Geological setting and characteristics of the tonalite-hosted Paleoproterozoic gold deposit at Osikonmäki, Rantasalmi, southeastern Finland

edited by Olavi Kontoniemi and Pekka A. Nurmi

Cover picture: A view northwards in the eastern part of the Osikonmäki gold mineralization. Here, the 10-15 m thick gold-bearing shear zone lies almost horizontally under the drilling machine (claim Osikko 1, profile L = 61.000, BH399).
Photo Olavi Kontoniemi

Geological setting and characteristics of the tonalite-hosted Paleoproterozoic gold deposit at Osikonmäki, Rantasalmi, southeastern Finland

edited by Olavi Kontoniemi and Pekka A. Nurmi

Kontoniemi, Olavi & Nurmi, Pekka A. (eds.) 1998. Geological setting and characteristics of tonalite-hosted Paleoproterozoic gold deposit at Osikonmäki, Rantasalmi, southeastern Finland. *Geological Survey of Finland, Special Paper 25.* 119 pages. 53 figures, 27 tables and 5 appendices.

The results of the Osikonmäki gold exploration project at Rantasalmi, SE Finland, carried out by the Geological Survey of Finland during 1986-1991 are reported in this Special Paper. Seven articles cover the following topics: geology of the Osikonmäki area and the granitoid host rock, geological setting, characteristics and fluid inclusion data of the gold deposit, and beneficiation properties of the ore.

The epigenetic Paleoproterozoic Osikonmäki gold deposit, is hosted by the synorogenic (1887±5 Ma) Osikonmäki tonalite pluton. The deposit exhibits a strong structural control, being closely associated with E-W trending shear zones that represent oblique ductile second order structures within the NW-trending crustal scale Raahe - Ladoga deformation zone. The granitoid is clearly I-type, calc-alkaline to subalkaline, metaluminous to marginally peraluminous, and is similar to calc-alkaline granitoids in modern collision zones.

The most common sulfide minerals associated with the ore are pyrrhotite, arsenopyrite, löllingite and chalcopyrite, which typically occur as irregular to somewhat banded disseminations. Gold and electrum, together with a number of Bi-Te-Se minerals, occur both as inclusions and at grain boundaries within and between arsenopyrite and silicate grains. Ore mineral parageneses indicate that gold mineralization took place under metamorphic conditions of amphibolite facies following the intrusion of synorogenic granitoids, but nevertheless prior to the peak of regional metamorphism. Fluid inclusion studies indicate that the main stage of mineralization was followed by influx of aqueous fluids of variable salinity, at least locally in the eastern part of the deposit, which transported gold and associated elements to higher structural levels during continued deformation within the shear zone.

Relative to the tonalite, As is the most enriched element in the deposit followed by Au, Se, S, Bi, Ag, Te, Sb, Cu, Pb, and Mo in decreasing order of enrichment. High concentrations of As, Au, and Se are characteristic of the Osikonmäki gold deposit. Gold is geochemically associated with Bi and Te whereas As-S-Se and Cu-Ag are distinct geochemical associations. The associations are interpreted as representing a temporal continuum of spatially overlapping episodes of precipitation.

In conventional bulk-flotation, gold recovery was only 70%, and the arsenic content in the bulk concentrate was 10-25%. Depending on the grinding fineness, the maximum recovery of gold by cyanide and bromide (Geobrom™3400A) leaching was 75-80%. Pressure oxidation increased gold recovery from the cyanide leaching by 10-25%. In kinetic tests, maximum gold recovery was achieved in only 8 hours by bromination as compared to the cyanidation which required nearly 24 hours to complete.

The publication provides new and detailed information on Osikonmäki tonalite and Osikonmäki gold deposit. Geological setting, mineralogy and geochemistry of this mainly premetamorphic deposit resemble other Paleoproterozoic (2000-1750 Ma) Svecofennian gold deposits.

Key words (GeoRef Thesaurus, AGI): gold ores, tonalite, mineralogy, geochemistry, fluid inclusions, beneficiation, Proterozoic, Paleoproterozoic, Osikonmäki, Rantasalmi, Finland

Olavi Kontoniemi
Geological Survey of Finland, P.O. Box 1237, FIN-70211 Kuopio, Finland
E-mail: Olavi.Kontoniemi@gsf.fi

Pekka Nurmi
Geological Survey of Finland, P. O. Box 96 FIN-02151 Espoo, Finland
E-mail: Pekka.Nurmi@gsf.fi

CONTENTS

PREFACE

The first indications of gold in the Rantasalmi district were found in the beginning of the 1970s during mineral exploration activities by the Geological Survey of Finland (GSF). During these investigations several gold-bearing erratics and quartz veins were discovered in the area west of lake Kolkonjärvi. The major impetus for gold exploration in the Osikonmäki area was provided in 1983 by the discovery of the Pirilä gold occurrence.

Gold exploration by the GSF began in earnest in the early 1980s motivated by high gold prices, improved analytical techniques for gold (rapid throughput with low detection limits) and the favorable geology in many parts of Finland for gold. Before 1980 only a few gold showings were known and there had not been much tought given to the gold potential of Finland. Rantasalmi was one of the project areas and after the discovery of the Pirilä occurrence, exploration was expanded into adjacent areas to the south and east. As a result of these investigations the first glacial erratics from the Osikonmäki deposit were found in late 1984. Follow-up studies led to the discovery of a gold-bearing shear zone in outcrop in summer of 1986. This was the beginning of the Osikonmäki gold project. The project involved collection of prospect-scale data that resulted in preliminary delineation of the gold deposit. Additional showings within the tonalite host rock were discovered between 1986 and 1991. GSF reported the deposit to the Ministry of Trade and Industry in 1991, and after a tender process the claim areas were transferred to Outokumpu Finnmines Oy.

Because the landscape of the Osikonmäki area is dominated by drumlinoid glacial till, boulder tracing was the main method used at the regional exploration stage. Magnetic, electromagnetic and IP measurements and finally detailed till/bedrock interface geochemistry and diamond drilling have been successively used during follow-up prospect stage investigations. Much of the material and data in this paper are based on the study of drill cores (comprising 120 holes, totalling about 16 km) recovered between 1986 and 1991. This Special Paper aims to give an overview on the tonalite-hosted Osikonmäki gold deposit which is representative of a distinct class of gold deposits in the Svecofennian terrain of Finland.

Turku, contributed to the project by studying the composition of fluid inclusions in different quartz vein types of the deposit. Outokumpu Finnmines Oy granted permission to publish the beneficiation results made by J. Leppinen, VTT Chemical Technology and Mineral Processing.

The combined efforts of exploration and multidisciplinary research made the Osikonmäki project successful. The project advanced our understanding of Svecofennian gold deposits and provided information that will aid in discovering similar deposits.

Espoo, February 24, 1998

Olavi Kontoniemi and Pekka A. Nurmi

AN OVERVIEW OF THE GEOLOGY IN THE OSIKONMÄKI AREA, RANTASALMI, SOUTHEASTERN FINLAND: ESPECIALLY AS A PROMISING ENVIRONMENT FOR EPIGENETIC GOLD MINERALIZATION

by

Olavi Kontoniemi

Kontoniemi, O. 1998. An overview of the geology in the Osikonmäki area, Rantasalmi, sotheastern Finland: especially as a promising environment for epigenetic gold mineralization. *Geological Survey of Finland, Special Paper 25.* 7-18. 5 figures.

The Osikonmäki gold deposit is situated in southeastern Finland, within the rural municipality of Rantasalmi. The area lies within the Ladoga-Bothnian Bay Zone, which is interpreted as a Paleoproterozoic collisional suture, expressed principally by NW-trending faults and dextral shear zones. The study area records a complex polyphase deformational and progressive metamorphic history and contains bimodal volcanic rocks characteristic of collisional settings. Metamorphic grade increases southwards towards the Sulkava thermal dome, and the gold mineralization is located within sillimanite-K-feldspar zone.

The bedrock of the study area consists predominantly of metaturbidites intruded by a variety of granitoids. The oldest supracrustal rocks are metasediments, overlain by a succession of volcanic lithologies commencing with felsic pyroclastics and followed by intermediate, mafic and ultramafic units. Intrusive rocks within the central part of the study area include the synkinematic Osikonmäki pluton (U-Pb zircon age = 1887±5 Ma), the Hiltula granitoid (U-Pb zircon age = 1850±7 Ma), which belongs to the late kinematic Putkilahti complex, and the post-tectonic Pirilä-type granites (U-Pb zircon age = 1815±7 Ma).

The gold deposit is located within the E-W trending Osikonmäki shear zone which deforms the synkinematic Osikonmäki pluton, and lies between the larger scale Kolkonjärvi and Haukivesi shear zones. Although the Kolkonjärvi shear zone has not been shown in outcrop to deform the Osikonmäki pluton, the occurrence of potassic alteration and chloritization, as well as interpretations of airborne magnetic data suggest that the shear zone was active after the pluton was intruded. Whether it was active prior to intrusion is difficult to ascertain, although it is concluded that shear zones developed during the early stages of collision. The similarities in appearance and monazite U-Pb ages of the late granites (including the Pirilä granite and Hiltula granitoid) on either side of the Kolkonjärvi lineament indicate that most of the movement took place before 1.80 Ga.

Convergence along the Ladoga-Bothnian Bay Zone provided appropriate conditions for the formation and transport of both metamorphic and magmatic fluids. Fluids have been channeled along complex fault systems and relatively competent rock units, such as granitoids, have preferentially focussed fluids in upper crustal levels.

Key words (GeoRef Thesaurus, AGI): metamorphic rocks, plutonic rocks, intrusions, tonalite, metamorphism, tectonics, shear zones, gold ores, Proterozoic, Paleoproterozoic, Osikonmäki, Finland

Olavi Kontoniemi
Geological Survey of Finland, P.O. Box 1237, FIN-70211 Kuopio, Finland

INTRODUCTION

The Osikonmäki gold deposit is situated in south-eastern Finland, in the rural municipality of Rantasalmi, some four kilometers WSW of the town of Rantasalmi (see Figure 1). The earliest published reference to the geology of this region was the 1:400 000 scale map of bedrock geology (Sheet D2 Savonlinna, Hackman and Berghell 1931), and the accompanying explanatory notes by Hackman (1933). The Rantasalmi area (Sheet 3233-Rantasalmi) was remapped on the scale of 1 to 100 000 by Korsman (1973).

In recent years the Rantasalmi area has been the focus for a number of detailed metamorphic and tectonic studies, commencing with Korsman (1977) and followed by Korsman et al. (1984), Korsman and Kilpeläinen (1986), Korsman et al. (1988), Kilpeläinen (1988) and Vaasjoki and Sakko (1988). In addition, the geochemistry and petrogenesis of metavolcanic rocks at Rantasalmi and nearby Juva were studied by Kousa (1985) and Viluksela (1988). Poutiainen (1992) has examined the tectono-metamorphic history of the Joroinen-Sulkava region, which includes Rantasalmi, on the basis of fluid inclusion investigations.

The Geological Survey of Finland commenced exploration in the Rantasalmi district during the 1960's and 1970's, in connection with the Juva Project (Pekkarinen 1972). Several erratics consisting of auriferous quartz rock and quartz diorite were already found during the course of these investigations, but the major impetus for gold exploration was provided by the discovery of the Pirilä deposit in 1983. Sustained high gold prices were an additional incentive for continuing exploration in the region, which became known as the Pirilä belt (see Makkonen and Ekdahl 1988), and in adjacent areas, to the south and east of the lake Kolkonjärvi (Figure 2). As a result of these investigations, the first erratics from the Osikonmäki deposit were found in late 1984, which in turn led to the finding of a mineralized shear zone in outcrop in the summer of 1986.
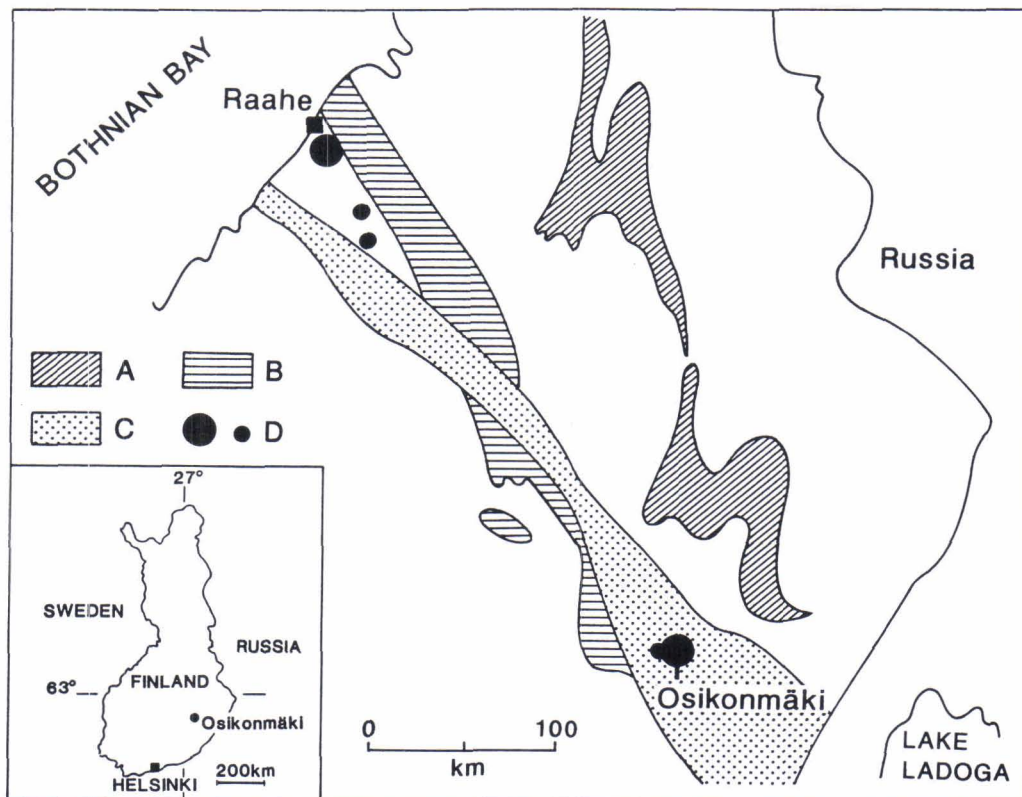

Fig. 1. The location of the Osikonmäki gold deposit and metallogenic provinces of the Ladoga-Bothnian Bay Zone after Ekdahl (1993). A = Kainuu-Outokumpu Back Arc, B = Pyhäsalmi Island Arc, C = Kotalahti Nickel Belt and D = Gold occurrences.

GEOLOGICAL SETTING OF THE STUDY AREA

The Rantasalmi area lies within a major geo-tectonic province variably known as the Main Sulfide Ore Belt (i.a. Kahma 1973, Neuvonen et al. 1981), Raahe-Ladoga Zone (i.a. Korsman 1988, Ekdahl 1993), and Ladoga-Bothnian Bay Zone (Gaál 1986 and 1990, Ward 1987). This zone contains most of the major sulfide deposits exploited in Finland to date, but recent discoveries, including the Osikonmäki deposit, indicate that there exists considerable potential for gold mineralization as well (Figure 1), particularly in association with shear zone systems in granitoids.

The Ladoga-Bothnian Bay Zone trends parallel to the Archean craton margin and represents the product of complex Paleoproterozoic subduction and collision processes (Gaál 1986 and 1990). The suture zone itself is considered to correspond to a pronounced negative Bouguer gravity anomaly, which also coincides with the surface expression of the Kolkonjärvi shear zone (see Figure 2). The heterogenity of the lithology and structure of the suture zone indicates that it is not a single structure but rather a tectonic junction between the Archean craton and obliquely orientated Paleoproterozoic formations (Koistinen et al. 1996).

It has been demonstrated that the tectono-metamorphic evolution of the Proterozoic crust in the Rantasalmi-Sulkava area differed from that in the central and northern part of the Ladoga-Bothnian Bay Zone (Korsman et al. 1988 and Vaasjoki and Sakko 1988). Korsman et al. (1988) suggested that there is a geosuture between the Kiuruvesi-Haukivesi complex and the Rantasalmi-Sulkava area (see Figure 3). Based on isotope data from Finland, Vaasjoki and Sakko (1988) suggested that the new Svecofennian crust was rapidly generated between 1930 and 1850 Ma ago by the collision of a Proterozoic oceanic plate with an Archean continent. Subsequent underplating in a W-E direction resulted in migmatization at about 1820 Ma and the emplacement of the ca. 1800 Ma post-tectonic granites in southern Finland (Vaasjoki and Sakko 1988).

Ekdahl (1993) considered that convergence took place along a SSW-NNE vector that generated an NW-SE dextral shear couple along the craton margin and caused variable overthrusting to the NW and NE. The resultant D_3 structures, including the SE-trending L_3 lineation strongly influenced the final geometry of massive sulfide ore bodies (Figure 4). Bimodal arc volcanism is characteristic of the zone, as indeed for the Svecofennian orogeny in general (Gaál 1990).

Lahtinen (1994) stressed the convergent plate tectonics and the complex nature of the evolution for the Svecofennian Domain. His model advocates three different collisional stages at 1.91-1.90 Ga, 1.89-1.88 Ga and 1.86-1.84 Ga where the third stage may be a direct continuation of the second stage. Lithospheric thickening during these events was followed by upwelling of the thermal boundary leading to magmatic underplating and high heat flow (Lahtinen 1994).

Koistinen et al. (1996) divide the tectonic evolution of southern Finland into two major parts: 1) a period of intense, large-scale tectonism, in which collision followed basin formation and destruction and 2) a synmetamorphic period with extensive crustal deformation. The E-W trending axis of recumbent F_1 and F_2 folds and thrusting of rocks onto basement in the east suggest tectonic transport due north. Because of rotation adjacent to the craton margin, the thrust sheets propagated to the northeast (Koistinen et al. 1996).

LITHOLOGIES IN THE STUDY AREA

Luukkonen and Lukkarinen (1986) classified the rocks of the Juva-Rantasalmi area as belonging to their so-called Svecofennian Supergroup. According to the Rantasalmi 1:100 000 map sheet (Korsman 1973), the most abundant lithologies in the area are metagraywackes and mica gneisses, with the central part of the region including a large proportion of granitoids, surrounded by amphibolites, quartzofeldspathic schists and ultramafic rocks. Small granitic intrusions are also present, including tourmaline granites.

Figure 2 is a geological map of the study area, based partly on the maps by Korsman (1973) and Makkonen and Ekdahl (1988), and partly on the results of subsequent exploration activity. The following review of lithologies is largely based on previous studies because the area of the present study consists principally of granitoids.

GEOLOGY OF THE OSIKONMÄKI AREA

Olavi Kontoniemi

3233

28° 10′ E

RANTASALMI

Haukivesi
shear zone

A 1169

Osikonmäki

Pirilä

Kolkonranta

Hakojärvi

LAKE KOLKON-JÄRVI

Tuusmäki

Kolkonjärvi shear zone

Pirilä belt

Hiltula

A 1170

Tuusjärvi

3555
6870

62°00′ N

OMK/AMK/-93

3 km

- Sample for U-Pb dating
✱ Gold occurrence

Osikonmäki granitoid:

Quartz diorite

Tonalite-granodiorite

Putkilahti complex:

Gabbro-diorite

Quartz diorite-granodiorite

Ultramafic rocks

Granite

Mafic-intermediate volcanite

Felsic volcanite and quartz-feldspar schist

Mica schist and gneiss

Conglomerate

Mafic or intermediate dyke

Granite dyke

Pegmatite dyke or vein

Inclusions:

Intermediate volcanite

Quartz-feldspar schist

Mica schist or gneiss

T   Tourmaline
⊙   Garnet
     Sillimanite
     Cordierite

Major fault

Fractures or lineament

Osikonmäki shear zone

Bedding

Foliation

Schistosity (S2)

Vertical schistosity (S3)

Lineation

⬠   Top of graded bedding

Modified from Korsman (1973) and Makkonen and Ekdahl (1988).

Fig. 2. Geological map of the study area. Modified from Korsman (1973) and Makkonen and Ekdahl (1988).
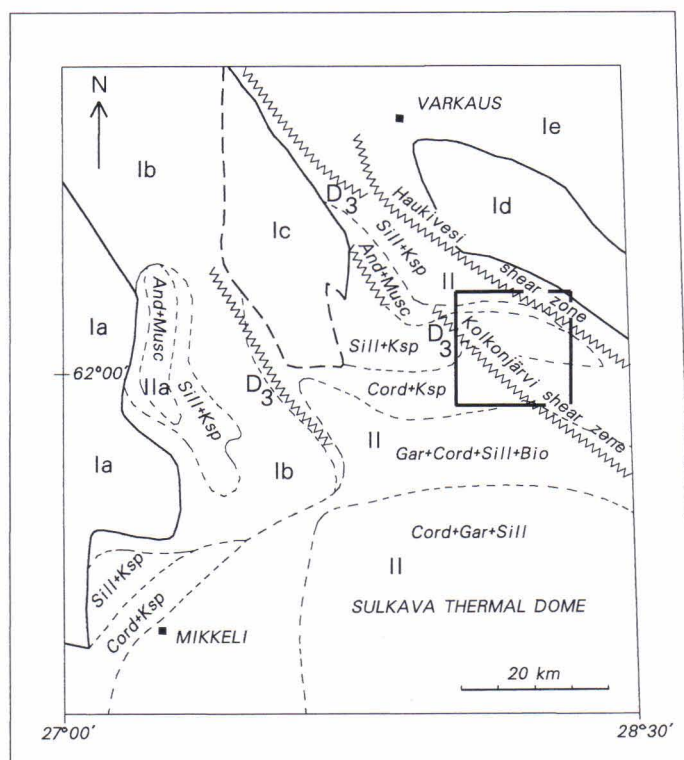
Fig. 3. Tectonometamorphic map of southern Savo (modified from Korsman et al. 1988) showing also the location of the study area (rectangle) and Kolkonjärvi and Haukivesi shear zones.
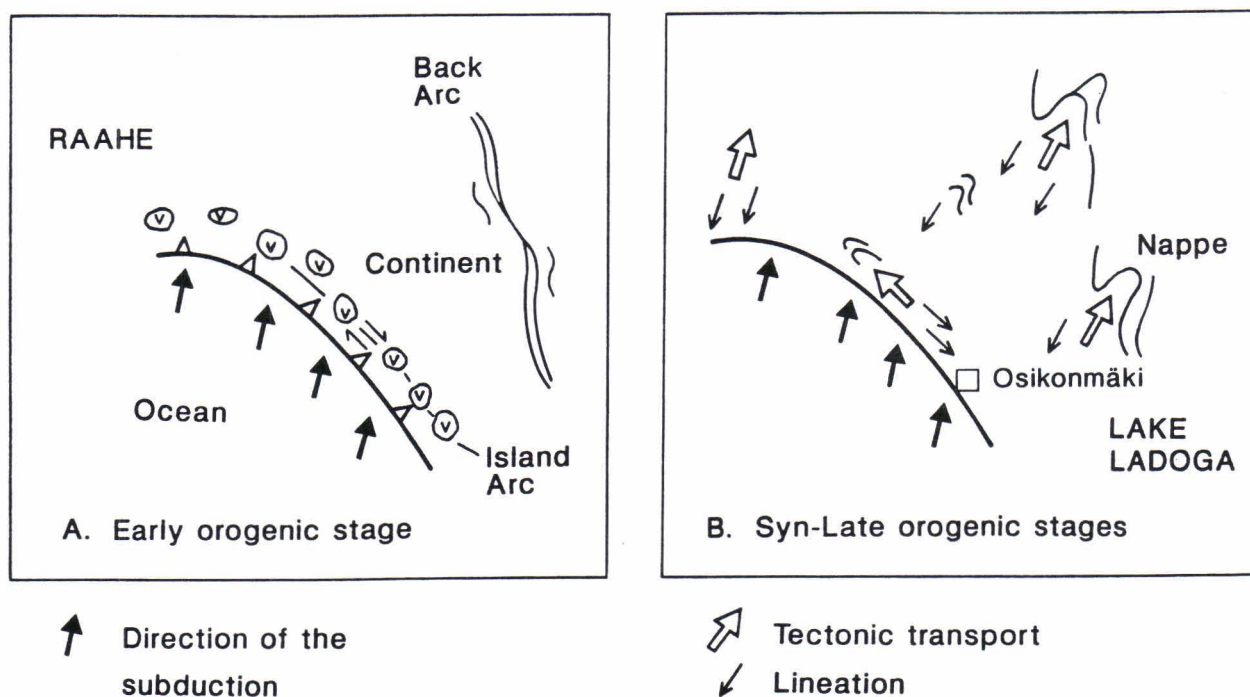

Fig. 4. Schematic illustration of tectonic events in the Ladoga-Bothnian Bay Zone showing also the location of the Osikonmäki gold deposit. Modified from Ekdahl (1993).

Supracrustal lithologies

Mica schists and mica gneisses

Mica schists in the study area commonly retain primary sedimentary features such as grading, slump structures and cross bedding, suggesting a turbiditic origin (Gaál and Rauhamäki 1971). With the southwards increase in metamorphic grade the mica schists gradually change into banded mica gneisses. Psammitic mica schists contain quartz, plagioclase and lithic fragments within a matrix of quartz, feldspar and mica. In contrast, pelitic layers consist principally of quartz and mica. Accessory minerals include apatite, sphene, tourmaline, opaques, carbonate and zircon. The metaturbidites contain narrow calc-silicate horizons and to the south of Kolkonjärvi a solitary conglomerate layer has been found (Makkonen 1992).

As metamorphic grade increases towards the south and southeast, pelitic compositions progressively show the development of porphyroblasts of andalusite, then K-feldspar with sillimanite, and finally, near the southern contact of the Osikonmäki pluton, cordierite and garnet.

Chemical sediments

In the so-called Pirilä belt (Makkonen and Ekdahl 1988), a narrow banded iron formation has been recognized that is considered to contain silicate, oxide and sulfide facies. The silcate facies is represented essentially by quartz-garnet-grünerite rock, but also contains sporadic hornblende, diopside, fayalite and cherty layers. The oxide facies layers consist predominantly of magnetite and quartz, with a little grünerite and diopside, while the sulfide facies comprises mangetite and pyrite with local chalcopyrite disseminations (Makkonen and Ekdahl 1988). The oxide facies attains a maximum thickness of about 5 m (Makkonen 1992).

Volcanic lithologies

The metavolcanic rocks of the region have been described previously by Kousa (1985), Makkonen and Ekdahl (1988) and Makkonen (1992). They occur within the Pirilä belt, near the Tuusmäki pluton (as at Kolkonranta), to the north of the Osikonmäki pluton, and in the vicinity of Hakojärvi and Tuusjärvi (Figure 2).

The felsic lithologies in the Pirilä belt are evidently lapilli tuffs in origin, with tectonically elongated but recognizable felsic fragments generally less than 5 cm in length, within a groundmass of quartz, plagioclase, biotite and K-feldspar. The dominant minerals in the lapilli are plagioclase and quartz, with accessory biotite, sericite, carbonate, opaques and zircon (Makkonen 1992).

Rocks of intermediate composition are present in the Pirilä belt, as well as at Kolkonranta and to the north of the Osikonmäki pluton. According to Makkonen (1992) those in the Pirilä belt show porphyritic and agglomeratic textures in some places but are generally strongly deformed and recrystallized. Uralite and plagioclase phenocrysts have been found in some cases at Pirilä, but at Kolkonranta a banded hornblende gneiss dominates (Kontoniemi 1991). Agglomeratic features are also present in intermediate metavolcanics occurring to the north of the Osikonmäki pluton, with pale highly elongate clasts varying in size from 2 to 40 cm.

Mafic intercalations, represented by amphibolites and diopside amphibolites, are also present within the intermediate volcanics. The amphibolites are interpreted as submarine flows because of the presence of pillow structures (cf. Kousa 1985, Makkonen 1992), while the banded diopside amphibolites represent their more highly strained equivalents. Chemically, the amphibolites are tholeiitic basalts (Kousa 1985), with trace element compositions being remeniscent of both MORB and island arc tholeiites (Viluksela 1988).

The western part of the study area contains ultramafic rocks of komatiitic affinity which appear to be either discordant or concordant with the amphibolites. Because of the presence of pillows, pyroclastic breccias and possible autoclastic lava breccias, the ultramafic rocks are interpreted as predominantly extrusive in origin (Kousa 1985).

Intermediate and mafic dykes

Intermediate and mafic dykes have been encountered during mapping in the vicinity of the Osikonmäki pluton. At the northern margin of the pluton there is a concordant intermediate uralite-plagioclase porphyry dyke that contains enclaves of mica schist. The largest uralite phenocrysts are about 1 cm in size and the principal minerals of the rock are plagioclase (An_{40}), uralitic hornblende and biotite. Accessory phases include quartz, opaques, apatite, sphene, sericite and zircon. The blasto-porphyritic texture of the rock is a consequence of incipient shearing and granulation.

An intermediate plagioclase porphyry dyke about 5 m in width crops out on the southern shore of the

lake Alanen. Contacts with the Osikonmäki granitoid are sharp and the western margin of the porphyry includes a narrow (1-2 cm) pegmatitic seam. Plagioclase, quartz, green hornblende and biotite predominate, with accessory opaques, sericite, sphene, apatite and zircon. The rock has a somewhat granoblastic texture, although the coarse plagioclase crystals also give an overall porphyritic appearance. Similar lithologies have been encountered in some of the Osikonmäki drill cores. Mafic and intermediate porphyry dykes are also present to the southeast of the Osikonmäki pluton, although intrusive relationships have not been well established. The dykes are compositonally very similar to the Alanen dyke.

Plutonic lithologies

Putkilahti complex

The Putkilahti intrusive complex (Gaál and Rauhamäki 1971) extends into the eastern part of the study area, and consists predominantly of heterogeneous diorite and gabbro alternating with coarser hornblendite. Marginal phases also include more quartz dioritic and granodioritic variants. The rocks of the complex are generally weakly foliated. The Putkilahti complex differs both texturally and petrographically from other gabbroic intrusions in the Haukivesi region. Nebulitic structures and magmatic layering are sometimes also present in the gabbroic phase. On the basis of truncating relationships, the youngest rocks within the complex are N-trending mafic dykes (Gaál and Rauhamäki 1971).

The predominant ultramafic lithology in the Putkilahti complex is hornblendite, which consists essentially of Mg-rich edenitic amphibole, although clinopyroxene is also sporadically present. Typical accessory minerals include sphene, apatite, carbonate and opaques (Gaál and Rauhamäki 1971). Gabbros and diorites differ from one another only with respect to plagioclase compositions, which are usually in the range An_{40}-An_{50}. Textures tend to be hypidiomorphic with intergrown pale green hornblende (possibly edenitic) and biotite. Typical accessory minerals are apatite, opaques, quartz and zircon, and plagioclase is somewhat sericitized and saussuritized.

Quartz diorites are generally somewhat finer grained than the diorites and are more distinctly hypidiomorphic. Plagioclase compositions vary from An_{35} to An_{40} and plagioclase constitutes about 50% of the rock, the remainder being green hornblende, biotite and quartz. Apatite is abundant,

forming up to 5% of the rock, with other accessory minerals being sphene, opaques, zircon, carboante, chlorite, sericite and K-feldspar.

Granodioritic compositions define a marginal phase, representing the most felsic lithologies in the complex. In conjunction with age determinations, they are referred as the Hiltula granodiorite (Vaasjoki and Kontoniemi 1991). Principal minerals are oligoclase, quartz, biotite and K-feldspar, while accessories include abundant apatite, sphene, zircon, opaques and amphibole, with some secondary sericite and epidote. The rock is weakly foliated and has a hypidiomorphic texture, with occasional myrmekite.

The Osikonmäki-type intrusion

The tonalitic Osikonmäki intrusion has been defined previously in connection with discussions of the Osikonmäki gold deposit (cf. Kontoniemi and Ekdahl 1990). This intrusion differs appreciably from the granitoids of the Putkilahti complex, with compositions ranging from quartz diorite to granodiorite, and also in having a highly deformed, in places gneissose fabric. The Osikonmäki intrusion and other related granitoids appear as discrete roundish magnetic minima on greyscale airborne magnetic pixel maps (Figure 5). Although they are broadly concordant with country rocks, they contain many kinds of supracrustal enclaves near their margins.

The Tuusmäki tonalite (Korsman et al. 1984) will be described in some detail here, since the Osikonmäki granitoid will be described elsewhere in this Special Paper. The Tuusmäki tonalite was originally termed the Peltue-Ronkala quartz diorite by Pekkarinen (1972), who considered it to be a domal intrusive mass surrounded by gneisses. He further described the quartz diorite as strongly deformed, almost gneissic, with an intense lineation and abundant pegmatitic and quartz veins in its central part.

Drillings carried out in connection with gold exploration at Kolkonranta (Kontoniemi 1991) revealed that the northern contact between the Tuusmäki tonalite and the surrounding metavolcanics is gradual, and intruded by pegmatites. Volcanic enclaves are also common within the margins of the intrusion, which in this area is granodioritic rather than tonalitic. The K-feldspar may however be partly secondary in origin. The rock has a granoblastic fabric as a result of metamorphic recrystallization and the principal minerals are plagioclase, quartz, biotite and K-feldspar. Accessory minerals are hornblende, diopside, epidote, carbonate, sphene, apatite and zircon (Kontoniemi 1991).

Granites

Two kinds of granite intrusion have been recognized in the study area, namely pinkish or greyish medium grained bodies such as the Pirilä granite (Vaasjoki and Sakko 1988), and a variety of pegmatitic veins and dykes. The former occur as discrete roundish intrusions, commonly intruded by related medium grained to pegmatitic dykes. Quartz, plagioclase, K-feldspar and in some places biotite are the dominant minerals, with typical accessory phases being apatite, muscovite, sphene and zircon. Some of the pegmatites exhibit complex mineralogies, with abundant tourmaline and in some cases brownish garnet, graphite and beryl. The area to the south of Kolkonjärvi is characterized by migmatites, commonly with microcline pegmatite dykes and leucosomes (Makkonen 1992).

AGE RELATIONSHIPS BETWEEN ROCK UNITS

Lithostratigraphical interpretations of the Rantasalmi area have been presented previously by Gaál and Rauhamäki (1971), Makkonen and Ekdahl (1988), and most recently, Makkonen (1992). According to Gaál and Rauhamäki (1971), the metapelites represent the oldest rocks in the Haukivesi area and are overlain by the mafic volcanics and metaturbidites. In contrast, Makkonen (1992) considered the mica schists and iron formation to be stratigraphically lowermost, followed by the volcanics, which commence with felsic pyroclastic deposits and are progressively overlain by intermediate, mafic and finally ultramafic lithologies.

Although the Osikonmäki pluton is broadly concordant with surrounding lithologies, the abundance of schistose supracrustal enclaves indicates the intrusive character of the granitoid. Two U-Pb zircon age determinations have been carried out for the Osikonmäki-type granitoids; the Tuusmäki tonalite gave an age of 1888±15 Ma (Korsman et al. 1984) and sheared Osikonmäki tonalite (Figure 2,

Sample A 1169) yielded an age of 1887±5 Ma (Vaasjoki and Kontoniemi 1991).

Field relationships indicate that the Putkilahti complex is less deformed than the Osikonmäki-type granitoids and therefore it was decided to attempt dating the felsic marginal phase, in order to test whether the Putkilahti complex is in fact younger. The resultant U-Pb zircon age determination, namely 1850±7 Ma (Figure 2, A 1170), obtained for the Hiltula granodiorite (Vaasjoki and Kontoniemi 1991), confirms this conclusion.

Intrusive relationships indicate that the mafic to intermediate porphyry dykes in the Osikonmäki area postdate the Osikonmäki pluton, and also the gabbros of the Putkilahti complex; relationships with the Hiltula granodiorite have not however, been established. The granites of the study area are still younger, as they cross cut all the other rock types of the area. The U-Pb zircon age for the Pirilä granite is consistent with field relationships, being 1815±7 Ma (Vaasjoki and Sakko 1988).

TECTONOMETAMORPHIC EVOLUTION OF THE STUDY AREA

Intensive structural and metamorphic studies have been carried out in the Rantasalmi area in recent years, notably by researchers from the Geological Survey of Finland. Results have been published by Korsman et al. (1984), Kilpeläinen (1988) and Korsman et al. (1988).

As noted earlier, the study area lies within a major suture zone associated with NW-trending faults and shear zones. The accompanying geological map (Figure 2) shows the Kolkonjärvi and Haukivesi shear zones, both of which are discernible in magnetic (Figure 5) and topographical data. The Osikonmäki pluton is situated between these two shear zones. Subsidiary shear zones interpreted from the grayscale magnetic pixel image (Figure 5) have also been marked on the map. However, the auriferous Osikonmäki shear zone does not have any topographical or magnetic expression.

The tectonometamorphic map of the Rantasalmi region (Korsman et al. 1988) includes the present study area and also shows the Kolkonjärvi and Haukivesi fault or shear zones (Figure 3). Being situated between Rantasalmi and Sulkava, the study area transects several progressive metamorphic zones. The Kiuruvesi-Haukivesi complex (I in Figure 3) and the Rantasalmi-Sulkava area (II in Figure 3) record quite different tectonothermal histories. For example, the high grade metamorphic Pieksämäki (Ic) and Haukivesi (Id) blocks were metamophosed during a D_1-D_2 tectonic event prior to the intrusion of granitoids around 1.88 Ga. In contrast, separate metamorphic evolution has been

recorded from the Sulkava area, where the thermal metamorphic peak postdated the local D_2 structures and culminated during D_3 at about 1.83-1.81 Ga (Korsman et al. 1988). Because movements took place on fault zones, including the D_3 shear zones, until a relatively late stage, some of the progressive metamorphic isograds have been truncated, and consequently zones of different metamorphic grade are tectonically juxtaposed. Metamorphic grade increases progressively in the Rantasalmi-Sulkava area towards the Sulkava thermal dome (Figure 3), as expressed by the following sequence of meta-morphic parageneses:

andalusite-muscovite zone
sillimanite-K-feldspar zone
K-feldspar-cordierite zone
garnet-cordierite-biotite zone
garnet-cordierite-sillimanite zone (Korsman et al. 1984)

The present study area is mostly within the sillimanite-K-feldspar zone, although the southern part also includes gneisses belonging to the K-feldspar-cordierite zone. Prograde progressive

metamorphism peaked during D_2 deformation in the Rantasalmi area (Kilpeläinen 1988). Andalusite formed at the expense of muscovite early during D_2, while further southwards, sillimanite and K-feldspar crystallized. Cordierite and K-feldspar formed as a result of biotite breakdown during the peak of D_2. In close proximity to the Sulkava thermal dome garnet equilibrated with cordierite after D_2, indicating that the age of the metamorphic peak becomes progressively younger as the Sulkava thermal dome is approached (Kilpeläinen 1988).

F_1 folds have only been identified within the andalusite-muscovite zone within the northern part of the study area. These folds are isoclinal with amplitudes varying from 10-20 m. F_2 folds tend to be tight with amplitudes ranging over hundreds of meters. The intensity of the S_2 foliation varies with metamorphic grade, being a penetrative schistosity in the sillimanite-K-feldspar zone. Fibrolitic sillimanite has also shown a tendency to crystallize within S_2 crenulation cleavage lithons. D_3 struc-tures are expressed in outcrop as asymmetrical folds of variable size with a NW-SE trending axial

**Magnetic map
Grayscale
Rantasalmi
Osikonmäki
Map 3233**

**Shading from south-west
at height angle 10 degrees**

6060
-19.4
-110
-200
-290
-2300
nT

.5   0   1.5   3

Kilometers

Lineaments:

.... **First order**
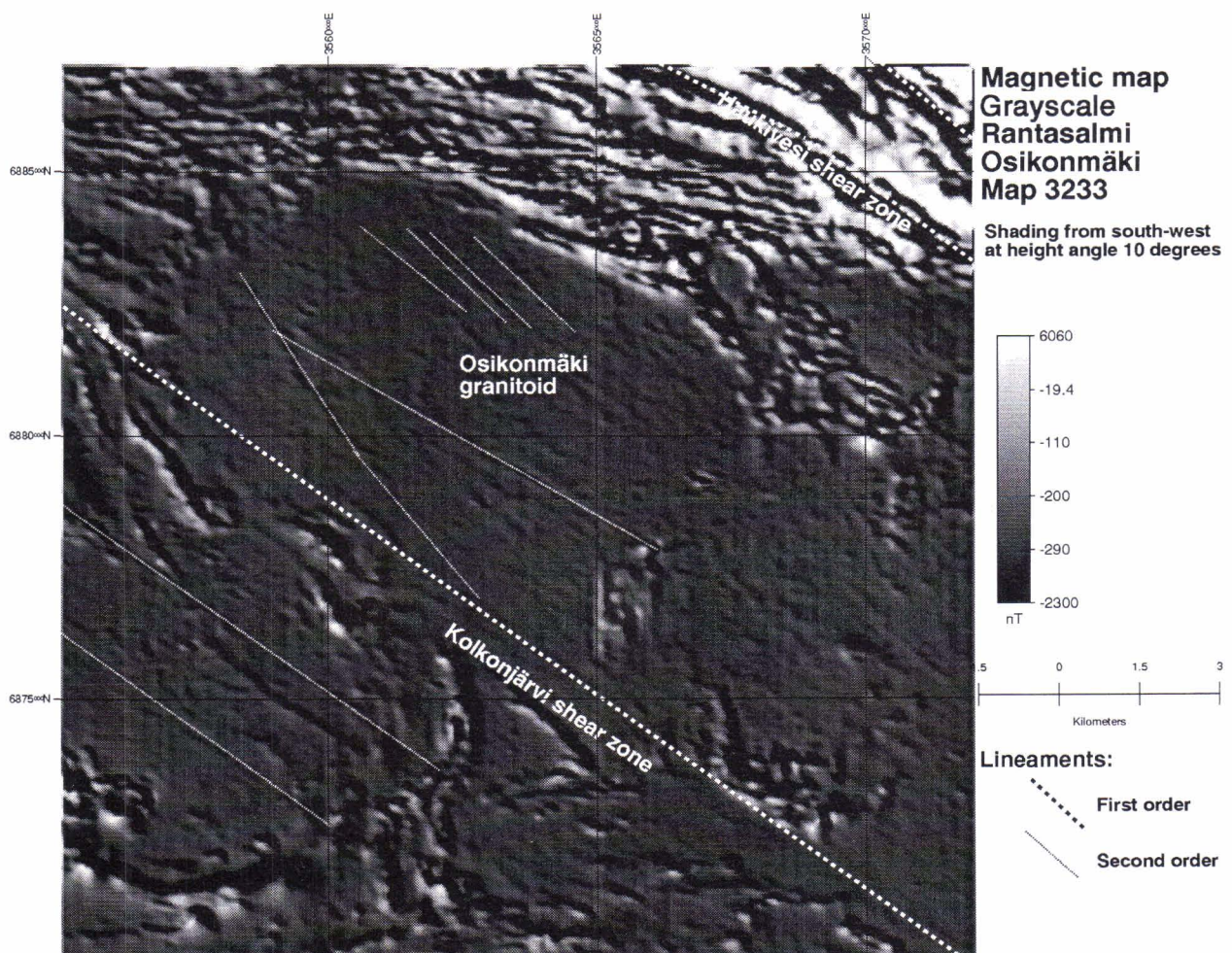
⁣ **Second order**

Fig. 5. Magnetic grayscale map of the study area showing also the location of possible major and subsidiary shears (lineaments).

plane and a generally southeastward plunge. This phase of deformation evidently continued after the climax of metamorphism since it has truncated and modified the distribution of metamorphic zones. This is also consistent with retrogressive formation of muscovite and the growth of axial planar biotite within the southern part of the sillimanite-K-feld-spar zone. D_4 is represented by a crenulation cleavage, but no associated folds have been identified; this foliation is also present within the younger (1.83-1.80 Ga) granites, which thus constrains the maximum possible age for this deformation (Kilpeläinen 1988).

Relationships between granitoid intrusions, deformation and metamorphism

Although the Osikonmäki-type intrusions predate the regional metamorphic peak, no evidence has been found for any thermal aureoles (Korsman et al. 1984). Moreover, although it is clear that the intrusions predate D_2, their relationship to earlier deformation has not been established (Korsman et al. 1988). This type of intrusion occurs predominantly within the sillimanite K-feldspar zone, with metamorphic grade increasing towards the south. Foliation in the granitoids conform with that in the enclosing supracrustal rocks. Observations from the Tuusmäki tonalite suggest that it was emplaced into a regional antiformal culmination, but that regional metamorphic isograds overprint structures within the pluton (Korsman et al. 1984). Within the classification of Finnish granitoids outlined by Nurmi and Haapala (1986), the Osikonmäki-type intrusions would fall into the synkinematic group.

The less deformed Putkilahti complex does not show the same range of structural features as the pre-D_2 Osikonmäki granitoids. Suitable metamorphic minerals for monitoring progressive metamorphism are not present within the complex, but there is nevertheless a distinct D_3 mineral alignment in proximity to the Kolkonjärvi lineament. Thus isotopic and structural criteria both suggest that the Putkilahti complex more likely represents the earliest stages of late kinematic magmatism

than the waning stages of synkinematic magmatism.

The Sulkava thermal dome is associated with abundant microcline granites interpreted as recording anatexis (Korsman et al. 1984). Within the sillimanite-K-feldspar zone however, and still further to the north, different kinds of granitic and pegmatitic intrusions are present. These might also represent the products of in situ anatexis (Korsman et al. 1984), but it is also possible that they have been intruded from greater depths, in which case they could be related to the Pirilä granite.

Although it has not been specifically demonstrated that the Kolkonjärvi fault cuts the Osikonmäki granitoids, the airborne magnetic data, as well as the presence of potassic alteration and chloritization suggest that the fault was active after granitoid emplacement. It is difficult to be certain as to whether the fault was active also prior to granitoid emplacement, but in general the shear zones along the suture must have formed at a relatively early stage during the overall deformation history. Because the Pirilä granite and the Hiltula granodiorite and related intrusions on either side of the Kolkonjärvi lineament are petrographically similar and have similar monazite $^{207}Pb/^{206}Pb$ ages, it is concluded that the main activity along this zone ceased before their emplacement (Vaasjoki and Kontoniemi 1991).

DISCUSSION

According to currently favoured concepts, mesothermal gold mineralization is closely associated with complex crustal scale deformation processes. With respect to plate tectonic processes, shear zones can either be extensional or compressional in nature, the former occurring during continental rifting and the latter during subsequent plate convergence. During oblique collision it is also probable that alternating zones and phases of extension and compression will exist. Within major convergence zones, as much as half of the total crustal thickness may be subjected to metamorphic

dehydration processes, with the metamorphic peak post-dating collision by as much as fifty million years (Murphy 1989).

The Rantasalmi area is located within a Paleoproterozoic collision zone that is recorded by the presence of NW-trending crustal scale shear zones, such as the Kolkonjärvi and Haukivesi zones. Previous interpretations of the Ladoga-Bothnian Bay Zone (Gaál 1986, Ekdahl 1993, Lahtinen 1994) involved convergence from the SW or SSW, resulting in a dextral wrench fault system. Koistinen et al. (1996) suggested that tectonic transport was due

north and because of rotation adjacent to the craton margin, the thrust sheets propagated to the northeast. Inspection of the airborne magnetic data from the Rantasalmi district suggests that the total displacement in this area was not great, so that a significant dip-slip component could also be inferred. During the later stages of collision, and during development of the Sulkava thermal dome, the overthrust tectonics and vertical fault movements were further accentuated.

Epigenetic ore processes inevitably require extensive hydrothermal activity and fluid flow, typically within major structural features. Fluid activity is closely linked with mobilization, transport and precipitation of ore metals, which is also greatly influenced by fluid compositions and ambient P-T conditions. Archean mesothermal gold deposits are considered to have formed from fluids that have both metamorphic (devolatilization) and magmatic (felsic intrusives) characteristics (Groves and Foster 1991). The Ladoga-Bothnian Bay Zone has experienced a range of metamorphic (subducting oceanic plate during convergence and/or thickening of the crust during collision, late thermal event) and magmatic (three phases of granitoid intrusion) processes that can have contributed to generation and migration of fluids. These fluids were focussed by major shear systems, particularly into obliquely oriented dilational sites, and the role of relatively competent rock units, such as the Osikonmäki intrusion, was important in chanelling fluids to higher crustal levels.

REFERENCES

Ekdahl, E. 1993. Early Proterozoic and Svecofennian formations and the Evolution of the Raahe-Laadoga Ore Zone, based on the Pielavesi area, central Finland. Geological Survey of Finland, Bulletin 373. 137 p.

Gaál, G. 1986. 2200 million years of crustal evolution: The Baltic shield. Bulletin of the Geological Society of Finland 58, 149-168.

Gaál, G. 1990. Tectonic styles of Early Proterozoic ore deposition in the Fennoscandian Shield. Precambrian Research 46, 83-114.

Gaál, G. & Rauhamäki, E. 1971. Petrological and structural analysis of the Haukivesi area between Varkaus and Savonlinna, Finland. Bulletin of the Geolgical Society of Finland 43, 265-337.

Groves, D.I. & Foster, R.P. 1991. Archaean lode gold deposits. In: Foster, R.P. (ed.) Gold metallogeny and exploration Blackie and Son Ltd, London, 63-103.

Hackman, V. 1933. Savonlinna. Suomen geologinen yleiskartta 1 : 400 000. Kivilajikartan selitys, lehti D2. 175 p.

Hackman, V. & Berghell, H. 1931. Savonlinna. Kivilajikartta, lehti D2. Suomen geologinen yleiskartta 1 : 400 000.

Kahma, A. 1973. The main metallogenic features of Finland. Geolgical Survey of Finland, Bulletin 265. 29 p.

Kilpeläinen, T. 1988. Evolution of deformation and metamorphism as a function of time in the Rantasalmi-Sulkava area, southeastern Finland. Geological Survey of Finland, Bulletin 343, 77-87.

Koistinen, T., Klein, V., Koppelmaa, H., Korsman, K., Lahtinen, R., Nironen, M., Puura, V., Saltykova, T.,

Tikhomirov, S. & Yanovskiy, A. 1996. Paleoproterozoic Svecofennian orogenic belt in the surroundings of the Gulf of Finland. In: Koistinen, T. (ed.) Explanation to the Map of Precambrian basement of the Gulf of Finland and surrounding area 1 : 1 million. Geological Survey of Finland, Special Paper 21, 21-57.

Kontoniemi, O. 1991. Kolkonrannan kultamalmitutkimukset Rantasalmen kunnassa vuosina 1989-1990. M19/3233/-91/2/10. Unpublished report, Geological Survey of Finland. 15 p.

Kontoniemi, O. & Ekdahl, E. 1990. Tonalite-hosted early Proterozoic gold deposit at Osikonmäki, southeastern Finland. Bulletin of the Geological Society of Finland 62, 61-70.

Korsman, K. 1973. Rantasalmi. Geological Map of Finland 1 : 100 000, Pre-Quaternary rocks, Sheet 3233. Geological Survey of Finland.

Korsman, K. 1977. Progressive metamorphism of the metapelites in the Rantasalmi-Sulkava area, southeastern Finland. Geological Survey of Finland, Bulletin 290. 82 p.

Korsman, K. 1988. Tectono-metamorphic evolution of the Raahe-Ladoga zone, Introduction. Geological Survey of Finland, Bulletin 343, 5-6.

Korsman, K., Hölttä, P., Hautala, T. & Wasenius, P. 1984. Metamorphism as an indicator of evolution and structure of the crust in eastern Finland. Geological Survey of Finland, Bulletin 328. 40 p.

Korsman, K. & Kilpeläinen, T. 1986. Relationship between zonal metamorphism and deformation in the Rantasalmi-Sulkava area, southeastern Finland. Geological Survey of Finland, Bulletin 339, 33-42.

Korsman, K., Niemelä, R. & Wasenius, P. 1988. Multistage evolution of the Proterozoic crust in the Savo schist belt, eastern Finland. Geological Survey of Finland, Bulletin 343, 89-96.

Kousa, J. 1985. Rantasalmen tholeiittisista ja komatiittisista vulkaniiteista. English summary: The tholeiitic and komatiitic metavolcanics in Rantasalmi, southeastern Finland. Geologi 37 (2), 17-22.

Lahtinen, R. 1994. Crustal evolution of the Svecofennian and Karelian domains during 2.1-1.79 Ga, with special emphasis on the geochemistry and origin of 1.93-1.91 Ga gneissic tonalites and associated supracrustal rocks in the Rautalampi area, central Finland. Geological Survey of Finland, Bulletin 378. 128 p.

Luukkonen, E. & Lukkarinen, H. 1986. Explanation to the stratigraphic map of Middle Finland. Geological Survey of Finland, Report of Investigation 74, 47 p.

Makkonen, H. 1992. 1.9 Ga tholeiittinen magmatismi ja siihen liittyvä Ni-Cu -malminmuodostus Juvan alueella, Kaakkois-Suomessa. Unpublished Licentiate thesis. University of Oulu. 200 p.

Makkonen, H. & Ekdahl, E. 1988. Petrology and structure of the early Proterozoic Pirilä gold deposit in southeastern Finland. Bulletin of the Geological Society of Finland 60, 55-66.

Murphy, J.B. 1989. Tectonic environment and metamorphic characteristics of shear zones. In: Bursnall, J.T. Mineralization and shear zones. Geological Association of Canada, Short Course Notes, Volume 6, 29-49.

Neuvonen, K. J., Korsman, K., Kouvo, O. & Paavola, J.
1981. Paleomagnetism and age relations of the rocks in the Main Sulphide Ore Belt in central Finland. Bulletin of the Geological Society of Finland 53, 109-133.

Nurmi, P.A. & Haapala, I. 1986. The Proterozoic granitoids of Finland: Granite types. metallogeny and relation to crustal evolution. Bulletin of the Geological Society of Finland 58, 203-233.

Pekkarinen, J. 1972. Selostus Juvan tutkimusprojektin malmitutkimuksista vuosina 1962-1971 (X=6880.0 eteläpuoli). M19/3231/-72/1/10. Unpublished report, Geological Survey of Finland. 48 p.

Poutiainen, M. 1992. Studies of fluid inclusions in metamorphic rocks and sulphide (-gold) deposits from the Svecofennian and Archean domains in Finland. Academic dissertation, University of Helsinki, Finland.

Vaasjoki, M. & Kontoniemi, O. 1991. Isotopic studies from the proterozoic Osikonmäki gold prospect at Rantasalmi, southeastern Finland. In: Autio, Sini (ed.) Geological Survey of Finland, Current Research 1989-1990. Geological Survey of Finland, Special Paper 12, 53-57.

Vaasjoki, M. & Sakko, M. 1988. The evolution of the Raahe-Ladoga zone in Finland: isotopic constraints. Geological Survey of Finland, Bulletin 343, 7-32.

Viluksela, A. 1988. Rantasalmen ja Parikkalan-Punkaharjun vulkaniittien petrografia, geokemia ja tektonomagmaattinen luonne. Unpublished Master of Science thesis. University of Helsinki. 96 p.

Ward, P. 1987. Early Proterozoic deposition and deformation at the Karelian craton margin in southeastern Finland. Precambrian Research 35, 71-93.

GEOLOGY OF THE PALEOPROTEROZOIC SYN-KINEMATIC OSIKONMÄKI GRANITOID INTRUSION AT RANTASALMI, SOUTHEASTERN FINLAND

by
Olavi Kontoniemi

Kontoniemi, Olavi 1998. Geology of the Paleoproterozoic synkinematic Osikonmäki granitoid intrusion at Rantasalmi, southeastern Finland. *Geological Survey of Finland, Special Paper 25*. 19-38. 11 figures, 4 tables and 2 appendices.

The Osikonmäki synkinematic granitoid intrusion is located in the Paleoproterozoic Ladoga-Bothnian Bay collision zone between the Kolkonjärvi and Haukivesi shear zones. The intrusion was emplaced before D_2 and has undergone, after that, the same deformational and metamorphic history as the surrounding supracrustal rocks. Its present domal form reflects location in an axial culmination.

The marginal areas of the granitoid intrusion are composed of quartz diorite that grades to tonalite (in places granodiorite) toward the center of the intrusion. An E-W-trending mineralized shear zone cuts the granitoid. In this zone, slightly altered hypidiomorphic tonalite has been sheared and the associated metamorphism gives the rock a granoblastic and gneissose appearance. In the shear zone, alteration is stronger than in the tonalite and the amount of K-feldspar, quartz and micas, particularly, has increased at the expense of plagioclase and hornblende. Throughout the intrusion, there are mafic microgranular enclaves (MME), which indicate mechanical mixing (mingling) of felsic and mafic magmas.

Declining concentration trends of major elements (Mg, Fe, Ca, Ti, P) and Ba and Zr with increasing SiO_2 reflect the fractionation of plagioclase, biotite, hornblende, Fe-Ti minerals, apatite and zircon in the Osikonmäki intrusion. Variations in K, Sr and Rb contents suggest that at first the fractionating mineral was biotite and only later potassium feldspar. Alternatively, the chemical trends may reflect a combination of fractional crystallization and alteration.

The Osikonmäki granitoid intrusion is clearly I-type, calc-alkaline and subalkaline, metaluminous to marginally peraluminous, and is highly similar to calc-alkaline granitoids in modern collision zones.

Key words (GeoRef Thesaurus, AGI): intrusions, tonalite, granodiorites, quartz diorites, inclusions, shear zones, geochemistry, genesis, Proterozoic, Paleoproterozoic, Osikonmäki, Finland

Geological Survey of Finland, P.O. Box 1237, FIN-70211 Kuopio, Finland

INTRODUCTION

The Osikonmäki granitoid intrusion is in the Paleoproterozoic Ladoga-Bothnian Bay collision zone (Gaál 1986), between the Kolkonjärvi and Haukivesi shear zones in southeastern Finland (Figure 1). It forms a dome-like structure within an axial culmination.

Kontoniemi and Ekdahl (1990) and Vaasjoki and Kontoniemi (1991) have earlier discussed the geology of the Osikonmäki intrusion. Kontoniemi gives an overview of the general geology of the area elsewhere in this Special Paper.

Zircon fractions from the partly gneissose, tonalitic Osikonmäki intrusion, emplaced at least before D_2, yield an upper intercept age of 1887±5 Ma (Vaasjoki and Kontoniemi 1991). Thus the intrusion belongs to the synkinematic group of Finnish Proterozoic granitoids (cf. Nurmi and Haapala 1986).

Petrogenetic classification of the granitoid rocks has traditionally been based on petrography, on inclusions in the granite, or on mineralization types. At present, they are often classified on the basis of major and trace element contents and tectonic characteristics. A classification frequently used is division into S-, I- and A-type granitoids based on major elements (White and Chappell 1983) and, based on trace elements, into the COL-, VA-, OR- and WP-granites of Pearce et al. (1984). Petrogenetic characteristics of Barbarin's (1990) granitoid classes are presented in Figure 2.

The samples from the Osikonmäki granitoids were collected during ore exploration. Surface samples were either hammered from outcrops or drilled with a portable drill. Ore samples were obtained from diamond-drill cores. The areal coverage of the sampling is only fair, because the outcrop density is relatively small and most of the outcrops are in the eastern and northern parts of the intrusion. All samples were analyzed in the laboratories of Geological Survey of Finland (GSF), with XRF, Leco, FAAS and Fire assay equipment at Espoo, GFAAS[*] at Kuopio and GFAAS at Rovaniemi. The methods used are presented in Table 1.

Table 1. Analytical methods used, detection limits and sample amounts.

Element	Method	GSF-code	n	Det. limit (ppm)
Major elements	XRF	713X	36	100
-"-	XRF	175X	19	100
V, Rb, Sr, Zr, Ba	XRF	170X	36	10
-"-	XRF	175X	19	10, 30 (V)
As, Cu, Zn, Pb	FAAS	511A	36	1
-"- (ore)	XRF	175X	19	10, 30 (As)
S	Leco	810L	55	100
H_2O	Leco	815L	55	100
Te, Se	GFAAS	519U	55	0.001, 0.01 (Se)
Sb (ore)	GFAAS	511U	19	0.01
Bi	GFAAS[*]	419U	55	0.1
Au	GFAAS	519U	36	0.001
Au (ore)	Fire assay	704A	19	0.1

XRF = X-ray fluorescence spectrometry
FAAS = Flame atomic absorption spectrometry
GFAAS = Graphite furnace AAS
Leco = Leco analyzer
  [*] = GFAAS after organic extraction
  n = number of analyses

GEOLOGY OF THE OSIKONMÄKI AREA

Olavi Kontoniemi

3233

___ 3 km

Gold occurrence ✶

Osikonmäki granitoid:

Quartz diorite

Tonalite-granodiorite

Putkilahti complex:

Gabbro-diorite

Quartz diorite-granodiorite

Ultramafic rocks

Granite

Mafic-intermediate volcanite

Felsic volcanite and quartz-feldspar schist

Mica schist and gneiss

Conglomerate

Mafic or intermediate dyke

Granite dyke

Pegmatite dyke or vein

Inclusions:

Intermediate volcanite

Quartz-feldspar schist

Mica schist or gneiss

T   Tourmaline

⊙   Garnet

Sillimanite

Cordierite

Major fault

Fractures or lineament

Osikonmäki shear zone

[83] Bedding

[85] Foliation

[85] Schistosity (S2)

Vertical schistosity (S3)

Lineation [25]

Top of graded bedding

Modified from Korsman (1973) and Makkonen and Ekdahl (1988).

OMK/AMK/-93

SWEDEN   RUSSIA   FINLAND   Osikonmäki   RAAHE-LADOGA ZONE   Helsinki   200 km

28° 10' E

RANTASALMI

Osikonmäki

Pirilä

Hakojärvi   Kolkonranta

LAKE KOLKON-JÄRVI

Tuusmäki

Kolkonjärvi shear zone

Haukivesi shear zone
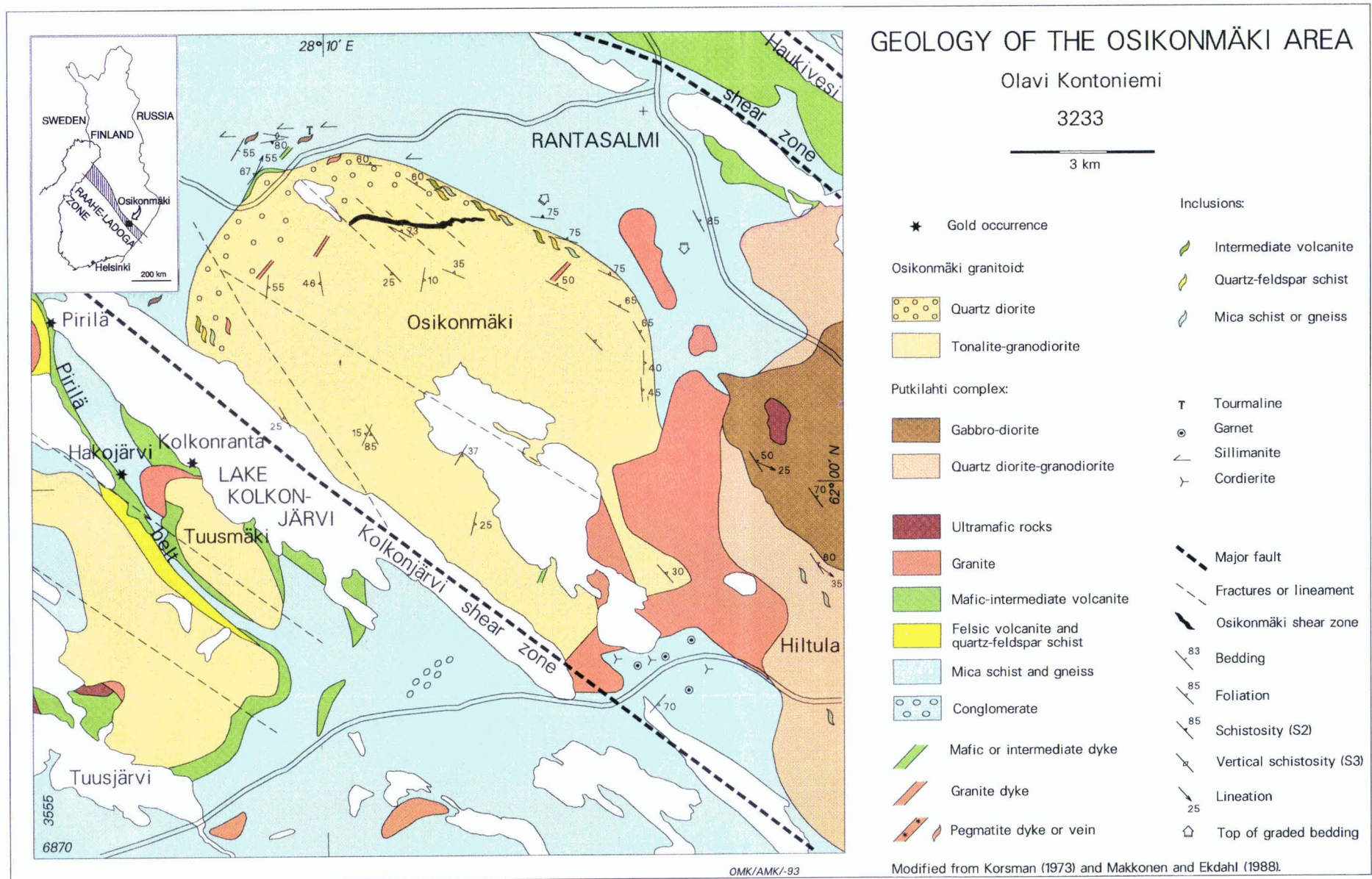
Hiltula

Tuusjärvi

62° 00' N

3555   6870

Fig. 1. Geological map of the Osikonmäki area showing also the location of the study area. Modified from Kontoniemi (1998, this volume).

FORM AND RELATION TO SURROUNDING SCHISTS

The Osikonmäki granitoid intrusion is roundish with a surface area of about 50 km². It is concordant to the surrounding schists and dips relatively gently toward E and SE under the schists. At the northern and northwestern corners of the intrusion, the wallrock schists are more vertical.

The dome-like structure of the intrusion is the result of polyphase deformation. The intrusion occupies an axial culmination, and structurally and geometrically it is a syntectonic phacolith or laccolith. The extent of the intrusion at depth is uncertain, but the nature of its deformation indicates that it was originally a sheet-like body, which was folded and sheared during D_2 and younger deformations. Based on drilling data, in the vicinity of the shear zone, the thickness of the granitoid is at least 400 m.

Although on a large scale the intrusion is concordant to the surrounding schists, especially at the northeastern contact, there are plenty of schistose inclusions or enclaves in the granitoid. The inclusions are more than a metre long at maximum and they have been deformed in the same way as the granitoids, showing elongated forms and rounded corners. Mica schist and porphyry inclusions are most common but also quartz-plagioclase schist inclusions are found. The porphyry inclusions are of intermediate composition and contain plagioclase and uralite phenocrysts. Besides these contact inclusions, small mafic inclusions occur throughout the intrusion.

Because of the strong deformation and regional metamorphism, the effects of contact metamorphism are not seen in the surrounding schists or inclusions in the contact zone. Pegmatite dyke and vein material is abundant close to the intrusion in its wallrocks, but this is due to structural rather than contact metamorphic factors.

INTERNAL STRUCTURE

Using Streckeisen's (1974) classification, the Osikonmäki intrusion's composition varies from quartz dioritic to granodioritic. The change from quartz diorite to granodiorite is gradual (Kontoniemi and Ekdahl 1990). The rocks on the eastern and northern margin are clearly more mafic than elsewhere in the intrusion. The granodioritic portions represent at least in part granodioritized tonalite, because, based on thin section investigations, most of K-feldspar is secondary, formed by alteration.

Mafic enclaves occur throughout the Osikonmäki intrusion (Figs 3a and b). The enclaves are roundish and usually less than 0.5 m in length. They are more mafic and finer-grained than the host rock and vary in

- ORIGIN -	- GRANITOID TYPES -		- TECTONIC SETTING -	
CRUSTAL ORIGIN	Intrusive Two-mica Leucogranites	C_{ST}	COLLISION OR POST-COLLISION ZONES	OROGENIC GRANITOIDS
	Peraluminous Autochtonous Granitoids	C_{CA}		
PERALUMINOUS ROCKS	Peraluminous Intrusive Granitoids	C_{CI}		
MIXED ORIGIN **(Crust + Mantle)**	Potassic Calc-Alkaline granitoids (High K – Low Ca)	H_{LO}		
METALUMINOUS OR CALC-ALKALINE ROCKS	Calc-Alkaline Granitoids (Low K–High Ca)	H_{CA}	SUBDUCTION ZONES	
MANTLE ORIGIN	Island Arc Tholeiitic Granitoids	T_{IA}		ANOROGENIC GRANITOIDS
	Midocean Ridge Tholeiitic Granitoids	T_{OR}	RIFTING OR DOMING ZONES	
THOLEIITIC, ALKALINE OR PERALKALINE ROCKS	Alkaline and Peralkaline Granitoids	A		

Fig. 2. The main petrogenetic classification of granitoids proposed by Barbarin (1990). Relationships between petrogenetic types of granitoids, origins of the magmas and tectonic settings. C_{ST} = shearing and thrusting granitoids, $C_{CA, CI}$ = Crustal collisional autochthonous or intrusive granitoids, H_{LO} = Hybrid late orogenic granitoids, H_{CA} = Hybrid continental arc granitoids, $T_{IA, OR}$ = Tholeiitic island arc or oceanic ridge granitoids, A = Alkaline anorogenic granitoids

composition from quartz diorite to diorite. Plagioclase and/or uralite phenocrysts can often be distinguished in the fine-grained groundmass, and occasionally the enclaves have a weak ophitic appearance.

The principal minerals of the enclaves are plagioclase, blue-green hornblende, biotite and occasionally quartz; accessory minerals are apatite, titanite, opaques and zircon. In particular, there is more apatite than in the host rock. Because the enclaves are also deformed and metamorphosed, their texture is nearly granoblastic and the original mineralogy has been partly altered. Vernon et al. (1988), Nironen (1989), Castro et al. (1990), and Barbarin and Didier (1992), among others, describe similar texturally magmatic, relatively mafic microgranular enclaves (MME) in granitoid plutons. According to present opinion (op. cit.), such enclaves indicate mixing of two magma types (hybridization) before the final cooling of the intrusion. Mixing of a felsic and a mafic magma may be mechanically and chemically perfect (mixing), where the result is a homogeneous "hybrid rock". If the mixing is mainly mechanical (mingling), the forming granitoid contains many types of MME, a fact which indicates interaction of mafic and felsic magma (Barbarin and Didier 1992).

The marginal area of the Osikonmäki intrusion, particularly, has a strong preferred orientation. The schistosity (foliation) follows the trend of the contact and dips towards the contact (Fig. 1). Because the intrusion was deformed during D_2, it is difficult to show how much of the foliation is an earlier fabric representing primary layering and how much was formed during deformation. In the central part of the intrusion, the trend and dip of schistosity vary, but usually planar and linear structures are nearly horizontal. This oldest observed schistosity is cut at a low angle by the shear schistosity of the Osikonmäki shear zone (Fig. 3c).

Outside the main shear zone in the intrusion (Fig. 1) there are discontinuous more narrow shear zones or seams which contain weak sulphide disseminations. In places there is a weak younger schistosity as a crenulation or orientated biotite. Near Lake Kolkonjärvi there is a NW-SE-trending schistosity that belongs to D_3 and a WSW-ENE-trending schistosity belonging perhaps to D_4. The latter is also associated with small sinistral faults with an offset of about 10 cm. In the shear zone there is clear, relatively strong, 20-25° ESE-plunging lineation and in the area of Lake Kolkonjärvi there is a slightly steeper SE-plunging lineation.
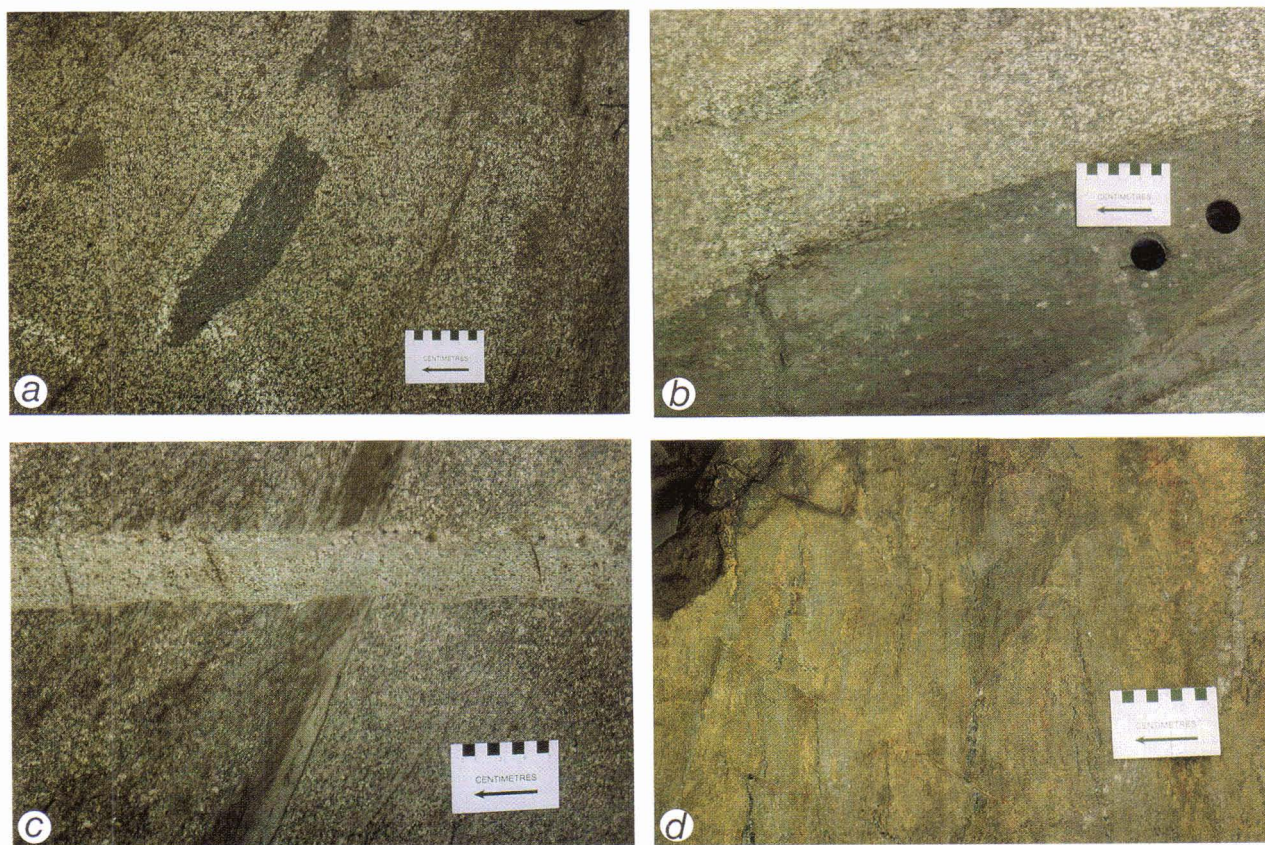
Fig. 3. a) Elongated quartz dioritic or dioritic enclaves in tonalite near the main shear zone, outcrop OMK-86-4. b) Close-up of MME in cataclastic porphyritic tonalite, outcrop OMK-88-15. c) Small-scale shear in outcrop OMK-86-4, with a cross-cutting, younger granite dyke (see text for further details). d) Strongly sheared and mineralized tonalite near the footwall contact of gold mineralization, exploration trench OMK-87-M1. Note the narrow concordant quartz veins. Length of the scale bar is 8 cm.

PETROGRAPHY

The Osikonmäki granitoid intrusion comprises the following structurally and mineralogically distinct units:
- quartz diorite - granodiorite
- mineralized shear zone
- granitic dykes and veins.

Figure 4 and Table 2 show the modal compositions of these units. The rock types plot in the fields of quartz diorite, tonalite, and granodiorite; the more felsic they are, the more quartz they contain. Ore samples contain, on the average, more quartz and K-feldspar than the rocks outside the shear zone.

Fig. 4. Modal compositions of the Osikonmäki granitoid intrusion presented on the QAP diagram of Streckeisen (1974). 500 points counted per thin section. 1 = granitoid, 2 = mineralized shear zone, 3 = granite dyke.
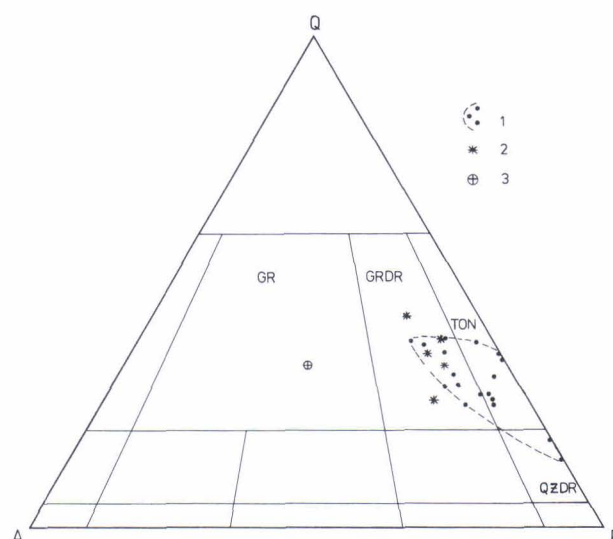
Table 2. Modal compositions of granitoids in the Osikonmäki area.

	n	Plag (%)	Plag An-%	Kfsp (%)	Qz (%)	Biot (%)	Af+Cpx (%)	Acs (%)
OSI[1]	18	37-69	25-35	0-11	12-33	7-20	0-11	1-5
OSI	mean	50.5	5.5	24.2	13.1	3.7	3.0	
ORE[2]	5	38-49	7-14	22-37	7-16		2-8	
GR[3]	1	29.6	30.8	31.4			8.2	

[1] = Osikonmäki granitoid intrusion   [3] = Younger granite dyke
[2] = Mineralized shear zone   n = number of samples

Quartz diorite - granodiorite

Generally these rock types are brownish grey, equigranular and medium-grained, but locally larger (5-10 mm) plagioclase grains give the rock a porphyritic appearance. In the marginal zone, quartz diorite is more strongly foliated than the tonalite or granodiorite of the central part of the intrusion. In places there are light coloured aplite lenses, which could represent felsic dykes deformed along with the granitoid.

Texturally, the slightly deformed tonalite is nearly hypidiomorphic (Figs 5a and b), but is increasingly granoblastic near the shear zone. The textural change is due to cataclastic events in the vicinity of the shear zone and subsequent recrystallization associated with metamorphism. Because of granulation of the hypidiomorphic texture, the rock contains porphyritic features and its texture is thus called here cataclastic porphyritic (Figs 5c and d). In Figures 5a-5d, the original plagioclase grain size can still be seen, even though the edges of the large grains are granulated. Figure 5e shows a totally recrystallized granoblastic granodiorite.

It is possible that the original magmatic mineral assemblage of the rock was: relatively calcic plagioclase + quartz + biotite + hornblende ± K-feldspar (Fig. 5a). The assemblage has been variably altered because of deformation and metamorphism and the principal minerals are now plagioclase (An_{25}-An_{35}), quartz, biotite and occasionally K-feldspar, amphibole and clinopyroxene. The accessory minerals are opaques, titanite, apatite and zircon and alteration products such as sericite, saussurite, chorite, carbonate and epidote.

In plagioclase there is no clearly-defined zoning, but in general, the central part of grains is richer in An than the margin. The central part, particularly, has commonly been saussuritized and sericitized. Quartz and biotite have remained relatively fresh. The amount of secondary quartz increases near the shear zone. In the rock there are a green-blue amphibole (hornblende) and a pale green and fibrous amphibole, the former being primary. Most
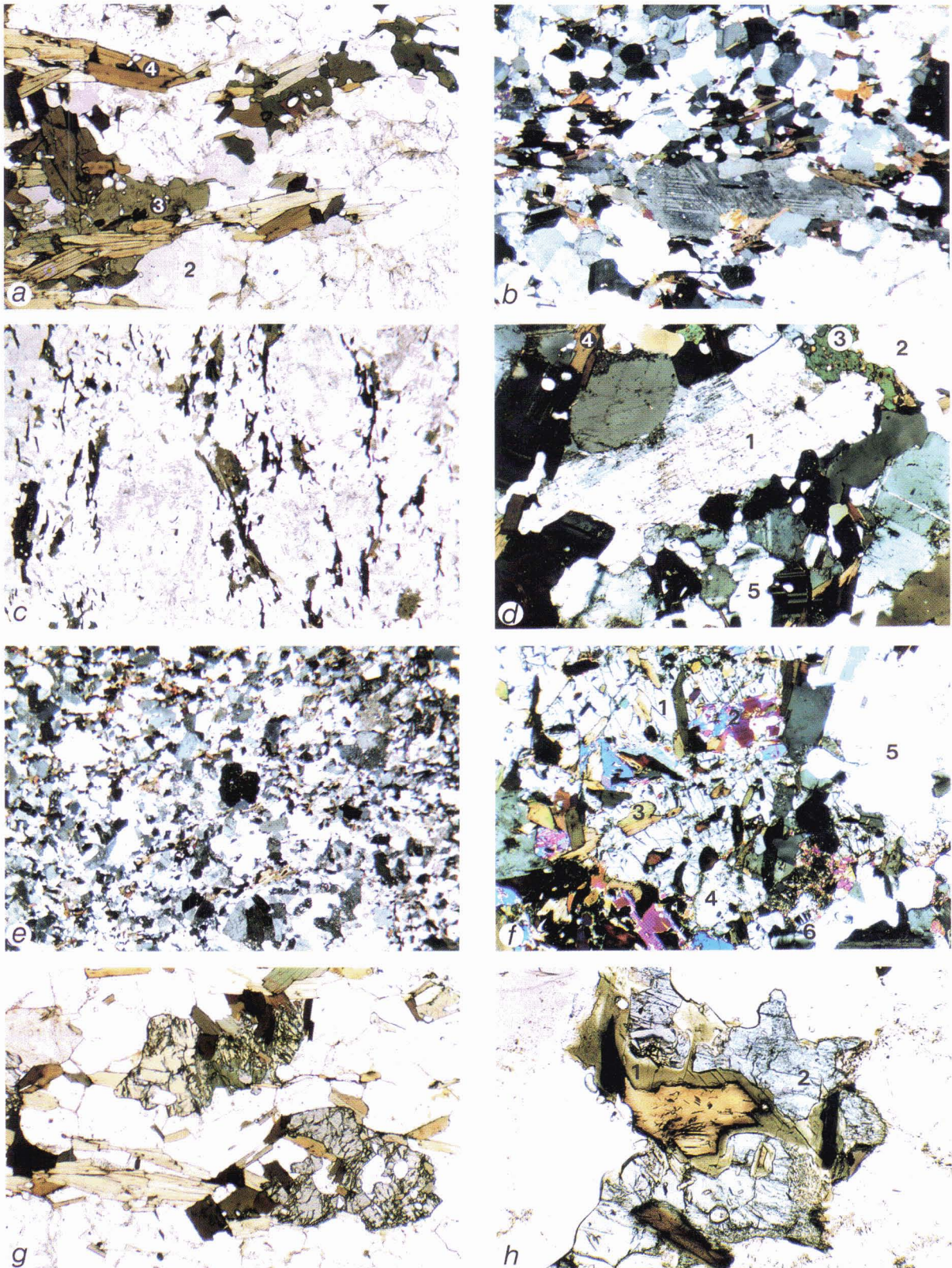
Fig. 5. Photomicrographs from Osikonmäki granitoid intrusion. a) Hypidiomorphic tonalite. 1 = plagioclase, 2 = quartz, 3 = primary amphibole (hornblende), 4 = biotite. 1 polarizer, sample ETK-87-127. Field of view is 4 mm in width. b) Slightly deformed tonalite. Crossed polarizers, sample BH 399/76.30 m. Field of view is 10 mm in width. c) Cataclastic porphyritic tonalite (blastomylonite). 1 polarizer, sample BH 404/104.20 m. Field of view is 16 mm in width. d) The breakdown of plagioclase about to begin in tonalite. 1 = plagioclase, 2 = quartz, 3 = amphibole, 4 = biotite, 5 = K-feldspar. Crossed polarizers, sample BH 468/44.90 m. Field of view is 4 mm in width. e) Totally granoblastic granitoid of the shear zone. Crossed polarizers, sample BH 403/203.90 m. Field of view is 16 mm in width. f) Diopside porphyroblast in metamorphosed granitoid. 1 = diopside, 2 = secondary amphibole, 3 = biotite, 4 = plagioclase, 5 = quartz, 6 = K-feldspar. Crossed polarizers, sample BH 399/76.30 m. Field of view is 4 mm in width. g) Diopside porphyroblasts (high relief) in tonalite. Note the green retrograde amphibole in fractures of diopside. 1 polarizer, sample ETK-87-127. Field of view is 4 mm in width. h) Metamorphic minerals amphibole (1) and diopside (2) around brown biotite. 1 polarizer, sample BH 399/76.30 m. Field of view is 1.6 mm in width.

of the K-felspar (microcline) is secondary, because it occurs as fine-grained "micro-veins" and its amount increases with increased degree of shearing.

Clearly metamorphic clinopyroxene and colourless or pale green amphibole occur throughout the intrusion (Figs 5f-5h). Pyroxene (diopside) grains contain inclusions of other minerals. It appears that the growth of secondary amphibole (actinolite) around biotite preceded poikiloblastic diopside or that amphibole represents a reaction rim between biotite and diopside (Fig. 5h). On the other hand, the secondary amphibole appears to have also crystallized in fractures and fissures of diopside (Fig. 5g). Similar to the other alteration products, these minerals (diopside and amphibole) are more abundant near the shear zones, where plagioclase and hornblende have broken down completely. This indicates that in the fractured rock metamorphic processes have been more efficient. In the shear zone, replacing the earlier presented mineral assemblage (plagioclase + quartz + biotite + hornblende + K-feldspar), there may be plagioclase + quartz + K-feldspar + biotite + actinolite + diopside.

Mineralized shear zone

Based on diamond drillings, the length of the mineralized shear zone is at least 3 km (Fig. 1) and its width varies from a few metres to tens of metres. In general, the zone dips 40-50° to the south, but the trend of both sheared and less sheared units within the zone is complex, especially in its eastern part. During exploration, the name "sheared tonalite" has been used, although mineralogically and structurally more suitable names are granodiorite gneiss and in places quartz-feldspar gneiss.

The cataclastic porphyritic character of tonalite becomes more marked near the shear zone. Figure 3c shows the texture of the shear zone in small scale. The right-handed footwall contact is extremely sharp, but to the left there is a transition from cataclastic porphyritic granitoid to normal
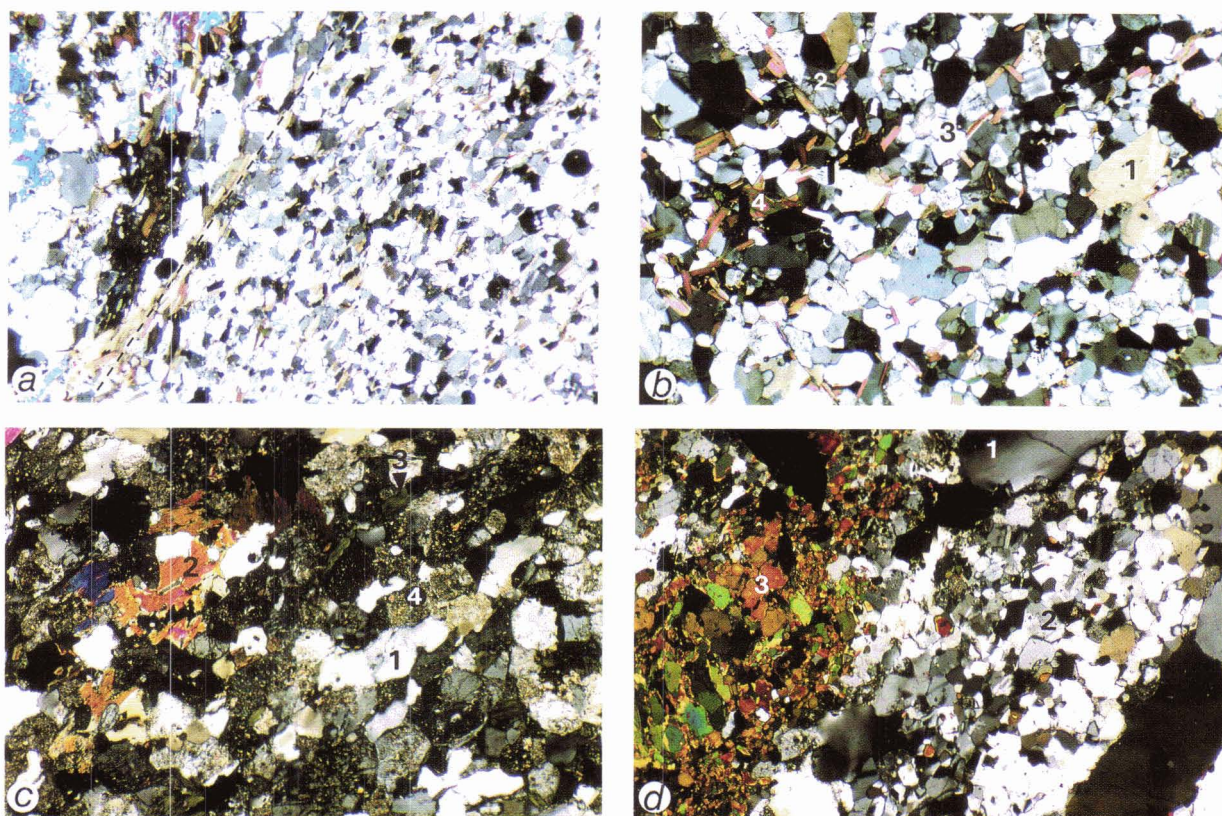
Fig. 6. Photomicrographs from texture and alteration of Osikonmäki granitoid intrusion in the shear zone. a) The contact (dashed line) of cataclastic porphyritic (left) and granoblastic tonalite. Crossed polarizers, sample BH 404/10.80 m. Field of view is 6.4 mm in width. b) Altered granitoid in the eastern part of the shear zone. 1 = quartz, 2 = plagioclase, 3 = K-feldspar, 4 = biotite. Crossed polarizers, sample BH 402/103.90 m. Field of view is 4 mm in width. c) Altered granitoid in the central part of the shear zone. 1 = quartz, 2 = amphibole, 3 = chlorite, 4 = saussuritized plagioclase. Crossed polarizers, sample OMK-88-15. Field of view is 3.7 mm in width. d) Altered granitoid in the western part of the shear zone. 1 = quartz, 2 = K-feldspar, 3 = tourmaline. Crossed polarizers, sample BH 520/143.70 m. Field of view is 3.7 mm in width.

granodiorite. Foliation follows the trend of the shear zone. The shear zone cross cut by younger granite dykes, which are associated with mainly vertical faulting.

The sheared tonalite is fine-grained and usually banded in the direction of the shear foliation. Particularly in the footwall contact there are narrow quartz veins (Fig. 3d) and pegmatite veins parallel to the banding. The sheared tonalite has a granoblastic texture (Fig. 6a). The mineralogy of the sheared host rock varies in different parts of the shear zone depending on the strength of shearing and alteration. Usually, the main minerals are quartz, plagioclase, biotite and K-feldspar with accessory minerals such as opaques, titanite and rutile, apatite and zircon.

Typical mineralogical changes associated with shearing and recrystallization have probably been:

1. at least partial breakdown of calcic plagioclase and hornblende,

2. formation of more albitic plagioclase, sericitization and saussuritization,

3. formation of secondary K-feldspar, biotite and quartz, and

4. formation of ore minerals.

In addition, there are typically diopside and actinolitic amphibole in the shear zone. The crystallization of these minerals is probably associated with regional metamorphism.

The character of alteration varies in different parts of the shear zone. In a sample from the eastern end of the shear zone (Fig. 6b), besides the major rock forming minerals, there is in places also sericite, chlorite and occasional fluorite. In the central part of the shear zone, the original granoblastic quartz-plagioclase-K-feldspar-biotite rock has been further altered, particularly regarding plagioclase and biotite (Fig. 6c). The present assemblage is quartz + K-feldspar + plagioclase + epidote + clorite with secondary accessory sericite, actinolitic amphibole and carbonate. Such alteration is common where there are many vertical fractures younger than the shear zone. Consequently, the alteration is younger than shearing and progressive metamorphism. The sample from the western part represents mineralized rock (Fig. 6d), in which there are quartz-tourmaline dykes and veins associated with shearing and alteration. There are also at least two generations of tourmaline, brown and black, the latter associated with younger crosscutting structures.

Granitic dykes and veins

Minor granitic material in the Osikonmäki area is represented by crosscutting granite dykes (Fig. 3c) and, in the shear zone, by pegmatite veins mostly with the same trend as the shear schistosity. The dykes are medium-grained and equigranular and range in width from 10 cm to several metres. Their colour varies from pale grey to a reddish grey, and close to the mineralized zone the colour of K-feldspar is mostly grey. The tonalite outside the shear zone has been granodioritized only in the surroundings of the reddish granite. The granites have a hypidiomorphic texture and show no clear fabric. The main minerals are quartz, K-feldspar and albitic plagioclase, and occasionally muscovite. Typical accessory minerals are biotite, apatite and zircon, but particularly in the granites of the shear zone there are also ore minerals such as pyrrhotite, pyrite, arsenopyrite and graphite as well as titanite and rutile.

GEOCHEMISTY

From the Osikonmäki rocks, a total of 123 wholerock analyses was made, most of them (82) representing the sheared and mineralized tonalite. Table 3 and Appendices 1 and 2 include only those samples that represent either unmineralized tonalite or clearly mineralized (Au content above 0.5 ppm) shear zone granitoid.

Major elements

The rocks of the Osikonmäki intrusion and the mineralized shear zone differ from each other in their alkali and alkali earth metal contents. In the mineralized rock there is less Mg, Ca and Na, but more K than in the unmineralized country rock. Figure 7 illustrates the enrichment and depletion of elements in the ore relative to the country rock.

Figure 8 shows how in unmineralized rock of

Table 3. Average chemical composition of the Osikonmäki intrusion (oxides are given as wt-%, Sb, Te, Se, Bi and Au as ppb and other trace elements as ppm). The values below the detection limit are replaced by 0. For comparison, column 3 gives values for I-type granites in the Lachlan Fold Belt, Australia (Chappell and White 1992).

	1 (n = 36)			2 (n = 19)			3 (n = 1074)
	mean	min.	max.	mean	min.	max.	mean
SiO_2	65.7	59.23	68.13	66.6	63.19	72.10	69.50
FeO_t	3.9	2.81	5.61	4.1	3.05	6.12	3.12
Al_2O_3	15.9	14.79	17.30	15.8	13.46	17.59	14.21
MgO	1.8	1.25	2.66	0.9	0.00	1.73	1.38
CaO	3.5	2.54	5.09	2.6	1.11	3.39	3.07
Na_2O	4.5	3.71	5.59	3.1	0.63	4.66	3.16
K_2O	2.3	0.99	3.12	3.2	1.96	5.59	3.48
TiO_2	0.6	0.39	1.03	0.5	0.31	0.54	0.41
MnO	0.1	0.05	0.11	0.1	0.03	0.09	0.07
P_2O_5	0.2	0.11	0.37	0.2	0.13	0.20	0.11
H_2O_t	0.7	0.44	1.23	0.9	0.21	1.89	
Sum	99.2			98.0			98.51
A/CNK	0.98			1.19			0.97
S	335	20	4170	12400	7900	19800	
As	35	0	530	12400	546	42331	
Rb	80	30	190	123	92	189	164
Sr	492	270	760	333	102	648	235
Zr	190	140	290	174	123	203	150
Ba	551	280	970	359	246	528	519
V	90	60	170	76	51	90	57
Cu	26	2	157	161	20	421	9
Zn	54	24	106	68	41	134	48
Pb	11	4	22	67	24	165	19
Sb				3000	40	13050	
Te	1	0	11	441	0	1830	
Se	17	0	280	21200	290	69820	
Bi	61	0	950	1550	0	7900	
Au	9	0	139	2780	600	6300	

1. Osikonmäki granitoid intrusion
2. Mineralized host rock from the Osikonmäki shear zone
3. I-type granites from the Lachlan Fold Belt
n = number of analyses

A/CNK = mol. $Al_2O_3/(CaO+Na_2O+K_2O)$
FeO_t = total Fe as FeO
H_2O_t = total water as H_2O

Osikonmäki intrusion, the trends of components related to mafic minerals (i.e. Mg, Fe, Ca, P and Ti) decrease with increasing SiO_2-content. Also, the trends of K and Al slightly decrease, while Na concentrations have no clear trend as a function of SiO_2. Thus, the falling trend of K_2O may indicate that the main carrier of K is biotite or that part of the potassium is derived from an external granitic fluid. The variation of the K/Na ratio as a function of SiO_2 also supports the latter alternative. Because the mineralized samples follow the same trend (not shown) as the samples from unmineralized rock, it is possible that the K/Na ratio reflects the alteration of the granitoid.

In general, there is no compositional gaps of elements in the Harker diagrams of Figure 8 and, thus, the geochemistry also reflects the lack of clear phase contacts in the Osikonmäki intrusion. Overall, major element data suggest that the rocks of the Osikonmäki intrusion were produced by fractional crystallization. The granodioritization of the tonalite in the surroundings of the reddish granite may be reflected on the declining concentrations of K as a function of SiO_2.
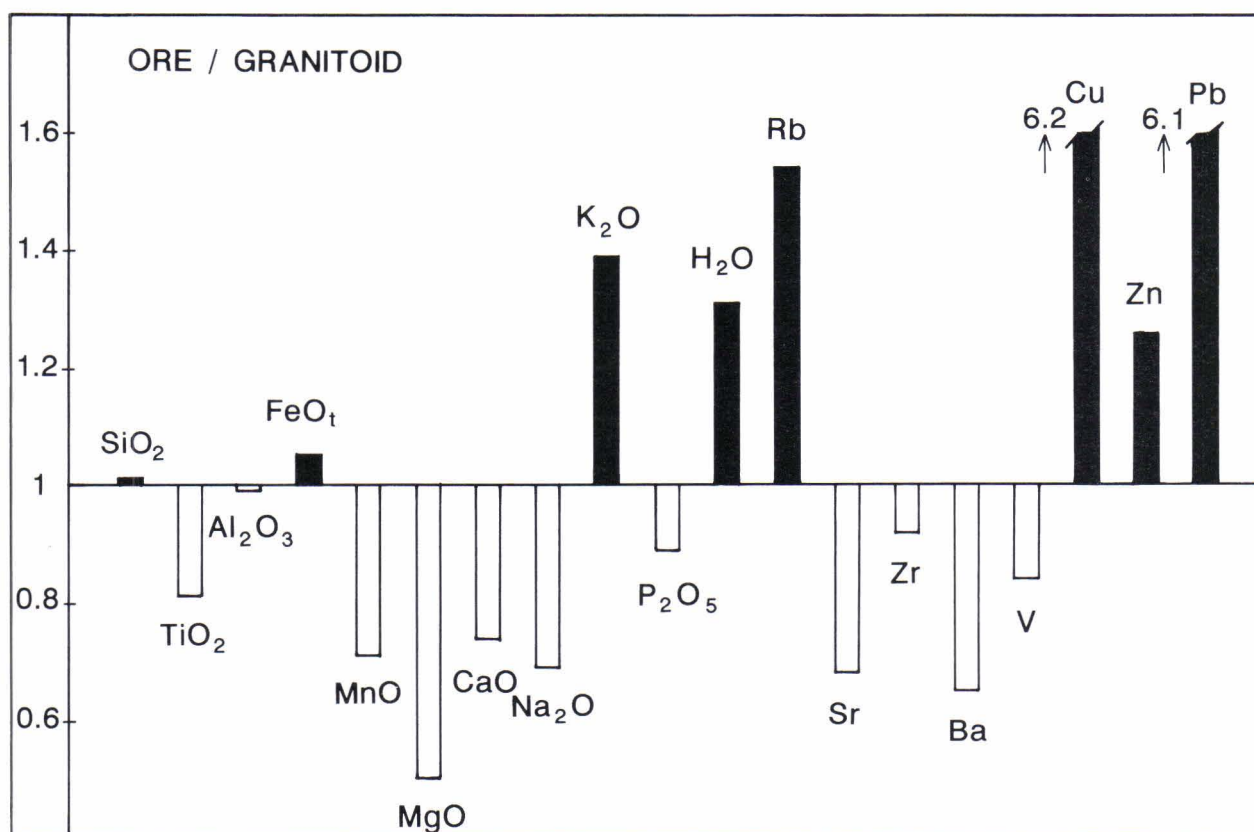
Fig. 7. Trends of enrichment and depletion of certain oxides and elements in the ore presented as ratios between concentrations in ore and unmineralized host rock. Same data as in Table 4.

Trace elements

Where possible, the analyzed samples from the intrusion were taken from unmineralized rock. However, trace element concentrations (Table 3) indicate that some samples contain a little pyrrhotite and arsenopyrite. Figure 9 presents variation diagrams for certain trace elements as well as major and trace element relations.

The declining concentrations of Mg, Fe, Ca, Ti and P (Fig. 8) and Ba and Zr (Fig. 9) with increasing SiO_2-content indicate fractional crystallization of plagioclase, biotite, hornblende, Fe-Ti-minerals, apatite and zircon. The behaviour of Sr is more complex. Figure 9 shows a gently declin-

ing trend, which would appear to indicate that Sr is bound to biotite. However, at > 65 % SiO_2 the rocks show higher Sr concentrations. This may be due to the crystallization of K-feldspar or indicate that the pattern is a combined result of fractional crystallization and alteration.

Falling K/Rb and increasing Rb/Sr ratios appear to indicate that the principal fractionating mineral concerning the elements in question has been K-feldspar (Rämö 1991). In the Osikonmäki case such trends do not exist (Fig. 9) and the principal mineral controlling the partitioning of these metals has probably been biotite.
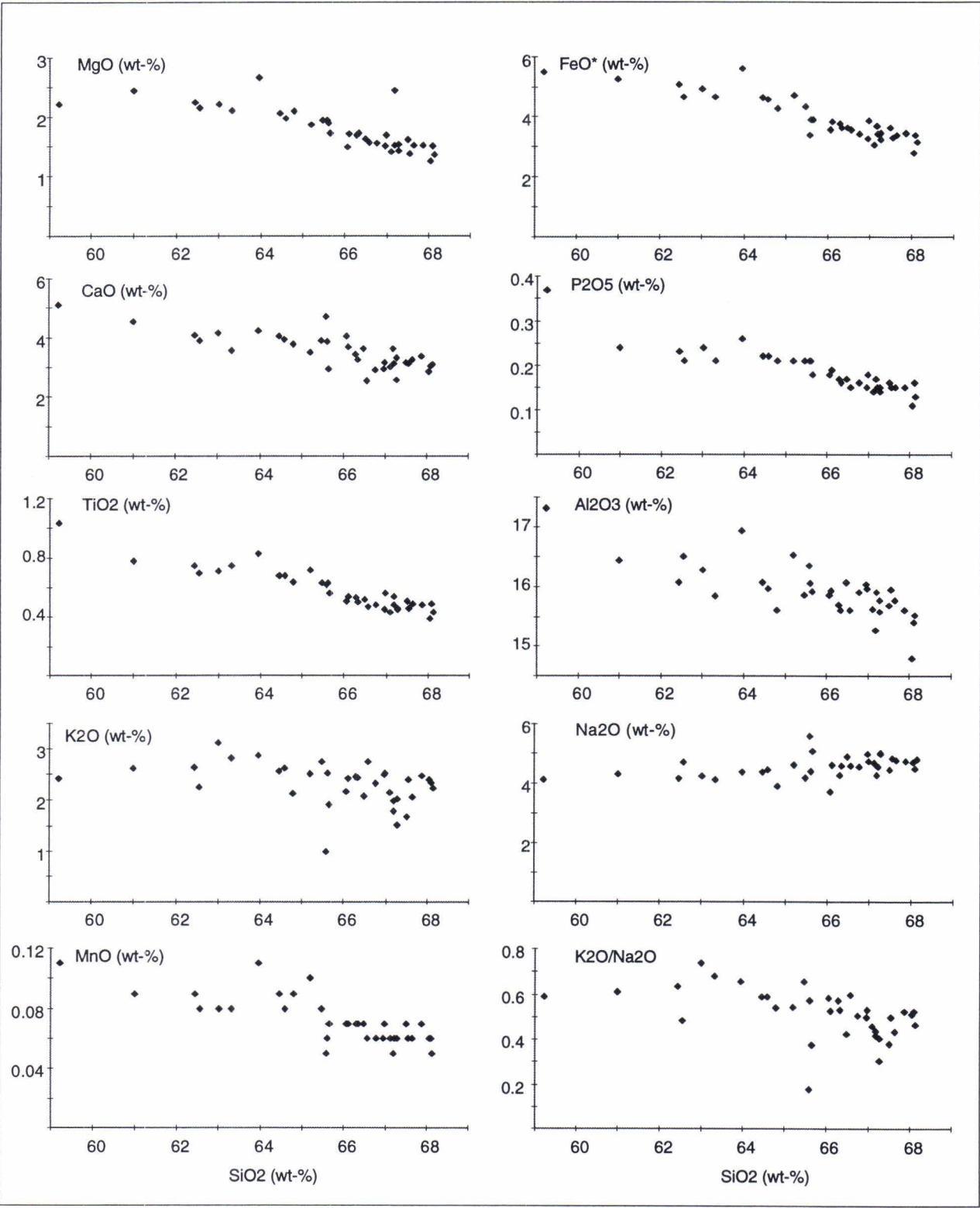
Fig. 8. Major element Harker diagrams for unmineralized Osikonmäki granitoid intrusion (36 analyses, App. 1). FeO* = total Fe as FeO.
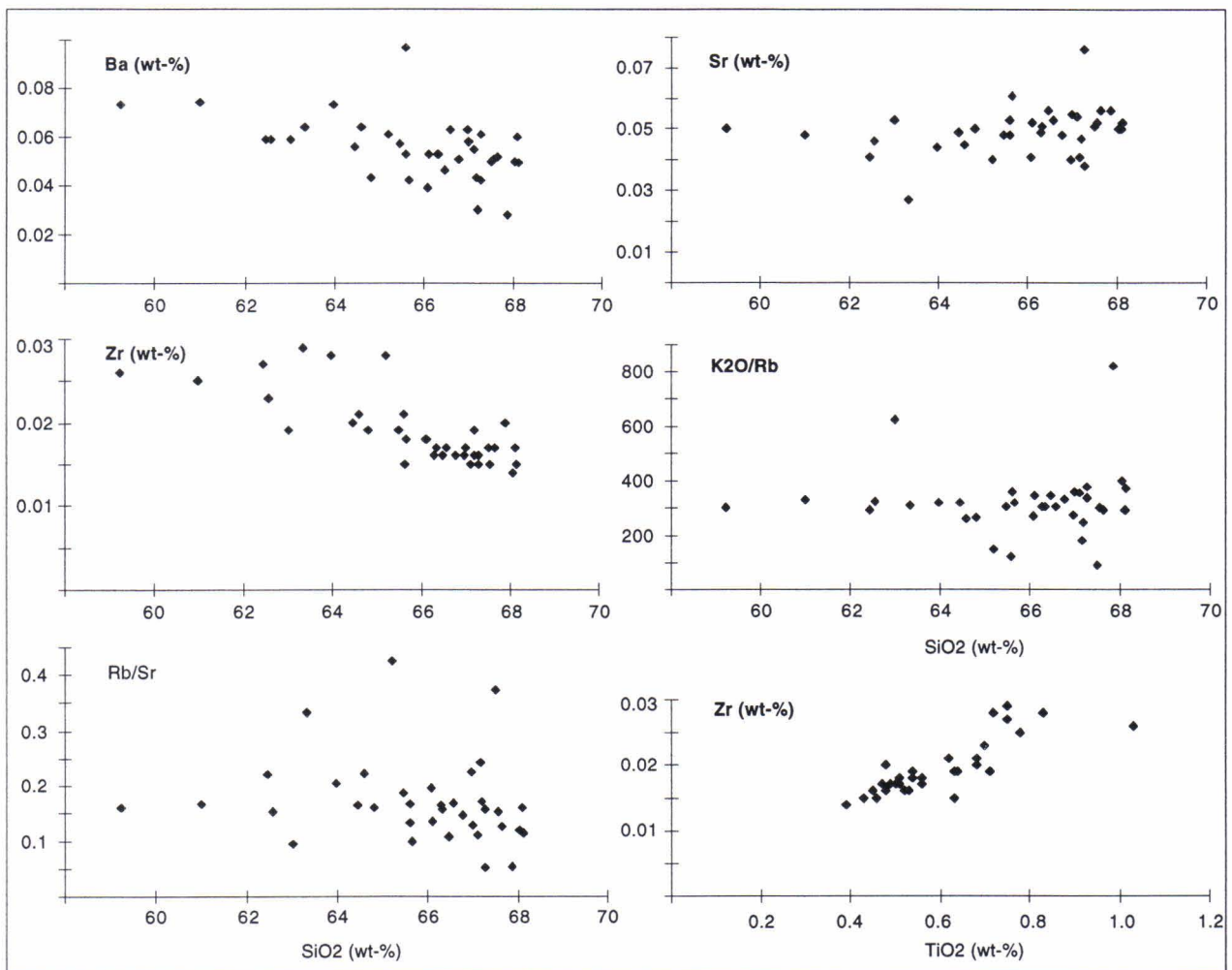
Fig. 9. Trace element Harker diagrams for unmineralized Osikonmäki granitoid intrusion (36 analyses, App. 2A).

Areal distribution of elements in the Osikonmäki intrusion

The Osikonmäki intrusion is unevenly exposed and, thus, the sample coverage is limited. However, the areal distribution of elements seems to follow a certain pattern and particular rules and also matches with field observations (Fig. 1). Metals bound to mafic minerals are enriched at the granitoid's margin and the enrichment is strongest in the northern, northwestern and western parts. Figure 10 shows, for example, the areal distributions of Fe, Ca and Ti, as well as K. Also here, the amount of K does not appear to simply illustrate the amount of K-feldspar but also that of biotite, because in part the higher K_2O concentrations occur in the quartz diorite area

(cf. Fig. 1).

Regarding trace elements, the distribution of Zr and Sr in the Osikonmäki granitoid intrusion is given as an example (Fig. 10). Zr has most probably been bound to zircon during crystallization, and thus its distribution is similar to that of elements (for example Fe) bound to mafic minerals. The distribution of Sr is more distinct than that of K. Probably, the distribution of Sr illustrates better than that of K the amount of K-feldspar in the Osikonmäki intrusion.
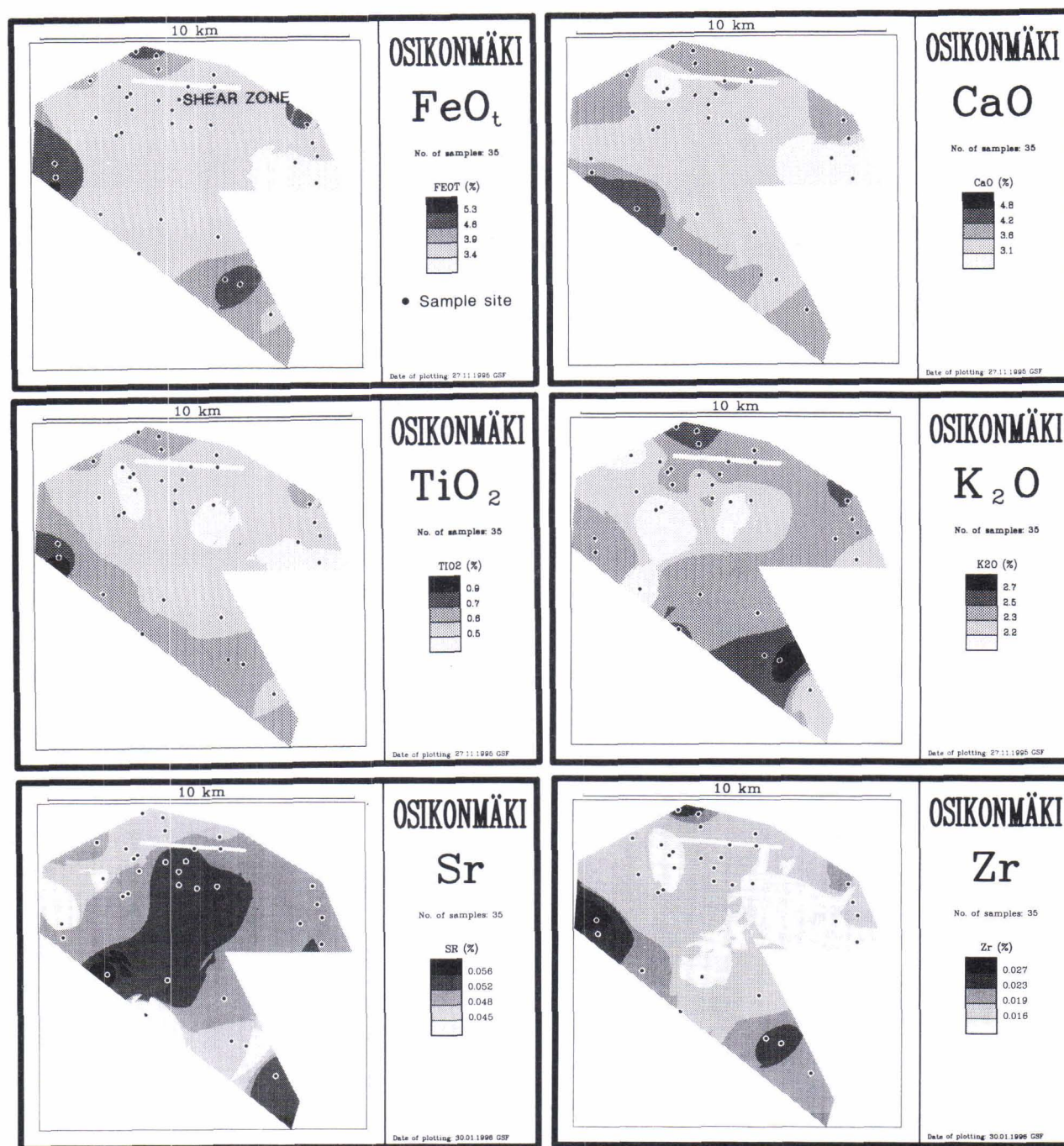
Fig. 10. Areal distribution of certain elements in the Osikonmäki granitoid intrusion. The maps are made by smoothing the original data (App. 1 and 2A) with GSF's ALKEMIA package. The smoothing area is circle with a radius of 3.5 km. In the SE-corner, the sample density is too small (one sample, ETK-87-140.1) for smoothing.

PETROGENESIS

It has been proposed that tonalitic granitoid magmas may originate either from mantle-derived tholeiitic magma by fractional crystallization (e.g. Condie and McCrink 1982), or by mixing of hot mantle magma and granitic magma formed by re-melting of the lower crust (e.g. Hyndman and Foster 1988), or by partial melting of a subducting oceanic slab (MORB) with subsequent crustal as-

similation (e.g. Defant et al. 1988).

Petrogenetically, Nurmi et al. (1984) classify the Svekokarelian synorogenic granitoids as having features of Phanerozoic I-type granitoids, which occur, for example, in an Andino-type plate tectonic setting. The tonalites form by the differentiation of tholeiitic basaltic mantle-derived magma, while granodiorites form by hybridization of man-

Table 4. Median compositions of specific synkinematic granitoids (tonalites) in Finland (Nurmi 1984). Oxides are given as wt-% and trace elements as ppm. N is the number of samples analyzed.

	1.	2.	3.	4.	5.	6.	7.	8.
n	27	3	45	18	4	10	7	15
SiO_2	61.7	62.0	65.5	65.6	66.9	61.7	64.0	66.8
TiO_2	0.48	0.43	0.34	0.32	0.31	0.34	0.38	0.24
Al_2O_3	15.3	17.4	16.7	17.7	17.4	16.4	15.7	16.8
FeO^*	4.2	5.6	4.0	3.6	3.5	5.3	3.8	3.2
MgO	3.8	3.4	2.7	2.4	2.6	2.4	3.7	1.3
CaO	3.7	5.2	3.7	4.1	3.9	5.2	3.2	4.6
Na_2O	3.7	3.8	3.6	3.9	3.7	2.5	4.3	4.0
K_2O	2.1	1.2	1.9	1.6	1.6	1.7	2.7	1.0
P_2O_5	0.18	0.15	0.11	0.13	0.12	0.11	0.39	0.10
Sum	95.2	99.2	98.6	99.4	100.0	95.7	98.2	98.0
A/CNK	1.02	1.02	1.14	1.14	1.17	1.07	0.99	1.05
Rb	76	27	41	37	46	65	79	35
Sr	690	530	490	600	570	290	780	530
Ba	530	420	630	540	590	450	620	590

1. Tonalite from Käkövesi batholith, Puumala
2. Hornblende tonalite from Tienpää tonalite complex, Halsua
3. Porphyritic tonalite, Tienpää
4. Equigranular tonalite, Tienpää
5. Tonalite porphyry, Tienpää
6. Tonalite porphyry from Kopsa stock, Haapajärvi

7. Tonalite from Salosaari stock, Ruokolahti
8. Tonalite from Silvola stock, Savonlinna.
FeO^* = Total Fe as FeO
A/CNK = mol. $Al_2O_3/(CaO+Na_2O+K_2O)$
n = number of analyses

tle-derived magmas and crustal melts (Nurmi et al. 1984, Nurmi and Haapala 1986). Nironen (1989) proposes that the synkinematic tonalites crystallized from magma that formed by mixing and mingling from crustal magma and either from mantle-derived magma, or from partial melts of a subducting oceanic slab.

The Osikonmäki analytical material has further been examined using petrogenetic discrimination diagrams (Fig. 11) and compared to certain synkinematic granitoids in the Ladoga - Bothnian Bay Zone (Table 4) (Nurmi 1984).

Figure 11 shows that the Osikonmäki intrusion is calc-alkaline (11 D and F), subalkaline (11 G) and I-type (11 B and C), and is metaluminous to slightly peraluminous (11 B) and its $FeO^*/(FeO^*+MgO)$ ratio is less than 0.8 in all samples (11 A). In Barbarin's (1990) classification (Fig. 2) the Osikonmäki intrusion's chemical and mineralogical features (hornblende + titanite) best fit the H_{CA}-type and in part also the C_{CI}-type. Examples of the former type are the Sierra Nevada and Andean batholiths and the granitoids of the Limousine tonalite zone in France (Barbarin 1990).

The tectonomagmatic classification scheme of Pearce et al. (1984) could not be used for the Osikonmäki data, because the required trace element analyses were too inaccurate or nonexistent. In classification of the Erzgebirge granites, Tischendorf and Förster (1990) have nevertheless adapted this classification terminology and principles for Ba-Rb-Sr diagram. In this diagram (Fig. 11 E), the Osikonmäki samples plot mainly in the field of volcanic arc granites and oceanic ridge granites (VAG+ORG).

The tectonomagmatic diagram developed by Batchelor and Bowden (1985) (Fig. 11 H) is based on the chemistry of tectonically-defined granitoids and on the R1-R2 multicationic diagram of de la Roche et al. (1980). In this diagram, the Osikonmäki data plot in groups 2 and 3 which represent collision zone calc-alkaline granitoids.

Compared to the reference material (Table 4, outlined field in Fig. 11) the Osikonmäki granitoid intrusion is more clearly I-type, slightly more alkaline, more iron-rich and the Na/K ratio in it is higher than in the comparison material. It is possible that the composition of the parental magma for the Osikonmäki intrusion was slightly more felsic and that contamination by crustal materials had been less than in the reference intrusions.

Chemical composition suggests that the Osikonmäki synkinematic granitoid intrusion fractionated from a calc-alkaline magma in a collision zone. Lower-crustal melts from a thickened crust were probably mixed with mantle-derived magma and/or magma produced by partial melting of a subducting oceanic slab.

Because mafic microgranular enclaves (MME) occur in the intrusion, hybridization associated with the magmatic evolution of the granitoid intrusion was mainly mechanical (mingling). The granitoid pluton, intruded as a conformable or sill-like body into the upper part of the crust in a
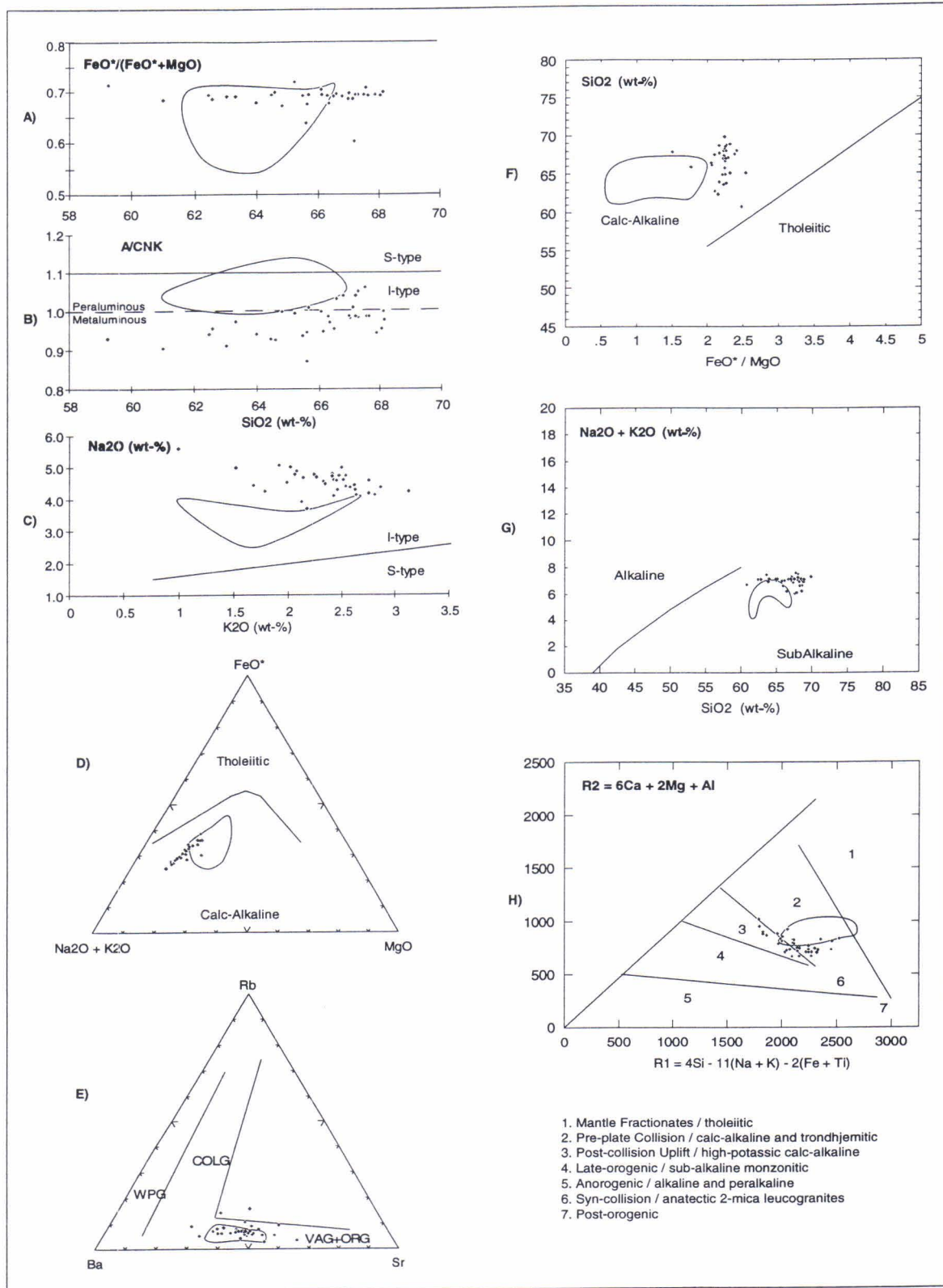
Fig. 11. Analytical data from the Osikonmäki granitoid intrusion (dots) presented in certain petrogenetic discrimination diagrams. The solid outlined area represents the median compositions of specific synkinematic granitoids given in Table 4. FeO* = total Fe as FeO. A) Fe index versus SiO_2 diagram. Solid line FeO*/(FeO*+MgO) = 0.8 after Barbarin (1990). B) Mol. $Al_2O_3/(CaO+Na_2O+K_2O)$ versus SiO_2 diagram. Fieds for S-type and I-type granitoids after White and Chappell (1983) and peraluminous/metaluminous line after Zen (1986). C) Na_2O versus K_2O diagram. Fields for S-type and I-type granitoids after Chappell and White (1974). D) AFM diagram separating tholeiitic and calc-alkaline fields with solid line after Irvine and Baragar (1971). E) Tectonomagmatic classification scheme of Pearce et al. (1984) adapted to Ba-Rb-Sr diagram. Granite fields after Tischendorf and Förster (1990). F) SiO_2 versus FeO*/MgO ratio diagram. Tholeiitic and calc-alkaline fields after Miyashiro (1974). G) Na_2O+K_2O versus SiO_2 diagram. Alkaline and subalkaline fields after Irvine and Baragar (1971). H) R1-R2 multicationic diagram of de la Roche et al. (1980). Tectonomagmatic fields (1 - 7) after Batchelor and Bowden (1985).

compressional regime and was deformed together with the supracrustal rocks that now flank the

intrusion.

ACKNOWLEDGEMENTS

REFERENCES

Barbarin, B. 1990. Granitoids: main petrogenetic classifications in relation to origin and tectonic setting. Geological Journal 25 (3-4), 227-238.

Barbarin, B. & Didier, J. 1992. Genesis and evolution of mafic microgranular enclaves through various types of interaction between coexisting felsic and mafic magmas. Transactions of the Royal Society of Edinburgh: Earth Sciences 83 (1-2), 145-153.

Batchelor, R.A. & Bowden, P. 1985. Petrogenetic interpretation of granitoid rock series using multicationic parameters. Chemical Geology 48, 43-55.

Castro, A., Moreno-Ventas, I. & de la Rosa, J.D. 1990. Microgranular enclaves as indicators of hybridization processes in granitoid rocks, Hercynian Belt, Spain. Geological Journal 25 (3-4), 391-404.

Chappell, B.W. & White, A.J.R. 1974. Two contrasting granite types. Pacific Geology 8, 173-174.

Chappell, B.W. & White, A.J.R. 1992. I- and S-type granites in the Lachlan Fold Belt. Transactions of the Royal Society of Edinburgh: Earth Sciences 83 (1-2), 1-26.

Condie, K.C. & McCrink, T.P. 1982. Geochemistry of Proterozoic volcanic and granitic rocks from the Gold Hill-Wheeler Peak area, northern New Mexico. Precambrian Research 19, 141-166.

Defant, M.J., Drummond, M.S., Arthur, J.D. & Ragland, P.C. 1988. An example of trondhjemite petrogenesis: the Blakes Ferry pluton, Alabama. U.S.A. Lithos 21, 161-181.

Gaál, G. 1986. 2200 million years of crustal evolution: The Baltic shield. Bulletin of the Geological Society of Finland 58, 149-168.

Hyndman, D.W. & Foster, D.A. 1988. The role of tonalites and mafic dikes in the generation of Idaho batholith. Journal of Geology 96, 31-46.

Irvine, T.N. & Baragar, W.R.A. 1971. A guide to the classification of the common volcanic rocks. Canadian Journal of Earth Sciences 8, 523-548.

Kontoniemi, O. 1998. An overview of the geology in the Osikonmäki area, Rantasalmi, southeastern Finland: Especially as a promising environment for epigenetic gold mineralization. In: Kontoniemi, O. & Nurmi, P.A. (eds.) Geological setting and characteristics of the tonalite-hosted Paleoproterozoic gold deposit at Osikonmäki, Rantasalmi, southeastern Finland. Geological Survey of Finland, Special Paper 25, 7-18.

Kontoniemi, O. & Ekdahl, E. 1990. Tonalite-hosted early Proterozoic gold deposit at Osikonmäki, southeastern Finland. Bulletin of Geological Society of Finland 62, 61-70.

Miyashiro, A. 1974. Volcanic rock series in island arcs and active continental margins. American Journal of Science 274, 321-355.

Nironen, M. 1989. Emplacement and structural setting of granitoids in the early Proterozoic Tampere and Savo Schist Belts, Finland - implications for contrasting crustal evolution. Geological Survey of Finland, Bulletin 346. 83 p.

Nurmi, P.A. 1984. Applications of lithogeochemistry in the search for Proterozoic porphyry-type molybdenum, copper and gold deposits, southern Finland. Geological Survey of Finland, Bulletin 329. 40 p.

Nurmi, P.A., Front, K., Lampi, E. & Nironen, M. 1984. Etelä-Suomen svekokarjalaiset porfyyrityyppiset molybdeeni- ja kupariesiintymät, niiden granitoidi-isäntäkivet ja litogeokemiallinen etsintä. Summary: Svecokarelian porphyry-type molybdenum and copper occurrences in southern Finland: their granitoid host rocks and lithogeochemical exploration. Geological Survey of Finland, Report of Investigation 67. 88 p.

Nurmi, P.A. & Haapala, I. 1986. The Proterozoic granitoids of Finland: Granite types, metallogeny and relation to crustal evolution. Bulletin of Geological Society of Finland 58, 203-233.

Pearce, J.A., Harris, N.B.W. & Tindle, A.G. 1984. Trace element discrimination diagrams for the tectonic interpretation of granitic rocks. Journal of Petrology 25, 956-983.

Rämö, O.T. 1991. Petrogenesis of the Proterozoic rapakivi granites and related basic rocks of southeastern Fennoscandia: Nd and Pb isotopic and general geochemical constraints. Geological Survey of Finland, Bulletin 355. 161 p.

De la Roche, H., Leterrier, J., Granclaude, P. & Marchal, M. 1980. A classification of volcanic and plutonic rocks using R1R2-diagram and major-element analyses - its relationships with current nomenclature. Chemical Geology 29, 183-210.

Streckeisen, A.L. 1974. Classification and nomenclature of igneous rocks. Geologische Rundschau 63, 773-786.

Tischendorf, G. & Förster, H-J. 1990. Acid magmatism and related metallogenesis in the Erzgebirge. Geological Journal 25 (3-4), 443-454.

Vaasjoki, M. & Kontoniemi, O. 1991. Isotopic studies from the Proterozoic Osikonmäki gold prospect at Rantasalmi, southeastern Finland. In: Autio, Sini (ed.) Geological Survey of Finland, Current Research 1989-1990. Geological Survey of Finland, Special Paper 12, 53-57.

Vernon, R.H., Etheridge, M.A. & Wall, V.J. 1988. Shape and microstructure of microgranitoid enclaves: indicators of magma mingling and flow. Lithos 22, 1-11.

White, A.J.R. & Chappell, B.W. 1983. Granitoid types and their distribution in the Lachlan Fold Belt, southeastern Australia. Geological Society of America, Memoir 159, 21-34.

Zen, E-an 1986. Aluminium enrichment in silicate melts by fractional crystallization: Some mineralogic and petrographic constraints. Journal of Petrology 27, 1095-1117.

Appendix 1. Major element data (as wt-%) for Osikonmäki granitoid intrusion.
N = 55. FeO_t: total Fe as FeO. H_2O_t = total water as H_2O.

Sample	S	SiO_2	FeO_t	Al_2O_3	MgO	CaO	Na_2O	K_2O	TiO_2	MnO	P_2O_5	H_2O_t
OMK-86-14.3	+	66.29	3.76	15.71	1.68	3.44	4.28	2.45	0.53	0.07	0.17	0.57
OMK-86-34.1	+	63.96	5.61	16.94	2.66	4.24	4.37	2.86	0.83	0.11	0.26	1.19
OMK-86-49.1	+	66.99	3.85	15.97	1.68	3.17	4.74	2.53	0.56	0.07	0.18	0.78
OMK-86-51.1	+	66.11	3.83	15.94	1.70	3.67	4.60	2.42	0.54	0.07	0.19	0.57
OMK-86-63.1	+	62.56	4.68	16.51	2.15	3.90	4.70	2.26	0.70	0.08	0.21	0.72
OMK-86-85.1	+	60.99	5.25	16.44	2.44	4.56	4.30	2.62	0.78	0.09	0.24	0.71
OMK-86-89.1	+	65.47	4.36	15.87	1.94	3.91	4.19	2.75	0.63	0.08	0.21	0.68
OMK-86-105.1	+	67.27	3.23	15.58	1.43	3.30	4.99	1.52	0.46	0.06	0.15	0.61
OMK-86-109.1	+	67.55	3.31	15.96	1.37	3.13	4.81	2.40	0.46	0.06	0.15	0.47
OMK-86-139.1	+	66.77	3.44	15.91	1.54	2.91	4.56	2.32	0.48	0.06	0.16	0.77
OMK-86-140.1	+	67.28	3.46	15.78	1.53	2.56	5.01	2.02	0.45	0.06	0.14	0.77
OMK-86-143.1	+	66.07	3.55	15.87	1.49	4.06	3.71	2.17	0.51	0.07	0.18	0.63
OMK-86-147.1	+	62.45	5.08	16.07	2.24	4.09	4.13	2.63	0.75	0.09	0.23	0.63
OMK-86-153.1	+	67.11	3.06	15.63	1.41	3.01	4.66	2.14	0.43	0.06	0.14	0.66
OMK-86-155.3	+	67.20	3.41	15.91	1.51	3.13	4.54	1.98	0.48	0.06	0.15	0.73
OMK-86-156.1	+	66.57	3.55	15.62	1.56	2.54	4.59	2.75	0.47	0.06	0.15	0.64
OMK-86-162.1	+	64.45	4.62	16.08	2.05	4.05	4.37	2.57	0.68	0.09	0.22	0.78
OMK-86-165.1	+	68.10	3.40	15.40	1.50	3.02	4.47	2.34	0.49	0.06	0.16	0.62
OMK-86-182.1	+	66.48	3.63	16.07	1.63	3.63	4.89	2.07	0.52	0.07	0.17	0.62
OMK-86-188.1	+	68.13	3.16	15.53	1.36	3.10	4.78	2.23	0.43	0.05	0.13	0.52
OMK-86-190.1	+	68.05	2.81	14.79	1.25	2.85	4.71	2.40	0.39	0.06	0.11	0.44
OMK-86-191.1	+	64.80	4.27	15.62	2.08	3.76	3.91	2.12	0.64	0.09	0.21	1.23
OMK-86-197.1	+	59.23	5.50	17.30	2.21	5.09	4.10	2.42	1.03	0.11	0.37	1.01
OMK-86-200.1	+	65.20	4.73	16.53	1.86	3.48	4.61	2.51	0.72	0.10	0.21	0.66
OMK-87-7.1	+	63.32	4.68	15.85	2.11	3.56	4.12	2.81	0.75	0.08	0.21	0.65
OMK-87-10.1	+	64.59	4.57	15.97	1.97	3.92	4.44	2.61	0.68	0.08	0.22	0.47
OMK-87-16.1	+	66.34	3.62	15.61	1.72	3.24	4.59	2.44	0.50	0.07	0.16	0.70
OMK-88-10.1	+	66.96	3.27	16.04	1.50	2.94	4.98	2.49	0.45	0.06	0.15	0.52
OMK-88-11.1	+	67.50	3.64	15.69	1.61	3.16	4.44	1.68	0.51	0.07	0.16	0.59
OMK-88-13.1	+	67.64	3.40	15.77	1.51	3.26	4.77	2.06	0.49	0.06	0.15	0.66
OMK-88-14.1	+	65.66	3.90	15.93	1.72	2.95	5.07	1.91	0.56	0.07	0.18	0.74
ETK-87-140.1	+	63.01	4.93	16.28	2.21	4.15	4.23	3.12	0.71	0.08	0.24	0.68
ETK-87-152.1	+	67.18	3.67	15.27	2.44	3.61	4.26	1.78	0.54	0.05	0.17	0.78
ETK-87-222.1	+	65.61	3.90	16.06	1.88	3.86	4.40	2.53	0.63	0.06	0.21	0.60
ETK-87-227.1	+	67.87	3.45	15.62	1.52	3.37	4.73	2.47	0.48	0.07	0.15	0.56
ETK-87-229.1	+	65.59	3.40	16.36	1.93	4.71	5.59	0.99	0.62	0.05	0.21	0.67
BH 460												
/45.00-46.00	*	71.46	3.39	13.98	1.56	2.80	0.74	3.53	0.46	0.087	0.166	1.48
/46.00-47.00	*	69.51	3.56	15.13	0.97	2.58	0.72	4.34	0.49	0.077	0.184	1.34
/47.00-48.00	*	72.10	3.29	14.93	0.79	1.11	0.63	4.14	0.46	0.071	0.176	1.35
/58.50-59.50	*	65.09	3.64	16.79	0.89	2.30	2.49	5.59	0.53	0.079	0.196	0.94
/59.50-60.50	*	67.73	3.44	15.67	1.01	2.64	2.85	3.81	0.51	0.093	0.191	0.80
/60.50-61.50	*	68.40	3.05	15.43	1.08	2.30	2.63	4.43	0.51	0.082	0.190	1.40
BH 464												
/135.00-136.00	*	65.42	4.45	16.88	1.42	2.79	4.66	2.30	0.48	0.042	0.162	0.64
/136.00-137.00	*	65.69	3.99	17.05	1.66	3.25	4.35	2.11	0.54	0.047	0.184	0.51
/137.00-138.00	*	63.40	5.17	16.60	0.61	3.39	4.28	1.97	0.51	0.038	0.178	0.41
/138.00-139.00	*	63.61	5.00	16.37	0.08	3.19	4.16	2.34	0.48	0.033	0.175	0.42
/141.00-142.00	*	70.38	3.30	14.16	0.52	2.70	3.29	2.58	0.40	0.037	0.140	0.21
/142.00-143.00	*	69.72	3.13	14.31	0.00	1.96	2.92	1.96	0.31	0.029	0.134	0.28
/147.00-148.00	*	65.26	3.60	16.98	1.10	2.97	4.01	3.32	0.49	0.042	0.176	0.78
/148.00-149.00	*	65.11	3.80	16.83	0.62	2.90	4.14	2.90	0.48	0.041	0.180	0.57
BH 478												
/57.00-58.00	*	64.70	4.28	17.37	1.73	3.28	4.26	2.23	0.53	0.051	0.194	1.48
/58.00-59.00	*	63.83	4.78	17.59	1.72	2.06	3.84	3.66	0.51	0.042	0.193	1.89
/59.00-60.00	*	63.19	5.64	15.22	0.00	2.77	3.57	2.85	0.46	0.039	0.162	1.15
/62.00-63.00	*	64.61	6.12	13.46	0.00	2.44	2.92	2.64	0.38	0.033	0.148	0.68
/63.00-64.00	*	65.37	3.86	16.01	0.39	2.80	3.38	3.83	0.48	0.044	0.175	0.50

Symbols (S):
+ = Unmineralized Osikonmäki intrusion
* = Mineralized host rock in the Osikonmäki shear zone

Appendix 2A. Trace element data for unmineralized Osikonmäki granitoid intrusion. Te, Se, Bi and Au as ppb, others as ppm. N = 36. The values below the detection limit are replaced by 0.

Sample	S	As	Rb	Sr	Zr	Ba	V	Cu	Zn	Pb	Te	Se	Bi	Au
OMK-86-14.3	280	230	80	490	160	530	80	19	40	7	7	110	0	7
OMK-86-34.1	210	20	90	440	280	730	130	21	74	13	2	0	100	5
OMK-86-49.1	260	10	70	550	170	580	90	17	50	9	3	0	250	17
OMK-86-51.1	90	0	70	520	180	530	80	14	43	5	1	0	0	1
OMK-86-63.1	40	0	70	460	230	590	110	13	60	9	3	0	0	0
OMK-86-85.1	220	0	80	480	250	740	120	25	61	9	1	10	0	0
OMK-86-89.1	60	0	90	480	190	570	100	7	49	5	1	0	50	0
OMK-86-105.1	110	0	40	760	150	610	70	15	32	5	1	0	50	0
OMK-86-109.1	90	0	80	520	150	510	70	6	39	4	11	0	950	43
OMK-86-139.1	80	0	70	480	160	510	70	4	50	7	1	0	0	0
OMK-86-140.1	70	50	60	380	160	420	70	8	44	5	0	0	50	6
OMK-86-143.1	4170	10	80	410	180	390	70	27	52	12	0	0	0	139
OMK-86-147.1	60	10	90	410	270	590	120	32	58	13	0	10	0	6
OMK-86-153.1	20	0	60	540	150	550	70	4	42	9	1	0	50	1
OMK-86-155.3	3700	530	80	470	160	300	70	100	106	22	2	90	50	18
OMK-86-156.1	60	0	90	530	170	630	70	5	58	12	0	0	0	1
OMK-86-162.1	50	0	80	490	200	560	100	12	53	14	0	0	0	2
OMK-86-165.1	70	0	80	500	170	600	80	4	49	11	0	0	0	1
OMK-86-182.1	70	0	60	560	160	460	80	3	47	11	0	0	0	1
OMK-86-188.1	80	10	60	520	150	490	70	2	39	8	0	0	0	1
OMK-86-190.1	40	0	60	500	140	500	60	12	37	9	0	0	0	2
OMK-86-191.1	1050	10	80	500	190	430	100	25	60	14	0	0	50	1
OMK-86-197.1	210	0	80	500	260	730	170	157	69	14	0	10	200	9
OMK-86-200.1	40	0	170	400	280	610	110	9	93	15	0	0	100	1
OMK-87-7.1	240	10	90	270	290	640	120	133	72	14	0	40	0	7
OMK-87-10.1	50	0	100	450	210	640	100	10	52	15	0	20	0	1
OMK-87-16.1	60	10	80	510	170	530	80	6	55	9	0	280	0	1
OMK-88-10.1	50	130	90	400	160	630	70	10	45	10	0	20	150	25
OMK-88-11.1	60	0	190	510	170	500	80	5	89	11	1	10	50	3
OMK-88-13.1	150	80	70	560	170	520	70	4	41	11	0	0	0	2
OMK-88-14.1	30	0	60	610	180	420	90	7	54	13	0	0	0	1
ETK-87-152.1	30	0	50	530	190	590	90	41	39	11	0	0	0	3
ETK-87-222.1	120	0	100	410	190	430	100	99	59	15	1	10	100	17
ETK-87-227.1	40	0	70	530	150	530	70	3	40	11	0	0	0	1
ETK-87-229.1	30	0	30	560	200	280	100	6	24	11	0	0	0	0
ETK-87-140.1	70	140	80	480	210	970	110	82	65	15	0	10	0	2

Appendix 2B. Trace element data (as ppm) for the mineralized and sheared host rock of Osikonmäki deposit (Au over 0.5 ppm). N = 19. The values below the detection limit are replaced by 0.

Sample	S	As	Rb	Sr	Zr	Ba	V	Cu	Zn	Pb	Sb	Te	Se	Bi	Au
BH 460															
45.0-46.0	10200	5572	114	196	171	319	76	21	89	32	2.69	0.02	0.32	0	1.3
46.0-47.0	11600	10102	142	171	170	322	75	20	57	39	4.87	0.02	0.29	0	1.0
47.0-48.0	12000	8826	134	102	167	287	77	33	67	46	5.16	0.01	0.55	0.1	4.5
58.5-59.5	12800	9256	147	223	180	444	88	86	131	124	13.05	0.01	1.15	0.1	6.2
59.5-60.5	12400	7009	117	202	176	326	82	73	128	100	11.03	0	1.02	0	0.7
60.5-61.5	8500	7121	123	202	181	294	80	46	134	128	8.78	0.01	0.79	0	0.6
BH 464															
135.0-136.0	11800	857	132	460	184	323	79	333	56	24	0.05	0.25	10.94	6.7	1.7
136.0-137.0	7900	546	93	648	202	528	85	126	41	24	0.04	0.18	9.25	2.2	1.0
137.0-138.0	16800	17684	98	465	186	298	84	259	48	26	0.51	0.82	46.87	0.8	4.2
138.0-139.0	17200	23447	92	390	170	246	72	195	45	33	2.20	1.08	65.65	0.8	3.6
141.0-142.0	8800	11198	97	335	145	340	67	171	46	66	0.55	1.83	19.16	1.3	5.2
142.0-143.0	11500	16965	127	284	123	429	51	93	50	165	1.46	1.77	35.34	1.9	6.3
147.0-148.0	9300	7284	115	410	181	417	77	310	60	72	0.82	0.32	12.88	0.4	0.6
148.0-149.0	10300	12957	126	357	181	420	71	211	60	68	0.89	1.02	26.56	0.4	0.7
BH 478															
57.0-58.0	10900	705	119	505	203	410	82	195	50	41	0.08	0.02	7.41	4.6	0.8
58.0-59.0	14400	2020	189	418	201	473	90	421	64	49	0.17	0.05	16.03	7.9	3.1
59.0-60.0	19600	33953	166	363	174	276	78	176	55	36	1.54	0.12	47.54	0.9	3.1
62.0-63.0	19800	42331	100	245	135	293	59	146	55	111	2.02	0.67	69.82	1.0	5.7
63.0-64.0	11000	18926	115	360	171	382	80	149	65	82	1.02	0.17	31.45	0.4	2.6

GEOLOGICAL SETTING AND CHARACTERISTICS OF THE PALEOPROTEROZOIC TONALITE-HOSTED OSIKONMÄKI GOLD DEPOSIT, SOUTHEASTERN FINLAND

by

Olavi Kontoniemi

Kontoniemi, Olavi 1998. Geological setting and characteristics of the Paleoproterozoic tonalite-hosted Osikonmäki gold deposit, southeastern Finland. *Geological Survey of Finland, Special Paper 25.* 39-80. 23 figures, 6 tables and 3 appendices.

The epigenetic Paleoproterozoic Osikonmäki gold deposit, near Rantasalmi in southeastern Finland, is hosted by the synorogenic I-type Osikonmäki tonalite pluton. The deposit exhibits a strong structural control, being closely associated with shear zones that represent oblique ductile second order structures within the NW-trending crustal scale Ladoga - Bothnian Bay deformation zone.

The highest gold concentrations occur at both the eastern and western parts of the footwall to the shear zone, which dips southwards at 40-50°. Gold-enriched zones occur as either tightly folded or en echelon lenses that typically plunge ESE at around 20°.

The most common sulfide minerals associated with the ore are pyrrhotite, arsenopyrite, löllingite and chalcopyrite, which typically occur as irregular to somewhat banded disseminations. Gold and electrum, together with a number of Bi-Te-Se minerals, occur both as inclusions and at grain boundaries within and between arsenopyrite and silicate grains. In contrast to many Archean mesothermal deposits, the effects of hydrothermal alteration appear to be rather limited; alteration is however difficult to discern due to subsequent prograde metamorphism above the sillimanite-K-feldspar isograd, followed by extensive retrograde recrystallization.

Although gold is the only commodity present of economic interest, the mineralization process caused marked enrichment in As, Bi, Te and Se, and moderate enrichment in Ag, Sb and Cu. At the deposit scale the distribution of Au correlates well with semimetals, Cu and Ag, while reasonably good correlation also exists with As and S. Where gold is most concentrated, the Au-As correlation becomes somewhat weaker, while conversely, Au and Ag correlate better. A geochemical aureole defined by Se, Bi, As, S and Cu is particularly prominent in the hanging wall country rock above the ore.

Transport of gold was presumably facilitated by thio- and thioarsenide complexes in fluids of either magmatic and/or metamorphic origin. Ore mineral parageneses indicate that gold mineralization took place under metamorphic conditions of amphibolite facies following the intrusion of synorogenic granitoids, but nevertheless prior to the peak of regional metamorphism. Fluid inclusion studies indicate that the main stage of mineralization was followed by influx of aqueous fluids of variable salinity, at least locally in the eastern part of the deposit, which transported gold and associated elements to higher structural levels during continued deformation within the shear zone.

Key words (GeoRef Thesaurus, AGI): gold ores, tonalite, shear zones, mineralogy, hydrothermal alteration, ore minerals, geochemistry, mineral deposits, genesis, Proterozoic, Paleoproterozoic, Osikonmäki, Finland

Geological Survey of Finland, P.O. Box 1237, FIN-70211 Kuopio, Finland

INTRODUCTION

The bulk of historical and present gold production has been from Archean shield areas and from Mesozoic to Cenozoic arc-collisional environments. Traditionally important types of gold deposit include the Witwatersrand paleoplacers in South Africa, mesothermal shear and vein-hosted deposits in late Archean (especially so-called rift-type) greenstone belts (such as Norseman-Wiluna and Abitibi), and Cordilleran and western Pacific epithermal, vein and porphyry type deposits (i.a. Boyle 1979, Kerrich & Cassidy 1994).

In contrast, rocks of Proterozoic age are less well known as major gold producers, although notable exceptions include the Ashanti gold belt in Ghana (Mumin et al. 1994) and the Homestake deposit, located within the Paleoproterozoic Trans-Hudson fold belt (Kerrich & Cassidy 1994). These deposits also tend to be associated within ductile shear systems developed during collisional processes involving Archean craton margins. Despite the relative importance of gold in most shields, the Fennoscandian shield has

never been a major gold producer, although significant amounts of the metal have been obtained from sulfide ores in Sweden, notably at Boliden and Aitik, and from Outokumpu, Vihanti and Pyhäsalmi in Finland (Gaál & Sundblad 1990). Small vein-type deposits have also been known in the Bergslagen and Skellefte districts of Sweden for many years, so that when the price of gold rose sharply towards the end of the 1970's, this led to a considerable increase in interest and investment in exploration. Within the next ten years five new gold mines came into operation at Enåsen, Björkdal and Åkerberg in Sweden, Bidjovagge in Norway, and Saattopora in Finland (Gaál & Sundblad 1990). Since then a further two mines have commenced production in Finland, namely Kutemajärvi, at Orivesi, within the southern part of the Svecofennian domain and Pahtavaara, near Sodankylä, within the Lapland greenstone belt.

According to Nurmi (1991) and Nurmi et al. (1991), gold occurrences in the Fennoscandian
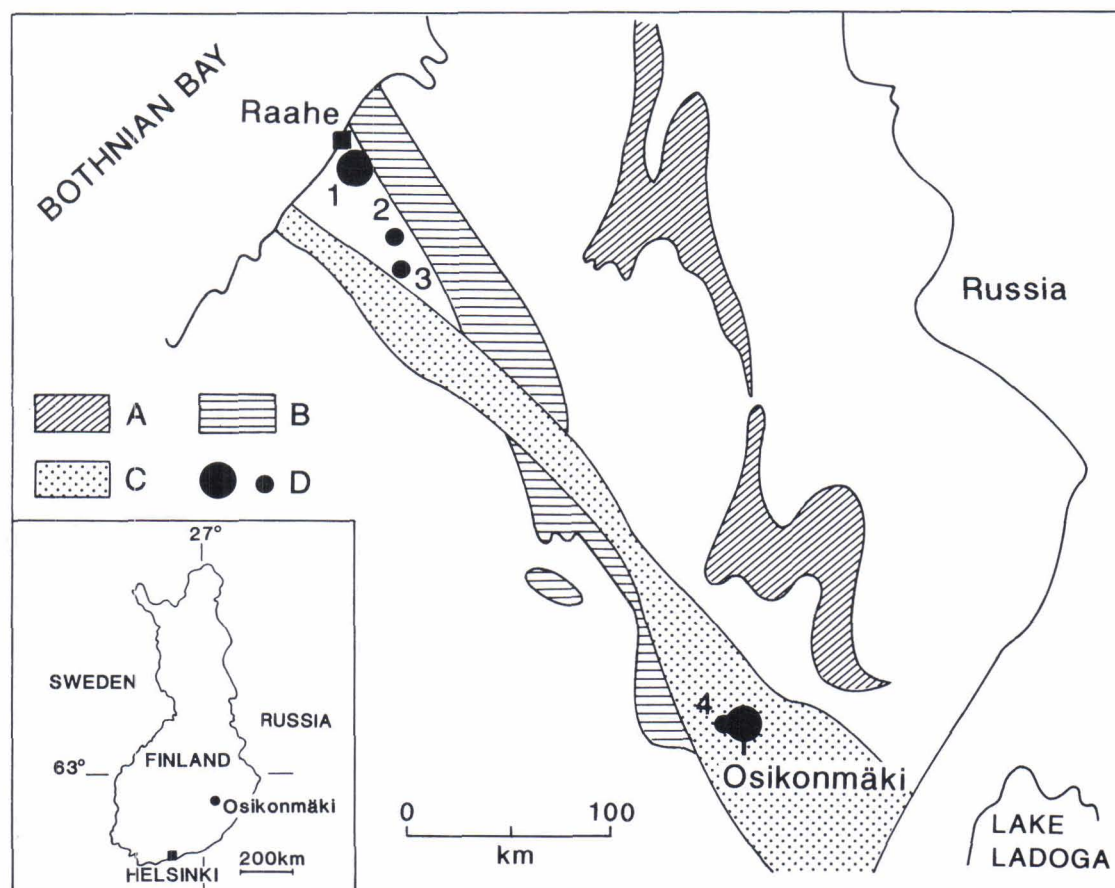

Fig. 1. Location of Osikonmäki and other promising gold deposits (large black circles) and occurrences and metallogenic provinces of the Ladoga - Bothnian Bay Zone after Ekdahl (1993). A = Kainuu-Outokumpu Back Arc, B = Pyhäsalmi Island Arc, C = Kotalahti Nickel Belt, D = Gold occurrences including Laivakangas (1), Vesiperä-Ängesneva (2), Kopsa (3) and Pirilä (4).

shield can be classified into three main categories (location of deposits e.g. in Gaál & Sundblad 1990 and Nurmi et al. 1991):

1. Deposits within late Archean (2.9-2.7 Ga) greenstone belts in eastern Finland (such as Pampalo and Rämepuro)

2. Deposits within the Paleoproterozoic (2.5-1.9 Ga) Lapland greenstone belt (such as Bidjovagge, Saattopora, Pahtavaara, Juomasuo)

3. Paleoproterozoic (2.0-1.75 Ga) Svecofennian deposits (such as Björkdal, Enåsen, Laivakangas, Osikonmäki, Kutemajärvi).

Deposits of the third group show a strong tendency to occur within the Ladoga - Bothnian Bay (i.a. Gaál 1986) zone and further along strike in the Skellefte district in Sweden - perhaps partly as a result of more intense exploration activity in this area. The most significant deposits so far found in Finland within this zone are Laivakangas, Osikonmäki, Kopsa and Vesiperä-Ängesneva (Figure 1).

Gold-bearing erratic boulders and quartz veins were first found in area surrounding Osikonmäki during the 1970's but systematic exploration did not commence until the 1980's. Pirilä was the first deposit to be found, in 1983, while Osikonmäki was discovered three years later. Gold is also present in subeconomic quantities in three deposits nearby, at Pirilä, Hakojärvi and Kolkonranta (Figure 2). Unlike Osikonmäki, each of these deposits is hosted by gneisses of volcanic and sedimentary origin metamorphosed under amphibolite-facies conditions. The Pirilä deposit is at the contact between sillimanite grade metasediments and intermediate and felsic metavolcanics (Makkonen & Ekdahl 1988). Ore-bearing quartz lenses at Pirilä are located within F_3 hinge zones or axial planes, with the high grade ore being concentrated in an F_3 antiform (Figure 3), that plunges SE at about 50 degrees. An evaluation of the deposit indicates reserves of 0.15 Mt grading 8g/t Au and 30g/t Ag (Makkonen & Ekdahl 1988).

The first indications that the Osikonmäki intrusion might have gold potential came from a few mineralized boulders of tonalite found by
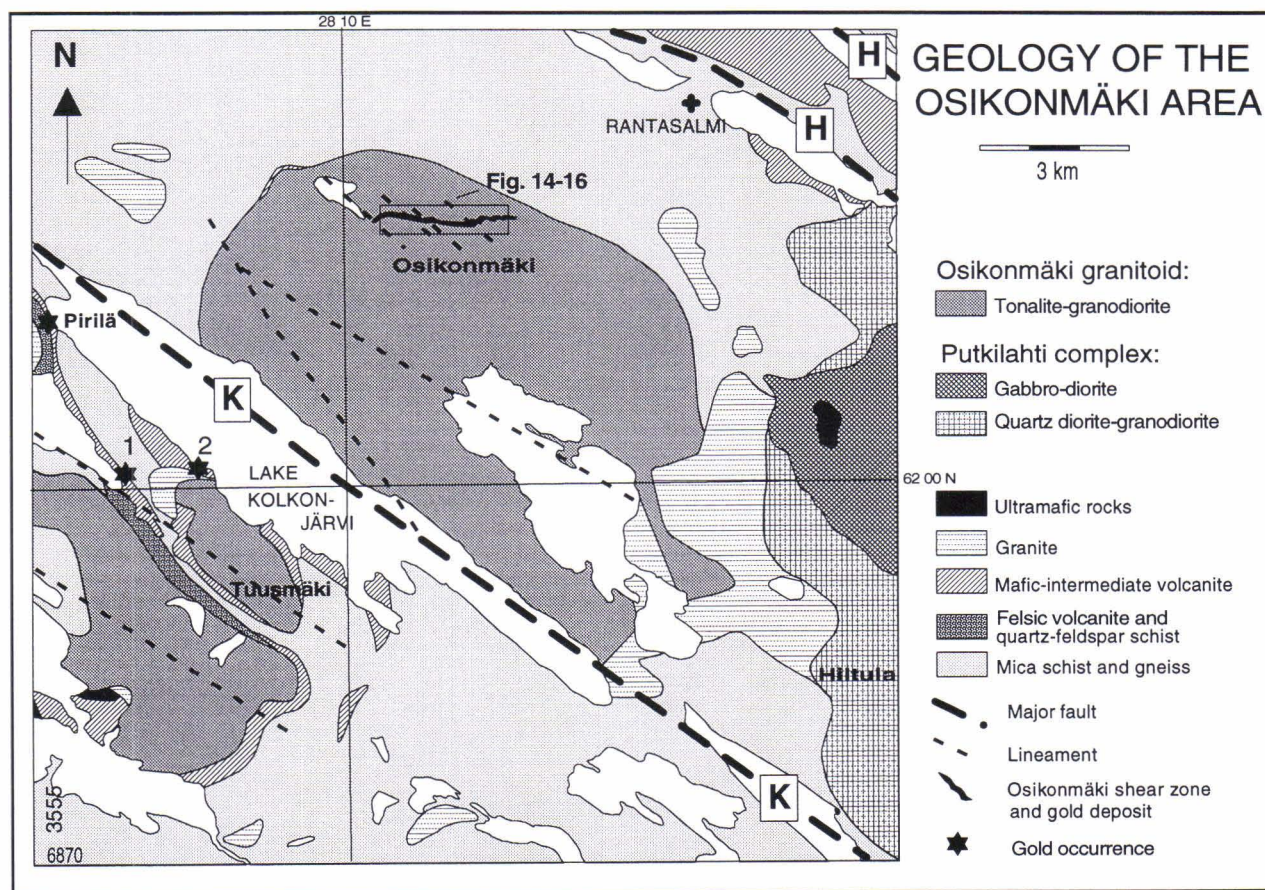

Fig. 2. Generalized geological map of the Osikonmäki area, also showing the area in Figures 14-16. Simplified from Kontoniemi (1998, this volume). K = Kolkonjärvi shear zone, H = Haukivesi shear zone. 1 = Hakojärvi, 2 = Kolkonranta.

Geological Survey field staff about 20 km to the southeast of Osikonmäki during autumn 1984. After once the boulders had been traced to their source, the total length of the mineralized shear zone at Osikonmäki was demonstrated to be at least 3 km (Figure 2), while the potential for finding more mineralization still exists both eastwards and westwards from the area proven by drilling. Proven and probable reserves in the area drilled in detail are (with a cutoff grade of 1 ppm) approximately 2 Mt with a mean concentration of 3 g/t Au and 0.77% As (Kontoniemi & Ekdahl 1990).

A number of publications already exist dealing with the general geology, ore mineralogy and isotope characteristics of the Osikonmäki deposit, including Kontoniemi (1989), Kontoniemi and Ekdahl (1990), Kontoniemi et al. (1991) and Vaasjoki and Kontoniemi (1991). The purpose of this Special Paper compilation is to consider the regional geological framework and the nature of the Osikonmäki tonalite from the perspective of ore genesis, in order to understand the origin of the deposit in detail.

Fig. 3. Cross section of the Pirilä gold deposit along profile X = 6880.920 (Makkonen & Ekdahl 1988).

GEOLOGICAL SETTING AND RELATIONSHIP TO SHEAR ZONES

The deposit is located within an E-W trending shear zone transecting the northern part of the Osikonmäki tonalite intrusion (Figure 2). Although mineralization is present throughout the entire shear zone, gold contents are highly variable. The shear zone itself dips overall towards the south at 40-50° but at least in the eastern part of the deposit, ore shoots tend to plunge towards ESE. Such angular discordances between the geometry of individual lodes within shear zones and the overall trend of the host shear zone is considered to be a typical feature of vein-hosted gold deposits (Peters 1993). The highest gold grades at Osikonmäki tend to occur at the footwall contacts of the shear zone, although rich intersections have also been recorded from the central and hanging wall regions. The boundaries of the deposit are based entirely on analytical data, rather than visually, however, anomalous gold values have been recorded only sporadically outside the shear zone. A number of subsidiary, discontinuous shear zones are present, subparallel to the main zone and containing weak sulfide disseminations. The shear zones are slightly oblique to the S_2 foliation present in the tonalite and have, together with the gold mineralization, been subsequently deformed and metamorphosed (Kontoniemi 1998, this volume). The Osikonmäki gold deposit thus clearly represents a shear zone related epigenetic style of mineralization.

INTERNAL STRUCTURAL FEATURES OF THE OSIKONMÄKI SHEAR ZONES

The principal structural elements present in the shear zone and the ore are banding parallel to the shear fabric, intrafolial folding and narrow concordant veins of quartz and quartzofeldspathic material. These features are distinctly truncated and overprinted by a variety of pale quartz and granite veins and dykes, arsenopyrite veins, quartz-tourmaline veins and breccias, and swarms of faults that disrupt the shear zone.

Ore minerals occur as disseminations throughout the shear zone, sometimes defining bands of sulfide parallel to the shear zone foliation (Figures 4a and 4d). High gold tenors are found in
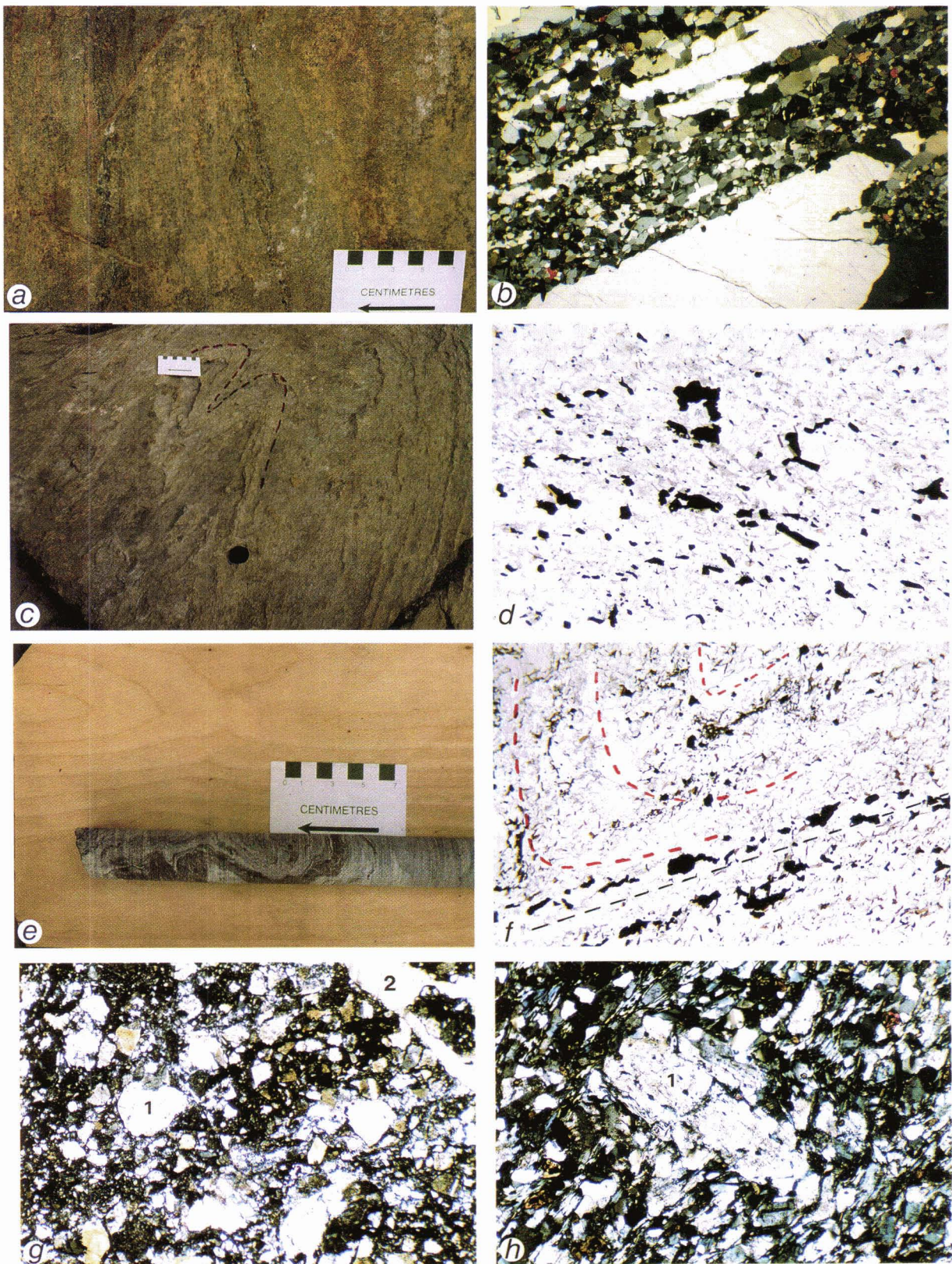
Fig. 4. a) Strongly sheared and mineralized tonalite near the footwall contact of the gold ore in exploration trench OMK-87-M1. Note the narrow dark quartz veins and younger nearly vertical offsets. b) Photomicrograph of narrow quartz veins in granoblastic granitoid of the Osikonmäki shear zone. Crossed polarizers, sample BH 505/93.50 m. Field of view is 10 mm in width. c) Intrafolial folding within the Osikonmäki shear zone in outcrop OMK-88-15. The shape of the fold is highlighted by red dashes. d) Photomicrograph of typical disseminations of ore minerals in the shear zone. Plane polarized light, sample OMK-87-M1. Field of view is 10 mm in width. e) Intrafolial small scale folding in drill core (BH 515) from the western part of the shear zone. Black tourmaline-bearing bands are clearly discernible. f) Photomicrograph of structurally controlled disseminated ore. Ore minerals are elongate and aligned within microfolds (red dashes) or subparallel to dislocations and axial planes (black dashes). Plane polarized light, sample OMK-88-15.27. Field of view is 10 mm in width. g) Photomicrograph of cataclastic fabrics in the younger brittle-ductile shear zone. 1 = quartz, 2 = carbonate. Crossed polarizers, sample BH 447/81.00 m. Field of view is 4 mm in width. h) Photomicrograph of mylonitic fabrics in the younger brittle-ductile shear zone. 1 = passively rotated plagioclase porphyroclast. Crossed polarizers, sample BH 447/92.30 m. Field of view is 4 mm in width.

OSIKKO 1

OMK-87-M 1

OSIKKO 1
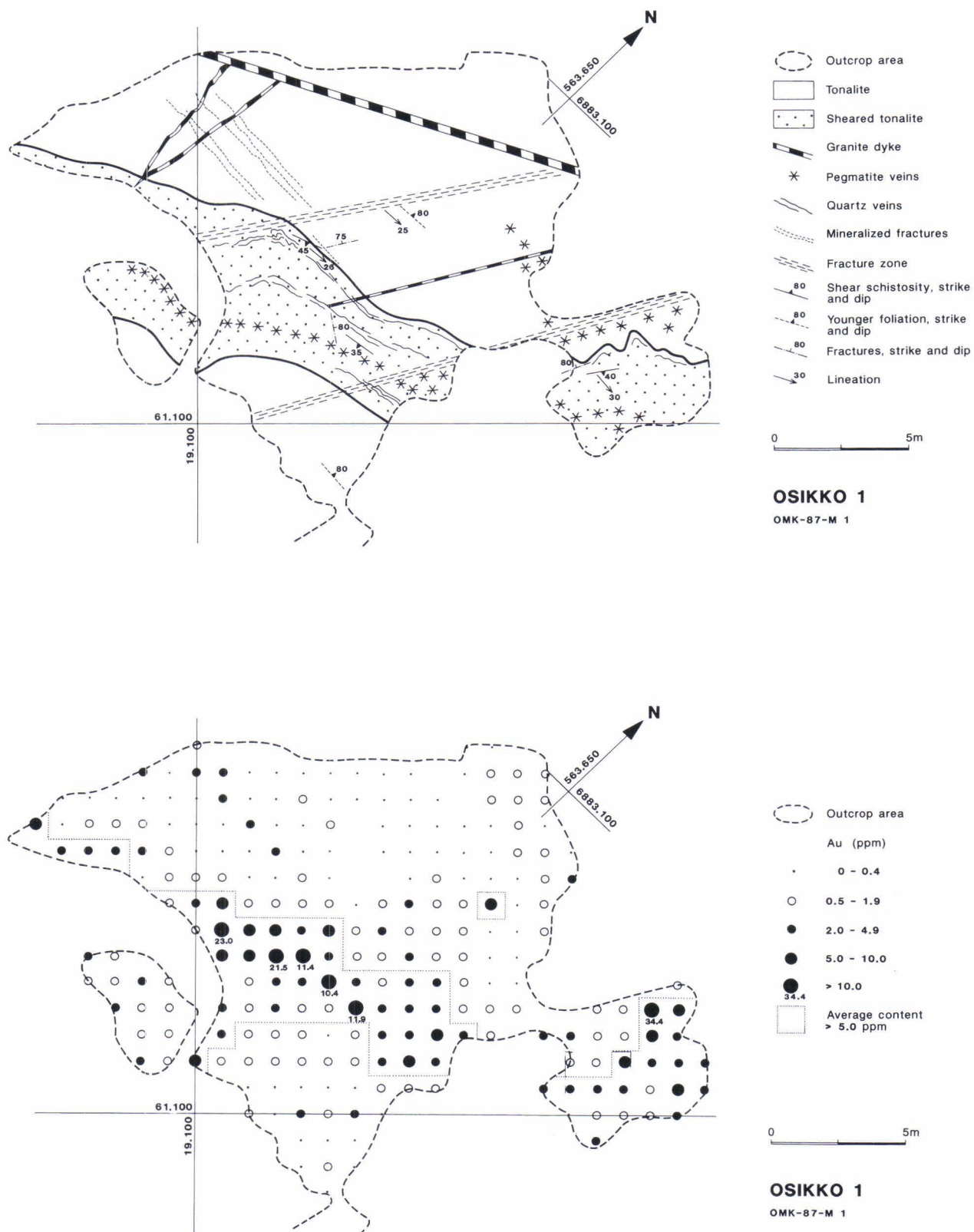
OMK-87-M 1

Fig. 5. Correspondence between structural and lithological features and gold abundances in exploration trench OMK-87-M1. The samples for gold analyses were drilled with a portable drill, about 20 cm long drill core from every sample site.
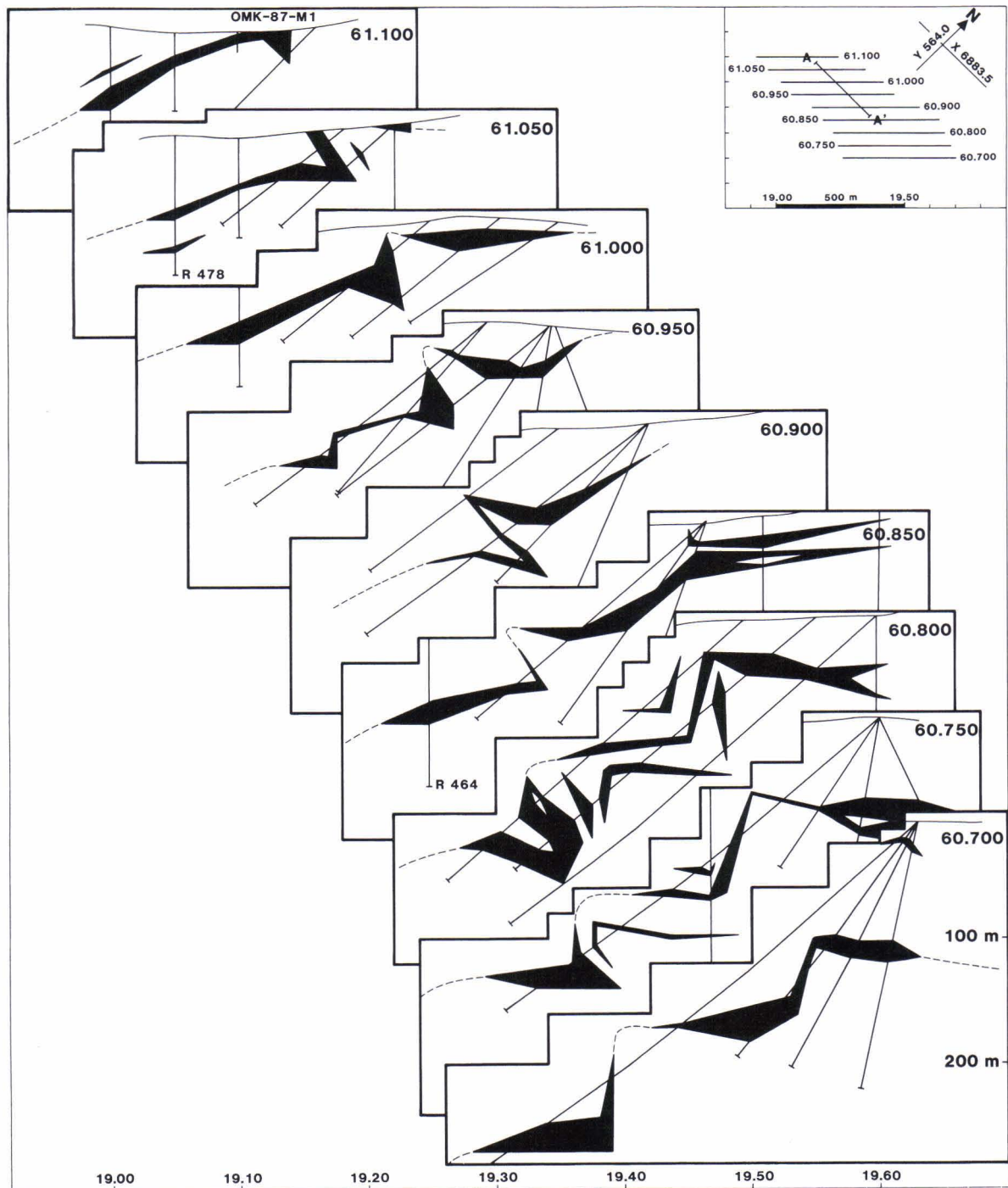
Fig. 6. Block diagram of claim Osikko 1 between profiles L = 60.700 and 61.100, also showing location of exploration trench OMK-87-M1 and drill holes 464 and 478. Black areas represent ore sections in different profiles (cut off 0.5 g/t). The inset shows the location of the profiles and the longitudinal section (A - A') in Fig. 9.

particular in certain horizons containing abundant narrow quartz veins near the footwall contact (Figures 4a and 4b). Intrafolial folding within the shear zone has been identified from drill core as well as in outcrop (Figures 4c and 4e). Although ore minerals and quartz veins are typically deformed around microfolds, sulfides are also aligned within axial plane orientations (Figure 4f). The close correspondence between such structural features and gold abundance is well developed in exploration trench OMK-87-M1, depicted in Figure 5.

Structures formed later under brittle conditions, such as different kinds of veins and breccias, appear to be more abundant towards the western end of the deposit, at least on the basis of observations from erratic boulders and drill core. The quartz-tourmaline breccias are of particular interest since in addition to arsenopyrite they also contain a number of Co and Sb minerals.

A number of late brittle-ductile shear zones that transect the main Osikonmäki shear zone have been marked on the map in Figure 2, based on both drill core information and magnetic characteristics determined from field measurements. The precise widths and displacements of these younger structures are not certain, although associated alteration haloes are commonly up to several meters wide. These shear zones are typically almost vertical and show both cataclastic (Figure 4g) and mylonitic (Figure 4h) fabrics using the nomenclature of Spry (1969). The mylonites show evidence for passive rotation of plagioclase porphyroclasts and incipient recrystallization but such features are nevertheless quite easily distinguishable from the blastomylonitic fabrics of the main shear zone.

Because the Osikonmäki shear zone is rather poorly exposed, interpretation of internal structure is largely based on information obtained from drill core observations. Such structural information has been necessary in both planning the drilling program and in estimating ore reserves. The eastern part of the shear zone is evidently somewhat more complex than the rest of it and because this area was not drilled in great detail, a number of different structural interpretations are possible, two of which will be discussed below: that of Kontoniemi and Ekdahl (1990), and that of Parkkinen (1992b).

The former interpretation (Figure 6) is based primarily on observations of angular relation-
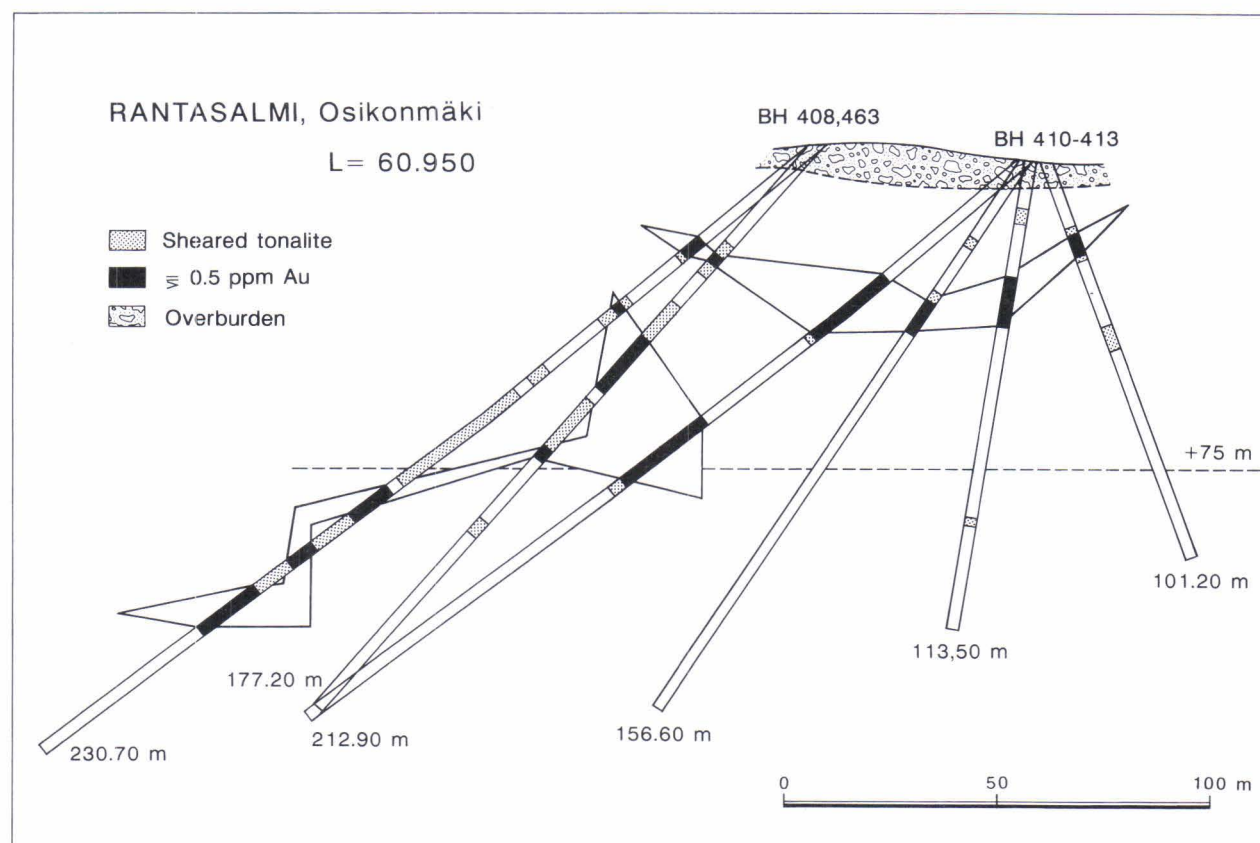
Fig. 7. Possible geometry of ore shoots in the cross section L = 60.950.

ships between foliation and drill core orientation in a series of drilling profiles combined with evidence for folding within the shear zone itself. According to this model the shear zone, which dips southwards at about 45°, contains alternating horizontal and vertical lenses of ore that plunge at about 20° ESE, or more precisely, at 22°/104° according to Parkkinen (1992a). The individual ore shoots apparently follow the trend shown in the densely drilled profile L = 60.950 (Figure 7) rather closely from profile to profile.

The alternative structural interpretation of Parkkinen shows the ore shoots as a stacked set of en echelon lodes (Figures 8 and 9).

According to the earlier model, the eastern part of the shear zone has been buckled during ductile deformation whereas the latter model emphasizes the role of low-angle thrusting following earlier ductile deformation. A simple en echelon interpretation does indeed seem more likely when progressing further westwards along the shear zone (Figure 10).
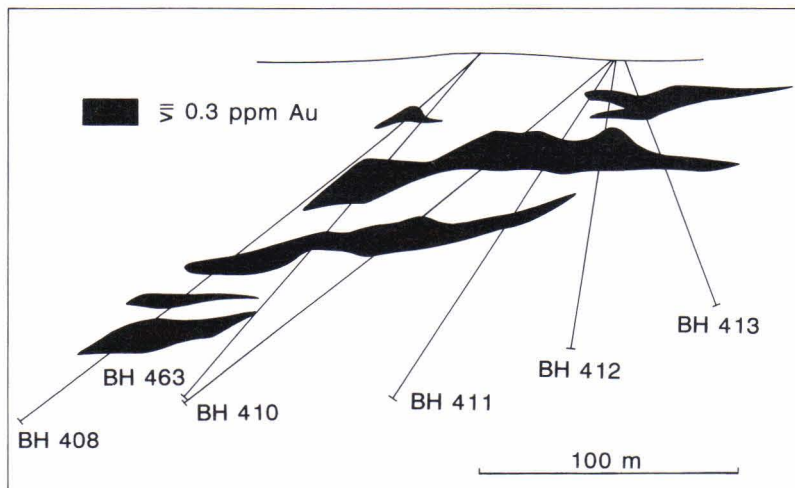
Fig. 8. Alternative structural model after Parkkinen (1992b) for the same cross section (L = 60.950) as in Fig. 7.
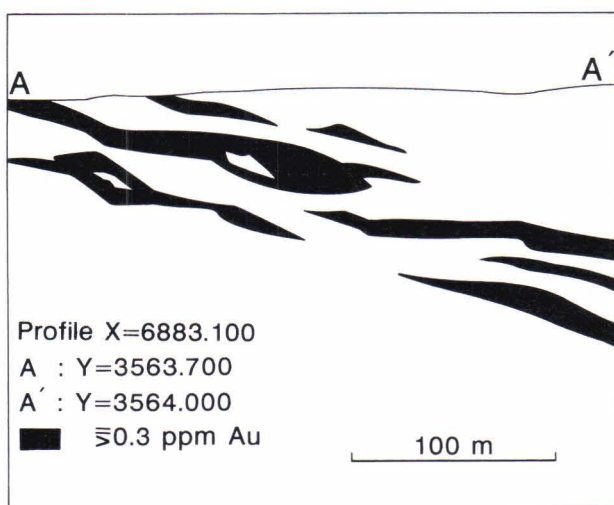
Fig. 9. Longitudinal section of ore shoots in claim Osikko 1 after Parkkinen (1992b). The location of profile A - A' is shown in Fig. 6.
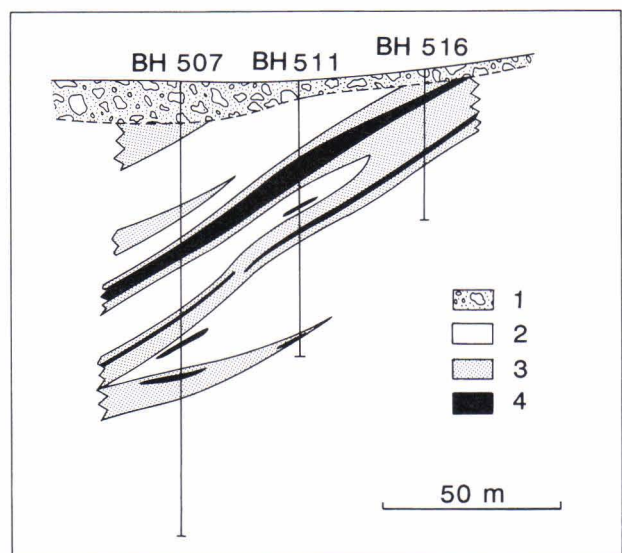
Fig. 10. Cross section of sheared and mineralized horizon in profile Y = 3561.780 in the western part of Osikonmäki shear zone. 1 = overburden, 2 = tonalite, 3 = sheared tonalite, 4 = ore with cutoff grade of 0.5 g/t.

MINERALOGY AND ALTERATION ASSEMBLAGES

The principal minerals present in the shear zone have already been alluded to in the general description of the Osikonmäki pluton. The original tonalite paragenesis, comprising plagioclase + quartz + biotite + hornblende ± K-feldspar has, as a result of deformation and mineralizing processes, been modified into distinct secondary assemblages (Table 1). The degree of alteration varies within the shear zone and can be subdivided into early hydrothermal alteration, regional prograde metamorphism in sillimanite-K-feldspar zone, and later retrograde alteration.

The mineral assemblage formed as a result of hydrothermal alteration associated with shear zone development and gold mineralization is difficult to ascertain due to the effects of superimposed prograde recrystallization. Breakdown of hornblende and plagioclase and replacement by biotite and quartz is characteristic of the whole shear zone, along with the widespread presence of K-feldspar, sulfides and, particularly in the western part of the deposit, tourmaline (Figure 11b). Figure 11a shows a section of drill core from the western end of the shear zone; the light-colored quartz vein (A) is almost devoid of gold (0.2-0.3 ppm), whereas the core below the lens cap (B+C) contains grades up to 4-5 ppm. Within the strongly sheared tonalite sillimanite porphyroblasts can be discerned (B), while quartz-tourmaline veins are well developed in the lowermost section of core (C).

The most characteristic prograde metamorphic minerals in the tonalite are diopside and actinolitic amphibole; fibrolitic sillimanite (Figure 11c), and sporadic poikiloblasts of garnet containing inclusions of all other minerals are also present within the shear zone, especially where alteration has been most intense, as at the western end of the deposit.

Later hydrothermal alteration occurs in proximity to the younger brittle-ductile shear zones and is characterized particularly by the presence of chlorite and epidote; in some instances carbonate veins and breccias have also been observed (Figures 11d and 11e).

Fluorite is sporadically present in association with ore mineral concentrations at the eastern end of the shear zone (Figure 11f), suggesting that the mineralizing fluid was at some stage fluorine-bearing, although the precise timing and nature of the fluid involved remains uncertain. Nevertheless, the spatial association of fluorite with late stage granitic material suggests that fluorine belongs to later rather than earlier mineralizing fluids.

Table 1. Alteration mineralogy and associated index minerals within the shear zone.

Early hydrothermal alteration	Prograde metamorphism	Late retrogression and hydrothermal alteration
biotite	diopside	chlorite
quartz	amphibole	epidote
K-feldspar	sillimanite	actinolite
titanite	garnet	sericite
rutile		carbonate
tourmaline (brown)		quartz
carbonate		tourmaline (black)
sericite[x]		K-feldspar
albite[x]		fluorite
saussurite[x]		ore minerals
chlorite[x]		
ore minerals		

[x] = inferred hypothetical minerals, destroyed by later metamorphic events
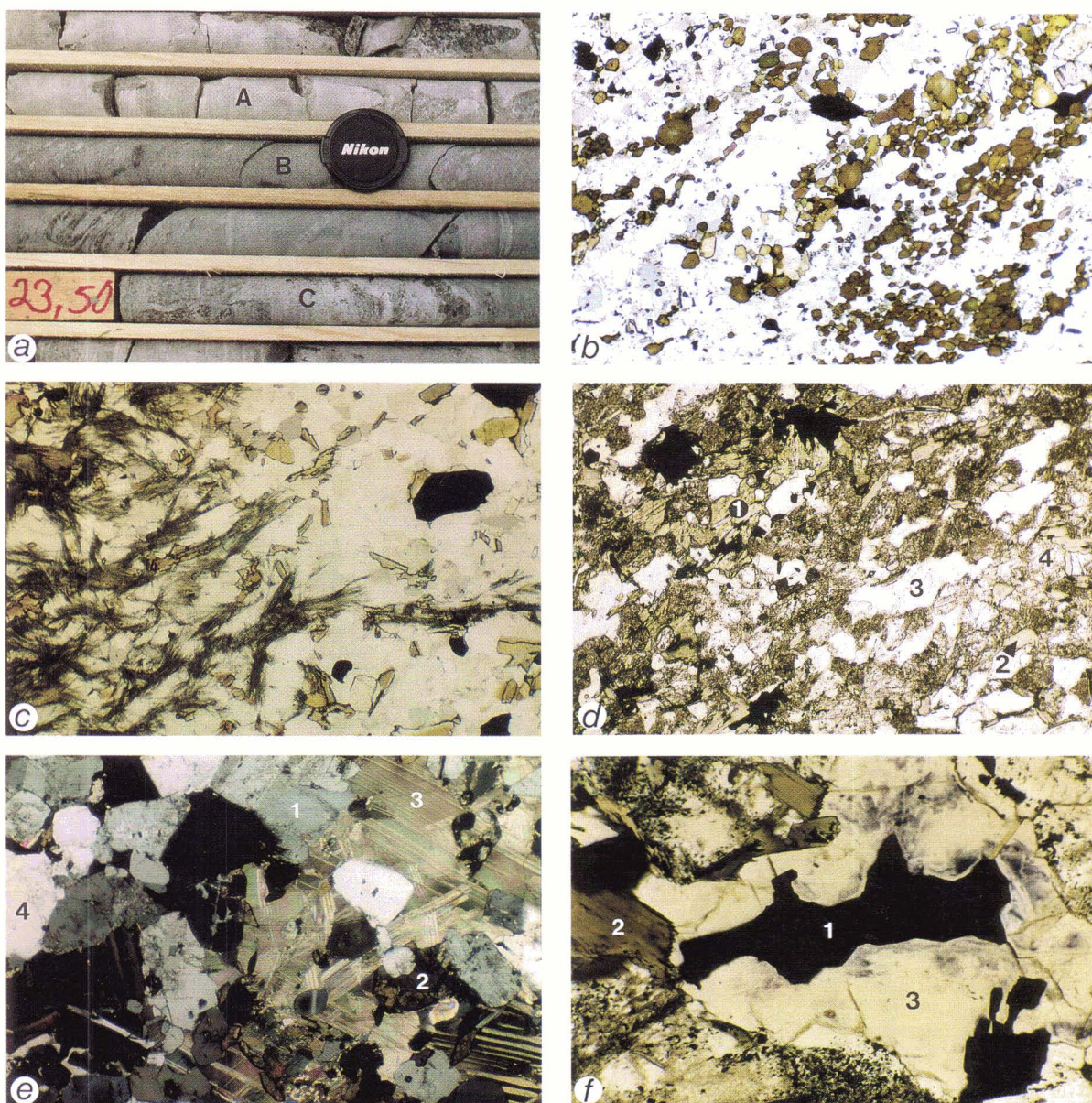
Fig. 11. Alteration mineralogy within the shear zone. a) Drill core section from BH 515 in the western part the shear zone. The light-colored quartz vein (A) curves towards the strongly sheared tonalite with sillimanite porphyroblasts (B) and quartz-tourmaline veins (C). Refer to text for more detailed explanation. b) Photomicrograph of quartz-tourmaline vein in the western part of the shear zone. Plane polarized light, sample BH 520/143.70 m. Field of view is 4 mm in width. c) Photomicrograph of fibrolitic sillimanite in the strongly sheared tonalite. Plane polarized light, sample BH 514/27.65 m. Field of view is 4 mm in width. d) Photomicrograph of late retrograde or hydrothermal minerals in the central part of the shear zone. 1 = actinolite, 2 = chlorite, 3 = quartz, 4 = epidote and plagioclase. Plane polarized light, sample OMK-88-15.12. Field of view is 4 mm in width. e) Photomicrograph of carbonate breccia in proximity to the younger brittle-ductile structures within the Osikonmäki shear zone. 1 = plagioclase, 2 = titanite, 3 = carbonate, 4 = quartz. Crossed polarizers, sample BH 505/62.90 m. Field of view is 4 mm in width. f) Photomicrograph of fluorite cavity in the strongly sheared granitoid. 1 = ore minerals, 2 = biotite, 3 = fluorite. Plane polarized light, sample OMK-86-L23.1. Field of view is 0.65 mm in width. Photo by Kari Kojonen.
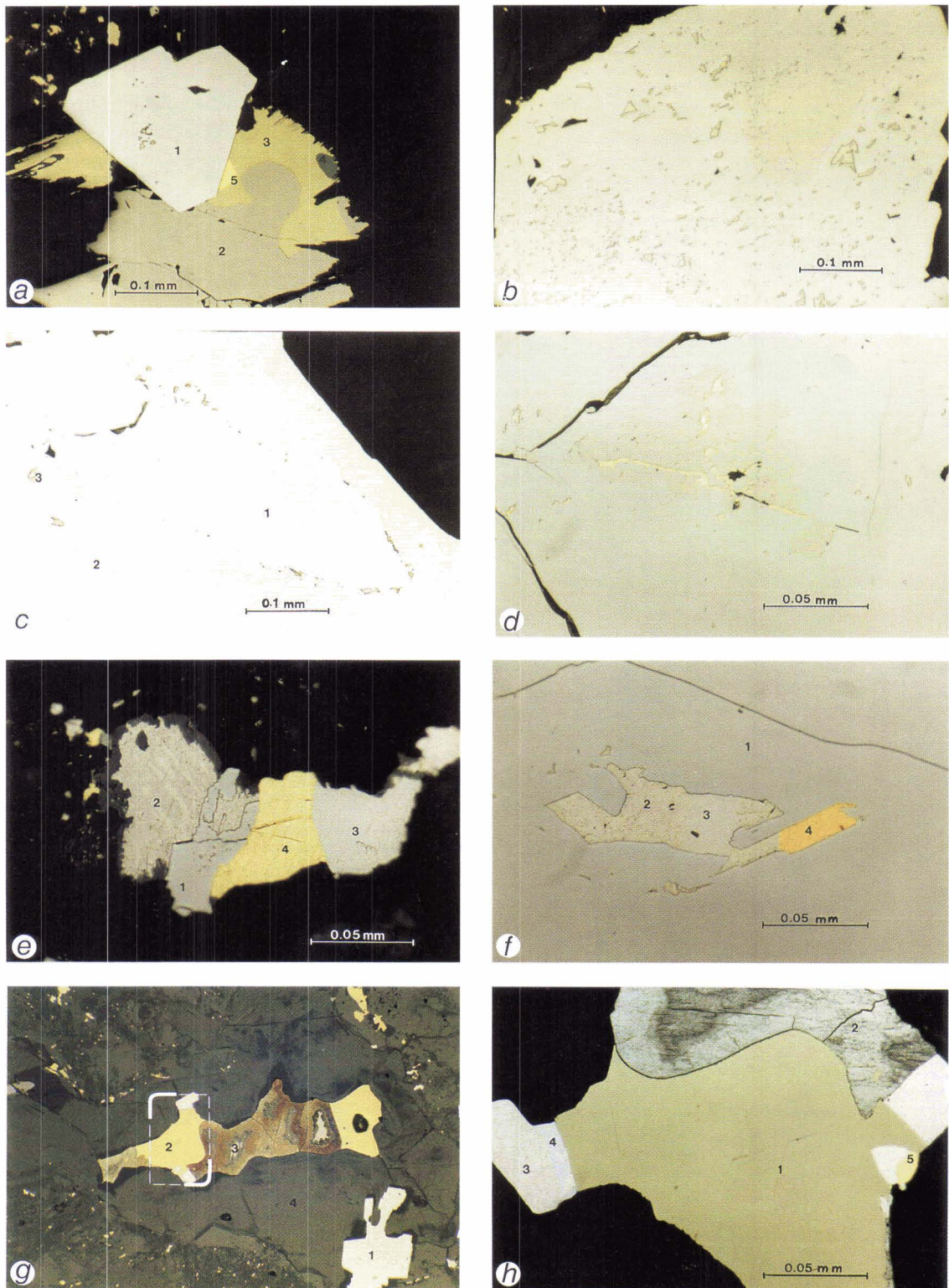
Fig. 12. Photomicrographs of ore minerals occurring in the Osikonmäki gold deposit. a) Typical ore mineral assemblage in the disseminated ore. 1 = arsenopyrite, 2 = pyrrhotite, 3 = chalcopyrite, 4 = sphalerite, 5 = gold. Reflected and plane polarized light, sample OMK-86-L23.2. b) Small inclusions of gold and Bi-Te-Se minerals inside the arsenopyrite grain. Reflected and plane polarized light, sample OMK-86-L23.1. c) Gold (3) and Bi-Te-Se mineral inclusions occurring along contact between mineral phase of arsenopyrite (2) and löllingite (1). Reflected and plane polarized light, sample OMK-86-L23.2. d) Worm-like and dust-like exsolutions of gold inside the arsenopyrite grain. Reflected and plane polarized light, sample BH 390/18.25 m. e) Ore mineral aggregate in narrow quartz vein. 1 = arsenopyrite, 2 = native bismuth, 3 = hedleyite, 4 = gold. Reflected and plane polarized light, sample TSP-85-L72. f) Gold and associated minerals as inclusions in arsenopyrite. 1 = arsenopyrite, 2 = native bismuth, 3 = hedleyite, 4 = gold. Reflected and plane polarized light, sample BH 390/18.25 m. g) Ore mineralogy in the same fluorite cavity as in Fig. 11f. 1 = arsenopyrite, 2 = chalcopyrite, 3 = altered pyrrhotite, 4 = fluorite. Reflected and plane polarized light, sample OMK-86-L23.1. h) Close-up of the restricted area in Fig. 12g. 1 = chalcopyrite, 2= altered pyrrhotite, 3 = native bismuth, 4 = unknown bismuth-tellurium selenide corresponding to the formula Bi_6Te_2Se (Kontoniemi et al. 1991), 5 = gold. Reflected and plane polarized light, sample OMK-86-L23.1.

ORE MINERALOGY

The ore minerals present at the Osikonmäki deposit have been described previously by Kontoniemi et al. (1991), so that only those aspects regarded as relevant to the genesis of the deposit will be considered here.

Ore minerals are typically present as irregular disseminations throughout the rocks of the shear zones, but locally they form discontinuous bands within the foliation. Compact sulfide veins are only rarely found. The abundance of disseminated sulfides decreases gradually towards the hanging wall of the shear zone, whereas the footwall contact is marked by a sharp decrease in sulfide content. The most characteristic ore minerals throughout the shear zone are pyrrhotite, arsenopyrite, löllingite and chalcopyrite, with accessory sphalerite, galena and ilmenite or rutile (Figure 12a).

Pyrrhotite commonly shows lamellar structure, consistent with it being a mixture of troilite and hexagonal pyrrhotite or hexagonal and monoclinic pyrrhotite (Kontoniemi et al. 1991); locally pyrrhotite has also been replaced by marcasite and pyrite (Figures 12g and 12h).

Arsenopyrite and löllingite have crystallized as euhedral to subhedral grains such that löllingite tends to form the central part of crystals (Figure 12c). Some of the arsenopyrite grains in erratic boulders of quartz-tourmaline rock from the western part of the shear zone are rimmed by cobaltite. A younger generation of poikiloblastic arsenopyrite is also present within the rare compact sulfide veins. Chalcopyrite occurs primarily in association with the other main sulfide minerals but also as discrete disseminations, particularly at the eastern end of the shear zone. Occasionally it has been replaced by covellite and contains cubanite lamellae. Sphalerite, galena and Ti-bearing phases occur either as small discrete grains or in association with chalcopyrite.

Gold and related minerals commonly occur together in either arsenides or silicates, with löllingite and arsenopyrite grains often being crowded with small inclusions of gold and a range of Bi-Te-Se phases (Figure 12b); alternatively the latter can also form small aggregates along contacts between arsenopyrite and löllingite grain boundaries (Figure 12c). Although gold grains are generally less than 5 μm in diameter, a scattered dust-like distribution of inclusions is only seldom seen (Figure 12d). Exceptional grains up to 1-2 mm in size have occasionally been recorded from drill core. The most common Bi-Te-Se minerals (Figures 12e-12h) are native bismuth, hedleyite

($Bi_{2+x}Te$) and ikunolite (Bi_2Se), and a previously undescribed bismuth-tellurium selenide whose composition corresponds to the formula Bi_6Te_2Se (Kontoniemi et al. 1991).

With respect to silicate minerals, gold and related ore phases are present either as inclusions in quartz and altered plagioclase, along fractures within individual silicate minerals, or at boundaries between two or more grains. Gold occurs mostly as discrete grains, either in native form or as electrum. Silver contents vary from 0.10% to 60.45% and alloys with bismuth, such as maldonite (Au_2Bi) are only seldom encountered. In general, it seems that the Au content of gold grains in silicate minerals is somewhat higher than that of grains within arsenide minerals (Kontoniemi et al. 1991).

Younger fractures and quartz-tourmaline vein systems sometimes contain scheelite, powellite and molybdenite. One sample (BH 505/87.10), obtained from immediately above a rather extensive quartz-tourmaline breccia, was also found to contain native antimony, dyscrasite [(Ag,Au)$_4$Sb], tetrahedrite, boulangerite and stannite (Kontoniemi et al. 1991).

The evidence from the Bogosu-Prestea mining district of southwestern Ghana suggests that most of the primary gold precipitated in solid-solution with sulphide/arsenide minerals. Gold evolved from primary solid-solution within sulphide/arsenide minerals, to colloidal and micrometre-size particles concentrated in voids, fractures and internal grain boundaries, and finally to microscopic and larger particles at sulphide/arsenide grain margins and in the gangue assemblage (Mumin et al. 1994).

On the basis of both ore mineral parageneses and arsenopyrite geothermometry (Kretschmar & Scott 1976) it appears that mineralization in Osikonmäki took place in conjunction with the crystallization of arsenopyrite at temperatures initially around 500°C (Kontoniemi et al. 1991). With a progressive fall in temperature, gold and various related phases evidently exsolved from solid solution with löllingite and arsenopyrite, forming discrete inclusions. Changes in ambient fluid composition during continued deformation and hydrothermal alteration (Liimatainen 1998, this volume) resulted in the crystallization of sulfides within silicate grains together with more gold and a range of Bi-Te-Se minerals.

Neumayr et al. (1993) have demonstrated that in Archean lode-gold deposits at Mt. York and Griffin's Find in Western Australia gold has been

liberated from the löllingite structure and concentrated at arsenopyrite-löllingite grain boundaries during the replacement of löllingite by arsenopyrite under slightly retrograde conditions. On the basis of natural and available experimental systems, it appears that the formation of native gold resulted from the inability of arsenopyrite to incorporate gold in its structure at high temperatures (Neumayr et al. 1993). This might have happened also at Osikonmäki. However, because in the Osikonmäki deposit gold seems to be relatively more abundant toward the centers of the early crystallized löllingite-arsenopyrite grains, it is conceivable that gold has been remobilized from the outer parts of these grains during subsequent hydrothermal processes. Fluids within the younger brittle-ductile shear zones precipitated sulfides (notably pyrite) and sulfosalts, as well as several Sb- and Ag-minerals (Kontoniemi et al. 1991).

GEOCHEMICAL INVESTIGATIONS

Geochemical features of the deposit have been examined previously by Kontoniemi and Ekdahl (1990) and in a broad synthesis of Fennoscandian gold deposits by Nurmi et al., (1991). In the latter study, Fennoscandian gold deposits were classified into three distinct groups, namely late Archean greenstone-hosted deposits, Paleoproterozoic deposits in the Lapland greenstone belt, and deposits of the juvenile Paleoproterozoic Svecofennian complex. Although deposits of all three groups show strong enrichment in gold and semimetals with respect to a hypothetical host rock of basaltic composition, the Svecofennian occurrences - including Osikonmäki - have some additional distinguishing features. For example they show a markedly greater enrichment in As, Bi, Te, Se, Ag, Sb, Cu and Sn, while conversely, they are relatively poorer in B and Mo. In general hydrothermal alteration is also less extensive than in other deposits (Nurmi et al. 1991).

The geochemical data considered here consist principally of routine analyses of ore, generally representing one meter long sections of drill core. The data have been analyzed as a single dataset, as well as in subgroups representing different parts of the deposit and also on the basis of ranking according to gold content. In addition, data from exploration trench OMK-87-M1 (n = 240, see Appendix 3) and several drill holes (BH 460, 464 and 478; n = 34, see Appendix 2) have been treated separately because of differencies in analytical methods used (Table 2).

Table 2. Analytical methods used, detection limits and number of samples (n).

Element	Method	GSF-code	n	Det. limit (ppm)
SiO_2, Al_2O_3, K_2O, Na_2O	XRF	175X	34	100
S	Leco	810L	5727	100
As, Cu, Zn, Pb, Ag	FAAS	511A	5727	1
Bi	FAAS	511A	240	20
Bi	GFAAS*)	419U	34	0.1
Te, Se	GFAAS	519U	34	0.01
Sb	GFAAS	511U	34	0.01
Au	Fire assay	704A	5727	0.1

XRF = X-ray fluorescence spectrometry
FAAS = flame atomic absorption spectrometry
GFAAS = graphite furnace AAS
Leco = Leco analyzer
*) = GFAAS after organic extraction

Statistical evaluation of data

Tables 3-5 present basic statistical parameters for those trace elements considered most relevant to ore genesis studies. Statistical analyses are presented for the whole dataset, as well for each exploration claim (areal distribution) and for different sets on the basis of gold content. Boundaries of the exploration claims are shown in Figure 14. The data have been analyzed using simple statistical procedures such as calculation of means, medians, maximum abundances, standad deviations (Table 3) and correlation coefficients for selected elements with respect to gold (Tables 4 and 5).

There are inherent problems in carrying out a more detailed statistical analysis of raw chemical data relating to mineralization since most analytical procedures assume a normal distribution for the data. On the other hand, exten-sive manipulation of the data prior to analysis might easily result in the loss of critical relationships from the point of view of ore-forming processes. Parkkinen (1992a) succeeded in nor-malizing the data for Cu, As and S from Osikonmäki using a relatively straightforward logarithmic transform operation but normaliza-tion of gold distribution is considerably more complicated. In the present study the "smooth-ing" and ranking is made in a somewhat more geological manner, by using a minimum inter-section length (4 m) and/or for longer sections a minimum gold value (cutoff 0.5 ppm). The mean concentrations for intersections are calcu-lated by weighting with length of the intersec-tions (Appendix 1). This modified dataset is then used for example in evaluating the areal distribution of particular elements.

Table 3. Statistical data for selected elements from Osikonmäki drill core samples. The values below the detection limit are replaced by 0 ppm. N = number of samples analyzed.

Data	Au (ppm)	Cu (ppm)	Zn (ppm)	Pb (ppm)	Ag (ppm)	As (ppm)	S (ppm)
MEAN VALUES							
Osi 1-4 (n=5487)	0.60	154	53	10	0.96	2090	5020
Osi 1+3 (n=3583)	0.78	214	47	9	0.94	2400	4430
Osi 2 (n=1364)	0.15	45	56	10	0.84	1540	5760
Osi 4 (n=540)	0.53	36	51	5	1.4	1400	7040
Ore (n=782)	3.10	465	51	12	1.6	7270	7680
IS (n=164)	1.60	307	61	12	1.5	4100	7150
MEDIAN VALUES							
Osi 1-4	0.10	59	46	8	1.0	300	4300
Osi 1+3	0.20	110	42	8	1.0	200	3500
Osi 2	0.10	33	56	6	1.0	400	5500
Osi 4	0.10	31	50	0	1.0	500	6600
Ore	1.90	270	45	9	1.0	2950	7600
IS	1.20	216	49	9	1.0	2000	7000
MAXIMUM VALUES							
Osi 1-4	68.8	3680	1700	460	25.0	77000	$1.02*10^5$
Osi 1+3	68.8	3680	1700	460	16.0	77000	$1.02*10^5$
Osi 2	9.0	1100	150	181	8.0	40000	19900
Osi 4	26.8	262	241	117	25.0	23200	48500
Ore	68.8	3680	578	460	25.0	77000	31600
IS	8.8	1540	288	88	9.3	28000	16000
STD. DEVIATION							
Osi 1-4	1.80	277	46	17	0.88	5340	4170
Osi 1+3	2.10	327	55	14	0.79	6170	4360
Osi 2	0.49	47	21	17	0.54	3470	3350
Osi 4	1.90	23	19	9	1.7	2300	3820
Ore	4.00	547	37	24	1.7	10500	4600
IS	1.50	344	37	12	1.2	4900	2950

Osi 1....4 = exploration claim areas Osikko 1....4 (see Figure 14)
Ore = ore samples with 1 ppm Au cutoff value in whole exploration area (Osikko 1-4)
IS = ore intersection data from bore holes in claims Osikko 1-4 (Appendix 1) with mean concentrations weighted with length of ore section. Minimum length for intersections is 4 m and the cutoff value for longer intersections is 0.5 ppm Au.

Table 4. Spearman correlation coefficients of selected elements with respect to gold. Same data as presented in Table 3, with coefficients having been calculated only for cases where values exceed analytical detection limits (see Table 2). N = number of cases. Correlations above 0.500 are shown in bold type.

Data	n	Au-Cu	Au-Zn	Au-Pb	Au-Ag	Au-As	Au-S
Osikko 1-4	3148 - 4064	**0.619**	-0.013	0.220	0.364	0.425	0.413
Osikko 1+3	2168 - 2917	**0.678**	0.156	0.274	0.414	0.477	**0.587**
Osikko 2	657 - 797	0.136	-0.069	0.091	0.253	0.440	0.320
Osikko 4	162 - 350	0.324	-0.109	0.058	0.354	0.400	0.203
Ore	658 - 718	0.186	0.131	0.150	0.374	0.165	0.202
IS	157	0.488	-0.111	0.208	**0.549**	0.369	0.300

The following features are evident from an inspection of the tabulated data:

Data for Osikko 1-4

- arithmetic means and median values for Au, Cu and As differ substantially from one another and std. deviation values are high, indicating a highly skewed distribution;

- Au shows strongest positive correlation with Cu and a moderate correlation with As, S and Ag

Data for Osikko 1+3, Osikko 2 and 4

- Osikko 2 has generally lower gold abundances

- Osikko 1+3 has high Cu and relatively high std. deviation value for As

- Zn and Pb concentrations are rather uniform throughout each area

- gold shows good positive correlation with Cu and S in Osikko 1+3 and moderate correlation with Ag, As and S throughout the whole area

Data for Ore and Intersections (IS)

- based on a restricted dataset defined by a cut-off grade of 1 ppm for Au, the mean Au and As concentrations are in reasonable agreement with mean values obtained in ore reserve estimations

- the mean and median values of all elements (except As) for the data Intersections (IS) are rather similar

- as expected, the ore itself has distinctly higher Au, Cu, As and S concentrations than those of the whole dataset, while the values of other elements are close to the mean for the whole dataset

- for the data Ore, only Ag shows consistent positive correlation with gold, but for IS also Cu and As show some degree of positive correlation.

Because of the inconsistent nature of gold distribution, correlation coefficients for other elements with respect to gold should be treated with caution. In the present case, correlation coefficients show considerable variation both areally and when ranked according to absolute gold concentration (Table 4 and Figure 13). The coefficients for four gold abundance intervals nevertheless display some mutually consistent trends (Figure 13):

- correlation of Zn and Pb with Au is everywhere poor

- correlation between Au and As systematically weakens with increasing Au concentration, while the opposite behaviour is observed with respect to Ag.

The data in Table 5 represent samples taken from the ore horizon as well as from the hanging wall and
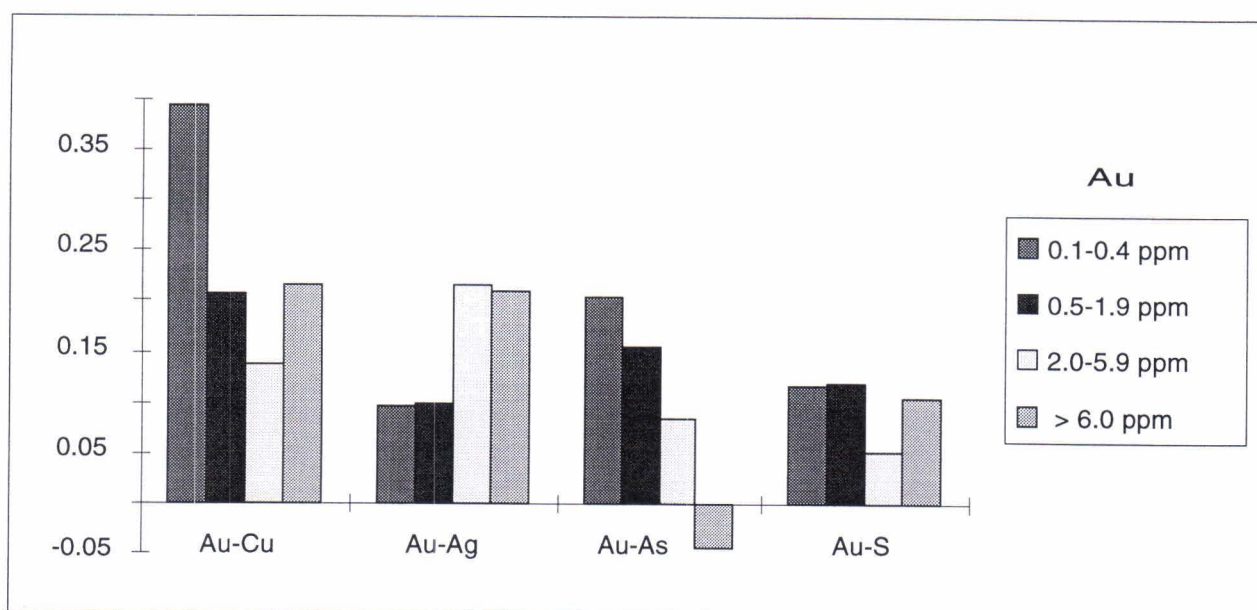

Fig. 13. Variation of Pearson correlation coefficients for Au-Cu, Au-Ag, Au-As and Au-S pairs in four different gold content classes. Number of cases in class 0.1-0.4 ppm = 1491, 0.5-1.9 ppm = 673, 2.0-5.9 ppm = 240 and > 6.0 ppm = 59.

footwall. On the basis of correlation coefficients for gold it is possible draw some conclusions concerning, for example, alteration phenomena associated with mineralization. Negative coefficients for Al_2O_3 and Na_2O and slightly positive coefficients for K_2O/Na_2O, SiO_2/Al_2O_3 and more strongly positive for S and As all reflect hydrothermal alteration processes

(such as potassium metasomatism, silicification and sulfidation). Moreover, good correlation exists between Au and Sb, Te and Se. Although there is generally only poor correlation between Au and Bi in the present case, exceptionally high positive correlations were found for samples from exploration trench OMK-87-M1 (Table 6).

Table 5. Spearman correlation coefficients (C) with respect to gold for analytical results from BH 460, 464 and 478 (Appendix 2, n = 34). Correlations above 0.500 or below -0.500 are shown in bold type.

Variable	C	Variable	C	Variable	C
SiO_2	-0.152	S	**0.860**	Sb	**0.605**
Al_2O_3	-0.464	As	**0.815**	Te	**0.671**
Na_2O	**-0.528**	Cu	0.350	Se	**0.636**
K_2O	0.118	Zn	0.414	Bi	0.316
K_2O/Na_2O	0.303				
SiO_2/Al_2O_3	0.262				

Table 6. Spearman correlation matrix for analytical data from exploration trench OMK-87-M1 (Appendix 3, n = 240), calculated only for cases where values exceed analytical detection limits (n_{min} = 86 for Au-Bi pair and n_{max} = 224 for Au-As, Au-S and Au-Cu pairs). Correlations above 0.500 are shown in bold type.

	As	S	Ag	Cu	Bi	Au
As	1.000					
S	**0.752**	1.000				
Ag	0.316	0.318	1.000			
Cu	0.214	0.131	0.214	1.000		
Bi	0.089	0.356	0.298	-0.008	1.000	
Au	**0.648**	**0.644**	0.244	-0.078	**0.743**	1.000

Spatial variations in element concentrations

In order to evaluate areal changes in the distribution of particular elements in ore grade material, the data listed in Appendix 1 (IS) have been processed with a routine procedure using the ALKEMIA software package developed at the Geological Survey of Finland (i.a. Ahlsved et al. 1991). For drill core intersections (IS) from exploration claims Osikko 1+3 and 4 (see Figure 14) a cut-off value of 0.5 ppm has been used, but in the case of the Osikko 2 claim, it has been necessary to compromise cut-off values in order to obtain a sufficiently comprehensive dataset; values for the data IS are nevertheless based on the best 4 m intersection in any given drill hole. Concentrations quoted in Appendix 1 for each intersection represent mean values weighted

with section length. For vertical drill holes the best interval represents the entire core. For inclined holes, positions on the map represent projections of centers of ore intersections to the ground surface.

Consideration will be given first to evaluation of the shear zone throughout the whole of the area drilled (Figures 14 and 15). High gold values are clearly concentrated towards the eastern and western ends of the shear zone, enabling the areas of greatest potential to be readily delineated. Maximum values of gold and arsenic do not appear to coincide, which is consistent with the evidence of the correlation coefficients for Au and As becoming poorer with increasing gold content. The highest concentrations of Zn are found in the area of the
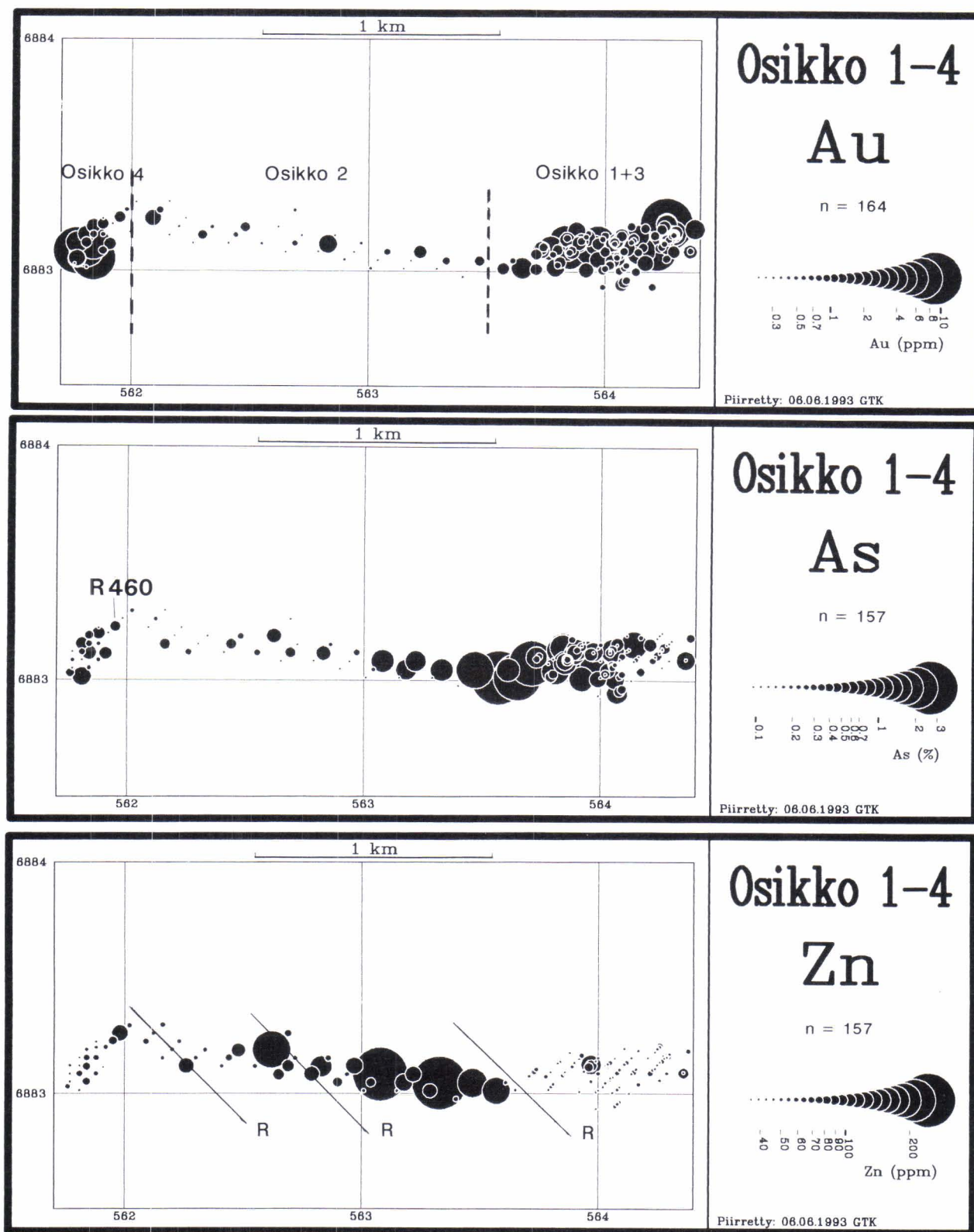
Fig. 14. Areal distribution of Au, As and Zn in the Osikonmäki shear zone (see Fig. 2) based on drill core analyses (see text). The location of claims (Au map) and younger brittle-ductile shears (R in Zn map) are also shown.
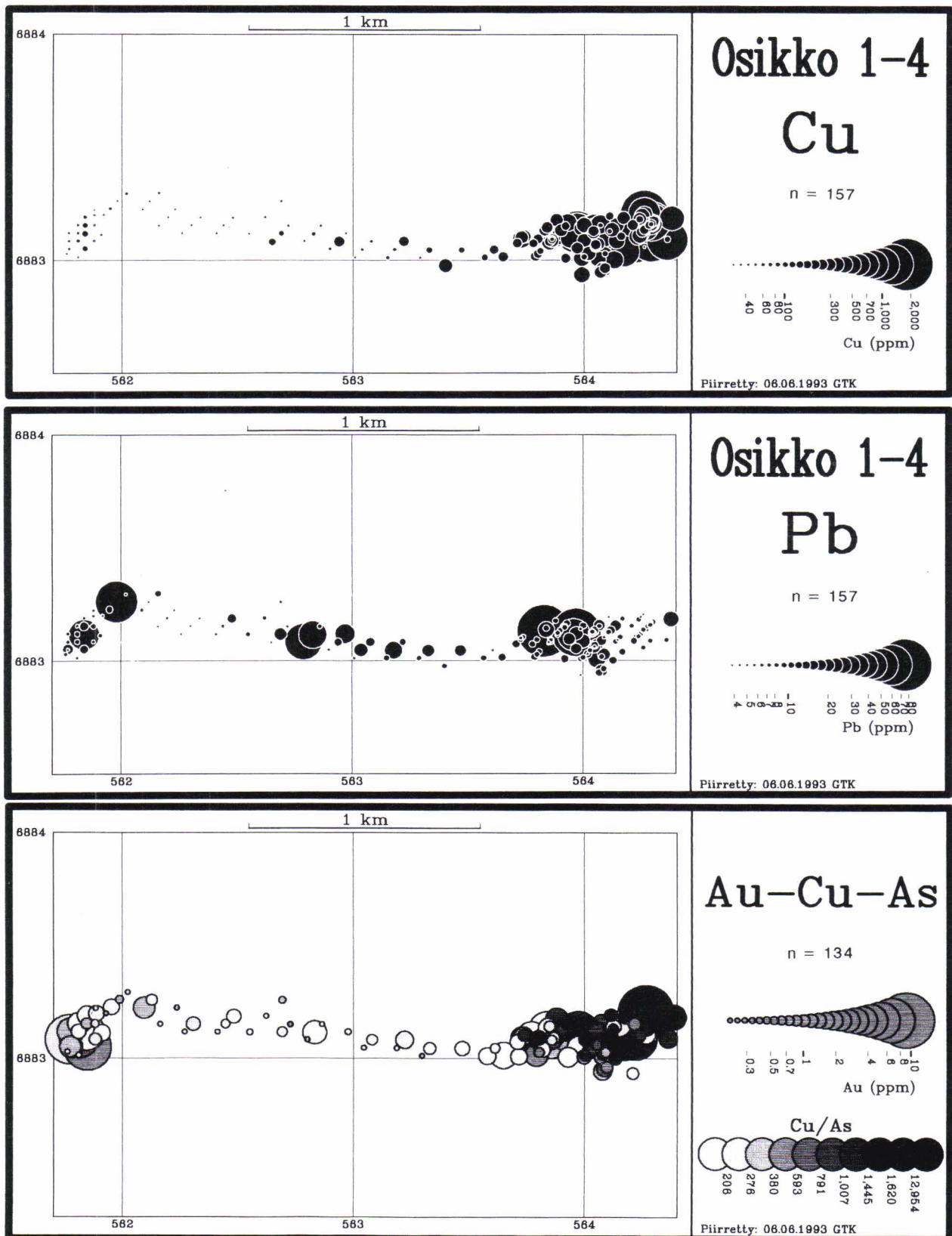
Fig. 15. Areal distribution of Cu, Pb and Au versus Cu/As in the Osikonmäki shear zone. Data as in Fig. 14.

Osikko 2 claim while Cu contents are greatest towards the eastern end of the deposit. No large scale features are discernible in the distribution of Pb but a positive correlation is evident between Au and the Cu/As ratio, particularly towards the east. The rocks from the Osikko 2 claim can clearly be distinguished from the rest of the shear zone on the basis of both mineralogy and geochemistry. This might be attributed to distinctive structural features as well as changes in fluid chemistry; because the younger brittle-ductile shear zones described earlier truncate and disrupt the main shear zone (cf. Figure 14), it is therefore possible that Osikko 2 represents different level through the deposit compared the eastern and western extremities.
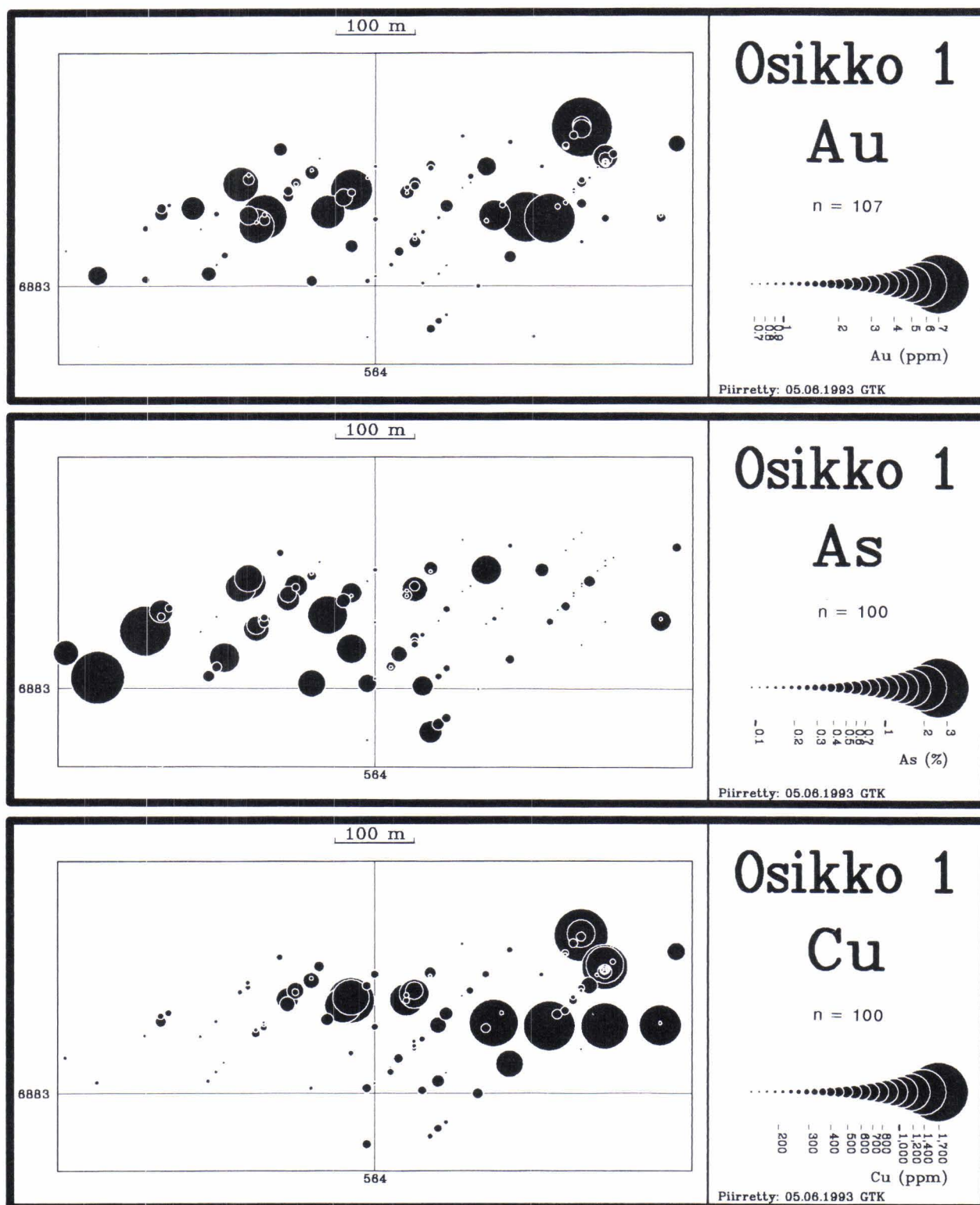
Fig. 16. Areal distribution of Au, As and Cu in the claim Osikko 1 and 3 (see Fig. 14) based on drill core analysis.

Mänttäri and Parkkinen (1990) and Parkkinen (1992a) have studied the internal chemical zonation in the Osikko 1 exploration claim using geostatistical software based on the PC-XPLOR program. The results of these studies indicated that the area can be separated into two distinct parts, namely a western part rich in As and S and an eastern part enriched in Cu. In the western part, Au is closely associated with As, while in the east there is only partial correlation with As but a strong association with Cu. Between these two areas is an E-W trending domain termed the "copper line", in which elevated gold concentrations are only accompanied by high values of copper.

The surface projection of Osikko 1 (Figure 16) reveals the same features, with As predominant in the west and Cu to the east, although on the basis of As distribution the boundary between the two domains trends NW-SE, which is parallel to that of the brittle-ductile shear zones shown in Figure 14. The trend of the Cu anomaly in the central part of the area is, in contrast, almost E-W and the highest gold abundances are also found along this anomaly; this might reflect the complex multistage history of gold enrichment. In ore mineralogy, there is a clear difference between western and eastern part of the claim Osikko 1. The abundance of löllingite and arsenopyrite decreases gradually eastwards while chalcopyrite is most abundant in the eastern part of Osikko 1. Based on thin section investigations, it is obvious that the amount of gold associated with silicates is larger in the eastern than the western part of the area.

Geochemical characteristics of alteration

Alteration processes related to mineralization within the Osikonmäki shear zone do not appear to be as extensive as those associated with most of well studied Archean gold deposits, nor those associated with the Proterozoic deposits in the Lapland greenstone belt (cf. Nurmi et al. 1991). A
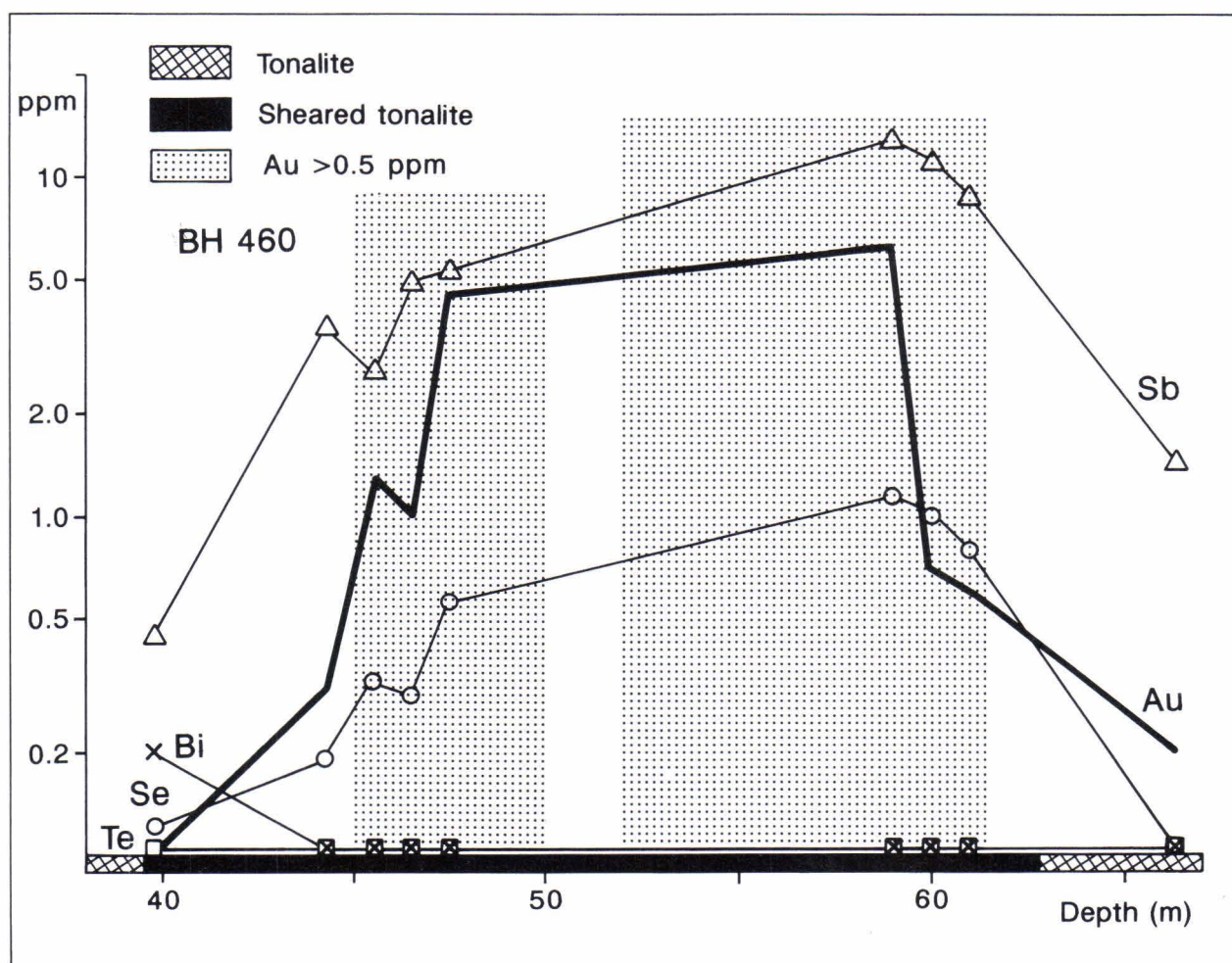
Fig. 17. Variation in concentration of Au and semimetals in BH 460 (location in Fig. 14). Note the logarithmic concentration scale.

further difference is the absence of intense carbonatization and lack of abundant quartz veins, with K and S metasomatism being the only readily discernible alteration phenomena. Moreover, the Osikonmäki deposit has undergone subsequent medium grade metamorphism which has modified the alteration assemblages and hence made it difficult to carry out conventional mass balance calculations with confidence. The present mineral assemblage therefore represents the product of several superimposed events.

The most obvious mineralogical manifestations of alteration, namely increases in the amount of biotite, K-feldspar, silica and sulfides, are reflected chemically by changes in the ratios of K_2O/Na_2O and SiO_2/Al_2O_3, S and As contents (Table 5 and Figures 20-22). Base metal concentrations are low, as is typically the case with epigenetic gold mineralization (Groves 1993, McCuaig & Kerrich 1994). All semimetals are, in contrast, strongly enriched, with selenium differing in this respect from many Archean gold deposits (Nurmi et al. 1991).
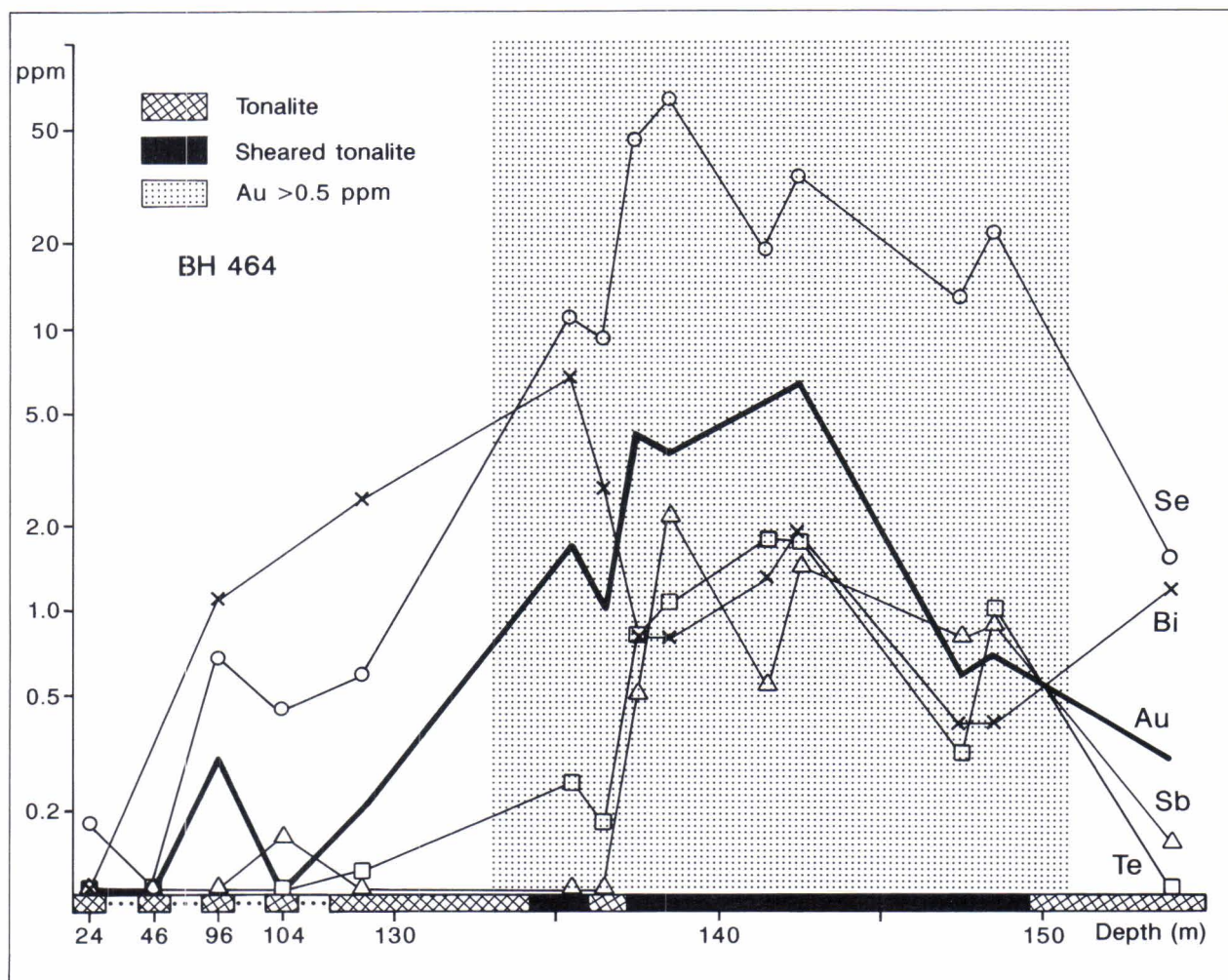
Fig. 18. Variation in concentration of Au and semimetals in BH 464 (location in Fig. 6). Note the logarithmic concentration scale.

The diagrams presented in Figures 17-22 illustrate the variations found in concentrations of several elements from drill holes BH 460, 464 and 478, within both the shear zone and immediately adjacent less sheared rock. Drill hole BH 460 (see location in Figure 14) is situated in the western part of the shear zone, while the other two are located in the eastern part (see Figure 6). These holes were chosen because they are almost perpendicular to the ore horizon, although it was not possible to obtain analyses for the hanging wall rocks overlying the shear zone in BH 460.

As might be expected from the nature of the ore mineralogy, concentrations of semimetals (Figures 17-19) closely follow the trend for gold, although some additional distinctive features can be recognized in certain areas and with respect to certain elements:

- on the whole, Se tends to most closely image Au distribution;

- Sb concentrations appear to increase west-
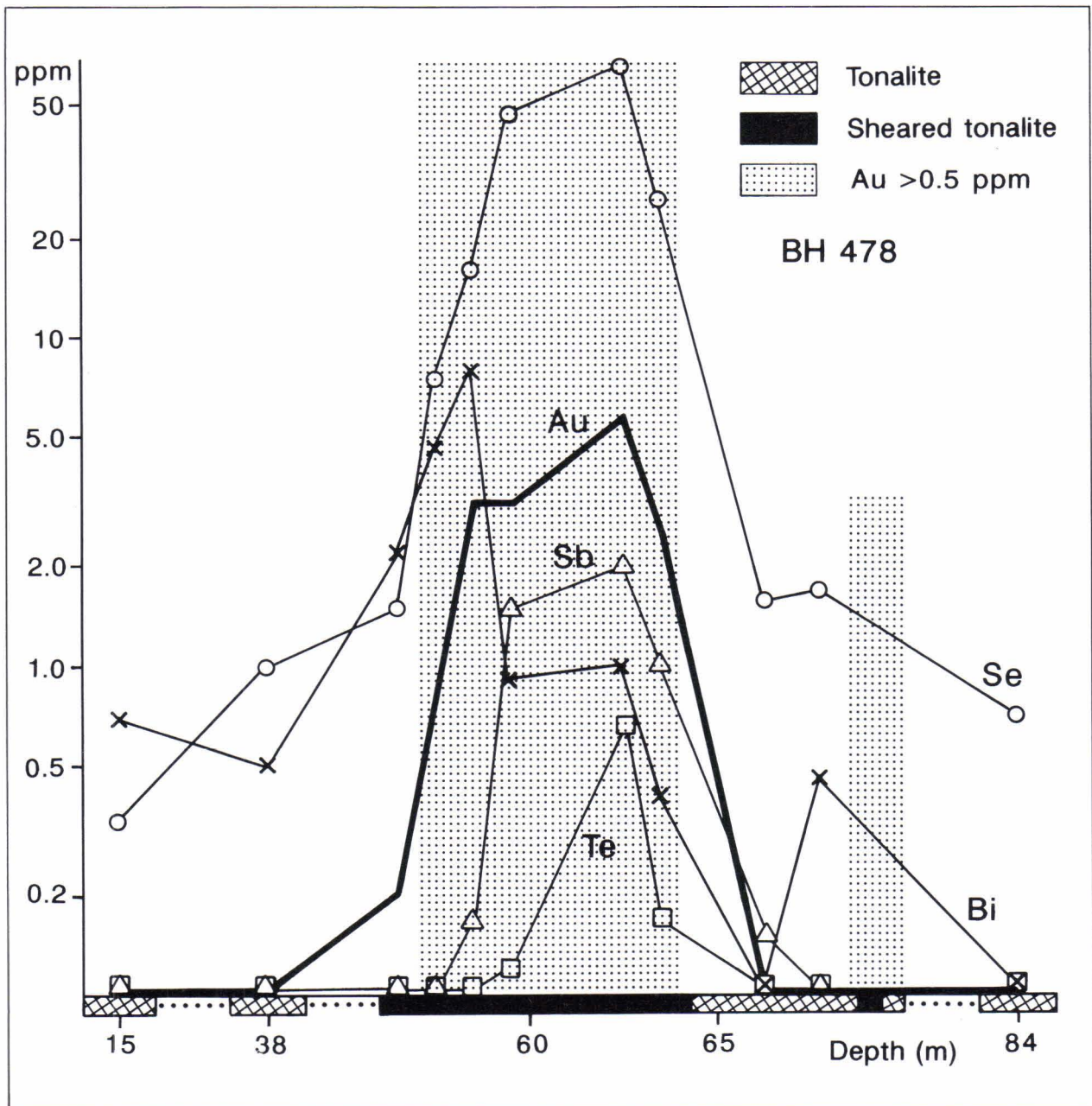
Fig. 19. Variation in concentration of Au and semimetals in BH 478 (location in Fig. 6). Note the logarithmic concentration scale.

wards, whereas other semimetals show the opposite trend;

- in the eastern part of the shear zone, Se and Bi define a positive aureole for up to several tens of meters from the ore;

- the aureole for Bi is only evident in the hanging wall rocks, while elevated Se concentrations are also present in the footwall beneath the shear zone.

Figures 20-22 show Si/Al and K/Na ratios and variations in S, As, Cu and Zn contents for the same drill holes. Also from these diagrams it is apparent that the samples from BH 460 (Figure 20) represent too short intersection outside the ore horizon for reliable conclusions concerning alteration anomalies. In general however, Si/Al and K/Na ratios tend to increase within the ore horizons. Higher values nevertheless indicate
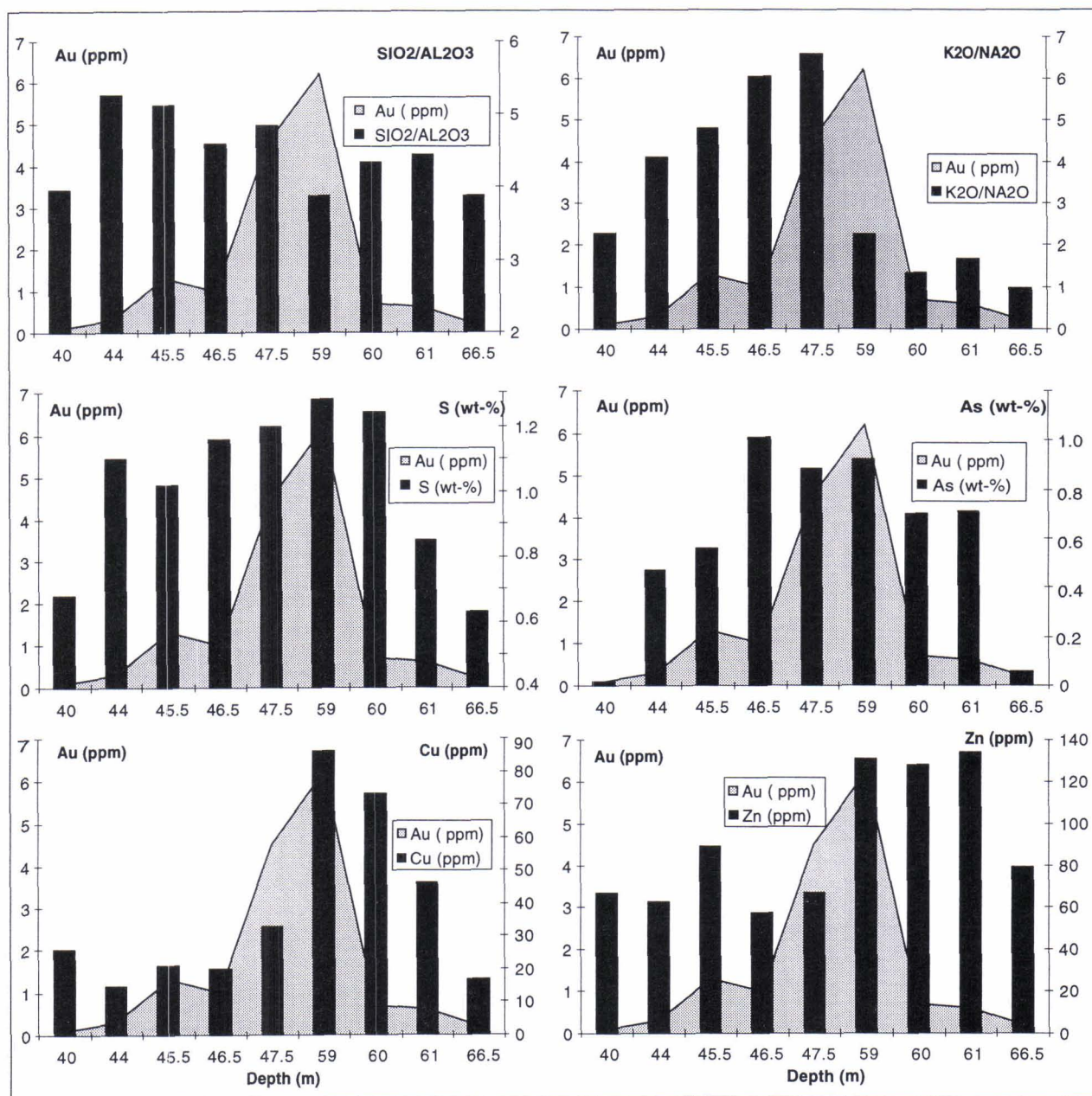
Fig. 20. Variation in SiO_2/Al_2O_3 and K_2O/Na_2O and in abundances of S, As, Cu and Zn with respect to gold content in BH 460.

more intensely deformed zones, characterized by a greater abundance of quartz veins and secondary K-feldspar. These features coincide with the upper contact of the shear zone in BH 460 but with the footwall contact in the eastern drill holes. A negative anomaly may exist with respect to the K/Na ratio immediately beneath the hanging wall contact (BH 464 and 478).

The positive correlation of gold with S, As and Cu is also apparent from the coincidence

between the ore and peak abundances for these elements in the profiles, together with aureoles in both the footwall and hanging wall resembling that for Se (BH 464 and 478). There is however only weak correlation between Zn and Au, particularly towards the eastern end of the shear zone, a feature which is evident from the erratic abundances in BH 464 and 478. The higher Zn values in BH 460 are nevertheless associated with the footwall contact.
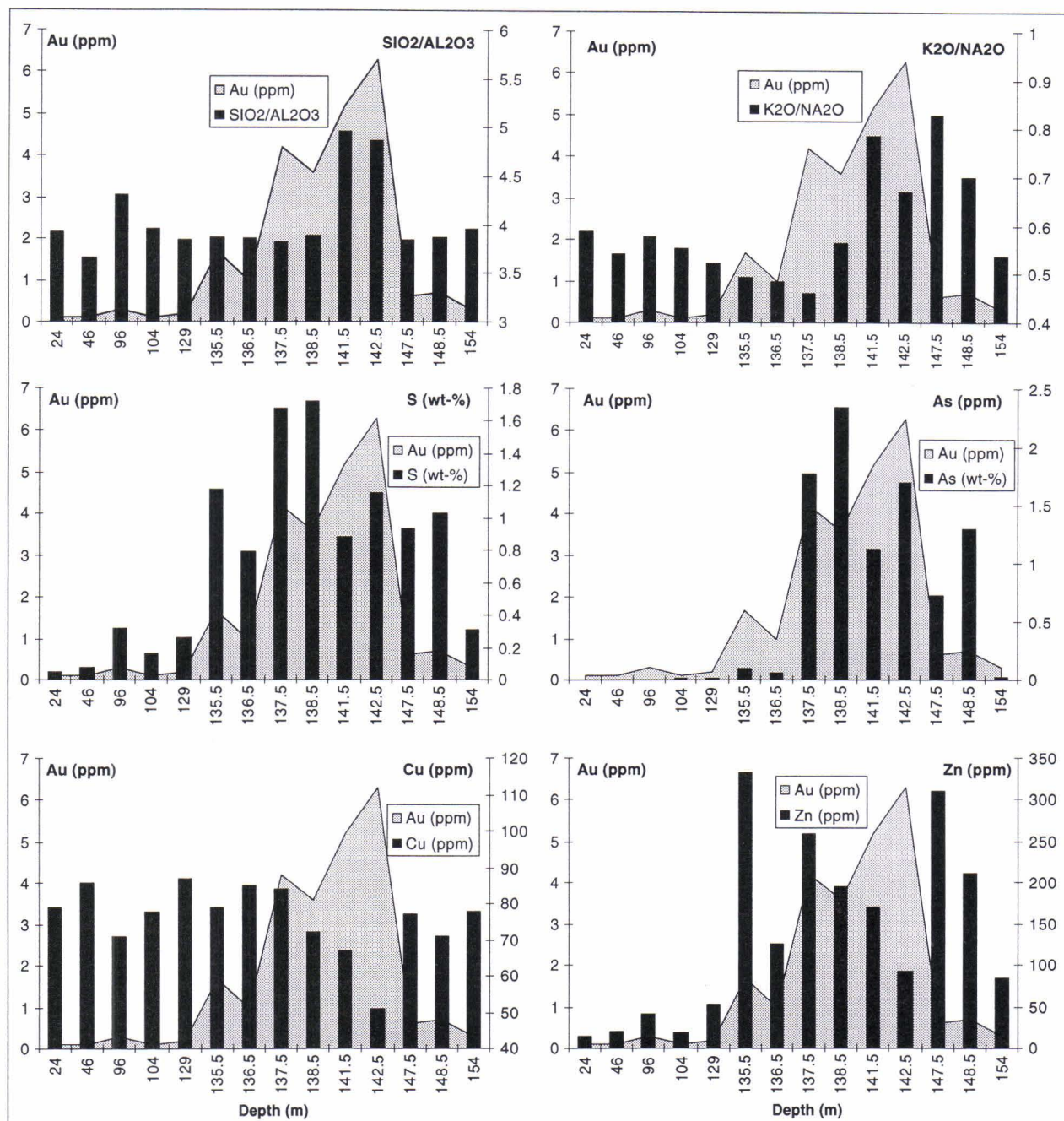
Fig. 21. Variation in SiO_2/Al_2O_3 and K_2O/Na_2O and in abundances of S, As, Cu and Zn with respect to gold content in BH 464.
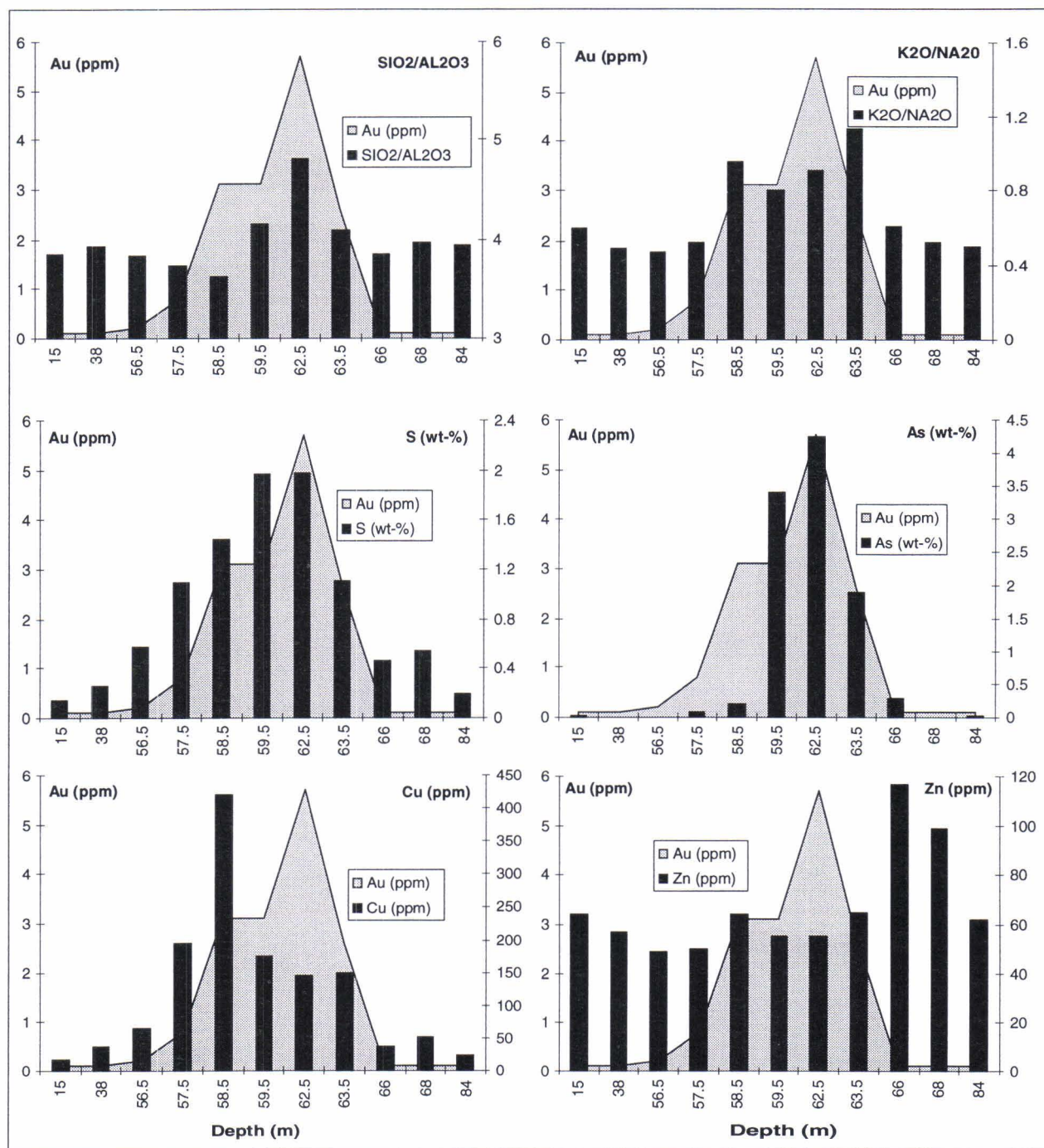
Fig. 22. Variation in SiO_2/Al_2O_3 and K_2O/Na_2O and in abundances of S, As, Cu and Zn with respect to gold content in BH 478.

DISCUSSION OF ORE FORMATION PROCESSES

Structural controls

Shear zones represent the loci of deformation and faulting in which the length of the deformation zone exceeds its width by a factor of at least 5 (Bursnall 1989). Depending on deformation mechanisms and conditions, shear zones may be further classified as brittle, ductile, or brittle-ductile. Shear zones typically record a range of superimposed brittle and ductile events. Brittle deformation processes dominate in the upper crust and at low metamorphic grade, occurring preferentially in competent massive rock types and at relatively rapid strain rates. Broader ductile shear zones form at deeper levels below depths at which earthquake failure occurs, corresponding to amphibolite and granulite facies metamorphic conditions (Bursnall 1989).

Within the plate tectonic context, reference is commonly made to both extensional and compressional shear zones, the former being typical of seafloor spreading and rift-related processes, while the latter predominate in convergent settings. Extension may however be broadly coeval with or alternate with episodes of compression, particularly in areas of oblique collision. Within collisional zones, up to half of the volume of tectonically overthickened crust may be subject to dehydration, with the metamorphic peak and thermal equilibration attained up to 50 Ma after the onset of collision (Murphy 1989).

Mesothermal deposits typically form in the region in which deformation styles are transitional from brittle to ductile, with alternations between brittle failure and plastic flow commonly being caused by cyclic changes in fluid pressure. Abrupt changes in shear zone trend, flexures and jogs all represent favorable sites for dilation and hence enhanced fluid flow and mineralization (Bursnall 1989, Murphy 1989).

Many Archean gold deposits have been shown to occur in association with crustal scale shear systems, although in detail gold is found in subsidiary oblique structures rather than within the major shear zones themselves (Groves & Foster 1991). Gold occurs in both brittle and ductile shear zones, and in many instances evidence for both brittle and ductile deformation is found within a single ore body; brittle structures tend to be characterized by more vein-type mineralization, whereas ductile shear zones exhibit more disseminated mineralization (Murphy 1989).

The Rantasalmi area lies within a Paleoproterozoic collision zone (Gaál 1986), represented by the NW-SE trending Kolkonjärvi and Haukivesi shear zones (Fig. 2). The Osikonmäki gold deposit occurs within an E-W trending shear zone between these two major shear zones. It has not been possible to trace this shear zone outside the tonalite intrusion, which may be explained by the difference in behaviour and orientation of the granitoid with respect to country rocks during deformation.

According to earlier studies (cf. Gaál 1986), convergence and subduction along the Ladoga - Bothnian Bay zone took place toward the NE or NNE, resulting in the formation of dextral NW-trending strike-slip shear systems (Ekdahl 1993). On the basis of regional aeromagnetic data however, the amount of displacement associated with the shear zones in the Rantasalmi area is rather limited, implying that a dip-slip component to deformation was significant.

One possibility for explaining the origin of the Osikonmäki shear zone is in terms of heterogeneous shear strain partitioning between two first order shear zones, with more competent units such as the tonalite intrusion promoting the development of discrete second order shear zones. During the early stages of deformation, these zones may have been dilatational and undergone brittle failure, focussing fluid flow; subsequent ductile deformation has overprinted and more or less obscured the early formed structures (cf. Hodgson 1989).

The Osikonmäki shear zone shows distinct plastic deformation features, including strong foliation development and blastomylonitic textures with concordant narrow quartz veins, indicating a strong simple shear component parallel to the boundaries of the zone, and/or prolonged deformation (cf. Bursnall 1989). Ductile deformation can be attributed to either lowering of fluid pressures or an increase in metamorphic grade.

On the basis of orientations of intrafolial minor folds and ore shoots within the shear zone a reverse dip-slip motion can be inferred for the main stage of ductile deformation. A commonly observed feature in ore deposits elsewhere is that lodes tend to lie within the intersection lineation defined by mylonitic S- and C-surfaces (cf. Poulsen & Robert 1989); in the case of Osikonmäki, this is consistent with the gentle ESE plunge observed for the ore lodes. Folding of the shear zone and the formation of en echelon shear zones in the eastern end of the shear zone could also have generated the possibility for a further stage of fluid activity, thereby explaining the anomalous Au-Cu enrichment in this area.

As a result of superimposed thermal metamorphism and regional uplift, the Osikonmäki shear

zone was disrupted by vertical brittle faulting, accompanied by the formation of quartz veins and quartz-tourmaline breccias, though these events did not lead to further mineralization, or significant redistribution of existing mineralization.

The age of mineralization at Osikonmäki

Svecofennian gold deposits are generally considered to have formed after the emplacement of synorogenic granitoids (Nurmi et al. 1991). Since the Osikonmäki shear zone also deforms such a synorogenic intrusion, dated at 1887±5 Ma (Vaasjoki & Kontoniemi 1991), this provides a maximum age for gold mineralization. Constraining the minimum age is less straightforward, since only the Pirilä-type granites, dated at 1815±7 Ma (Vaasjoki & Sakko 1988) are observed to cut the mineralization. Deformation and recrystallization of textures within the already mineralized shear zone during prograde regional metamorphism requires that ore formation took place prior to D_3 (at around 1830 Ma)

(Kilpeläinen 1988). Granitoids of the Putkilahti complex in the Hiltula area (see Figure 2), dated at 1850±7 Ma (Vaasjoki & Kontoniemi 1991), do not contain shear zones such as that affecting the Osikonmäki intrusion, from which it is inferred that gold mineralization took place rather soon after the intrusion of the Osikonmäki tonalite. However, gold has apparently undergone some local later enrichment, particularly in the eastern part of the area, where Au-Cu fluids were evidently active during the final stages of D_3, if not still later. Brittle-ductile shear zones containing chalcopyrite have also been found within gabbros and granitoids of the Putkilahti complex.

Fluid activity

Epigenetic gold deposits are invariably associated with considerable fluid flow through zones of active deformation, thus providing physical and chemical mechanisms and opportunities for dissolution, transport, enrichment and precipitation of gold and related elements. The origin of such fluids, and hence the source of gold, can be studied by using stable isotopes (C, O, H, S) and fluid inclusions. It is generally considered however, that the source composition itself is not as significant as the availability of fluid and pathways for efficient fluid flow combined with suitable chemical and physical sites for metal precipitation.

Gold mineralizing fluids in Archean mesothermal deposits are generally attributed to devolatilization reactions during regional metamorphism of the lower crust, with the additional possibility of an input from magmatic activity, mostly felsic intrusions (Groves & Foster 1991). During hydrothermal processes gold occurs principally as HS^- and Cl^- complexes in a multicomponent electrolyte fluid (Seward 1991). Because fluids related to mesothermal gold mineralizations in general appear to have been of relatively low salinity and H_2O - CO_2 dominated (Phillips 1996), bisulfide complexes would have dominated gold transport. However, in the absence of sufficient experimental data, the role of complexes containing Bi, Te, Sb, Se and As in gold transport remains uncertain.

It has been documented from modern active epithermal systems in New Zealand that a sudden drop in fluid pressure leads to boiling, which promotes rapid precipitation of gold from solution. A consequence of adiabatic boiling and loss of a vapour phase is that a temperature drop of as little as 15° is sufficient to lead to gold precipitation (Seward 1989).

Gold precipitation may also occur due to breakdown of gold-bearing complexes through reaction with wallrock. Sulfidation of iron-rich wallrocks or other replacement reactions, with carbonate-bearing horizons for example, tend to destabilize gold complexes. Metamorphic reactions also show strong fluid buffering capabilities; for this reason slower and more pervasive fluid flow in and around ductile shear zones enhances the opportunity for fluids to equilibrate with a larger volume of rock than is the case with rapid fluid flow through transient brittle pathways. As a consequence, brittle deformation zones commonly show more intense wallrock alteration (Murphy 1989).

Poutiainen (1993) has studied fluid inclusions from the Pirilä deposit, which has the same Pb isotope characteristics as Osikonmäki (Vaasjoki & Kontoniemi 1991), but is situated to the west of the Kolkonjärvi shear zone. Four different inclusion types were identified: a weakly saline H_2O-CO_2 type fluid interpreted as being of relict primary origin, together with secondary CO_2-, CH_4- and H_2O types. The first fluid type would have been

associated with D_2 and D_3 deformation and amphibolite facies metamorphism, while the latter fluids were presumable related to D_4 (Poutiainen 1993).

Fluid inclusions within quartz from the Osikonmäki shear zone have been studied recently by Liimatainen (1998, this volume), with four separate types of inclusion-bearing quartz being recognized:

QA: Sheared tonalite quartz, forming the host rock to the deposit, together with feldspars and mica. Recrystallization has resulted in a granoblastic texture with equigranular quartz grains.

QB: Disrupted thin quartz veins concordant with foliation and which may also have been folded; these veins are noticeably thinner than QD-type veins.

QC: A distinctive spotty quartz type containing small exsolutions of K-feldspar, found only in association with QD quartz.

QD: Forms widest veins, with clear and unbroken large crystals.

The oldest, QA-type quartz contains sporadic small CO_2-type inclusions, which is rather typical of amphibolite facies rocks in general. Inclusions formed prior to recrystallization related to metamorphism have been destroyed so that it is not possible to infer the nature and history of the fluids associated with arsenides and gold. Inclusions within the three younger types of quartz (QB, QC and QD) have apparently formed under similarly water-rich conditions. The primary and early secondary inclusions are characterized by low salinities, ranging from 2% in the western part to 5% in the east. The late secondary inclusions show both low and higher (10%) salinities. One of the high salinity late secondary inclusions from the eastern part of the deposit was found to contain grains of gold and bismuth (Liimatainen, this volume).

The Ladoga - Bothnian Bay collision zone has presumably been subjected to fluids of both metamorphic (related to subduction and the late metamorphic Sulkava thermal dome) and magmatic (three stages of granitoid emplacement) origin. Fluids have in particular been focussed into second order shear zones during ductile deformation. On the basis of associated mineral parageneses it appears that formation of early sulfides commenced at relatively high temperatures (about 500°C), probably precipitating from fluids in which gold was transported as thio- and thioarsenide complexes. The fluid also apparently contained abundant Bi, Te and Se, as indicated by the presence of inclusions in löllingite and arsenopyrite. More saline aqueous fluids were active during later stages of deformation within the shear zone and to some extent remobilized gold from deeper levels. Fluorite-bearing cavities near the area affected by later granites also supports an interpretation involving late saline fluids.

THE OSIKONMÄKI DEPOSIT - A SYNTHESIS AND MODEL

The Osikonmäki gold deposit represents an epigenetic, tonalite-hosted ore body within a ductile second order shear oriented obliquely between two major crustal scale shear zones. The shear zone formed and underwent continued ductile deformation during amphibolite facies metamorphism related to arc-continent collision. The deposit was subsequently disrupted somewhat by approximately N-S trending brittle-ductile shear zones.

The ore is characterized by disseminated pyrrhotite and arsenopyrite and forms a series of en echelon and folded lodes exhibiting an overall gentle plunge towards the ESE.

Ore fluids were probably metamorphic or mixed metamorphic-magmatic in origin and gold was presumably transported by thio- and thioarsenide complexes. Halogen complexes were evidently not important since the base metal abundances in the deposit are generally low. On the basis of ore mineralogy, it is inferred that gold exsolved from arsenic-bearing minerals under a high mesothermal or hypothermal (Lindgren 1933) temperature regime soon after the emplacement of the synorogenic Osikonmäki tonalite intrusion, yet before the regional metamorphic peak. Fluid inclusion studies indicate that this main mineralizing phase was followed, especially in the eastern part of the deposit, by the local influx of more saline aqueous fluids that resulted in some redistribution of gold and associated elements to higher structural levels.

Although gold is the only metal of economic interest at Osikonmäki, the deposit nevertheless shows strong enrichment in As, Bi, Te, Se, Ag, Sb, Cu and Sn, which is characteristic of Svecofennian gold deposits in general (Nurmi et al. 1991). The median Au/Ag ratio is around two, which is low when compared with Archean mesothermal gold deposits but quite typical for Svecofennian occurrences (Nurmi et al. 1991).

Within the deposit, Au concentrations correlate particularly well with Se, Te, Sb, Bi and Cu, and moderately As, S and Ag abundances. At high Au

concentrations however, the correlation between Au and As is less apparent, while correlation between Au and Ag conversely improves, suggesting perhaps late enrichment of gold. Based on ore mineralogy, the correlation between gold and semimetals varies regionally. Inclusions of native gold and bismuth, hedleyite and ikunolite are common within arsenide minerals, but Sb minerals only occur in the western part of the deposit. In high grade ore, gold grains typically also occur outside the arsenide phase and the amount of chalcopyrite is clearly larger, particularly in the eastern part of the deposit.

In addition to the effects of hydrothermal altera-

tion, the shear zone mineralogy and textures also record superimposed prograde and retrograde metamorphic events, the latter being mainly restricted to younger brittle-ductile shear zones. Away from the immediate vicinity of the mineralized shear zone, metamorphic processes appear to have been isochemical, while within the shear zone, alteration is manifest by the abundance of biotite, quartz, sulfides, K-feldspar and locally tourmaline. A positive geochemical halo, in places up to several tens of meters in thickness, is defined by anomalous abundances of Se, Bi, As, S and Cu, especially in the cataclastic porphyritic tonalite in the hanging wall of the deposit.

COMPARISONS WITH OTHER SVECOFENNIAN GOLD DEPOSITS

There is significantly less published information available for Proterozoic mesothermal granitoid-hosted gold deposits than for Archean greenstone-hosted gold deposits and Phanerozoic collision zone deposits. There is no reason to suppose however, that ore forming processes differed substantially in the Proterozoic. Hence, Proterozoic epigenetic deposits are also found in extensive deformation zones exhibiting a wide range of mineralization style and host rock lithology.

Svecofennian gold deposits have some distinctive geochemical characteristics (Nurmi et al. 1991), and tend to occur in four separate geographic provinces, namely Skellefte, Central Ostrobothnia, the Tampere region and southern Savo (Figure 23). Gold mineralization was approximately coeval in all four provinces and varies in style from vein-type deposits, which are the most common, through porphyry and stockwork types, to disseminated shear zone hosted deposits.

Fig. 23. Logation of Svecofennian gold provinces. Modified from Nurmi et al. (1991).

Tampere area

The gold deposits of the Tampere area (Kutema-järvi, Järvenpää) are typically found within rock associations containing pyroclastic volcanogenic deposits and are evidently closely related to magmatic activity (Luukkonen 1994). Mineralization in many occurrences postdated at least the earliest stages of regional deformation and metamorphism and was controlled by shear zones. Intense hydrothermal alteration is recorded by assemblages containing quartz, sericite, andalusite, topaz,

phlogopite, magnetite and fluorite, in particular at Kutemajärvi. Early sulfide and gold mineralization was post-peak metamorphic and took place at greenschist to lower amphibolite facies PT conditions in the presence of low-salinity H_2O-CO_2-CH_4 fluid, a setting similar to that of typical mesothermal gold deposits (Poutiainen & Grönholm 1996). Secondary enrichment and remobilization of gold was associated with ductile-brittle deformation and late CO_2-CH_4+N_2 fluids could have caused

late epithermal telluride deposition (op. cit.). Gold is present principally in native form and as electrum and shows a strong geochemical association with Ag, Te and Bi (Luukkonen 1994).

Skellefte area

The Björkdal deposit, which is the largest currently mined in the Skellefte district, is hosted by steeply dipping quartz veins in tonalite immediately beneath the contact with overlying supracrustal rocks (Löfgren 1987). With respect to mineralogy, lithology, structural features, alteration style, nature of fluids and tectonic setting, the deposit is reminiscent of mesothermal deposits. Gold mineralization throughout the Skellefte field was closely associated with island arc volcanism around 1.9 Ga and the role of magmatic processes prior to regional metamorphism appears to have been significant (Broman et al. 1994). The Middagsbergen stockwork and vein-complex deposit occurs within a shear zone transecting a diorite intrusion and is characterized mineralogically by the abundance of sericite and chlorite, and enrichments in As, S, Sb and W (Öhlander & Markkula 1994). The Åkerberg gold deposit is hosted by swarms of narrow quartz veins within a ductile shear zone occurring in a gabbroic intrusion. The Ersmarksberget occurrence is similarly hosted by a network of quartz veins located around the contact of an even-grained albitized tonalite intrusion of age around 1.9 Ga.

Central Ostrobothnian area

The most important of the Central Ostrobothnian deposits is the subeconomic vein-type Laivakangas prospect, where gold is present both within a tonalite intrusion and the surrounding basaltic lithologies. Vein parageneses variably comprise quartz, quartz-arsenopyrite, quartz-chalcopyrite and arsenopyrite (Mäkelä et al. 1988). Other similar occurrences include Pöhlölä, Kangaskylä, Hietajärvi and Antinoja. The Kiimala-Ängäsneva occurrences form an en echelon array within a NW-SE trending fault system. The host rock consists of a subvolcanic feldspar porphyry and gold occurs in quartz veins, arsenopyrite veins or with disseminated arsenides and sulfides and with massive sulfide breccias (Kojonen et al. 1991). The mineralization is also associated with potassium metasomatism and silicification, sericitization and chloritization (Västi 1997). The Kopsa stockwork-type Cu-Au occurrence forms two gently dipping disseminated zones of mineralization within a porphyritic tonalite intrusion (cf. Nurmi & Haapala 1986). The predominant sulfide minerals are chalcopyrite, arsenopyrite and pyrrhotite and gold occurs in native form, in tellurides, and closely associated with arsenopyrite. The main types of alteration accompanying mineralization are potassium metasomatism and silicification; also Bi, Mo, Sb, Te and W are enriched within the mineralization (Karvinen 1997).

Conclusions

The Swedish and Central Ostrobothnian deposits generally seem to have formed relatively late during orogenic processes compared to Osikonmäki, with the possible exception of Björkdal, being predominantly vein-type in character. For these reasons, subsequent deformation and metamorphism have not overprinted or obscured alteration assemblages related to ore formation. In each case however, it appears that mechanically competent rock units have been favourable for mineralization, with vein arrays preferentially forming in the contact zone between granitoids and surrounding supracrustal lithologies. The Kopsa deposit is the only one that shows porphyry-type characteristics and although it is geochemically very similar to Osikonmäki, the latter is distinctive in being the only deposit hosted by ductile rather than brittle deformation zones.

Hydrothermal alteration seems to be most intensive in the Tampere area (at Kutemajärvi) and the alteration style and mineralogy resembles that of Andean epithermal aduladia-sericite type deposits (P. Grönholm, personal comm.). In the deposits of Skellefte area and Central Ostrobothnia the alteration is more lode-bound and the mineral assemblage corresponds to greenschist facies PT conditions. In the Osikonmäki deposit, the early hydrothermal alteration is possibly weak and difficult to ascertain due to the effects of superimposed prograde and retrograde metamorphic events. The existing mineral assemblage in the main part of the shear zone at Osikonmäki corresponds to amphibolite facies PT conditions.

In general, Svecofennian gold deposits show

Olavi Kontoniemi

strong enrichment in semimetals and locally also Cu, Ag and W. In different areas and even in

different parts of the deposit the order and contents of semimetals can vary considerably.

ACKNOWLEDGEMENTS

REFERENCES

Ahlsved, C., Lampio, E & Tarvainen, T. 1991. Alkemia - a database and program package for regional geochemistry. In: Pulkkinen, E.(ed.) Environmental Geochemistry in Northern Europe. Geological Survey of Finland, Special Paper 9, 291-296.

Boyle, R.W. 1979. The geochemistry of gold and its deposits. Geological Survey of Canada, Bulletin 280. 584 p.

Broman, C., Billström, K., Gustavsson, K. & Fallick, A.E. 1994. Fluid inclusions, stable isotopes and gold deposition at Björkdal, northern Sweden. Mineralium Deposita 29, 139-149.

Bursnall, J.T. 1989. Introduction: Review of mechanical principles, deformation mechanisms and shear zone rocks. In: Bursnall, J. T. (ed.) Mineralization and shear zones, Geological Association of Canada, Short Course Notes, Vol. 6, 1-27.

Ekdahl, E. 1993. Early Proterozoic Karelian and Svecofennian formations and the Evolution of the Raahe-Ladoga Ore Zone, based on the Pielavesi area, central Finland. Geological Survey of Finland, Bulletin 373. 137 p.

Gaál, G. 1986. 2200 million years of crustal evolution: The Baltic shield. Bulletin of the Geological Society of Finland 58, 149-168.

Gaál, G. & Sundblad, K. 1990. Metallogeny of gold in the Fennoscandian Shield. Mineralium Deposita 25, 104-114.

Groves, D.I. 1993. The crustal continuum model for late-Archaean lode-gold deposits of the Yilgarn Block, Western Australia. Mineralium Deposita, 366-374.

Groves, D.I. & Foster, R.P. 1991. Archaean lode gold deposits. In: Foster, R.P. (ed.) Gold metallogeny and exploration, London: Blackie and Son Ltd, 63-103.

Hodgson, C. Jay 1989. Patterns of mineralization. In: Bursnall, J. T. (ed.) Mineralization and shear zones,. Geological Association of Canada, Short Course Notes, Vol. 6, 51-88.

Karvinen, W. 1997. The Kopsa gold-copper prospect. In Excursion Guidebook A2: Volcanic hosted massive sulfide deposits and gold deposits in the Skellefte district, Sweden and western Finland, ed. by P. Weihed & T. Mäki. 4th Biennial SGA Meeting, August 11-13, 1997, Turku, Finland. Geological Survey of Finland, Guide 41, 75-76.

Kerrich, R. & Cassidy, K.F. 1994. Temporal relationships of lode gold mineralization to accretion, magmatism, metamorphism and deformation - Archean to present: A review. Ore Geology Reviews 9, 263-310.

Kilpeläinen, T. 1988. Evolution of deformation and metamorphism as a function of time in the Rantasalmi-Sulkava area, southeastern Finland. Geological Survey of Finland, Bulletin 343, 77-87.

Kojonen, K., Johanson, B. & Sipilä, E. 1991. The Kiimala gold deposit in Haapavesi, western Finland. In: Autio, Sini

(ed.) Geological Survey of Finland, Current Research 1989-1990, ed. by Geological Survey of Finland, Special Paper 12, 75-79.

Kontoniemi, O. 1989. The Osikonmäki gold occurrence at Rantasalmi, southeastern Finland. In: Autio, Sini (ed.) Geological Survey of Finland, Current Research 1988. Geological Survey of Finland, Special Paper 10, 107-110.

Kontoniemi, O. 1998. Geology of the Paleoproterozoic synkinematic Osikonmäki granitoid at Rantasalmi, southeastern Finland. In: Kontoniemi, O. &Nurmi, P.A. (eds.) Geological setting and characteristics of tonalite-hosted Paleoproterozoic gold deposit at Osikonmäki, Rantasalmi, southeastern Finland. Geological Survey of Finland, Special Paper 25, 19-38.

Kontoniemi, O. & Ekdahl, E. 1990. Tonalite-hosted early Proterozoic gold deposit at Osikonmäki, southeastern Finland. Bulletin of the Geological Society of Finland 62, 61-70.

Kontoniemi, O., Johanson, B., Kojonen, K. & Pakkanen, L. 1991. Ore mineralogy of the Osikonmäki gold deposit, Rantasalmi, southeastern Finland. In: Sini Autio, Sini (ed.) Geological Survey of Finland, Current Research 1989-1990. Geological Survey of Finland, Special Paper 12, 81-89.

Kretschmar, U. & Scott S.D. 1976. Phase relations involving arsenopyrite in the system Fe-As-S and their application. The Canadian Minereralogist 14, 346-386.

Liimatainen, J. 1998. A fluid inclusion study of the Osikonmäki gold deposit, Rantasalmi, southeastern Finland. In: Kontoniemi, O. & Nurmi, P.A. (eds.) Geological setting and characteristics of tonalite-hosted Paleoproterozoic gold deposit at Osikonmäki, Rantasalmi, southeastern Finland, Geological Survey of Finland, Special Paper 25, 91-99.

Lindgren, W. 1933. Mineral Deposits (4th edn). New York: McGraw-Hill. 933 p.

Löfgren, C. 1987. The Björkdal gold deposit. In: GOLD '87: Program and abstracts. University of Turku, Department of Geology, Publication No 19, p. 24.

Luukkonen, A. 1994. Main geological features, metallogeny and hydrothermal alteration phenomena of certain gold and gold-tin-tungsten prospects in southern Finland. Geological Survey of Finland, Bulletin 377. 153 p.

Mäkelä, Merja, Sandberg, E. & Rantala, O. 1988. Geochemical exploration of gold-bearing veins associated with granitoids in western Finland. *In* Prospecting in areas of glaciated terrain - 1988, ed. by D.R. MacDonald. CIM and IMM, symposium volyme, 255-270.

Makkonen, H. & Ekdahl, E. 1988. Petrology and structure of the early Proterozoic Pirilä gold deposit in southeastern Finland. Bulletin of the Geological Society of Finland 60, 55-

66.

Mänttäri, Irmeli & Parkkinen, J. 1990. PC-XPLOR - ohjelmiston tilastografiikka malmitutkimuksessa; Osikonmäki. M19/3233/-90/3/10. Unpublished report, Geological Survey of Finland, 23 p.

McCuaig, T.C. & Kerrich, R. 1994. P-T-t-deformation-fluid characteristics of lode gold deposits: evidence from alteration systematics. In: Lentz, D.R. (ed.) Alteration and Alteration Processes Associated with Ore-forming Systems. Geological Association of Canada, Short Course Notes 11, 339-379.

Mumin, A.H., Fleet, M.E. & Chryssoulis, S.L. 1994. Gold mineralization in As-rich mesothermal gold ores of the Bogosu-Prestea mining district of the Ashanti Gold Belt, Ghana: remobilization of "invisible" gold. Mineralium Deposita 29, 445-460.

Murphy, J.B. 1989. Tectonic environment and metamorphic characteristics of shear zones. In: Bursnall, J. T. (ed.) Mineralization and shear zones, Geological Association of Canada, Short Course Notes, Vol. 6, 29-49.

Neumayr, P., Cabri, L.J., Groves, D.I., Mikucki, E.J. & Jackman, Jennifer A. 1993. The mineralogical distribution of gold and relative timing of gold mineralization in two Archean settings of high metamorphic grade in Australia. The Canadian Mineralogist 31, 711-725.

Nurmi, P.A. 1991. Geological setting, history of discovery and exploration economics of Precambrian gold occurrences in Finland. Journal of Geochemical Exploration 39, 273-287.

Nurmi, P.A. & Haapala, I. 1986. The Proterozoic granitoids of Finland: Granite types, metallogeny and relation to crustal evolution. Bulletin of the Geological Society of Finland 58, 203-233.

Nurmi, P.A., Lestinen, P. & Niskavaara, H. 1991. Geochemical characteristics of mesothermal gold deposits in Fennoscandian Shield, and a comparison with selected Canadian and Australian deposits. Geological Survey of Finland, Bulletin 351. 101 p.

Öhlander, B. & Markkula, H. 1994. Alteration associated with the gold-bearing quartz veins at Middagsberget, northern Sweden. Mineralium Deposita 29, 120-127.

Parkkinen, J. 1992a. Osikonmäki: tomografia. In: Parkkinen, J. (ed.) Kullanetsinnän tila ja tulevaisuus - Workshop in Rovaniemi 11.-12.11.1991, M10.2/-92/1. Unpublished report, Geological Survey of Finland, 149-164.

Parkkinen, J. 1992b. Osikonmäki: kultaesiintymän rakennegeologinen mallitus ja mineraalivarantoarvion tarkistus. M19/3233/-92/1/10. Unpublished report, Geologi-cal Survey of Finland, 12 p.

Peters, S.G. 1993. Nomenclature, concepts and classification of oreshoots in vein deposits. In: Groves, D.I. & Bennet, J.M. Structural Setting and Controls on Mineral Deposits. Ore Geology Reviews 8, 3-22.

Phillips, G.N. 1996. Fluids and gold deposits. In: Mesothermal gold deposits: A global overview. Mesothermal Gold Conference, 11-12 July 1996, UWA, Perth, WA. Extended Abstracts, 104-108.

Poulsen, K.H & Robert, F. 1989. Shear zones and gold: practical examples from the southern Canadian shield. In: Bursnall, J.T. (ed.) Mineralization and shear zones. Geological Association of Canada, Short Course Notes, Vol. 6, 239-266.

Poutiainen, M. 1993. Fluid inclusion geochemistry of the early Proterozoic Pirilä gold deposit in Rantasalmi, southeastern Finland. Mineralium Deposita 28, 129-135.

Poutiainen, M. & Grönholm, P. 1996. Hydrothermal fluid evolution of the Paleoproterozoic Kutemajärvi gold telluride deposit, Southwest Finland. Economic Geology 91, 1335-1353.

Seward, T.M. 1989. The hydrothermal chemistry of gold and its implications for ore formation: boiling and conductive cooling as examples. In: Keays, Reid R., Ramsay, R.H. & Groves, D.I. The geology of gold Deposits: the perspective in 1988, Economic Geology Monograph 6, 398-404.

Seward, T.M. 1991. The hydrothermal geochemistry of gold. In: Foster, R.P. Gold metallogeny and exploration, London: Blackie and Son Ltd, 37-62.

Spry, A. 1969. Metamorphic textures. Oxford: Pergamon Press Ltd. 350 p.

Vaasjoki, M. & Kontoniemi, O. 1991. Isotopic studies from the proterozoic Osikonmäki gold prospect at Rantasalmi, southeastern Finland. In: Autio, Sini (ed.) Geological Survey of Finland, Current Research 1989-1990. Geological Survey of Finland, Special Paper 12, 53-57.

Vaasjoki, M. & Sakko, M. 1988. The evolution of the Raahe-Ladoga zone in Finland: isotopic constraints. Geological Survey of Finland, Bulletin 343, 7-32.

Västi, K. 1997. The Vesiperä gold mineralisation in Haapavesi. In: Weihed, P. & Mäki, T. Excursion Guidebook A2: Volcanic hosted massive sulfide deposits and gold deposits in the Skellefte district, Sweden and western Finland, e 4th Biennial SGA Meeting, August 11-13, 1997, Turku, Finland. Geological Survey of Finland, Guide 41, 76.

Appendix 1. Data for ore grade intersections (IS in Table 3) from the Osikonmäki deposit. Symbol -1 means "not determined". Values are means weighted with section length.

Northing	Easting	Sect./m	Au (ppm)	As (wt-%)	S (wt-%)	Ag (ppm)	Cu (ppm)	Pb (ppm)	Zn (ppm)
6882.976	563.402	4.0	0.28	0.0	0.9	1.3	338	9	57
6883.045	563.330	4.0	1.00	1.1	0.7	1.0	124	20	254
6883.011	563.296	4.0	0.15	0.1	0.4	1.0	38	9	109
6883.083	563.222	4.0	1.78	1.0	1.0	0.8	224	11	119
6883.046	563.187	4.0	0.18	1.0	1.2	1.0	60	28	126
6883.011	563.152	4.0	0.10	0.0	0.6	0.9	62	10	47
6883.083	563.081	4.0	0.85	1.1	0.7	1.0	51	15	288
6883.047	563.046	4.0	0.25	0.2	1.0	0.9	44	22	84
6883.011	563.011	4.0	0.35	0.0	0.5	1.0	25	5	49
6883.119	562.977	4.0	0.35	0.3	0.4	1.0	34	31	124
6883.082	562.940	4.0	0.15	0.0	0.7	2.0	242	13	58
6883.152	562.864	4.0	0.20	0.2	0.4	0.6	41	7	67
6883.115	562.832	4.0	2.70	0.7	0.9	1.0	71	42	143
6883.084	562.799	4.0	0.10	0.1	0.9	1.0	38	54	116
6883.152	562.727	4.0	0.28	0.1	0.4	1.0	44	5	60
6883.118	562.692	4.0	0.75	0.5	1.2	1.0	94	20	101
6883.081	562.655	4.0	0.08	0.0	0.9	1.0	150	3	98
6883.260	562.693	4.0	0.43	0.1	0.2	1.0	38	5	74
6883.189	562.623	4.0	0.20	0.7	0.5	1.0	41	7	198
6883.117	562.551	4.0	0.35	0.3	0.4	0.5	22	8	58
6883.187	562.483	4.0	1.28	0.3	0.3	1.5	38	15	111
6883.154	562.446	4.0	0.63	0.5	1.0	1.0	33	6	74
6883.118	562.411	4.0	0.15	0.1	0.3	1.0	27	5	55
6883.188	562.341	4.0	0.48	0.0	0.5	1.0	32	3	58
6883.154	562.306	4.0	1.23	0.1	0.5	1.0	22	3	56
6883.119	562.269	4.0	0.08	0.3	0.7	0.9	26	3	118
6883.225	562.235	4.0	0.23	0.1	0.5	0.6	30	3	56
6883.189	562.200	4.0	0.30	0.0	0.5	1.0	23	5	56
6883.153	562.164	4.0	0.16	0.5	0.5	1.0	21	4	54
6883.297	562.166	4.0	0.14	0.0	0.2	0.8	40	11	63
6883.260	562.127	4.0	0.88	0.2	0.9	1.0	28	3	52
6883.225	562.094	4.0	2.38	0.1	0.9	1.8	28	6	68
6883.294	562.022	4.0	0.13	0.2	0.5	1.0	51	4	60
6883.261	561.987	4.0	0.53	0.1	0.9	1.0	29	61	121
6883.228	561.952	9.5	1.52	0.5	1.3	3.1	57	11	83
6883.049	562.905	4.0	0.35	0.0	0.6	1.0	52	5	90
6883.154	561.881	4.0	0.55	0.2	1.0	2.8	51	9	67
6883.200	561.928	4.0	0.23	0.1	1.2	1.0	37	3	59
6883.085	561.811	4.0	5.33	0.1	0.9	7.3	68	8	69
6883.116	561.843	5.0	5.12	0.7	0.8	7.0	121	46	78
6883.029	561.761	4.0	0.19	0.4	0.6	1.0	30	7	62
6883.050	561.778	6.0	2.50	0.1	0.7	1.0	43	4	41
6883.199	561.887	4.0	1.48	0.6	1.3	1.8	43	5	49
6883.154	561.845	4.0	0.88	0.3	1.0	4.5	98	14	70
6883.119	561.810	5.0	1.34	0.3	0.7	2.0	41	8	37
6883.084	561.775	4.0	7.78	0.2	0.8	3.8	44	6	42
6883.052	561.774	4.5	2.31	0.2	0.9	5.8	59	17	50
6883.223	561.883	4.1	0.23	0.1	1.0	1.3	27	5	39
6883.190	561.847	4.0	2.00	0.4	1.3	2.9	65	5	52
6883.155	561.811	4.0	2.43	0.6	0.7	1.3	38	5	15
6883.120	561.776	4.0	3.20	0.1	0.6	1.8	37	6	45
6883.013	561.810	4.0	0.28	0.9	0.5	1.0	22	5	40
6883.085	561.882	4.0	1.03	0.2	1.1	3.3	53	5	59

Appendix 1. Continued 2/3

Northing	Easting	Sect./m	Au (ppm)	As (wt-%)	S (wt-%)	Ag (ppm)	Cu (ppm)	Pb (ppm)	Zn (ppm)
6883.113	561.911	5.0	1.64	0.6	0.5	1.2	38	7	33
6883.159	564.292	4.0	1.00	0.0	0.9	1.0	335	10	40
6883.038	564.171	5.0	2.26	0.4	1.0	2.4	936	11	54
6883.000	564.133	5.0	1.08	0.1	0.7	1.0	458	13	40
6882.963	564.096	6.0	0.97	0.4	0.8	1.5	233	10	48
6882.955	564.087	6.0	1.48	0.5	0.9	1.5	375	20	45
6882.945	564.078	6.0	1.80	1.0	0.7	1.7	280	12	50
6883.163	564.296	10.0	2.36	0.1	1.1	3.0	1364	8	85
6883.159	564.293	4.0	1.40	0.2	0.5	1.0	180	8	44
6883.153	564.286	4.0	0.70	0.1	0.5	1.0	150	9	36
6883.139	564.272	5.0	0.80	0.5	0.5	2.0	642	11	56
6883.133	564.267	4.0	1.95	0.1	0.4	1.0	192	9	37
6883.124	564.257	9.0	0.82	0.0	0.4	1.0	238	11	31
6883.120	564.253	4.0	0.70	0.0	0.4	1.0	375	9	44
6883.107	564.240	9.0	0.93	0.4	0.8	1.0	361	8	40
6883.102	564.236	6.0	1.10	0.1	0.8	1.0	413	11	46
6883.087	564.221	44.0	6.13	0.3	0.6	2.8	1487	11	63
6883.170	564.303	6.0	1.73	0.0	0.4	1.0	234	10	46
6883.160	564.293	4.0	0.82	0.0	0.6	1.0	413	9	41
6883.157	564.291	6.0	1.40	0.1	0.4	1.3	553	9	48
6883.093	563.730	7.0	2.41	0.3	1.0	1.1	461	9	61
6883.074	563.711	14.0	1.42	2.2	1.6	1.0	192	13	45
6883.093	563.801	8.0	1.31	0.1	0.9	1.0	208	9	38
6883.073	563.780	4.0	0.75	0.1	0.8	1.0	173	10	55
6883.095	563.946	8.0	4.68	1.7	1.1	1.6	516	19	44
6883.143	563.849	8.0	0.89	1.2	1.1	1.0	253	10	45
6883.137	563.843	10.0	2.04	1.5	0.9	1.3	277	25	40
6883.131	563.838	6.0	4.83	1.3	1.0	3.2	255	88	36
6883.139	563.990	8.0	0.68	0.0	0.3	1.3	373	5	39
6883.124	563.975	4.0	5.40	0.9	0.5	2.5	1145	70	136
6883.120	563.971	5.0	1.56	0.0	0.4	3.0	1390	21	97
6883.114	563.965	11.0	2.86	0.6	0.6	3.2	1154	48	83
6883.154	564.146	24.5	3.16	1.3	0.7	1.4	343	18	41
6883.133	564.125	8.0	0.71	0.1	0.6	1.1	341	14	56
6883.103	564.095	7.5	2.37	0.3	0.6	1.5	547	5	46
6883.088	564.080	4.5	0.97	0.1	0.5	1.4	640	16	57
6883.070	564.063	5.0	1.10	0.2	0.6	1.0	292	19	39
6883.061	564.054	4.0	0.73	0.3	0.5	1.0	220	5	40
6883.057	564.050	6.0	2.17	0.3	0.6	1.2	229	18	37
6883.045	564.037	25.0	1.89	0.7	0.9	1.6	414	8	42
6883.028	564.020	13.4	1.12	0.0	0.7	1.1	331	4	40
6883.185	564.177	13.0	1.20	0.2	0.7	1.0	298	8	43
6883.126	564.117	5.0	0.64	0.0	0.2	0.8	84	9	42
6883.067	564.058	10.0	0.96	0.4	0.7	1.4	216	12	36
6883.029	564.020	4.0	1.23	0.4	0.6	1.5	397	13	48
6883.013	564.004	4.0	0.80	0.1	0.3	1.0	107	9	31
6883.007	563.998	15.0	1.22	0.8	0.9	1.7	409	10	42
6883.104	563.740	6.0	1.05	0.3	0.4	1.0	312	8	56
6883.100	563.736	6.0	1.88	1.0	0.8	1.0	298	7	63
6883.040	563.817	7.0	1.51	1.3	0.9	1.0	129	9	44
6883.028	563.804	7.0	0.76	0.4	0.7	1.0	186	9	46
6883.016	563.792	16.0	2.59	0.5	0.7	0.8	220	12	39
6883.122	563.897	14.0	1.88	0.7	1.1	1.2	804	8	55
6883.115	563.890	7.0	2.06	1.0	1.2	1.0	597	9	49
6883.092	563.867	4.0	1.00	0.3	0.2	1.0	68	7	37

Appendix 1. Continued 3/3

Northing	Easting	Sect./m	Au (ppm)	As (wt-%)	S (wt-%)	Ag (ppm)	Cu (ppm)	Pb (ppm)	Zn (ppm)
6883.089	563.864	4.0	5.70	0.5	0.5	1.0	160	10	39
6883.085	563.861	4.0	1.95	0.4	0.6	1.0	315	9	42
6883.133	563.908	4.0	1.98	1.0	1.0	1.3	645	9	40
6883.131	563.906	4.0	0.93	0.3	0.8	1.0	295	10	51
6883.149	563.923	4.0	0.60	0.1	0.6	1.0	170	10	39
6883.146	563.921	12.0	2.50	0.4	0.8	1.4	625	9	42
6883.164	563.938	4.0	0.65	0.0	0.7	1.0	450	11	59
6883.154	564.005	5.0	0.94	0.2	0.9	1.0	368	11	40
6883.120	564.042	4.0	0.65	0.0	0.3	0.5	285	9	42
6883.086	564.007	9.0	1.27	0.1	0.6	1.0	326	22	55
6883.052	563.974	11.0	2.36	1.3	1.0	0.9	266	17	47
6883.133	564.054	9.0	2.21	0.4	0.6	1.7	664	13	55
6883.129	564.050	9.0	1.70	1.1	1.0	2.1	986	13	71
6883.121	564.041	15.0	2.52	0.4	0.7	2.1	1082	13	73
6883.156	564.076	15.0	1.87	0.6	0.9	1.7	491	18	50
6883.152	564.073	4.0	1.35	0.0	0.4	1.0	82	8	37
6883.127	564.047	6.0	1.17	0.0	0.3	1.0	227	8	39
6883.104	564.169	6.0	1.17	0.0	0.3	1.0	167	9	42
6883.084	564.149	7.0	0.97	0.0	0.5	1.0	389	9	42
6883.027	564.092	4.0	0.75	0.3	0.4	1.0	101	20	34
6883.016	564.080	4.0	0.80	0.3	0.8	1.0	525	9	46
6883.004	564.068	30.0	0.95	0.9	1.0	1.5	387	27	39
6883.154	564.217	4.0	1.10	0.6	0.8	1.0	235	8	38
6883.181	564.244	8.7	1.27	0.1	0.4	1.0	292	9	43
6883.179	564.242	5.0	1.30	0.1	0.4	1.0	146	10	39
6883.045	563.472	10.0	1.33	1.8	1.3	1.7	113	19	171
6883.082	563.858	10.0	0.76	0.8	0.9	1.0	212	4	56
6883.077	563.854	4.0	4.75	1.1	1.0	2.0	374	5	52
6883.007	563.929	18.0	2.10	1.2	1.0	1.6	211	13	38
6882.934	563.998	4.0	0.70	0.0	0.6	1.0	403	3	38
6882.935	564.209	4.0	0.95	-1.0	-1.0	-1.0	-1	-1	-1
6883.088	564.363	5.0	1.88	0.9	0.9	2.9	1289	11	94
6883.091	564.366	4.0	0.75	0.0	0.2	0.5	110	8	24
6883.057	564.261	4.0	1.00	0.0	0.0	0.0	17	8	47
6883.087	564.291	11.0	1.65	0.0	0.4	1.8	1407	8	50
6883.166	564.299	6.0	3.72	0.1	0.9	3.2	1167	9	55
6883.157	564.290	4.0	0.65	0.0	0.3	0.0	80	8	15
6883.136	564.269	14.0	1.42	0.1	0.5	1.0	302	8	32
6883.194	564.256	4.5	1.58	0.0	0.7	0.8	369	3	42
6883.202	564.264	5.0	2.96	0.1	0.7	1.0	388	6	47
6883.204	564.266	4.0	8.77	0.1	0.9	2.8	1541	4	72
6883.206	564.267	6.0	3.02	0.1	0.6	1.7	933	4	68
6883.091	564.155	4.0	4.43	0.2	0.6	2.5	1436	4	63
6883.193	564.115	4.0	1.05	0.1	0.5	1.0	161	0	41
6883.011	563.579	6.0	1.67	2.8	1.6	0.8	128	10	164
6883.014	563.650	7.0	3.19	2.3	1.5	1.3	223	13	43
6883.046	563.613	8.0	0.70	1.1	0.9	1.0	198	5	51
6883.183	564.387	6.5	2.89	0.4	0.6	1.9	691	25	58
6883.106	564.267	12.0	1.88	-1.0	-1.0	-1.0	-1	-1	-1
6883.089	564.196	6.0	6.23	-1.0	-1.0	-1.0	-1	-1	-1
6883.141	564.125	4.0	1.37	-1.0	-1.0	-1.0	-1	-1	-1
6883.009	563.716	12.0	1.60	-1.0	-1.0	-1.0	-1	-1	-1
6883.100	563.772	5.0	3.66	-1.0	-1.0	-1.0	-1	-1	-1
6883.091	563.840	21.0	3.05	-1.0	-1.0	-1.0	-1	-1	-1

Appendix 2. Major and trace element data for certain drill core intersections within the Osikonmäki shear zone. Symbol 0 means values below detection limit.

BH/Depth (m)		Au (ppm)	SIO2 (%)	AL2O3 (%)	K2O (%)	NA2O (%)	S (ppm)	As (ppm)	Cu (ppm)	Zn (ppm)	Sb (ppm)	Te (ppm)	Se (ppm)	Bi (ppm)
BH460/	40.0	0.1	66.68	16.81	3.80	1.67	6800	141	26	67	0.44	0.01	0.12	0.2
	44.0	0.3	71.76	13.67	4.53	1.10	11000	4691	15	63	3.63	0.01	0.19	0
	45.5	1.3	71.46	13.98	3.53	0.74	10200	5572	21	89	2.69	0.02	0.32	0
	46.5	1.0	69.51	15.13	4.34	0.72	11600	10102	20	57	4.87	0.02	0.29	0
	47.5	4.5	72.10	14.93	4.14	0.63	12000	8826	33	67	5.16	0.01	0.55	0.1
	59.0	6.2	65.09	16.79	5.59	2.49	12800	9256	86	131	13.05	0.01	1.15	0.1
	60.0	0.7	67.73	15.67	3.81	2.85	12400	7009	73	128	11.03	0	1.02	0
	61.0	0.6	68.40	15.43	4.43	2.63	8500	7121	46	134	8.78	0.01	0.79	0
	66.5	0.2	65.82	16.95	3.12	3.17	6300	570	17	79	1.45	0	0.08	0
BH464/	24.0	0.1	65.91	16.78	2.64	4.49	500	34	79	14	0.04	0.01	0.18	0
	46.0	0.1	64.57	17.66	2.44	4.50	700	24	86	20	0.04	0.01	0.07	0
	96.0	0.3	68.22	15.84	2.46	4.26	3200	23	71	42	0.05	0.02	0.68	1.1
	104.0	0.1	66.27	16.75	2.46	4.44	1600	77	78	19	0.16	0.01	0.46	0.1
	129.0	0.2	65.44	17.00	2.34	4.48	2600	81	87	53	0.01	0.12	0.59	2.5
	135.5	1.7	65.42	16.88	2.30	4.66	11800	857	79	333	0.05	0.25	10.94	6.7
	136.5	1.0	65.69	17.05	2.11	4.35	7900	546	85	126	0.04	0.18	9.25	2.2
	137.5	4.2	63.40	16.60	1.97	4.28	16800	17684	84	259	0.51	0.82	46.87	0.8
	138.5	3.6	63.61	16.37	2.34	4.16	17200	23447	72	195	2.20	1.08	65.65	0.8
	141.5	5.2	70.38	14.16	2.58	3.29	8800	11198	67	171	0.55	1.83	19.16	1.3
	142.5	6.3	69.72	14.31	1.96	2.92	11500	16965	51	93	1.46	1.77	35.34	1.9
	147.5	0.6	65.26	16.98	3.32	4.01	9300	7284	77	310	0.82	0.32	12.88	0.4
	148.5	0.7	65.11	16.83	2.90	4.14	10300	12957	71	211	0.89	1.02	26.56	0.4
	154.0	0.3	66.08	16.71	2.36	4.41	3100	258	78	84	0.15	0.09	1.52	1.2
BH478/	15.0	0.1	65.99	17.15	2.86	4.75	1400	113	17	64	0.03	0	0.34	0.7
	38.0	0.1	65.67	16.70	2.35	4.74	2600	9	38	57	0.05	0	1.00	0.5
	56.5	0.2	65.41	17.06	2.15	4.51	5700	74	65	49	0.04	0	1.48	2.2
	57.5	0.8	64.70	17.37	2.23	4.26	10900	705	195	50	0.08	0.02	7.41	4.6
	58.5	3.1	63.83	17.59	3.66	3.84	14400	2020	421	64	0.17	0.05	16.03	7.9
	59.5	3.1	63.19	15.22	2.85	3.57	19600	33953	176	55	1.54	0.12	47.54	0.9
	62.5	5.7	64.61	13.46	2.64	2.92	19800	42331	146	55	2.02	0.67	69.82	1.0
	63.5	2.6	65.37	16.01	3.83	3.38	11000	18926	149	65	1.02	0.17	31.45	0.4
	66.0	0.1	65.46	16.98	2.57	4.21	4600	2855	38	117	0.15	0.01	1.56	0.1
	68.0	0.1	66.11	16.67	2.25	4.31	5400	93	51	99	0.08	0.01	1.70	0.5
	84.0	0.1	66.55	16.86	2.24	4.43	1900	116	24	62	0.03	0	0.73	0.1

Appendix 3. Trace element data for exploration trench OMK-87-M1. Symbol 0 means values below detection limit.

Sample	Northing	Easting	As (wt-%)	S (wt-%)	Ag (ppm)	Cu (ppm)	Bi (ppm)	Au (ppm)
1.1	6883.084	563.634	2.40	1.15	1	260	60	9.9
1.2	6883.084	563.635	2.60	1.38	1	240	28	3.7
1.3	6883.085	563.635	0.09	0.20	0	39	0	0.1
1.4	6883.085	563.634	0.20	0.58	1	200	0	0.1
1.5	6883.081	563.640	3.50	1.89	4	64	0	1.2
1.6	6883.082	563.639	3.40	2.16	1	110	34	3.6
1.7	6883.085	563.636	1.90	1.03	1	210	24	3.2
1.8	6883.085	563.635	1.20	0.85	3	110	0	0.7
1.9	6883.086	563.635	0.01	0.21	2	33	0	0
1.10	6883.081	563.641	6.60	1.79	2	58	0	2.1
1.11	6883.082	563.640	5.90	2.35	2	71	0	1.6
1.12	6883.082	563.640	0.61	1.65	1	91	27	1.6
1.13	6883.085	563.637	1.20	1.10	2	260	28	4.6
1.14	6883.086	563.636	0.46	0.49	2	140	0	0.6
1.15	6883.087	563.635	0.31	0.57	1	140	0	0.2
1.16	6883.080	563.643	11.30	4.69	2	410	29	4.9
1.17	6883.081	563.642	1.00	0.54	1	38	0	0.9
1.18	6883.082	563.642	2.20	1.32	2	89	0	1.1
1.19	6883.082	563.641	10.70	4.46	2	160	21	2.5
1.20	6883.083	563.640	0.09	0.45	1	23	0	0.2
1.21	6883.085	563.638	0.20	0.59	2	200	0	0.1
1.22	6883.086	563.638	1.40	0.86	2	190	0	2.3
1.23	6883.087	563.637	0.82	0.64	2	130	0	0.6
1.24	6883.087	563.636	0.20	0.50	2	180	0	0.2
1.25	6883.088	563.635	3.20	1.38	2	190	0	2.1
1.26	6883.081	563.644	0.47	1.25	2	230	0	0.8
1.27	6883.082	563.643	1.10	0.98	1	92	0	0.7
1.28	6883.082	563.642	2.00	1.27	1	99	0	0.7
1.29	6883.083	563.642	3.00	1.78	2	78	0	1.6
1.30	6883.085	563.640	1.10	1.94	4	320	0	1.1
1.31	6883.086	563.639	1.20	1.27	2	420	0	1.0
1.32	6883.087	563.638	0.81	0.84	2	200	0	0.7
1.33	6883.087	563.638	0.30	0.75	2	220	0	0.4
1.34	6883.088	563.637	0.30	0.54	2	190	0	0.4
1.35	6883.089	563.636	0.22	0.66	2	230	0	0.3
1.36	6883.082	563.645	0.37	1.84	2	370	0	8.8
1.37	6883.085	563.641	10.30	4.43	3	210	63	0.6
1.38	6883.086	563.640	2.30	1.27	2	170	23	3.1
1.39	6883.087	563.640	0.82	0.87	2	160	0	0.8
1.40	6883.087	563.639	0.27	0.57	2	150	0	0.4
1.41	6883.088	563.638	0.31	0.62	2	220	0	0.2
1.42	6883.089	563.638	0.16	0.60	2	220	0	0.2
1.43	6883.090	563.637	0.08	0.31	1	150	24	3.6
1.44	6883.090	563.636	0.21	0.50	2	270	0	0.6
1.45	6883.082	563.645	0.25	1.22	2	210	0	0.5
1.46	6883.083	563.645	5.90	2.77	1	36	39	3.3
1.47	6883.084	563.644	4.50	2.01	2	63	29	2.5
1.48	6883.085	563.642	4.00	2.17	1	76	36	5.5
1.49	6883.086	563.642	6.50	2.99	3	78	150	23.0
1.50	6883.087	563.641	2.60	1.38	2	180	42	5.3
1.51	6883.087	563.640	0.90	0.83	2	170	0	1.5
1.52	6883.088	563.640	0.36	0.53	1	170	0	0.2
1.53	6883.089	563.639	0.49	0.55	1	220	0	0.4
1.54	6883.090	563.638	0.27	0.80	1	350	0	2.0

Sample	Northing	Easting	As (wt-%)	S (wt-%)	Ag (ppm)	Cu (ppm)	Bi (ppm)	Au (ppm)
Appendix 3. Continued 2/5								
1.55	6883.090	563.638	0.34	0.38	1	110	28	3.1
1.56	6883.082	563.647	0.08	1.11	1	270	0	1.4
1.57	6883.082	563.647	0.09	1.09	1	200	0	0.4
1.58	6883.083	563.646	0.62	1.33	1	200	0	1.4
1.59	6883.084	563.645	4.60	2.18	1	61	23	1.8
1.60	6883.085	563.645	2.40	1.13	1	57	0	0.9
1.61	6883.085	563.644	0.06	0.43	1	38	0	0.5
1.62	6883.086	563.643	5.50	2.53	2	100	59	8.8
1.63	6883.087	563.642	4.70	2.18	2	76	47	6.1
1.64	6883.087	563.642	1.60	0.84	1	160	0	1.5
1.65	6883.088	563.641	0.11	0.45	1	180	0	0.1
1.66	6883.089	563.640	0.20	0.38	1	210	0	0.4
1.67	6883.090	563.640	0.36	0.42	2	260	34	4.3
1.68	6883.090	563.639	0.30	0.50	1	210	0	0.4
1.69	6883.091	563.638	0.29	0.39	1	160	0	0.3
1.70	6883.082	563.648	0.04	1.08	1	190	0	0.2
1.71	6883.083	563.647	0.10	1.27	1	260	0	0.4
1.72	6883.084	563.647	4.20	1.98	1	62	0	1.4
1.73	6883.085	563.646	5.10	2.37	1	31	20	1.3
1.74	6883.085	563.645	6.70	3.50	2	170	25	3.2
1.75	6883.086	563.645	1.30	1.24	1	67	32	3.0
1.76	6883.087	563.644	5.50	2.41	2	110	130	21.5
1.77	6883.087	563.643	5.60	2.46	1	50	45	5.9
1.78	6883.088	563.642	0.43	0.63	1	190	0	0.8
1.79	6883.089	563.642	0.20	0.74	2	320	0	0.2
1.80	6883.090	563.641	0.30	0.26	2	130	22	4.3
1.81	6883.090	563.640	0.11	0.42	1	140	0	0.4
1.82	6883.091	563.640	0.05	0.37	1	140	0	0.1
1.83	6883.092	563.639	0.02	0.12	1	46	0	0.0
1.84	6883.082	563.650	0.01	0.62	1	150	0	0.3
1.85	6883.082	563.650	0.01	0.96	1	160	0	0.2
1.86	6883.083	563.649	3.20	1.53	1	110	21	2.3
1.87	6883.084	563.648	0.04	1.01	1	300	0	0.2
1.88	6883.085	563.647	0.14	1.29	1	280	0	0.5
1.89	6883.085	563.647	3.00	1.48	1	46	0	0.8
1.90	6883.086	563.646	1.90	1.01	1	42	0	0.7
1.91	6883.087	563.645	0.11	1.28	1	61	22	2.3
1.92	6883.087	563.645	8.30	3.62	2	51	82	11.4
1.93	6883.088	563.644	2.20	1.06	2	230	20	2.5
1.94	6883.089	563.643	1.00	0.98	2	460	0	1.5
1.95	6883.090	563.642	0.65	0.57	1	260	0	1.3
1.96	6883.090	563.642	0.15	0.46	1	150	0	0.2
1.97	6883.091	563.641	0.10	0.27	1	84	0	0.2
1.98	6883.092	563.640	0.05	0.34	1	130	0	0.8
1.99	6883.092	563.640	0.02	0.32	1	92	0	0.1
1.100	6883.082	563.652	0.04	0.92	1	150	0	0.3
1.101	6883.082	563.651	0.02	0.94	1	150	0	0.7
1.102	6883.083	563.650	0.04	1.08	1	190	0	0.2
1.103	6883.084	563.650	0.10	1.15	1	260	0	1.3
1.104	6883.085	563.649	0.30	1.10	1	280	0	0.4
1.105	6883.085	563.648	4.40	1.97	1	48	0	0.9
1.106	6883.086	563.647	1.20	0.81	1	43	0	0.4
1.107	6883.087	563.647	0.32	1.28	1	77	29	1.7
1.108	6883.087	563.646	6.00	2.98	2	130	61	10.4
1.109	6883.088	563.645	4.20	1.84	2	91	25	4.3

Sample	Northing	Easting	As (wt-%)	S (wt-%)	Ag (ppm)	Cu (ppm)	Bi (ppm)	Au (ppm)
Appendix 3. Continued 3/5								
1.110	6883.089	563.645	2.90	1.17	2	250	51	7.7
1.111	6883.090	563.644	0.46	0.58	2	230	0	0.6
1.112	6883.090	563.643	0.13	0.60	2	200	0	0.2
1.113	6883.091	563.642	0.07	0.35	1	120	0	0.2
1.114	6883.092	563.642	0.16	0.52	1	160	0	0.8
1.115	6883.092	563.641	0.04	0.32	1	92	0	0
1.116	6883.093	563.640	0.03	0.25	1	58	0	0
1.117	6883.083	563.652	0.10	1.26	1	200	0	0.2
1.118	6883.084	563.651	0.03	1.24	1	250	0	0.1
1.119	6883.085	563.650	0.73	1.31	1	230	0	2.6
1.120	6883.085	563.650	1.80	1.03	1	48	0	0.3
1.121	6883.086	563.649	4.00	2.04	1	39	24	0.8
1.122	6883.087	563.648	3.70	1.84	1	69	23	1.2
1.123	6883.087	563.647	3.60	1.67	2	93	82	11.9
1.124	6883.088	563.647	3.20	1.73	1	86	34	3.9
1.125	6883.089	563.646	1.20	0.95	1	160	21	1.5
1.126	6883.090	563.645	0.66	0.94	1	260	21	1.0
1.127	6883.090	563.645	0.21	0.67	1	200	0	0.4
1.128	6883.093	563.642	0.04	0.24	1	53	0	0
1.129	6883.094	563.641	0.02	0.13	1	29	0	0
1.130	6883.085	563.651	1.80	1.18	1	65	0	0.3
1.131	6883.086	563.650	4.00	1.76	1	29	30	1.2
1.132	6883.087	563.650	9.40	4.69	2	180	41	3.1
1.133	6883.087	563.649	0.68	1.42	1	77	99	4.0
1.134	6883.088	563.648	4.80	2.36	1	84	43	4.2
1.135	6883.089	563.647	1.50	1.06	1	130	0	1.7
1.136	6883.090	563.647	0.48	0.70	1	200	0	1.1
1.137	6883.090	563.646	4.40	1.48	2	250	25	2.1
1.138	6883.091	563.645	1.50	0.80	1	110	0	0.9
1.139	6883.092	563.644	0.14	0.32	1	79	0	0.1
1.140	6883.093	563.643	0.03	0.30	1	64	0	0.1
1.141	6883.094	563.642	0.02	0.12	0	32	0	0
1.142	6883.094	563.642	0.04	0.17	1	34	0	0
1.143	6883.087	563.651	4.80	2.09	1	82	21	1.6
1.144	6883.087	563.650	0.05	1.18	1	190	170	7.9
1.145	6883.088	563.650	0.02	1.26	1	96	57	3.2
1.146	6883.089	563.649	3.10	1.62	2	140	35	4.3
1.147	6883.090	563.648	0.99	0.80	1	150	23	2.0
1.148	6883.090	563.647	7.90	2.66	2	380	25	2.5
1.149	6883.091	563.647	1.30	0.83	1	100	0	1.1
1.150	6883.092	563.646	2.20	1.23	2	140	0	2.2
1.151	6883.092	563.645	0.24	0.43	1	100	0	0.4
1.152	6883.093	563.645	0.14	0.39	1	99	0	0.2
1.153	6883.094	563.644	0.20	0.48	1	140	0	0.3
1.154	6883.094	563.643	0.04	0.25	1	71	0	0.2
1.155	6883.095	563.642	0.01	0.10	1	27	0	0
1.156	6883.087	563.652	2.50	1.91	1	210	0	0.7
1.157	6883.088	563.651	0.04	1.44	1	88	97	4.1
1.158	6883.089	563.650	4.40	1.93	1	81	43	6.0
1.159	6883.090	563.650	1.60	1.02	1	140	27	3.1
1.160	6883.090	563.649	1.80	1.18	1	180	23	2.6
1.161	6883.091	563.648	1.00	0.69	1	100	0	0.9
1.162	6883.092	563.647	1.30	0.87	1	170	0	0.9
1.163	6883.092	563.647	1.30	0.72	1	160	0	1.0
1.164	6883.093	563.646	1.80	0.73	1	150	0	1.2

Sample	Northing	Easting	As (wt-%)	S (wt-%)	Ag (ppm)	Cu (ppm)	Bi (ppm)	Au (ppm)
Appendix 3. Continued 4/5								
1.165	6883.094	563.645	0.26	0.46	1	120	0	0.3
1.166	6883.094	563.645	0.12	0.46	1	130	0	0.2
1.167	6883.095	563.644	0.02	0.23	1	47	0	0
1.168	6883.090	563.651	2.00	1.16	1	190	26	2.7
1.169	6883.090	563.650	1.80	0.99	1	150	0	1.2
1.170	6883.091	563.650	2.60	1.36	1	120	0	1.3
1.171	6883.092	563.649	0.77	0.90	1	250	0	0.9
1.172	6883.092	563.648	0.69	0.29	1	55	0	0.5
1.173	6883.093	563.647	0.23	0.33	1	77	20	1.5
1.174	6883.094	563.647	0.24	0.37	1	110	0	0.2
1.175	6883.094	563.646	0.10	0.34	1	87	0	0
1.176	6883.095	563.645	0.01	0.09	0	21	0	0
1.177	6883.097	563.644	0.03	0.28	1	68	0	0
1.178	6883.097	563.643	0.02	0.05	1	37	0	0
1.179	6883.090	563.652	0.63	0.80	1	180	0	1.0
1.180	6883.091	563.651	0.98	0.67	1	69	0	1.0
1.181	6883.092	563.650	0.20	0.51	1	110	0	0.4
1.182	6883.092	563.650	0.22	0.50	1	130	0	0.3
1.183	6883.093	563.649	0.09	0.27	1	72	0	0
1.184	6883.094	563.648	0.56	0.47	1	110	51	6.8
1.185	6883.094	563.647	0.09	0.44	1	120	0	0.2
1.186	6883.095	563.647	0.09	0.51	1	160	0	0
1.187	6883.096	563.646	0.65	0.58	1	170	0	0.4
1.188	6883.097	563.645	0.27	0.85	1	440	0	0.8
1.189	6883.097	563.645	0.13	0.80	1	600	0	0.5
1.190	6883.098	563.644	0.34	0.67	1	360	0	0.4
1.191	6883.092	563.652	1.30	0.92	1	160	0	1.2
1.192	6883.092	563.651	0.12	0.48	1	110	0	0.2
1.193	6883.093	563.650	0.08	0.41	1	130	0	0.2
1.194	6883.094	563.650	0.03	0.39	1	82	0	0.3
1.195	6883.094	563.649	0.35	0.60	1	160	0	0.4
1.196	6883.095	563.648	0.19	0.66	1	230	0	0.4
1.197	6883.096	563.647	0.34	0.64	1	280	0	0.8
1.198	6883.097	563.647	0.35	0.73	1	350	0	0.6
1.199	6883.097	563.646	0.81	0.65	1	280	0	0.7
1.200	6883.098	563.645	0.38	0.27	1	91	0	0.6
1.201	6883.090	563.654	2.50	1.20	1	130	26	2.8
1.202	6883.092	563.653	3.80	1.72	1	230	25	2.3
1.203	6883.094	563.650	0.36	0.60	1	310	0	1.5
1.204	6883.095	563.650	0.79	0.56	1	260	0	0.8
1.205	6883.096	563.649	0.66	0.39	1	170	0	0.8
1.206	6883.097	563.648	0.99	0.92	1	490	0	0.8
1.207	6883.097	563.647	0.47	0.81	1	270	0	0.4
1.208	6883.098	563.647	0.10	0.73	1	220	0	0.5
1.209	6883.099	563.646	0.83	1.44	1	340	0	1.2
1.210	6883.090	563.656	0.02	0.34	0	60	0	0.4
1.211	6883.091	563.655	1.80	0.92	1	100	44	3.1
1.212	6883.092	563.654	1.00	0.70	1	91	0	0.6
1.213	6883.092	563.654	1.30	0.79	1	120	27	2.6
1.214	6883.093	563.653	0.04	0.16	1	31	0	0.2
1.215	6883.097	563.650	2.00	0.87	1	220	33	3.7
1.216	6883.097	563.649	0.06	0.61	1	190	0	0.2
1.217	6883.090	563.657	2.50	1.15	1	75	24	2.6
1.218	6883.091	563.657	0.07	0.13	1	55	0	0.5
1.219	6883.092	563.656	0.68	1.86	1	210	57	4.4

Sample	Northing	Easting	As (wt-%)	S (wt-%)	Ag (ppm)	Cu (ppm)	Bi (ppm)	Au (ppm)
Appendix 3. Continued 5/5								
1.220	6883.092	563.655	1.20	0.89	1	140	0	1.0
1.221	6883.093	563.654	0.98	0.79	1	170	23	1.6
1.222	6883.094	563.654	0.02	0.84	1	120	37	1.8
1.223	6883.092	563.657	3.40	1.38	1	150	29	1.4
1.224	6883.092	563.657	2.40	1.04	1	140	23	2.0
1.225	6883.093	563.656	1.60	1.11	1	120	48	5.2
1.226	6883.094	563.655	1.40	0.91	1	130	24	1.9
1.227	6883.094	563.654	0.09	0.32	1	55	21	0.9
1.228	6883.092	563.658	1.20	0.53	1	53	22	0.9
1.229	6883.093	563.657	1.90	1.04	1	140	20	1.7
1.230	6883.094	563.657	1.50	1.24	1	160	30	3.1
1.231	6883.094	563.656	1.90	1.81	2	120	70	7.5
1.232	6883.095	563.655	1.90	2.88	4	250	490	34.4
1.233	6883.093	563.659	1.30	0.99	1	85	48	3.5
1.234	6883.094	563.658	5.20	1.99	1	79	44	5.7
1.235	6883.094	563.657	0.96	0.98	1	82	40	3.3
1.236	6883.095	563.657	1.80	2.12	2	170	56	3.8
1.237	6883.096	563.656	0.04	1.77	2	130	110	6.1
1.238	6883.097	563.655	0.01	0.50	1	76	26	1.1
1.239	6883.094	563.659	1.50	1.14	1	98	29	3.1
1.240	6883.095	563.658	0.59	1.11	1	100	34	2.2

GEOCHEMISTRY OF GOLD AND ASSOCIATED ELEMENTS IN THE PALEOPROTEROZOIC OSIKONMÄKI GOLD DEPOSIT, SOUTHEASTERN FINLAND

by

Theodore J. Bornhorst, Pekka A. Nurmi and Olavi Kontoniemi

Bornhorst, Theorore J., Nurmi, Pekka A. & Kontoniemi, Olavi 1998.
Geochemistry of gold and associated elements in the Paleoproterozoic
Osikonmäki gold deposit, southeastern Finland. *Geological Survey of
Finland, Special Paper 25.* 81 - 90. 3 figures and 4 tables.

The Osikonmäki gold deposit is related to a shear zone within a Paleo-
proterozoic tonalite. Relative to the tonalite, As is the most enriched
element in the deposit followed by Au, Se, S, Bi, Ag, Te, Sb, Cu, Pb, and Mo
in decreasing order of enrichment; all have median enrichment of more than
5 times background. High concentrations of As, Au, and Se are character-
istic of the Osikonmäki gold deposit. Gold is geochemically associated with
Bi and Te whereas As-S-Se and Cu-Ag are distinct geochemical associa-
tions. The geochemical associations are interpreted as representing a tem-
poral continuum of spatially overlapping episodes of precipitation.

Key words (GeoRef Thesaurus, AGI): gold ores, tonalite, geochemistry
gold, arsenic, selenium, pathfinders, statistical analysis, Proterozoic,
Paleoproterozoic, Osikonmäki, Finland

*Theodore J. Bornhorst, Department of Geological Engineering and Sci-
ences, Michigan Technological University, Houghton, MI 49931 U.S.A.*
*Pekka A. Nurmi, Geological Survey of Finland, P.O.Box 96, FIN-02151
Espoo, Finland*
*Olavi Kontoniemi, Geological Survey of Finland, P.O.Box 1237, FIN-
70211 Kuopio, Finland*

INTRODUCTION

The Osikonmäki gold deposit of southeastern Finland was discovered in 1986 (Kontoniemi 1989). Since its discovery the deposit has been subjected to a variety of geologic studies including lithologic characterization, ore mineralogy and geochronology. Kontoniemi and Ekdahl (1990) give a sketch of the geochemical character of the host rocks and ore-bearing zones. As part of the continuing study of this deposit by the Geological Survey of Finland, the abundance of a selected suite of elements was determined for 362 samples in and adjacent to the gold-bearing zone. This detailed geochemical sampling allows us to better understand the behavior of gold and its related elements at the Osikonmäki deposit. Such knowledge provides important input to developing techniques for geochemical exploration.

GEOLOGIC SETTING

Gold at Osikonmäki is hosted by a syntectonic 1887 Ma tonalite (Vaasjoki and Kontoniemi 1991) within the NW-trending Ladoga-Bothnian Bay deformation zone (Kontoniemi 1998a, this volume). The suture zone is interpreted as an early Proterozoic continental margin involving subduction and subsequent collision (Gaál 1986).

The bedrock of the study area consist predominantly of metaturbidites and metavolcanics intruded by a variety of granitoids (Fig. 1). The area records a complex polyphase deformational and progressive metamorphic history. Metamorphic grade increases southwards towards the Sulkava thermal dome, and the gold mineralization is located within the sillimanite-K-feldspar zone (Kontoniemi 1998a, this volume).

Within the tonalite intrusion gold is localized in an at least 3 km long zone within an E-W trending shear zone (Fig. 1). The highest gold concentrations occur at both the eastern and western parts of the shear zone, which dips southwards at 40-50°. Gold-enriched zones occur as either tightly folded or en-echelon lenses that typically plunge ESE at around 20° (Kontoniemi 1998b, this volume). Proven and probable reserves in the area drilled in detail (Fig. 2) are approximately 2 Mt with a mean concentration of 3 g/t Au and 0.77 % As (Kontoniemi and Ekdahl 1990).

The age of the synorgenic Osikonmäki intrusion provides a maximum age for gold mineralization, but constraining the minimum age is less straightforward. It is obvious that the main stage of mineralization started before the peak of metamorphism. Fluid inclusion studies indicate that the main stage was followed by influx of aqueous fluids of variable salinity, at least locally. The late fluids transported gold and associated elements to higher structural levels during continued deformation within the shear zone (Kontoniemi 1998b, this volume).

The host rock, Osikonmäki tonalite, is foliated and it has a gneissose and locally porphyritic appearance. In comparison to many mesothermal deposits, the effect of hydrothermal alteration is difficult to discern due to subsequent prograde metamorphism above the sillimanite-K-feldspar isograd, followed by extensive retrograde recrystal-
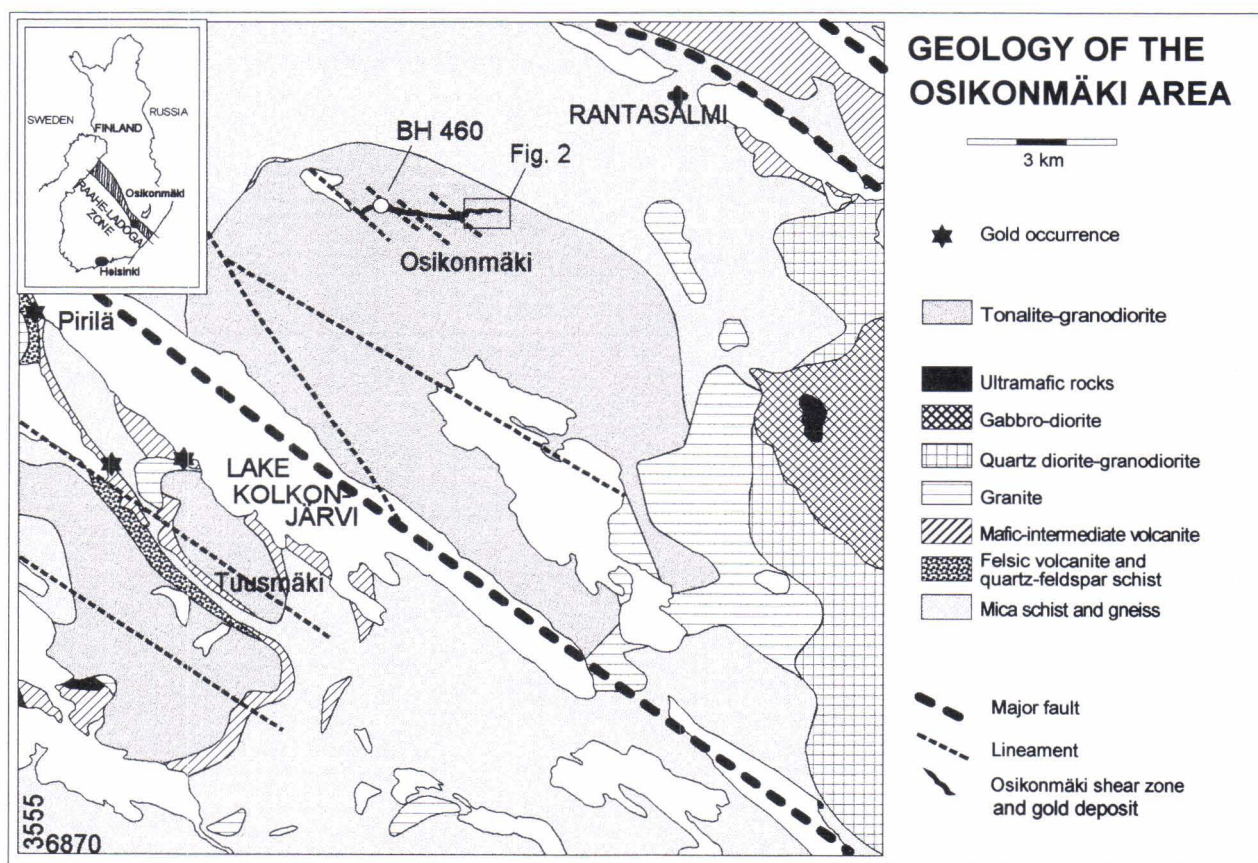
Fig. 1. Generalized geological map of the Osikonmäki area, also showing location of drill hole BH 460 and the claim Osikko 1. Simplified from Kontoniemi (1997a, this volume).

lization. In the shear zone, alteration is stronger than in the tonalite and the amount of K-feldspar, quartz and mica, have increased at the expense of plagioclase and hornblende. Typical prograde minerals are diopside, green amphibole, sillimanite, and garnet. Late retrograde minerals are chlorite, epidote, actinolite, sericite, carbonate, and quartz (Kontoniemi 1998b, this volume).

The most common ore minerals in the shear zone are pyrrhotite, arsenopyrite, löllingite, and chalcopyrite, which occur as irregular or banded disseminations. Typical accessory minerals are sphalerite, galena, and ilmenite or rutile and occasionally also stannite, tetrahedrite, boulangerite, and

molybdenite. Pyrite, marcasite and some covellite occur as secondary minerals (Kontoniemi et al. 1991).

Gold occurs in native form and electrum as inclusions in arsenopyrite-löllingite aggregates with native Bi, Bi-Te and Bi-Se minerals; in fractures of arsenopyrite; and as inclusions in quartz and plagioclase with native Bi and Bi-Se-Te minerals, arsenopyrite, chalcopyrite, and pyrrhotite. Although gold is seldom found as inclusions in chalcopyrite, chalcopyrite has higher lattice gold contents. Sb-bearing minerals were only found in one sample in association with gold, pyrrhotite, chalcopyrite, arsenopyrite, stannite, and galena (Kontoniemi et al. 1991).

METHODS

Three-hundred sixty-two samples of core from 10 different diamond drill holes were analyzed for 11 elements. Holes were selected to represent three profiles penetrating the main mineralized bodies (Osikko 1 and Osikko 3) at the center and at both ends (Fig. 2). The total distance between these profiles is about 600 m. One hole was sampled from Osikko 2 ore body some 2 km west from the main prospect. Each core was split in to halves and sampled with 1 to 1.5 m intervals using gold assays and drill-core logs as to ensure a continuous section including the ore horizon and unmineralized wallrocks on both sides. The samples were crushed with a jaw crusher and a representative portion (about 100 g) milled for analysis.

Gold, Ag, Te, Se and Bi were analyzed by graphite furnace atomic absorption spectrometry using a 20 g sample for Au and Ag and 0.5 g sample for Te, Se, and Bi (Niskavaara & Kontas 1990). This method yields very high quality data for these elements (Nurmi et al. 1991) with detection limits of 0.01 ppm. Copper, Mo, Pb, Sb, and S were determined by inductively coupled plasma atomic emission spectrometry (ICP-AES) after 90°C aqua regia leach. Detection limits are Cu and Mo, 0.5 ppm; Pb, 3 ppm; Sb, 4 ppm; and S, 5 ppm. Cu, Mo Pb, and Sb are likely of good quality as aqua regia leach is

expected to mostly liberate these elements. S data are high quality. Although a large suite of additional elements were analyzed by ICP-AES, they are not included here because their quality is suspect due to incomplete liberation by the low temperature aqua regia leach.

The samples were carefully selected to include the spectrum of rock and ore types observed by hand specimen study within and in close proximity to the mineralized zone. The samples also provide both vertical and lateral coverage of the ore body (Fig. 2). The computerized geochemical data base was manipulated via the programs SYSTAT and SYGRAPH (Wilkinson 1990a, b).

A significant number of values are below the detection limit (i.e. censored) so that the concentration bracketed rather than precisely known. This hampers statistical analysis. These censored values can be objectively replaced as described by Sanford et al. (1992) or nonparametric (rank) statistical procedures can be used. For this study nonparametric methods were used. As the Osikonmäki geochemical data are not normally distributed and contain outliers, nonparametric procedures also provide the advantage of being less sensitive to these problems, yielding more robust statistical estimates (e.g., Rock 1988).
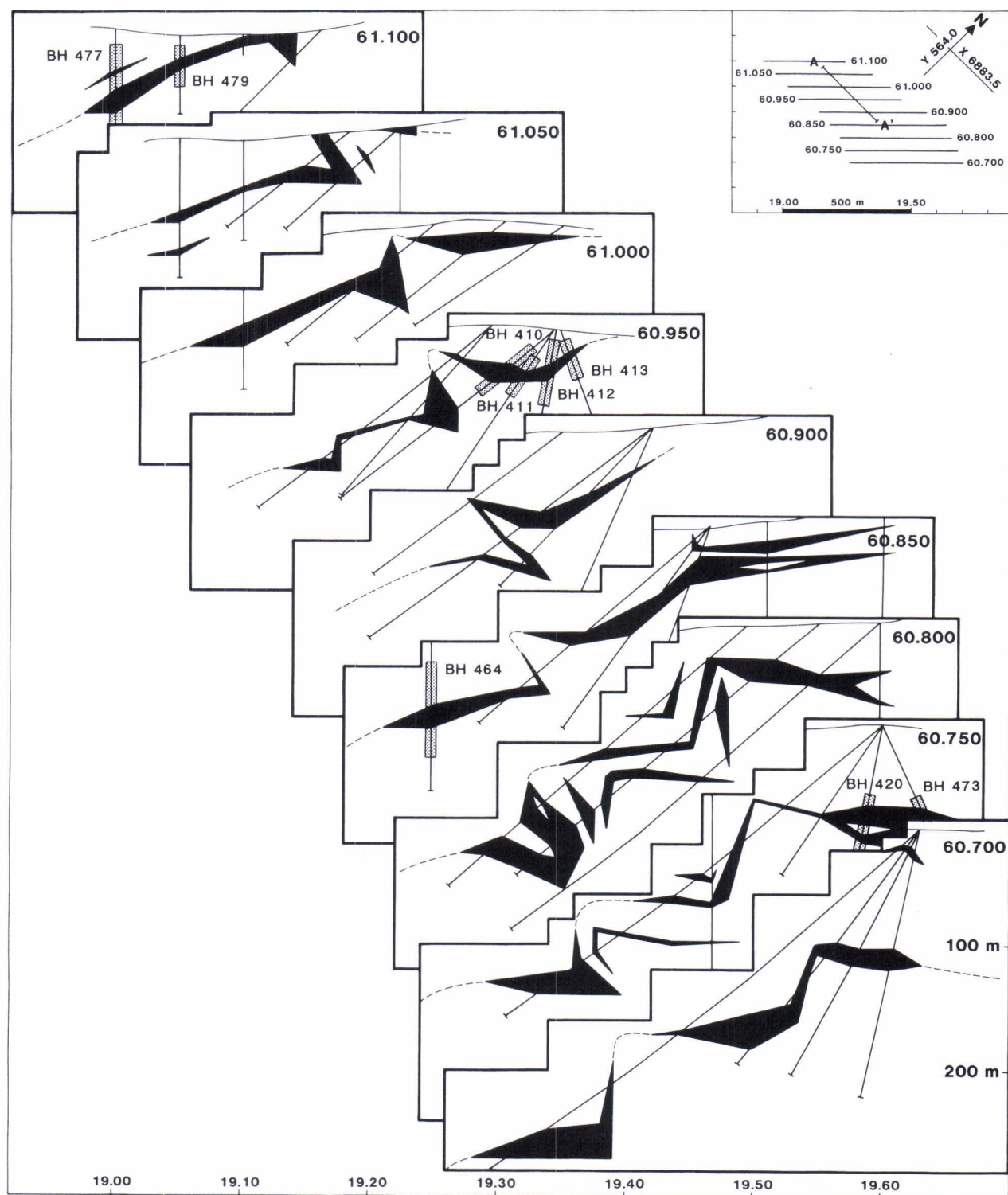
Fig. 2. Block diagram of the claim Osikko 1 between profiles L=60.700 and 61.000, also showing location of sample sites in drill holes (stippled). Black areas represent ore sections (cut off 0.5 g/t Au).

ELEMENTAL ABUNDANCE

The Osikonmäki ore body has been defined by Kontoniemi and Ekdahl (1990) using 0.5 and 1.0 ppm Au cutoffs which yields an ore body of about 4 Mt averaging 2 ppm Au or 2 Mt averaging 3 ppm Au, respectively. Out of the 362 samples analyzed for this study, 142 samples contain Au greater than 0.5 ppm and 100 samples contain Au greater than 1.0 ppm Au. The average Au contents of 2.5 and 3.3 ppm using the 0.5 and 1.0 ppm Au limits, respectively, for samples from this study are similar to those reported by Kontoniemi and Ekdahl (1990). In addition, using a 1.0 ppm Au cutoff Kontoniemi and Ekdahl (1990) report average As contents of 7700 ppm. The geochemical data used here yield an average As abundance of 8640 ppm using a 1.0 ppm Au cutoff. These comparisons suggest that the data reported here are a good representation of the Osikonmäki ore geochemistry. The entire 362 samples reported here range from barren (<0.01 ppm Au) to high-grade (42 ppm Au) (Table 1). Overall distribution of Au, Ag, As, Bi, Cu, S, Se, and Te

approximate log-normal with some outliers. Pb and Mo are approximately normally distributed with some outliers at high concentrations. Sb is between normally and log-normally distributed.

Since the Osikonmäki deposit is hosted by only one rock type (tonalite), variable starting rock composition should have minimal effect on the observed geochemical variations. Relative to unmineralized tonalite the ore body is extremely enriched in As compared to other elements (Fig. 3). All elements considered here are enriched in the ore and surrounding host rocks with Mo the lowest at 5 times unmineralized tonalite. This is a clear indication that secondary (hydrothermal) processes are responsible for geochemical variations in the data. The singular host rock and high degree of enrichment of all elements considered here makes quantitative mass transfer calculations such as those done by Bornhorst et al. (1993) not a necessary prerequisite to accurate geochemical interpretations.

Table 1. Geochemical character of the Osikonmäki gold deposit (in ppm). Includes drill hole 460.

A. Entire geochemical data set, N = 362.

ppm	Au	Ag	As	Bi	Cu	Mo	Pb	S	Sb	Se	Te
Minimum	<0.01	0.01	<3.	0.01	5.	0.6	3.	108.	<4.	<0.01	<0.01
Maximum	42.	4.97	58600.	119.	2430.	24.3	142.	23900.	25.	94.3	6.88
Median	0.30	0.20	413.	1.49	105.	2.6	10.0	5085.	5.1	3.34	0.04
Median deviation from median	0.28	0.17	401.	1.26	79.	0.5	3.1	3060.	6.2	3.18	0.05

B. Samples with >0.5 ppm Au, N = 142

ppm	Au	Ag	As	Bi	Cu	Mo	Pb	S	Sb	Se	Te
Minimum	0.5	0.05	14.3	0.11	22.6	0.8	3.5	108.	<4.	0.33	< 0.01
Maximum	42.	4.97	58600.	119.	2430.	24.2	142.	23900.	25.	94.3	6.98
Median	1.40	0.80	5060.	5.22	276.	2.8	11.2	8560.	5.3	11.7	0.21
Median deviation from median	0.70	0.32	4224.	2.68	177.	0.5	4.1	2140.	6.7	6.9	0.18

C. Samples with >1.0 ppm Au, N = 100

ppm	Au	Ag	As	Bi	Cu	Mo	Pb	S	Sb	Se	Te
Minimum	1.0	0.11	24.7	0.22	24.	1.3	3.5	108.	<4.	0.40	<0.01
Maximum	42.	4.97	58600.	42.	2430.	24.2	142.	23900.	23.	94.3	6.88
Median	2.05	0.96	5080.	6.62	391.	2.9	12.5	9395.	5.7	11.9	0.29
Median deviation from median	0.85	0.36	4006.	2.80	277.	0.5	4.7	2105.	5.5	6.8	0.22

D. Background tonalite from Nurmi et al. (1991)

	Au	Ar	As	Bi	Cu	Mo	Pb	S	Sb	Se	Te
	.001	0.013	<0.6	<0.1	14.6	<1.	<2.	30.	0.2	<0.02	0.005

The difference between the enrichment in all samples as compared to samples only from the gold ore body (>1.0 ppm Au) provides a first approximation of those elements geochemically part of the hydrothermal system that deposited gold. Arsenic, Se, Bi, Te, Cu and to a lesser degree S show preferential enrichment in the gold orebody. Antimony, Pb, and Mo show little preferential enrichment in the gold enriched portion of the system.

Nurmi et al. (1991) have demonstrated that Paleoproterozoic Svecofennian gold deposits from the Fennoscandian Shield are relatively enriched in As, Bi, Se, Sb, and Cu and depleted in Mo relative to comparable gold deposits from the Paleoproterozoic Lapland greenstone belt, Archean of Finland, and Archean of Australia and Canada. Since these elements of ten show a positive correlation with Au within a single deposit, it is necessary to compare deposits with one another at similar levels of Au. Using elemental ratios with gold shows that Osikonmäki is extremely enriched in As and Se relative to other deposits, including those of the Paleoproterozoic Svecofennian group in which Osikonmäki is a member (Table 2). To a lesser degree enrichment in Sb, Mo, and Cu characterizes Osikonmäki.

Although a certain amount of spatial geochemical variability is expected for a gold deposit, that is the product of a complex hydrothermal system, such as Osikonmäki, it necessary to identify outliers with respect to the overall deposit. Previous geologic study of the Osikonmäki deposit (petrology and geochemistry) by Kontoniemi suggested that the ore body in vicinity of hole 460 (Fig. 1) was quite different from the rest of the ore body. Alteration in this area looks different than elsewhere and includes tourmaline, not found in other parts of the ore body. Antimony-bearing minerals were only found in one sample near this hole.

For those samples from hole 460 with Au > 0.5 ppm, the concentrations of As, S, Mo and Au itself fall within the variation shown by the rest of the ore body and Ag and Pb are within the high concentration end of the variation. However, Te, Bi, and Cu define the low concentration end of the variation with most samples having concentrations outside those from other drill holes. Te and Bi are almost completely outside the range shown by the rest of the ore body (compare Tables 1 and 3). Sb defines the high concentration end of the variation with most samples outside those from other drill holes. Spearman (rank) correlation coefficients for element-element pairs were calculated for the entire data set (with data from hole 460) and for each individual drill hole. For most drill holes the element-element rank correlation coefficients are usu-
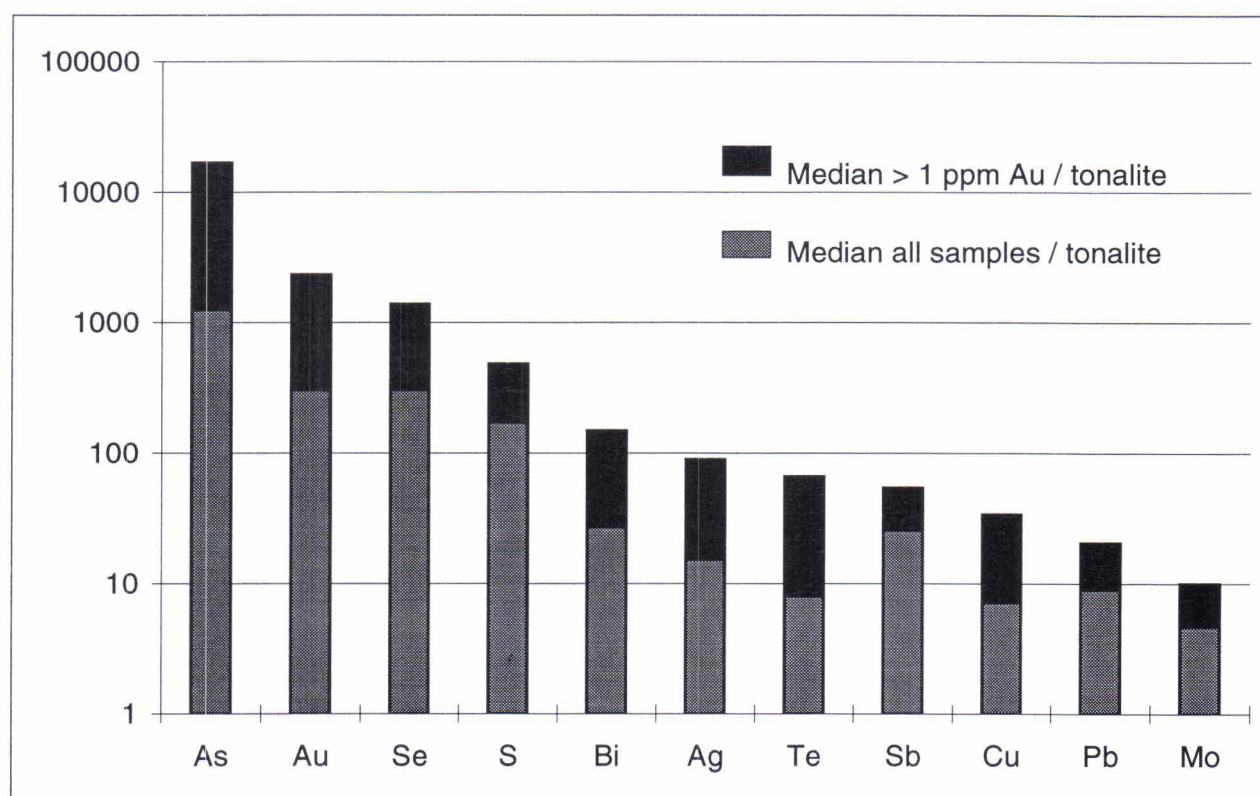
Fig. 3. Geochemical enrichment in the Osikonmäki gold deposit relative to unmineralized tonalite. Data are given in Table 1 (0.55 times the detection limit substituted for values in the tonalite at the detection limit).

Table 2. Comparison of Osikonmäki to other gold deposits.

	Median ratios								
	As/Au	Se/Au	Sb/Au	Mo/Au	Cu/Au	Bi/Au	Te/Au	S/Au	Ag/Au
Archean Australia and Canada*	30.	0.04	0.27	0.53	18.	0.02	0.07	3150.	0.35
Archean Finland*	12.	0.05	0.06	0.90	16.	0.42	0.48	1976.	0.14
Early Proterozoic Lapland*	11.	0.28	0.10	0.77	57.	0.56	0.13	8769.	0.06
Early Proterozoic* Sveco-fennian (includes Osikonmäki)	592.	0.92	0.97	0.24	112.	4.0	0.42	2632.	0.45
Osikonmäki[1]	2478.	5.8	2.8	1.4	190.	3.2	0.14	4582.	0.46

* Data from Nurmi et al (1991)
[1] Data table 1 (>1.0 ppm Au) this study

Table 3. Geochemical composition of samples with > 0.5 ppm Au in drill hole 460 (in ppm). See Figure 1 for location of drill hole 460. N = 15

	Au	Ag	As	Bi	Cu	Mo	Pb	S	Sb	Se	Te
Minimum	0.60	0.82	1430	0.11	22.6	2.1	13.5	8460.	5.2	0.33	<0.01
Maximum	6.20	3.57	13200.	1.12	96.2	4.4	45.2	16300.	25.	3.97	0.03
Median	1.10	1.52	6120.	0.48	31.6	3.1	27.1	12600.	13.5	0.94	0.01
Median deviation from median	0.30	0.43	2090.	1.15	7.6	0.5	5.3	1200.	4.9	0.47	0.01

ally within 0.25 correlation units of those for the entire data set. If hole 460 is excluded, only 3 pairs are different by more than 0.5 correlation units. For hole 460, 24 out of 55 pairs or 44 % are more than 0.5 correlation units from the entire data set. For example, the Spearman correlation coefficient for Au-Te in the entire data set (with hole 460) is 0.767 (N=362) and eight individual drill holes have Au-Te correlation coefficients of between 0.813 and 0.942 (N between 18 and 48) and one hole has 0.691 (N=52). In contrast, drill hole 460 has a Spearman correlation coefficient for Au-Te of 0.169 (N=48). We conclude that drill hole 460 is an outlier. To provide more homogenous dataset that better represents the overall Osikonmäki ore body, the data from hole 460 will be dropped from further statistical analysis.

GEOCHEMICAL ASSOCIATIONS

Graphical and statistical analysis have been used to define geochemical associations i.e., elements that are geochemically linked or follow each other. Simple inspection of Spearman correlation coefficients for the Osikonmäki geochemical data set (without data from drill hole 460) shows that Ag, As, Bi, Cu, S, Se, and Te are well correlated with Au (Table 4). These correlations are remarkably high given the complex nature of hydrothermal systems. Although the magnitude of correlation varies, these elements also correlate well with each other. Molybdenum, Pb and Sb are not closely associated with Au and its associated elements, but seem to be related to each other. Varimax rotated principal components models of these rank correlations yield one component dominated by Au, Ag, As, Bi, Cu, S, Se, and Te and includes Mo with a moderate loading (association). Pb and Sb form separate components, consistent with inspection. In some models, Sb, Mo, Pb form separate components, As, S and Se form a separate component with some association to Au, Ag, and Cu, and Cu and Ag show a tendency to form a separate component. These latter results give indication of a more complex geochemical system.

Some of the correlation within individual element-element pairs for the entire data set is likely the result of zoning as concentrations decrease away from the ore body. Such correlation masks the real geochemical associations of the core of the hydrothermal system. A more restrictive data set utilizing only samples within the ore body partially eliminates this problem and provides geochemical associations within the ore body in the main part of the hydrothermal system.

Two ore body data sets were analyzed, >0.5 ppm Au and >1.0 ppm Au. Spearman correlations for the >0.5 ppm ore body are quite different than those using the entire data set (Table 5). Simple inspection shows that Bi and to a slightly lesser degree Te are very well correlated with Au and Ag and to a lesser degree Cu are correlated with Au. Arsenic, Se, and S are very well correlated with each other. Other relationship are less clear. Varimax rotated

Table 4. Matrix of Spearman correlation coefficients for barren to ore grade samples in the Osikonmäki geochemical data set, excluding drill hole 460. Correlations above 0.07 are statistically significant at the 90 % confidence level. N=314.

	Au	Ag	As	Bi	Cu	Mo	Pb	S	Sb	Se	Te
Au	1.000										
Ag	0.827	1.000									
As	0.759	0.755	1.000								
Bi	0.882	0.761	0.633	1.000							
Cu	0.785	0.907	0.651	0.746	1.000						
Mo	0.370	0.404	0.361	0.320	0.376	1.000					
Pb	0.203	0.210	0.170	0.206	0,135	0.184	1.000				
S	0.755	0.855	0.807	0.703	0.777	0.421	0.183	1.000			
Sb	0.043	0.028	-0.083	0.002	-0.006	0.031	0.112	-0.040	1.000		
Se	0.817	0.825	0.910	0.699	0.750	0.410	0.168	0.924	-0.025	1.000	
Te	0.858	0.766	0.652	0.826	0.762	0.276	0.230	0.616	0.010	0.671	1.000

Table 5. Matrix of Spearman correlation coefficients for ore grade samples with > 0.5 ppm Au in the Osikonmäki geochemical data set, excluding drill hole 460. Correlations above 0.11 are statistically significant at the 90 % confidence level. N=127

	Au	Ag	As	Bi	Cu	Mo	Pb	S	Sb	Se	Te
Au	1.000										
Ag	0.504	1.000									
As	0.054	0.244	1.000								
Bi	0.843	0.337	-0.107	1.000							
Cu	0.410	0.681	-0.198	0.388	1.000						
Mo	0.306	0.224	0.224	0.297	0.146	1.000					
Pb	0.134	0.034	0.133	0.099	-0.197	0.241	1.00				
S	0.189	0.418	0.774	0.071	0.032	0.383	0.198	1.000			
Sb	0.195	0.246	-0.044	0.112	0.113	0.070	0.162	0.004	1.000		
Se	0.114	0.336	0.900	-0.042	-0.087	0.293	0.171	0.892	-0.029	1.000	
Te	0.667	0.486	-0.133	0.561	0.479	-0.008	0.095	-0.060	0.242	-0.092	1.000

Number of observatios: 127

Table 6. Representative varimax rotated principal components model of Spearman correlation coefficients given in Table 5.

	1	2	3	4	5	6
Ag	0.272	0.336	0.826	0.162	0.026	0.038
As	-0.037	0.949	-0.076	-0.006	0.009	0.021
Au	0.915	0.112	0.219	0.087	0.128	0.041
Bi	0.915	-0.058	0.113	-0.009	0.223	-0.006
Cu	0.246	-0.142	0.894	-0.006	0.112	-0.161
Mo	0.164	0.213	0.094	0.031	0.917	0.132
Pb	0.079	0.110	-0.089	0.082	0.117	0.970
S	0.041	0.902	0.147	-0.009	0.210	0.085
Sb	0.097	-0.027	0.095	0.985	0.024	0.079
Se	-0.010	0.971	0.041	-0.016	0.083	0.061
Te	0.713	-0.098	0.422	0.141	-0.287	0.155

Percent of total varience explained by component

1	2	3	4	5	6
21.491	26.136	16.144	9.372	9.714	9.352

principal component models of rank correlations for both the >0.5 ppm Au (N=127) and >1.0 ppm Au (N=90) data sets yield quite similar results. The two major components in most models consist of two uncorrelated associations: Au, Bi, and Te and As, S, and Se. Cu and Ag form another independent geochemical association with a weak affinity to the Au association. The three major and consistent components account for much (~65 to 75 %) of the total variance of the geochemical data (Table 6). Relationships between Mo, Pb, and Sb are less clear. They tend to form components independent from each other and the other three main associations. Mo does show a weak affinity for the Au

association.

Because of limited data continuity, spatial analysis of the Osikonmäki geochemical data is somewhat limited. Overlays of element concentration contoured on an east versus depth profile clearly shows similarity between Au, Bi, and Te, between As, S, and Se, and between Cu and Ag. The patterns of Mo, Pb, and Sb are dissimilar to each other and the other groupings. The same relationships are shown by contoured concentrations on north versus depth profile but with less clarity. These same geochemical groupings are also observed by visual inspection of concentration versus depth plots within drill holes.

DISCUSSION

Analysis of the geochemical data from the Osikonmäki gold deposit indicates three distinct geochemical associations: 1) Au, Bi, and Te; 2) As, S, and Se; and 3) Cu and Ag. Molybdenum, Pb, and Sb vary independent of each other and other associations. Ore mineralogical observations of Kontoniemi et al. (1991) provide a means of confirming the geochemical associations and providing geologic context. Gold at Osikonmäki is closely associated with Bi and Te minerals, mostly as inclusions in quartz with lesser frequency as inclusions in As-bearing arsenopyrite and löllingite and in pyrrhotine. Gold is found in fractures in arsenopyrite indicating a later and separate episode of deposition. Gold is seldom found as inclusions in chalcopyrite but chalcopyrite has high lattice Au. The Au, Bi, and Te geochemical association distinct from As and Cu is compatible with mineralogical observations. Arsenic-bearing arsenopyrite and löllingite probably precipitated before sulfides such as pyrrhotite and chalcopyrite. This is compatible with separate episodes of As and Cu precipitation. Mineralogical data suggest that the Au, As, and Cu associations were deposited as part of a continuous hydrothermal event. Younger fractures and fissures contain scheelite and powellite (Mo-bearing) compatible with a distinct episode of Mo precipitation. Antimony-bearing minerals are rare at Osikonmäki.

Mineralogical observations of Kontoniemi et al. (1991) are consistent with the geochemical associations recognized here. Although paragenesis is not well defined, the geochemical associations are best interpreted as episodes of metal precipitation from the hydrothermal fluids that were likely mostly distinct but somewhat overlapping in time. The early As association was followed by the Au and Cu associations in undetermined order. The apparent lack of S in the Cu association is best explained by the volumetric dominance of As-bearing minerals as compared to Cu-bearing minerals. The fluid pathways for each episode were likely spatially different in detail but overlapped on the scale of the ore body. These data are not sufficient to determine whether or not any of the geochemical associations were the product of a more regional rather than local hydrothermal system, although the As, Au, and Cu associations are best interpreted as part of a continuously evolving hydrothermal system. Perhaps Mo, Pb, and Sb represent a later and more regional event. Since a tonalite intrusion has low overall permeability and porosity, fluid movement is limited. Hydrothermal fluids, whether of regional or local extent will be localized by fractures and faults, including the shear zone at Osikonmäki. Complex superposition of hydrothermal fluids over time would be enhanced by continuing structural adjustments.

All elements studied here are good indicators of focused hydrothermal activity, as they are significantly enriched over background tonalite. However, only one episode of this evolving hydrothermal system resulted in the precipitation of the economic target, Au. This episode also resulted in deposition of Bi and Te. Local geochemical exploration should use a combination of Au+Te+Bi as an indicator of Au potential hydrothermal fluids. While As and Cu associations are not directly related to Au they too are indicators of a long-lived, evolving, complex hydrothermal system which may be an important prerequisite to generation of economic Au ore. The Au+Te+Bi association has been recognized as important for gold exploration elsewhere in Finland for the Late Archean Hattu schist belt (Rasilainen et al. 1993; Rasilainen 1993).

CONCLUSIONS

The Osikonmäki gold deposit is hosted by a shear zone in a single rock type, tonalite. The deposit contains a suite of enriched elements, including Au, As, Se, S, Bi, Ag, Te, Sb, Cu, Pb, and Mo. It is particularly characterized by high concentrations of As, Au, and Se. Drill holes at the extreme east end of the ore body intersected mineralized rock with a much different geochemical signature than the rest of the ore body. The significance of this geochemical outlier is not certain. Although the ore body is characterized by As, Au, and Se, graphical and statistical analysis of variations with the geochemical data are consistent with distinct episodes of precipitation of Au, Bi, and Te and As, S, and Se. Although all of these elements are quite enriched at Osikonmäki, they are interpreted as temporally different but continuous episodes of precipitation which spatially overlap on the scale of the ore body. In detail, the different fluids followed slightly different pathways as a result of filling of earlier pore spaces and on-going movement in the shear zone. Cu and Ag also were deposited during the main part of the evolving Osikonmäki hydrothermal system, but as a separate episode. The precipitation of Mo, Pb, and Sb was separate from the other elements and of uncertain relationship to the main hydrothermal event. A combination of Au+Bi+Te is the best geochemical indicator for Au potential fluids in the Osikonmäki ore system.

REFERENCES

Bornhorst, T.J. & Rasilainen, K. 1993. Mass transfer during hydrothermal alteration associated with Au mineralization within the Late Archean Hattu schist belt, Ilomantsi, eastern Finland. In: Nurmi, P.A. & Sorjonen-Ward, P. (ed.) Geological Development, Gold Mineralization and Exploration Methods in the Late Archean Hattu Schist Belt, Ilomantsi, Eastern Finland. Geological Survey of Finland, Special Paper 17, 273-289.

Gaál, G. 1986. 2200 million years of crustal evolution: The Baltic Shield. Bulletin of the Geological Society of Finland 58, 149-168.

Kontoniemi, O. 1989. The Osikonmäki gold occurrence at Rantasalmi, southeastern Finland. In: Autio, Sini (ed.) Geological Survey of Finland, Current Research 1988. Geological Survey of Finland, Special Paper 10, 107-110.

Kontoniemi, O. 1998a. An overview of the geology in the Osikonmäki area, Rantasalmi, southeastern Finland: Especially as a promising environment for epigenetic gold mineralization. In: Kontoniemi, O. & Nurmi, P. A. (eds.) Geological setting and characteristics of the tonalite-hosted Paleoproterozoic gold deposit at Osikonmäki, Rantasalmi, southeastern Finland. Geological Survey of Finland, Special Paper 25, 7-18.

Kontoniemi, O. 1998b. Geological setting and characteristics of the Paleoproterozoic tonalite-hosted Osikonmäki gold deposit, southeastern Finland In: Kontoniemi, O. & Nurmi, P.A. (eds.) Geological setting and characteristics of the tonalite-hosted Paleoproterozoic gold deposit at Osikonmäki, Rantasalmi, southeastern Finland, Geological Survey of Finland, Special Paper 25, 39-80.

Kontoniemi, O. & Ekdahl, E. 1990. Tonalite-hosted Early Proterozoic gold deposit at Osikonmäki, southeastern Finland. Bulletin of the Geological Society of Finland 62, 61-70.

Kontoniemi, O., Johanson, B., Kojonen, K. & Pakkanen, L. 1991. Ore mineralogy of the Osikonmäki gold deposit, Rantasalmi, southeastern Finland. In: Autio, Sini (ed.) Geological Survey of Finland, Current Research 1989-1990. Geological Survey of Finland, Special Paper 12, 81-89.

Niskavaara, H. & Kontas, E. 1990. Reductive coprecipitation as a separation method for the determination of gold, pallarium, platinum, rhodium, silver, selenium, and tellurium in geological samples by graphite furnace atomic absorption spectrometry. Analytica chimica Acta 231, 273-282.

Nurmi, P. A., Lestinen, P. & Niskavaara, H. 1991. Geochemical characteristics of mesothermal gold deposits in the Fennoscandian Shield, and a comparison with selected Canadian and Australian deposits. Geological Survey of Finland, Bulletin 351. 101 p.

Rasilainen, K. 1993. Differences in geochemistry of Au and the semimetals As, Bi, and Te in gold occurences at the Late Archean Hattu schist belt, Ilomantsi, eastern Finland. In: Autio, Sini (ed.) Geological Survey of Finland, Current Research 1991-1992. Geological Survey of Finland, Special Paper 18, 113-117.

Rasilainen, K., Nurmi, P.A. and Bornhorst, T.J. 1993. Rock geochemical implications for gold exploration in the Late Archean Hattu schist belt, Ilomantsi, eastern Finland. In: Nurmi, P.A. & Sorjonen-Ward, P. Geological Development, Gold Mineralization and Exploration Methods in the Late Archean Hattu Schist Belt, Ilomantsi, Eastern Finland. Geological Survey of Finland, Special Paper 17, 353-362.

Rock, N.M.S. 1988. Summary statistics in geochemistry: A study of the performance of robust estimates: Mathematical Geology 20, 243-275.

Sanford, R.F., Pierson, C.T., & Crovelli, R.A. 1992. An objective replacement method for censored geochemical data: Mathematical Geology 25, 59-80.

Vaasjoki, M. & Kontoniemi, O. 1991. Isotopic studies from the Proterozoic Osikonmäki gold prospect at Rantasalmi, southeastern Finland. In: Autio, Sini (ed.) Geological Survey of Finland, Current Research 1989-1990. Geological Survey of Finland, Special Paper 12, 53-57.

Wilkinson, L. 1990a. SYSTAT: The system for statistics. Evanston, IL, U.S.A., SYSTAT, Inc., 677p.

Wilkinson, L. 1990b. SYGRAPH: The system for graphics. Evanston, IL, U.S.A., SYSTAT, Inc., 547p.

FLUID INCLUSION DATA FROM THE OSIKONMÄKI GOLD DEPOSIT, RANTASALMI, SOUTHEASTERN FINLAND

by
Jyrki Liimatainen

Liimatainen, Jyrki 1998. Fluid inclusion data from the Osikonmäki gold
deposit, Rantasalmi, southeastern Finland. *Geological Survey of Finland,
Special Paper 25.* 91 -99. 6 figures and 3 tables.

Four different quartz types in the Osikonmäki gold deposit were studied
by fluid inclusion microthermometry. No inclusion data was available
where there had been early shearing or from deposition of early arsenopyrite.
The oldest fluid inclusions, which contain carbon dioxide, were found from
recrystallized sheared tonalite. These inclusions have 5 % methane and a
density around 0.75 g/cm^3. Primary and early secondary aqueous inclusions
in the vein quartz contain saline water with 2 - 5 wt % equivalent NaCl.
Calculated isochores for these early fluids reach the pressure-temperature
conditions of regional D_2 - D_3 deformation at 690°C and 2.9 kbars. Late
secondary aqueous fluid inclusions appear in several types with salinity
range from 0 to 14 wt % NaCl. One of these fluid types with 8 - 14 wt % NaCl
is related to secondary enrichment of gold. The isochores of different late
secondary fluids suggest, that the appearance of this saline fluid has
accompanied with minor reheating of the area.

INTRODUCTION

Osikonmäki is a small gold deposit (2 Mt 3 g/t gold and 0.77 % arsenic) near Rantasalmi in southeastern Finland. The bedrock of the area, at regional scale, consists of granitoids and metamorphic sedimentary and volcanic rocks. The deposit is hosted by a shear zone cutting through an Early Proterozoic tonalite intrusion. The tonalite intrusion is a synkinematic I-type granitoid with calc-alkaline affinity and a U-Pb zircon age of 1887 Ma (Kontoniemi and Ekdahl 1990; Vaasjoki and

Kontoniemi 1991). Amphibolite facies regional metamorphism has altered the mineralogy and D_2 deformation has resulted in a gneissose texture in the weakly porphyritic tonalite. The E-W-trending, gently (40-45°) southwards dipping shear zone is at least 3 km long. The texture of the sheared rock is foliated and granoblastic. Shearing probably occurred before the intrusion of granitoids at 1850 Ma; these granitoids lack E-W-trending shear zones. Gold-bearing arsenides and some sulphides were

precipitated in the shear zone forming banded disseminations. Later, the zone was deformed during the regional D_3-phase, which was active 1830 - 1810 Ma ago, and some gold-bearing arsenopyrite and quartz veins crystallized during this late shearing and folding event. The gold-bearing parts of the zone are 2 - 20 m thick (Kontoniemi and Ekdahl 1990). Detailed descriptions of regional and depositional geology are given in the other articles of this volume.

SAMPLE SELECTION

Material for this fluid inclusion research was selected from the core samples that the Geological Survey of Finland had drilled from the shear zone. Three samples are from the eastern part of shear zone that contain the highest amounts of gold. Two samples are from quartz-tourmaline veins at the western end and one is from barren middle part (Table 1).

Different quartz types were recognized and classified from the oldest sheared tonalite quartz, QA, through broken vein quartzes, QB and QC, to the unbroken vein quartz, QD (Fig. 1). These vein

Table 1. Quartz and fluid inclusion types in the samples.

Part of shear zone		Quartz type			
Drill hole/depth	QA	QB	QC	QD	
East:					
R403/ 180.20 m	SE	SL,SG,SE,P	-	SL,SG,SE,P	
R403/ 302.30 m	SL,SG	-	SL,SG,SE,P	SL,SG,SE,P	
R477/ 47.80 m	-	SL,SG,SE,P	-	-	
Middle:					
R427/ 48.10 m	SG,SE	SL,SG,SE,P	-	-	
West:					
R505/ 93.50 m	SG	SL,SE	-	SL,SG,SE,P	
R520/ 143.70 m	P	SL,SG,P	-	SL,SG,SE,P	

quartz types are probably genetically close to each other, but their appearance is different. QA is recrystallized quartz from sheared tonalite, which forms the host rock of the deposit. Equigranularity and grain contacts of triple junction type suggest that this small grained foliated rock recrytallized during metamorphism. Broken thin quartz veins that follow the foliation, and which may have been folded, belong to QB type. QC is a peculiar spotted quartz type that contains many small exsolutions. These have a low refractive index suggesting that they are potassium feldspar. So far this type has been found only from one sample. QD quartz forms the widest veins with clear and unbroken large crystals. These veins are parallel to the foliation and may be deformed by open folds (Fig. 1).
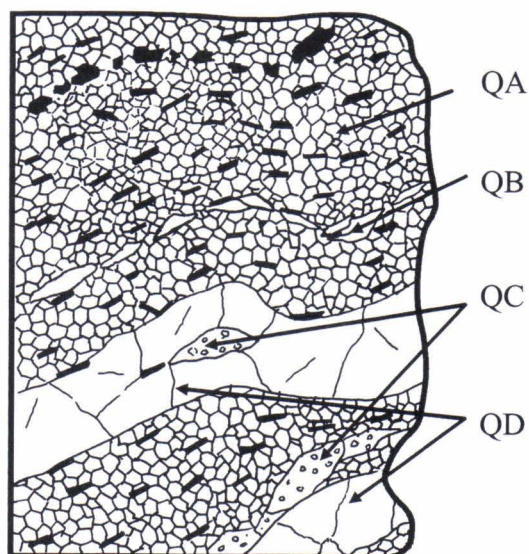
Fig. 1. Schematic diagram showing the different quartz types in the Osikonmäki samples. More detailed explanation is in the text.

METHODS

Doubly-polished 0.5 mm thick sections prepared at the University of Turku were examined with polarizing microscope. Despite fluorite and tourmaline grains in some samples, the only inclusions suitable for microthermometry were found in quartz. Microthermometry of selected inclusions was carried out using a Fluid Inc. heating/freezing gas-flow stage. The stage is cooled by nitrogen gas flowing from a liquid nitrogen container. The temperature is controlled with an electric heating element, with a range of -180 °C to 500 °C, and it is measured from the upper surface of sample by a thermocouple. The thermocouple was calibrated against standards at 0 °C and -56.6 °C. At temperatures below 40 °C, the reproducibility of results is about 0.1 °C , but it increases to few degrees when temperature is over 200 °C.

The temperatures measured during microthermometry were melting temperature (Tm) and homogenization temperature (Th). Freezing experiments were carried out prior to heating. The composition and molar volume of the carbon dioxide inclusions were estimated from the melting point of carbon dioxide ice and their homogenization temperature by using the phase diagrams of Heyen et al. (1982) and Kerkhof (1990). Isochores for these inclusions were calculated from an equation given by Kerrick and Jacobs (1981). The salinity of the sole clathrate forming inclusion was estimated from the stability diagrams of Diamond (1992). The salinities of aqueous inclusions were calculated from the melting point depression of ice with the equation of Bodnar (1993). Salinity is expressed as weight percent equivalent to sodium chloride. The densities and isochores of aqueous inclusions were calculated from the salinities and homogenization temperatures using the equations of Zhang and Frantz (1987).

MICROTHERMOMETRY

Inclusions from different samples and quartz types were selected and classified by their appearance. Samples usually have only part of the quartz types present and some inclusion classes might be absent especially from QA tonalite quartz (Table 1.). Primary inclusions (P) do not show any of those crystal growth relating structures summarized in Roedder (1984), but they occur as single or small groups of inclusions without any obvious planar structure (Fig. 2). Secondary inclusions were divided into three different types (SE, SG, SL). Early secondary inclusions (SE) form sparse clusters and the inclusions usually have a negative crystal shape. Some of these inclusions might have pseudosecondary or even primary origin. Normally secondary inclusions occur along healed fractures as dense planar groups. Some of these inclusions have quite regular shape and hence these kind of groups of secondary inclusions (SG) are separated from late secondary inclusions (SL), which form planar groups of inclusions with different size and shape (Fig. 2).

In QA quartz fluid inclusions are very rare and usually small - less than 10 mm in diameter. The probable primary fluid for recrystallized QA quartz is carbon dioxide, which was found from one sample (R403/302.20m). These inclusions have a melting temperature (Tm) for solid carbon dioxide of -

58 °C and a temperature of homogenization (Th) of 16.2 - 20.5 °C. Secondary inclusions in QA and QC have a similar Tm, but their Th is over 21 °C (Table 2. and Fig. 3). All these inclusions homogenized to a liquid phase. The estimated methane amount in the carbon dioxide inclusions is about 5 mole % and the molar volumes for primary inclusions are 55 - 60 cm^3/mol and 60 - 65 cm^3/mol for secondary inclusions (Heyen et al. 1982, Kerkhof 1990). Those few early aqueous inclusions of QA (both P/SE and SE types) have similar properties as inclusions in the QB and QD vein quartzes (Fig. 4) described later in this chapter. Therefore these early aqueous inclusions are classed as secondary in QA type quartz. Later secondary inclusions in QA quartz are also comparable to secondary inclusions in the vein quartzes.

Most of the fluid inclusions in all quartz types and samples consist of low salinity water without notable amounts of carbon dioxide. These inclusions contain a relatively small gas bubble and the normal method of homogenization is filling with liquid until the gas bubble disappears. Inclusions that homogenize to a gas phase (Table 3. marked as (V) and Fig. 4. filled symbols in Th versus salinity diagrams) usually have the same salinity, but higher homogenization temperature than those similar type of inclusions that homogenize to a liquid phase.

Therefore, these inclusions are probably a result of post trapping leakage or necking-down of inclusions, which is a common process in secondary inclusion planes when the fracture heals (Roedder 1979).

Primary and some early secondary aqueous inclusions, P/SE and SE, in all vein quartzes (QB,QC,QD) have a quite similar Th-range and salinity (Table 3. and Fig. 4). These early aqueous fluid inclusions have salinities around 5 wt % in the eastern part of the shear zone, where the mineralized body is and about 2 wt % in the weakly mineralized western part.

Homogenization temperatures are from 300 °C to 360 °C and calculated densities are between 0.63 g/cm^3 and 0.75 g/cm^3 for these early aqueous flu-
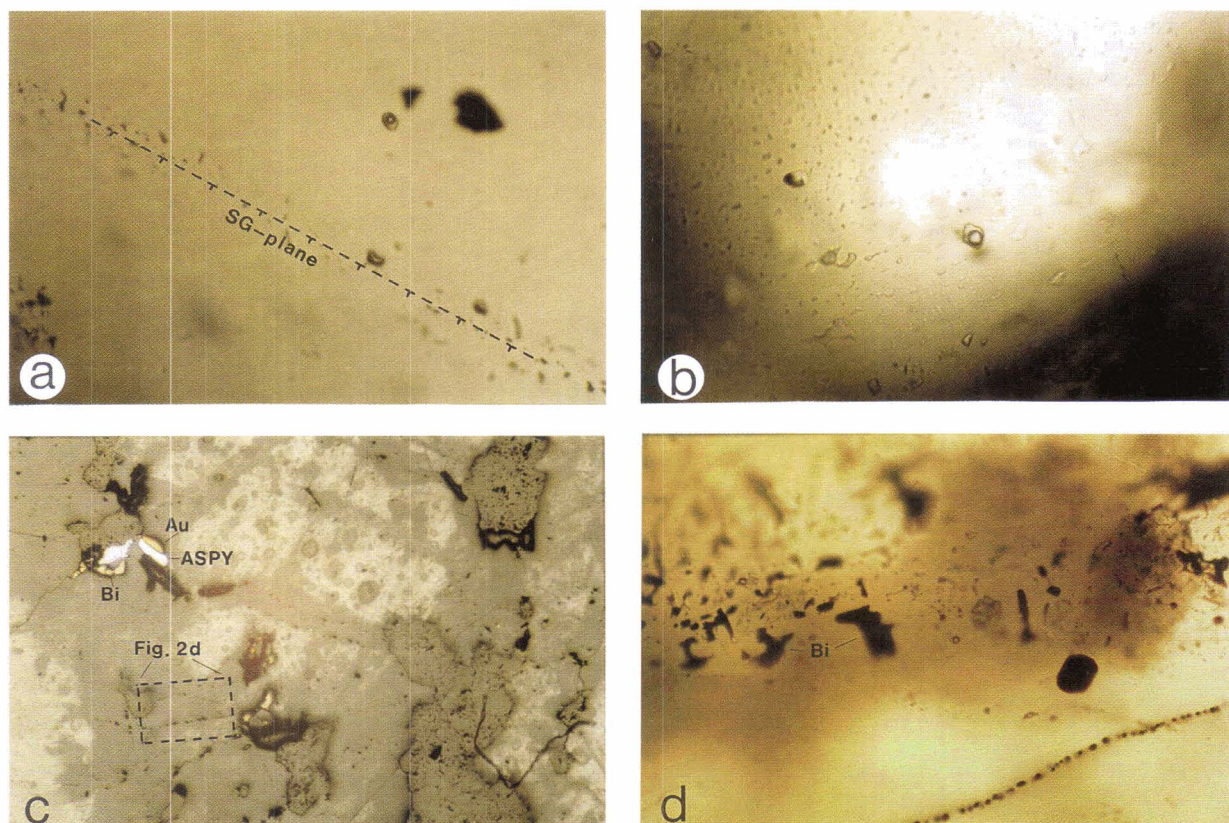
Fig. 2. Different fluid inclusion types in the Osikonmäki gold deposit: a) Primary inclusion (P) in QD-type quartz beside two opaque grains and diagonal plane of secondary SG inclusions. Length of primary inclusion is 8 mm, Tm is -3.4 °C (5.6 %) and Th 359.8 °C. b) Flat plane of late secondary inclusions (SL). Largest inclusion is 15 mm long, Tm range from -0.6 °C to -1.5 °C (1.1 - 2.6 %), Th around 210 °C, but most inclusions have no bubble. c) Gold (Au), bismuth (Bi) and arsenopyrite (ASPY) grains in spotted quartz (QC) with secondary inclusion trails, width of picture 7 mm. d) Detail of secondary inclusion plane, which has ameboidal bismuth (Bi) grains. Salinities of inclusion are from 8 wt % to 14 wt % equivalent to NaCl, width of picture 1.2 mm

Table 2. Microthermometric data of carbonaceous inclusions.

Type		Melting Tm (°C)			median	N	Homogenization Th (°C)			median	N
QA	SG		to	-57.8	-57.8	2	22.8	to	23.3	23.1	2
	P/SE	-58.0	to	-57.9	-57.9	4	16.2	to	20.5	18.0	4
QC	SE		to	-57.9	-57.9	3	21.0	to	22.2	22.1	3
	P/SE		to	-57.8	-57.8	4		-		-	0

N = Number of measurements

Table 3. Microthermometric data and salinity of aqueous inclusions.

Type		Melting Tm (°C)			median	N	Homogenization Th (°C)			median	N	Salinity wt-% NaCl			median
QA	SL	-			-	0		to	215	215	1			-	-
	SG(L)	-13.4	to	-0.5	-3.5	13	155	to	285	190	10	0.9	to	17.3	5.7
	SG(V)	-0.5	to	4.6	2.0	2	350	to	462	406	2	0.9	to	9.6	5.3
	SE	-3.7	to	-2.5	-3.3	6	180	to	315	181	3	4.2	to	6.0	5.4
	P/SE	-7.6	to	-0.7	-3.8	4	171	to	310	211	4	1.2	to	11.2	6.2
QB	SL	-2.2	to	-0.5	-0.7	9	178	to	283	256	6	0.9	to	3.7	1.2
	SG	-8.9	to	-0.7	-2.9	20	93	to	350	185	22	1.2	to	12.7	4.8
	SE(L)	-3.5	to	-0.5	-0.8	12	207	to	349	284	10	0.9	to	5.7	1.4
	SE(V)	-3.5	to	-0.7	-2.1	2	368	to	387	370	3	1.2	to	5.7	1.2
	P/SE(L)	-2.6	to	-0.5	-1.6	8	248	to	380	349	6	0.9	to	4.3	2.7
	P/SE(V)		to	-1.5	-1.5	1		to	380	380	1		to	2.6	2.6
QC	SL	-10.0	to	-0.6	-6.8	18	118	to	370	277	14	1.1	to	13.9	10.2
	SG	-4.3	to	-1.6	-1.8	4	178	to	313	289	4	2.7	to	6.9	3.1
	SE(L)	-2.5	to	-2.3	-2.4	4	293	to	372	360	5	3.9	to	4.2	4.0
	SE(V)		to	-11.5	-11.5	1	375	to	460	406	3		to	15.5	15.5
	P/SE		to	-3.4	-3.4	2			-		-	0	to	5.6	5.6
QD	SL	-9.8	to	-0.3	-1.2	19	112	to	341	215	15	0.5	to	13.7	2.1
	SG(L)	-3.6	to	-0.4	-3.2	22	222	to	385	299	17	0.7	to	5.9	5.3
	SG(V)	-3.5	to	-3.2	-3.4	13	386	to	500	410	14	5.3	to	5.7	5.6
	SE(L)	-1.4	to	-0.5	-0.5	3	292	to	369	298	3	0.9	to	2.4	0.9
	SE(V)		to	-2.0	-2.0	1		to	379	379	1		to	3.4	3.4
	P/SE(L)	-9.0	to	-0.6	-2.6	16	160	to	371	305	13	1.1	to	12.8	4.3
	P/SE(V)	-3.6	to	-1.2	-2.4	2	402	to	405	404	2	2.1	to	5.9	4.0

N = Number of measurements
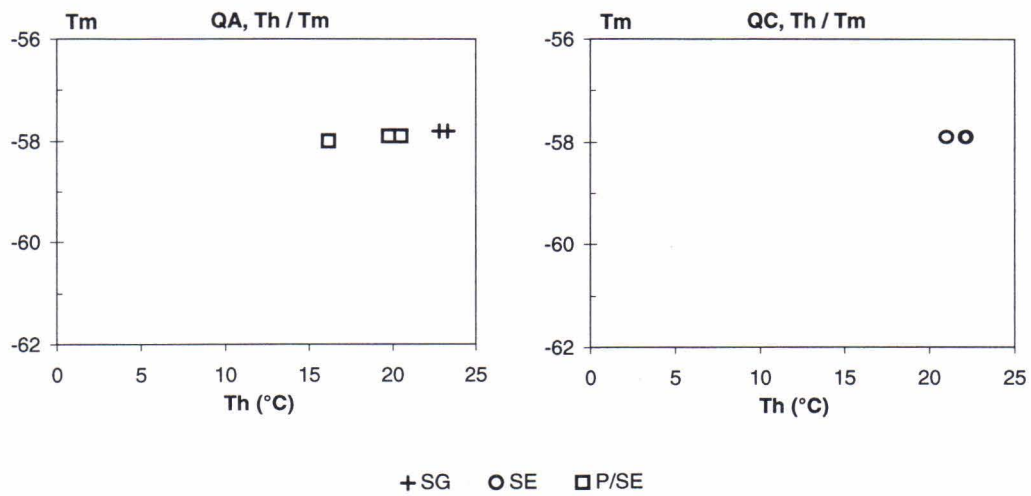
Fig. 3. Homogenization versus melting temperature diagrams of carbon dioxide inclusions in QA and QC quartz types.

ids. In the later aqueous fluids a distinct group of SG-type secondary aqueous inclusions is present in samples from the eastern part of the shear zone. These inclusions consist of fluid with salinity between 4 wt % and 6 wt %. Their homogenization temperature is between 160 °C and 230 °C in QA and QB types of quartz (Table 3. and Fig. 4). In QD quartz homogenization temperatures are higher, from 220 °C up to 300 °C. Densities calculated for

these inclusions vary from 0.86 g/cm³ to 0.95 g/cm³. SL-type late secondary aqueous inclusions occur in two broad groups, which have low homogenization temperature (usually under 260 °C) and either low salinity (0-4 wt %) or high salinity (over 10 wt %) (Table 3. and Fig. 4). Densities for low salinity fluids are close to 1 g/cm³, and for high salinity fluids from 0.88 g/cm³ to 0.93 g/cm³.
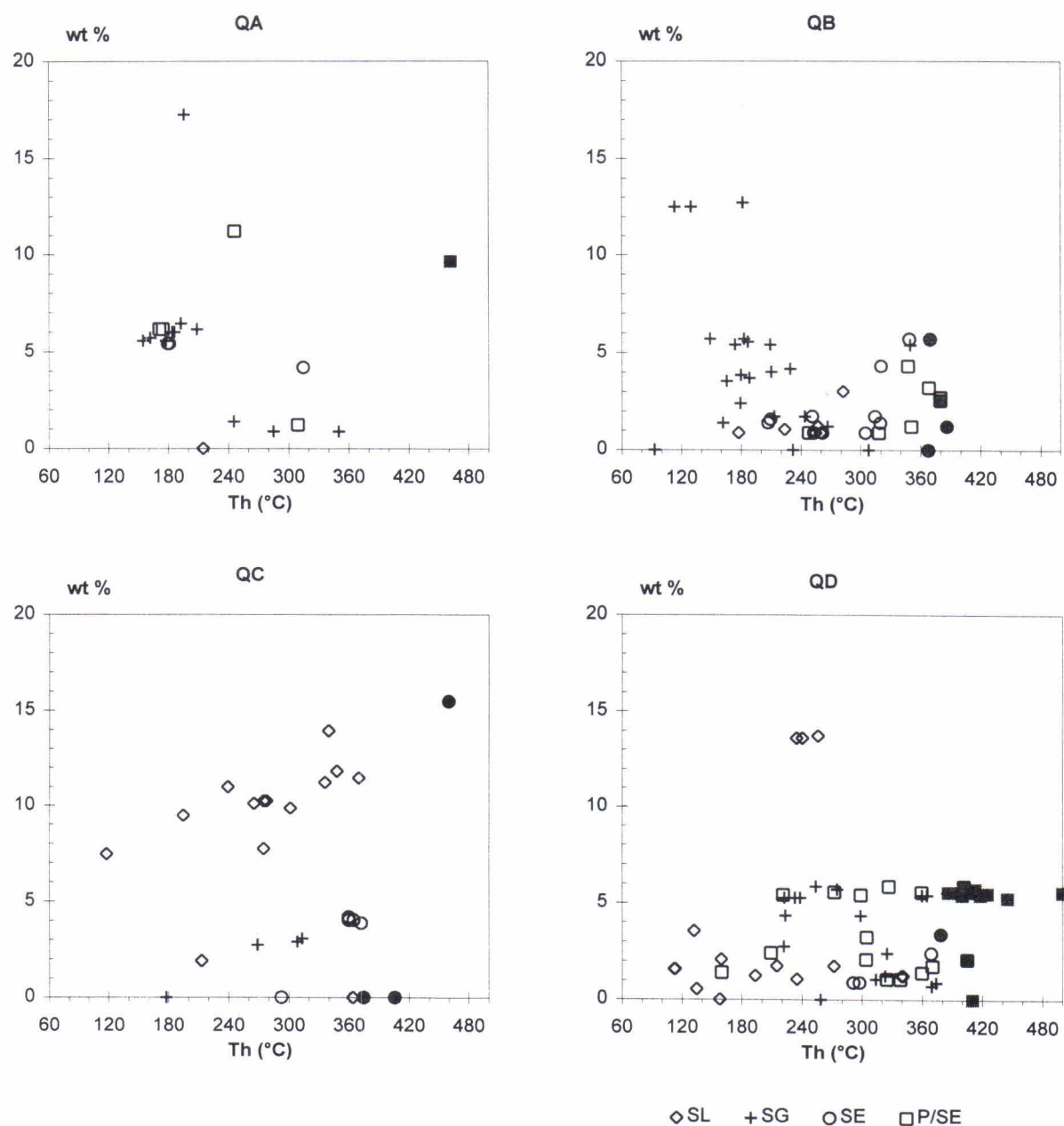
Fig. 4. Homogenization temperature versus salinity diagrams of aqueous inclusions in QA, QB, QC and QD quartz types. Filled symbols indicate inclusions homogenizing to vapor phase.

DISCUSSION AND CONCLUSIONS

Fluid inclusions are closed systems and they will have constant composition and density after they have become trapped in a mineral. In the pressure-temperature field, the isochores represent lines along which the inclusions have trapped. The isochores were calculated for early carbon dioxide fluids in tonalite quartz (QA) and for aqueous fluids of early P/SE-, late SG- and late saline SL-types in vein quartzes (Fig. 5). Each fluid type is presented as a minimum and maximum isochore.

Recrystallization of sheared tonalite has de-

stroyed those fluid inclusions that represent conditions before and during shearing. As primary arsenopyrite and gold deposited before recrystallization, the fluid related to that stage is still unknown. The earliest inclusions show that during the recrystallization the fluid phase was carbon dioxide, which is quite normal fluid during amphibolite facies metamorphism. Isochores of this fluid go through the same pressure - temperature area around 2.9 kbar and 670 °C that Poutiainen (1990) presented for CO_2 fluid inclusions in quartz
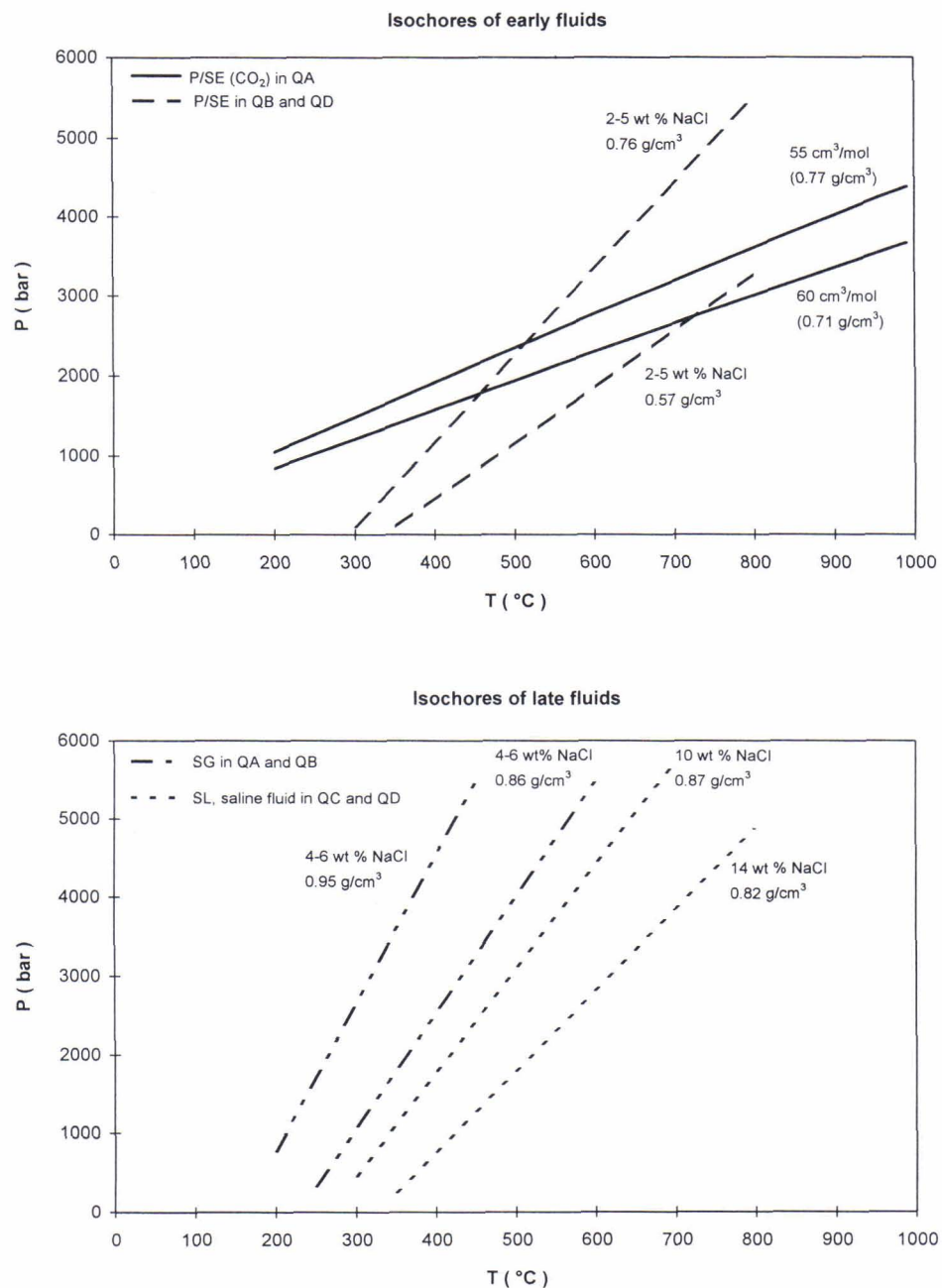
Fig. 5. Calculated sets of isochores for early carbonaceous and aqueous fluids and late aqueous fluids.

veins related to regional D_2-D_3 deformation (Fig. 6). In that paper the p-T area of D_2-related fluids is located in few hundred bars higher pressures, close to the crystallization conditions of potassium feldspar - sillimanite zone rocks. Mineral geobarometry and metamorphic assemblages give the p-T estimate of 3.4 kbar and 645 °C for these rocks in the Rantasalmi region (Korsman et al. 1984). In the fluid inclusion study of Pirilä gold deposit, which is less than 8 km westward from Osikonmäki, Poutiainen (1993) found that the primary fluid inclusions for D_2-D_3 deformation related vein quartz contain weakly saline H_2O-CO_2 fluid. The properties of these inclusions - less than 10 mole % methane in carbonaceous phase, salinity between 1.8 wt % and 4.3 wt %, total homogenization temperature range from 300 °C to 325 °C and bulk density between 0.75 g/cm³ and 0.79 g/cm³ - have similarities to early fluid inclusions of Osikonmäki. However in Osikonmäki the carbonaceous and aqueous fluids are mainly found as separate inclusions and from different quartz types. These fluids have not formed by phase separation of single fluid because it requires pressure lower than 700 bars, which is the vapour pressure of Pirilä-type primary

H_2O-CO_2 fluid (Poutiainen 1993). As carbonaceous fluid inclusions are usually found from tonalite quartz, the next stage is the introduction of the early aqueous fluid, which was present when the QB-QD type quartz veins formed (Fig. 6). Pressure and temperature have probably lowered slightly, but this lowering must have roughly followed the isochores of CO_2-inclusions, as they have survived. The inclusions larger than 10 µm in quartz will usually break, if the pressure difference between inclusion and surrounding exceeds 1 kbar (Roedder 1984). Therefore, if cooling and uplift have followed CO_2-isochores, then the formation temperature of vein quartzes has been 500-700 °C and the pressure has been around 2 kbars.

Secondary inclusions do not normally give very useful data because their genetic relation to a mineral may represent a large time and condition interval. Late secondary inclusions with low salinity are commonly found, and usually discarded, in fluid inclusion work. Secondary inclusions could however give some idea of events after the minerals have formed. The distinct group of SG-type inclusions (Fig. 4) from eastern part of the shear zone clearly represent secondary fluid that differs from
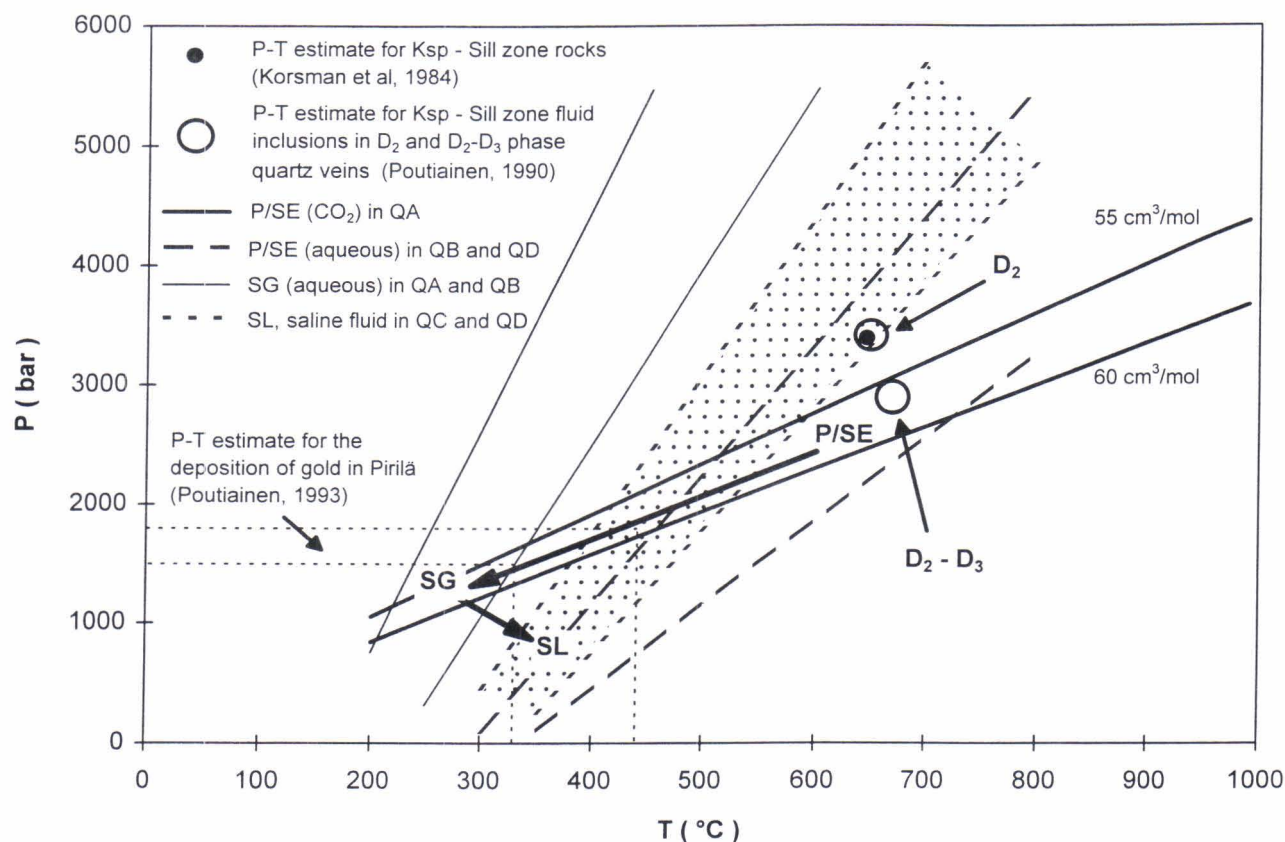
Fig. 6. Isochores of discussed fluids and proposed fluid evolution path with pressure-temperature estimates of previous studies.

the fluid of those early secondary inclusions by their higher salinity and lower homogenization temperature. Some other, even later SL-type inclusions are of special interest as they were formed at the same time as secondary enriched gold. These saline fluid inclusions were found from a fracture in QC-type quartz with bismuth and gold grains. The salinity of the fluid varies from 8 wt % to 14 wt %. In the Pirilä gold deposit the precipitation of gold and remobilization of sulphides has occured in the presence of methane and saline aqueous fluids (about 25 wt % NaCl). From these fluids Poutiainen (1993) estimated p-T conditions of pre-

cipitation to be between 1.5 kbars/330 °C and 1.8 kbars/440 °C (Fig. 6). In Osikonmäki there is no signs of methane in late secondary fluids and the salinity of aqueous inclusions is clearly lower. This fluid probably carried gold in chloride complexes and enriched it in small fractures in vein quartz. The temperature range of this gold precipitation might be close to temperatures of Pirilä, but the pressure have been lower. The presence of SG-type secondary fluid suggest, that irrespective of the cooling and uplift path the appearance of saline SL fluid has accompanied with minor reheating of the area (Fig. 6).

ACKNOWLEDGEMENTS

REFERENCES

Bodnar, R.J. 1993. Revised equation and table for determing the freezing point depression of H_2O-NaCl solutions. Geochimica et Cosmochimica Acta 57, 683-684.

Diamond, L.W. 1992. Stability of CO_2 clathrate hydrate + CO_2 liquid + CO_2 vapour + aqueous KCl-NaCl solutions: Experimental determination and application to salinity estimates of fluid inclusions. Geochimica et Cosmochimica Acta 56, 273-280.

Heyen, G., Ramboz, C. & Dubessy, J. 1982. Simulation des Èquilibres de phases dans le systéme CO_2-CH_4 en dessous de 50 EC et de 100 bar. Application aux inclusion fluides. Comptes Rendus des Seances de l´Acádemie des Sciences, serie 2, Mécanique-Physique-Chimie 294, 203-206.

Kerkhof, A.M. van den 1990. Isochoric phase diagrams in the systems CO_2-CH_4 and CO_2-N_2: Application to fluid inclusions. Geochimica et Cosmochimica Acta 54, 621-629.

Kerrick, D.M. & Jacobs, G.K. 1981. A modified Redlich-Kwong equation for H_2O, CO_2 and H_2O-CO_2 mixtures at elevated pressures and temperatures. American Journal of Science 281, 735-767.

Kontoniemi, O. & Ekdahl, E. 1990. Tonalite-hosted early Proterozoic gold deposit at Osikonmäki, southeastern Finland. Bulletin of the Geological Society of Finland 62, 61-70.

Korsman, K., Hautala, T., Hölttä, P. & Wasenius, P. 1984. Metamorphism as an indicator of evolution and structure of the crust in eastern Finland. Geological Survey of Finland, Bulletin 328. 40 p.

Poutiainen, M. 1990. Evolution of a metamorphic fluid during progressive metamorphism in the Joroinen-Sulkava area, southeastern Finland, as indicated by fluid inclusions. Mineralogical Magazine 54, 207-218.

Poutiainen, M. 1993. Fluid inclusion geochemistry of the early Proterozoic Pirilä gold deposit in Rantasalmi, southeastern Finland. Mineralium Deposita 28, 129-135.

Roedder, E. 1979. Fluid inclusions as samples of ore fluids. In: Barnes, H.L Geochemistry of hydrothermal ore deposits, 2nd edn. New York: John Wiley & Sons, Inc., 684-737.

Roedder, E. 1984. Fluid inclusions. Mineralogical Society of America, Reviews in Mineralogy 12. 644 p.

Vaasjoki, M. & Kontoniemi, O. 1991. Isotopic studies from the Proterozoic Osikonmäki gold prospect at Rantasalmi, southeastern Finland. In: Autio, Sini (ed.) Geological Survey of Finland, Current Research 1989-1990. Geological Survey of Finland, Special Paper 12, 53-57.

Zhang, Y-G. & Frantz, J.D. 1987. Determination of the homogenization temperatures and densities of supercritical fluids in the system NaCl-KCl-$CaCl_2$-H_2O using synthetic fluid inclusions. Chemical Geology 64, 335-350.

BENEFICIATION STUDY OF THE OSIKONMÄKI REFRACTORY-TYPE GOLD ORE AT RANTASALMI, SOUTHEASTERN FINLAND

by

Jaakko Leppinen and Olavi Kontoniemi

Leppinen, Jaakko & Kontoniemi, Olavi 1998. Beneficiation study of the
Osikonmäki refractory-type gold ore at Rantasalmi, southeastern Finland.
Geological Survey of Finland, Special Paper 25. 101-110. 4 figures, 5 tables
and 4 appendices.

Osikonmäki is a Paleoproterozoic, epigenetic, tonalite-hosted and shear zone
related gold deposit. The ore minerals: pyrrhotite, arsenopyrite, löllingite and
chalcopyrite and the accessories: sphalerite, galena and ilmenite or rutile, occur
as uneven or banded disseminations throughout the c. 3 km long shear zone.
Gold or electrum and associated minerals occur as inclusions in and also on the
grain boundaries of sulphide, arsenide and silicate phases. The most com-
mon associated minerals are native bismuth, hedleyite and ikunolite.

Beneficiation studies on the refractory-type Osikonmäki ore were carried
out with a composite sample made of three subsamples taken from the study
pit. Froth-flotation, cyanide leaching and pressure oxidation were used to
test the recovery of gold from the ore. In conventional bulk-flotation, gold
recovery was only 70% although sulphides and arsenides were almost
completely recovered. The arsenic content in the bulk concentrate is 10 -
25%. Depending on the grinding fineness, the maximum recovery of gold by
cyanide leaching was 75 - 80%. Pressure oxidation increased gold recovery
from the cyanide leaching by 10 - 25%, the maximum recovery then being
about 93%. Conventional processes may not provide satisfactory gold
recovery or acceptable arsenic content. More sophisticated technologies
and/or new process options must therefore be considered in processing the
Osikonmäki ore.

Key words (GeoRef Thesaurus, AGI): gold ores, ore minerals, beneficiation,
flotation, leaching, oxidation, Proterozoic, Paleoproterozoic, Osikonmäki,
Finland

*Jaakko Leppinen, VTT Chemical Technology, Mineral Processing, FIN-
83500 Outokumpu, Finland*

*Olavi Kontoniemi, Geological Survey of Finland, P.O. Box 1237, FIN-
70211 Kuopio, Finland*

INTRODUCTION

Gold ores of epigenetic origin often differ in
their mode of occurrence and character. Moreo-
ver, their economic exploitation is affected by the
heterogenity of ores and the limitations of visual
estimation. Native gold generally occurs in frac-
tures in, or in spaces between, silicates. At their
largest the grains are tens of microns in size, but
they also occur as intergrowths with sulphides or
arsenides. In some cases, "invisible" gold occurs
in the lattice of sulphides and arsenides.

Depending on the size of an ore deposit, even very low gold concentrations (3-5 g/t) can be economically viable. Detailed knowledge of the special features of the ore and of beneficiation methods is therefore required. Typically, coarse gold is recovered from ores by gravity separation, and fine-grained gold by flotation and cyanide leaching. In refractory ores (Jha 1987), total breakdown of the sulphide phase is necessary to render the gold locked in sulphide mineral grains amenable to cyanide leaching. For free-milling ores, the most commonly used process is direct cyanide leaching. This is appropriate for ores in which the gold is well liberated and cyanide consumption is moderate.

Several options are currently available for processing refractory gold ores (Kontopoulos and Stefanikis 1990). With the exception of ultra-fine grinding, all the processes comprise oxidation pretreatment steps in which gold is liberated from sulphides and arsenides. The options for oxidation pretreatment comprise roasting, pressure oxidation, bio-oxidation and chemical oxidation, the latter including a number of suboptions. Roasting and pressure oxidation are most widely applied on an industrial scale. Bio-oxidation is still at the development stage although small-scale industrial operations, predominantly for gold concentrates, are already in existence.

In recent years, pressure oxidation in autoclaves has been the preferred pretreatment method for refractory ores, and several full-scale processes are in operation throughout the world (Berezowsky 1989). Pressure oxidation with subsequent cyanide leaching generally results in very high gold recovery. The major disadvantages of pressure oxidation are high capital and operating costs and the problems created by the disposal of a large volume of low bulk density effluents in tailing ponds. Unfortunately, as with all the pretreatment process options, beneficiation of small ores with pressure oxidation does not appear very promising economically.

On the basis of mineralogy (e.g. Kontoniemi et al. 1991) and preliminary cyanide leaching tests, the Osikomäki deposit consists only partly of free-milling ore. Cyanide leaching studies (Nurmi et al. 1992) and the bromine leaching studies conducted at Michigan Technical University (Wahyudi 1993) both showed 75 - 80% gold recovery, depending on the ore type and leaching conditions.

Beneficiation of the Osikonmäki ore sample was here evaluated by means of different process methods at laboratory scale. Gold and sulphide/arsenide minerals were concentrated with froth-flotation. Direct cyanide leaching was applied to the ore and the bulk concentrate. The effect of pressure oxidation pretreatment was tested on both the ore and the concentrate. The prospects for processing the Osikonmäki ore are discussed in relation to mineralogical factors.

GEOLOGY OF THE ORE PROSPECT

Osikonmäki is an Paleoproterozoic epigenetic, mainly mesothermal and shear zone-related gold deposit. It is located in a second-order shear that is oblique to a crustal-scale deformation zone and cuts a synorogenic granitoid (Fig. 1). The ductile shear zone was deformed under approximately amphibolite facies conditions. Late brittle deformation (splitting) occurred during retrogression.

The ore minerals occur as uneven or banded disseminations throughout the c. 3-km-long shear zone. The highest gold contents have been encountered in its western and eastern parts, close to the footwall contact. Here and there, narrow quartz veins have the same orientation as the contact.

The most common ore minerals are pyrrhotite, arsenopyrite, löllingite and chalcopyrite with sphalerite, galena and ilmenite or rutile as accessories. Gold or electrum and associated minerals occur as inclusions in and also on the grain boundaries of sulphide, arsenide and silicate phases. The most common associated minerals are native bismuth, hedleyite and ikunolite.

It is difficult to distinguish between the effects of prograde metamorphism in the sillimanite - K-feldspar zone and those of later retrogression in this epigenetic hydrothermal mineralization. The most probable index minerals of the ore formation are biotite, K-feldspar, quartz, rutile, tourmaline and, generally, the ore minerals listed above.

Although gold is the only economically significant metal present, the Osikonmäki deposit is also strongly enriched in As, Bi, Te, Se, Ag, Sb, Cu and Sn. At low concentrations Au correlates reasonably well with concentrations of As and S. At high Au concentrations the Au - As correlation weakens and the Au - Ag correlation strengthens. Se, Bi, As, S and Cu form, at best, a positive aureole tens of metres wide, especially in the cataclastic porphyritic hanging-wall tonalite.
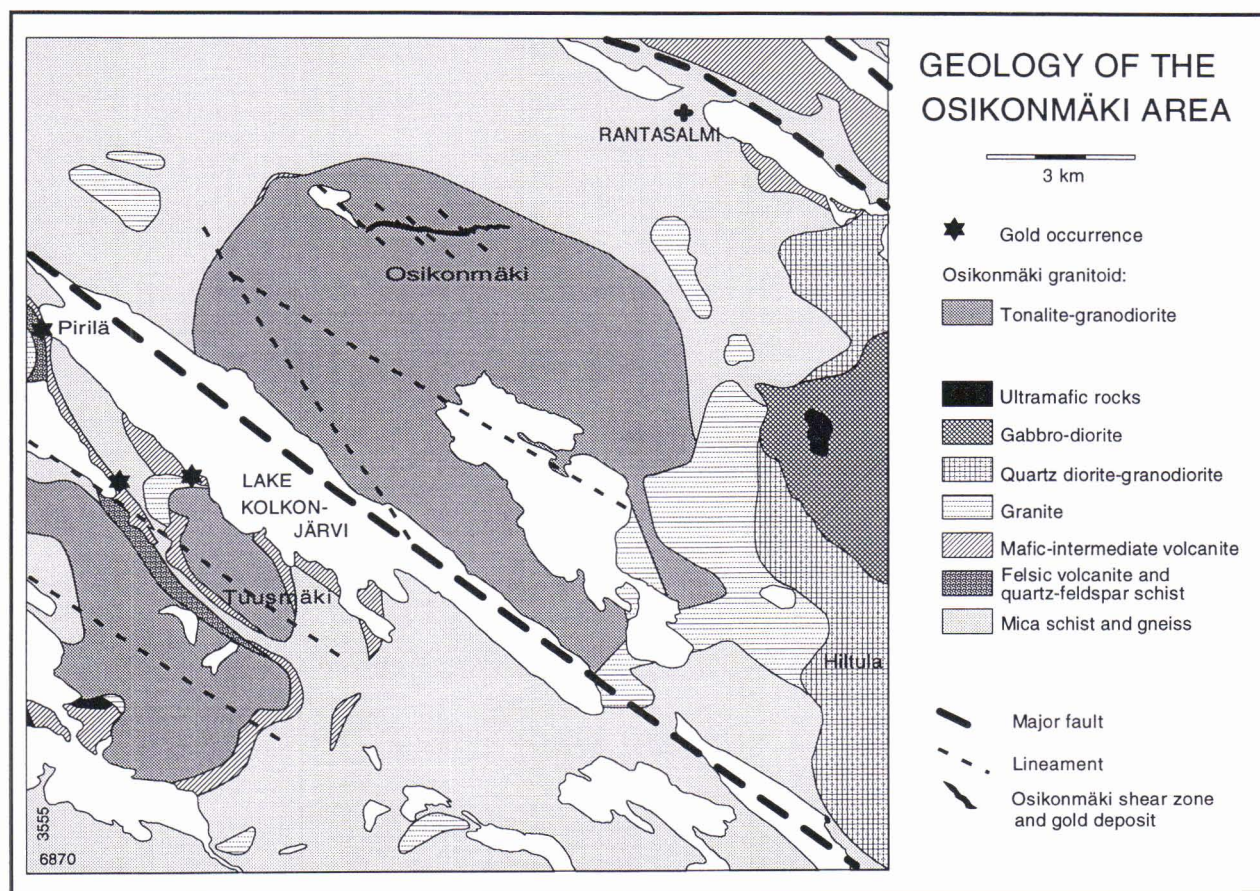
Fig. 1. Generalized geological map of the Osikonmäki area. Simplified from Kontoniemi (1998, this volume).

SAMPLE SELECTION

Tests of beneficiation techniques require ore samples that weigh c. 1000 kg and are both geologically and chemically as close as possible to the "average ore". It is usually impossible to blast an average sample directly from the rock because of the special characteristics of gold ore. Better results can be obtained with appropriate mixing of subsamples.

The average Au content in the eastern part of the mineralization is slightly over 3 g/t (cut off 1 g/t) and the average As content, which is the second most important component in beneficiation techniques, c. 0.8%. Figure 2 shows that the As content of the mineralization falls systematically from profile 61.100 (2.5%) to profile 60.700 (0.3%)

(Kontoniemi 1990). A test sample was taken from profile 61.100 despite its high As content, because only there is a study pit suitable for blasting available.

The test sample was blasted from the eastern part of study pit OMK-87-M1 (Fig. 3). Here, as shown by previous sampling, the Au content averages c. 3 g/t and the As content 0.5 - 2.0%. The host rock is mainly sheared tonalite containing more pegmatitic vein material than usual. Due to the heterogeneous nature of the sample, it was divided by visual estimation into three subsamples: an arsenopyrite-rich one (388.5 kg), an arsenopyrite-poor one (136.1 kg) and a pegmatitic one (241.6 kg).
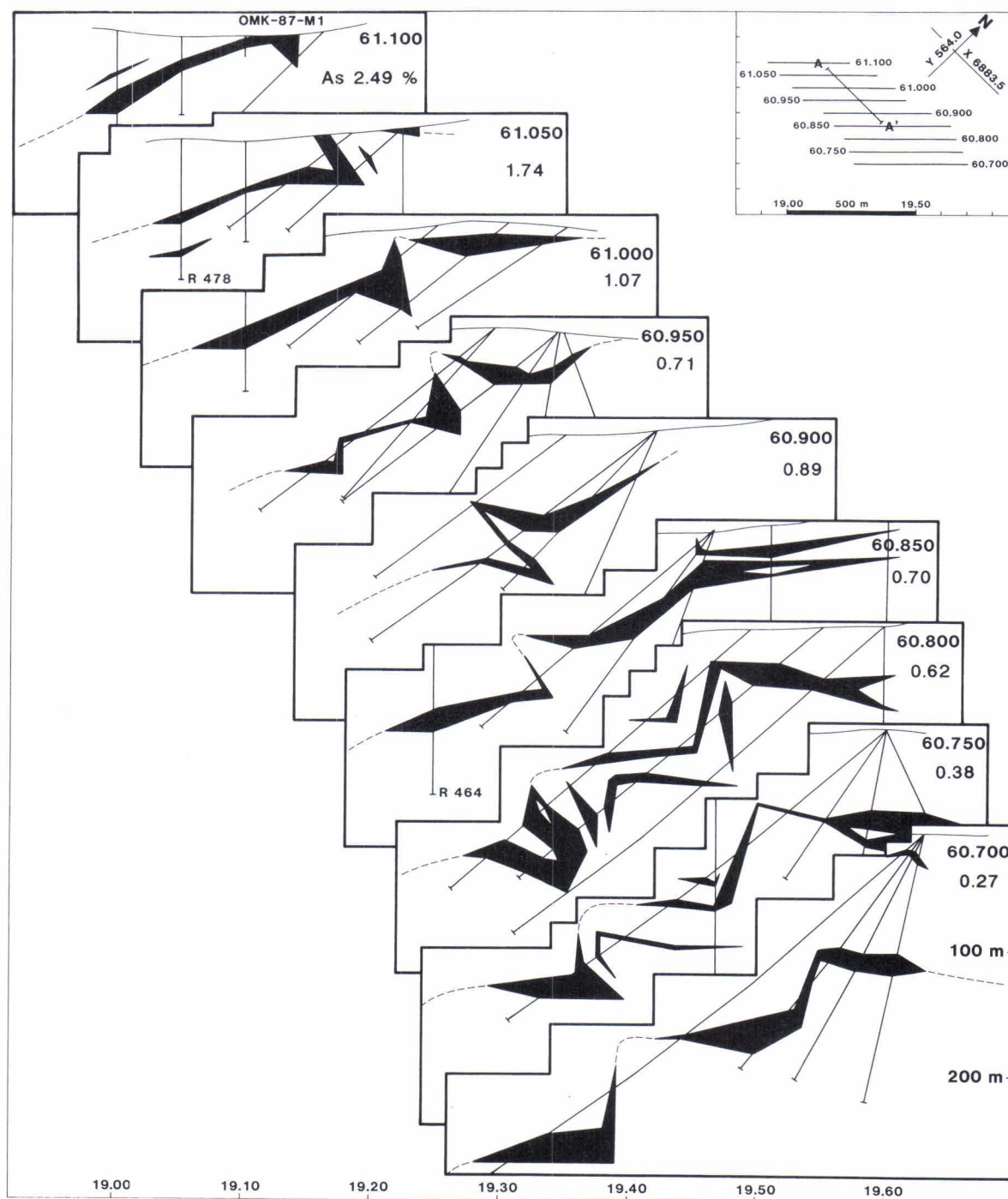
Fig. 2. Three-dimensional model of the claim, Osikko 1, between profiles L = 60.700 and 61.100. Black areas refer to ore sections (Au ≥ 0.5 g/t). Average As contents are shown in each profile. The inset shows the location of the profiles.
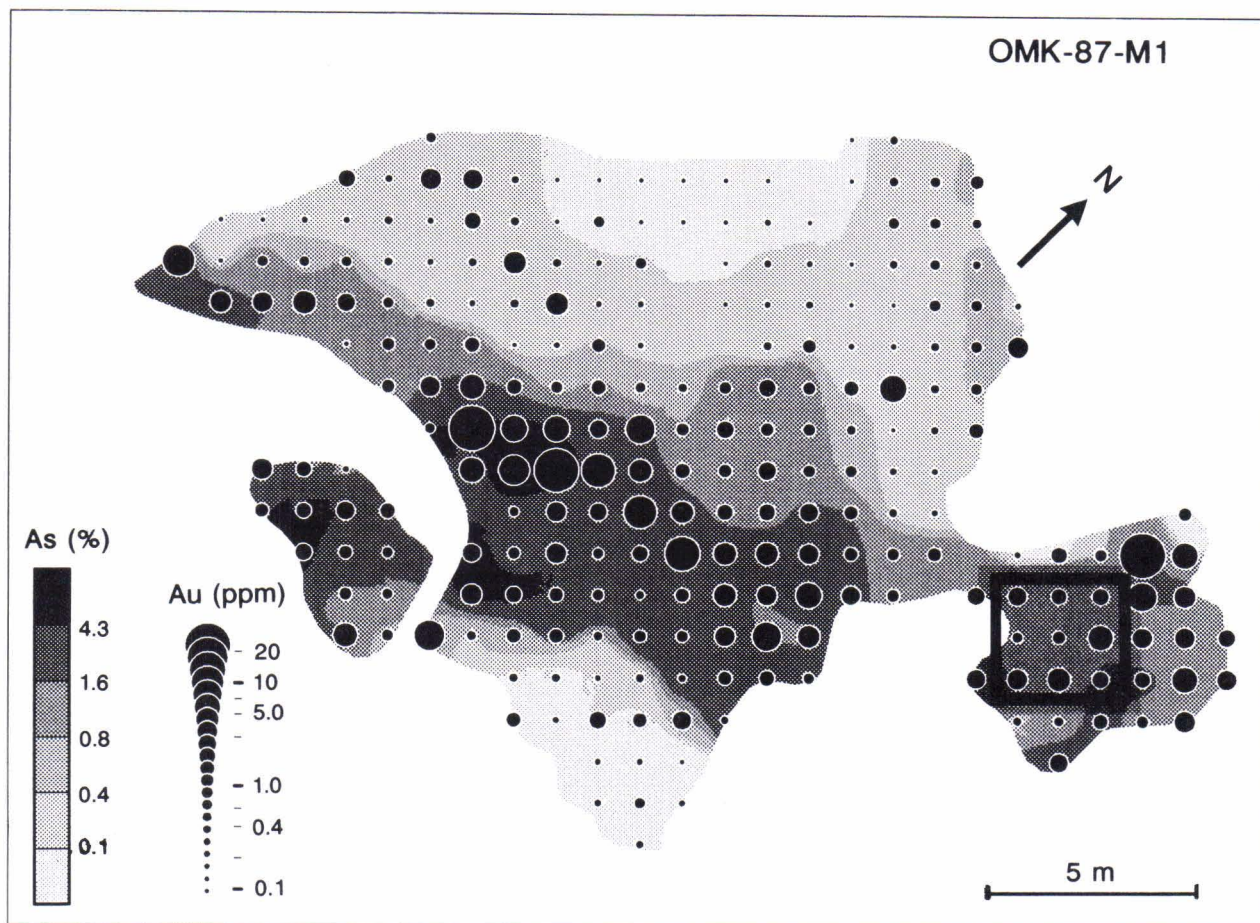
Fig. 3. The distribution of gold and arsenic in outcrop OMK-87-M1. The site of the test sample is marked with an open square.

MINERALOGY OF THE SAMPLES

The ore mineralogy of the Osikonmäki deposit has been described by Kontoniemi et al. (1991) and the mineralogy of the samples taken specifically from the study pit by Wahyudi (1993). The deposit varies in mineralogy and chemistry throughout the shear zone, as reported by Kontoniemi elsewhere in this Special Paper.

During the prograde metamorphism following the formation of the shear zone, the rock recrystallized totally, forming a granoblastic texture. The main silicates are quartz, K-feldspar, plagioclase and biotite, and common accessory minerals are opaques, apatite, zircon, rutile and titanite. The large primary plagioclase grains are often granulated at their edges and altered into saussurite and sericite in their central parts. Where shearing has been weakest, diopside is a product of the breakdown of plagioclase and primary hornblende. Other rare alteration products are carbonate, chlorite and epidote.

The main ore minerals are pyrrhotite, arsenopyrite and löllingite with chalcopyrite.

Sphalerite and galena occur locally. Pyrrhotite usually has a lamellar structure and in composition varies from a mixture of troilite and hexagonal pyrrhotite to a mixture of hexagonal and monoclinic pyrrhotite (Kontoniemi et al. 1991). In places, pyrrhotite has altered into marcasite. Arsenopyrite and löllingite occur as subhedral or euhedral intergrowths in which löllingite forms the central part of the grain. Locally, chalcopyrite has cubanite lamellae and in places is altered at its rim into covellite.

Gold mainly occurs as fine-grained native gold or electrum with sulphide, arsenide or silicate phases. Rarely, maldonite (Au_2Bi) is present and in places, arsenopyrite and chalcopyrite contain a small amount of lattice gold ($< 0.1\%$). Other minerals associated with gold are native bismuth, hedleyite ($Bi_{2+x}Te$), ikunolite (Bi_2Se) and an unknown bismuth tellurium selenide with the chemical formula Bi_6Te_2Se (Kontoniemi et al. 1991).

According to Wahyudi (1993), approximately 65% of the gold grains are in silicate phases and the

remainder in sulphide phases. On the basis of prospecting works, there seems to be a substantial increase in the amount of "silicate-gold" at a higher Au content (> 2-3 g/t). In silicate phases, gold generally occurs on the rims of quartz grains and in fractures or, in the worst case, as small inclusions inside the quartz. Gold and associated

minerals also occur inside altered plagioclase structures. In sulphide phases, gold and the Bi-Te-Se minerals generally occur as inclusions in löllingite and arsenopyrite. Most of the inclusions are at the contacts of the above minerals, and may simply be gold or electrum grains or granules mixed with associated minerals.

BENEFICIATION OF THE OSIKONMÄKI GOLD ORE

The beneficiation studies of the Osikonmäki ore sample were conducted at the Mineral Processing laboratory of VTT (Technical Research Centre, Finland) Chemical Technology. In addition to pressure oxidation as a pretreatment method, the ore

sample was subjected to froth-flotation and cyanide leaching. The mineralogy of the ore sample was studied using VTT's eMAX image analysis (Laukkanen and Leppinen 1994) and chemical analyses at various process stages.

Composition of the ore sample

The compositions of the three subsamples and a composite sample are presented in Table 1. Subsample OMK1 has the characteristics of an arsenopyrite-poor ore type, subsample OMK2 that of an arsenopyrite-rich ore type, and subsample

OMK3 that of a pegmatitic ore type. The mineralogical composition of the composite sample is presented in Table 2. In the following report on the process studies, this sample is referred to the Osikonmäki ore.

Table 1. Compositions of the Osikonmäki ore subsamples and the composite sample.

Ore type	mass (%)	Au (g/t)	As (%)	Fe (%)	Cu (%)	S (%)
OMK1	47.5	4.2	0.57	3.50	0.016	1.14
OMK2	47.5	7.1	2.80	4.96	0.023	1.87
OMK3	5.0	3.6	0.10	2.91	0.012	0.99
Composite	100.0	5.7	1.44	3.56	0.019	1.23

Table 2. Mineralogical composition of the Osikonmäki ore.

Mineral	Content (%)
Arsenopyrite	2.21
Löllingite	0.63
Pyrrhotite	1.05
Pyrite	0.76
Chalcopyrite	0.05
Sulphides total	4.69
Silicates	95.31
Carbonates	0.00

Flotation of the Osikonmäki ore

The froth-flotation experiments were carried out at laboratory scale with 1-kg samples using a 4-litre flotation cell and an Outokumpu-type flotation machine. During flotation, pH was 5.0, and 30 g/t

dithiophosphinate collector (Aerophine 3418A) and 170 g/t sodium amyl xanthate were used as flotation reagents. The recovery and grade of gold, arsenic, iron and sulphur were determined as a

Table 3. Rougher flotation data of the Osikonmäki ore.

Grinding (min)	Fineness (%)-45μm	mass (%)	C/Au (g/t)	R/Au (%)	C/As (%)	R/As (%)	C/Fe (%)	R/Fe (%)	C/S (%)	R/S (%)
10	16.6	7.0	48.3	65.7	23.1	99.7	27.4	49.3	18.3	93.2
20	26.0	6.7	52.7	66.6	24.0	94.3	28.1	47.6	18.8	90.0
30	37.6	6.9	51.9	68.0	23.4	93.2	27.5	46.4	18.2	88.7
180	98.3	19.5	25.7	86.2	5.1	67.1	9.1	39.9	5.4	70.5

function of grinding fineness (Table 3). Only rougher flotation tests were made, i.e. no attempt was made to upgrade the concentrate by cleaner flotation.

At a conventional grinding fineness (grinding time 10 - 30 min), a gold concentrate of about 50 g/t was obtained with a recovery of 65 - 68%. Recoveries of slighly over 70% were achieved in separate flotation tests on larger samples. Practically all sulphides/arsenides were floated, the recovery of arsenic being 93 - 100% and that of sulphur about 90%. The arsenic content in the concentrate was very high (23 - 24%) and the sulphur content 18 - 19%. The mass of the concentrate was about 7%, which is higher than the calculated mass of sulphides, 4.7% implying that the abundance of silicates in the concentrate was about 30%. Most of the silicates can probably be removed by cleaner flotation, with an increase in the gold content in the concentrate. It may also be possible to depress some of the sulphides/arsenides. Depression of silicates and sulphides/arsenides might, however, lead to a significant decrease in gold recovery.

Gold recovery was significantly higher with ultra-fine grinding (180 min) than at shorter grinding times, and the gold content (25.7 g/t) was correspondingly lower. The increase in gold recovery was, however, not much higher than the increase in mass of the concentrate. The higher mass with ultra-fine grinding was mainly due to an increase in silicates in the concentrate indicating that some gold occurs in association with silicates. It is likely that the higher mass recovery also increased the recovery of poorly floatable gold particles. An advantage of ultra-fine grinding was that arsenic, iron and sulphur recoveries were lower than at shorter grinding times. Although ultra-fine grinding leads to better metallurgical performance, the

energy consumption required would very likely make this an unprofitable alternative.

Using cyanide leaching, gold recovery from flotation tailings was 60 to 70%, which would represent a total recovery up to 90%. After a 10 min grinding time for flotation, the gold content in the cyanide leaching residue was 0.8 g/t, compared with 0.4 g/t at 30 min grinding time. This indicates that some gold is present as inclusions in silicates that are not amenable to cyanidation, while some also occurs as "free" particles amenable to cyanide leaching but not recoverable by flotation. Consequently, the flotation tailings contain a great number of gold particles which are non-floatable or whose flotation rate is very low. Gold recovery could potentially be improved by using a more specific reagent combination or more favourable solution conditions. It is possible, however, that the non-floatable gold particles are coated by passivating layers, comprised for example of oxides, which are common in certain gold ores, making the improvement in flotation recovery difficult. Some non-floatable gold is likely to occur as mixed grains, at silicate grain boundaries or as films on silicate grains. Although there is no direct evidence, gold grains associated with bismuth may not be floatable using conventional flotation reagents. Mineralogical studies indicated that gold occurs in the flotation tailings as very fine particles enclosed by plagioclase and potassium feldspar. Gold was also observed in association with native bismuth and other Bi-Te-Se minerals.

The conclusion from the froth-flotation tests is that gold recovery is low except with ultra-fine grinding. The arsenic content in the bulk concentrate containing all sulphides/arsenides is far too high for conventional metallurgical processing such as copper smelting. Alternative processing methods to flotation must therefore be carefully studied.

Cyanide leaching of the Osikonmäki ore

Standard cyanide leaching tests were made on the Osikonmäki ore using 0.3% sodium cyanide solution at pH 11.5. Typically, the leaching time was 24 h. The results of the cyanide leaching tests at different grinding finenesses are presented in

Table 4.

The recovery of gold into the solution was not clearly dependent of the grinding fineness at the grinding times studied indicating that even the shortest grinding time provided sufficient degree

Table 4. Results of standard cyanide leaching tests on the Osikomäki ore.

Grinding time (min)	Fineness (% -30µm)	Au recovery (%)	Consumption of NaCN (kg/t)	Comsumption of lime (kg/t)
30	31.7	78.5	1.12	1.75
60	52.3	74.8	2.98	1.10
120	80.1	80.2	8.04	0.42

of liberation for gold. Gold recovery in cyanide leaching was 75 - 80%, which is clearly higher than in flotation. The recovery indicates that 75 - 80% of the gold must be sufficiently free after grinding for the cyanide solution to react with it. Because the gold from sulphides and arsenides was probably not recovered in cyanide leaching, to obtain 80% recovery, gold leached from "non-floatable" particles must be 10 to 20%. Consumption of sodium cyanide increased as a function of grinding fineness up to a grinding time of 120 min; that of lime decreased correspondingly.

Effect of pressure oxidation on cyanide leaching

Pressure oxidation is currently the preferred method for pretreating refractory gold ores. Over 10 plants in various parts of the world use pressure oxidation technology in gold processing, and several new plants are being planned. Pressure oxidation aims at the decomposition of all sulphides containing gold as fine grains or "invisible gold". After the decomposition, all gold, especially that from the sulphide phase, is amenable to cyanide leaching. Pressure oxidation with VTT's autoclave system was applied to the Osikonmäki ore and the flotation concentrate. Typically, a total pressure of 15 bars and a temperature of 180 °C were used. Pulp density was 31% in autoclaving the ore and 10% for the concentrate. A retention time of about 2 hours was sufficient for the complete breakdown of all sulphides except chalcopyrite. At 210 °C the retention time was about 50% of that at 180 °C. For the ore, the pulp density could be increased up to 60% without any loss in the breakdown rate of the sulphide/arsenide phase. The breakdown of minerals in the pressure oxidation is presented in Table 5.

Table 5 shows that sulphide and arsenide minerals were almost completely broken down in 2 hours.

More detailed analysis showed that practically all the sulphur of the ore was oxidised into sulphuric acid. Iron was predominantly converted into ferric arsenate, and hematite and arsenic completely into ferric arsenate. Consequently, the autoclave residue consisted of silicates, ferric arsenate and hematite. Due to a minor change in total mass
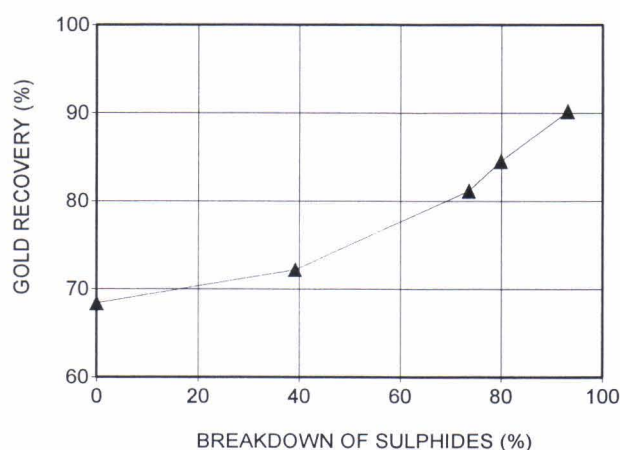

Fig. 4. The relationship between sulphide/arsenide breakdown and gold recovery in cyanide leaching.

Table 5. Pressure oxidation of Osikonmäki ore. T = 180 °C, ptot = 15 bar, pulp density = 31%.

Mineral	Amount of minerals (%)				
	Feed	15 min	30 min	60 min	120 min
Chalcopyrite	0.1	0.1	0.1	0.1	0.1
Pyrrhotite	0.5	0.5	0.0	0.0	0.0
Pyrite	0.4	0.4	0.1	0.1	0.0
Arsenopyrite	1.2	1.2	0.4	0.4	0.1
Löllingite	0.3	0.3	0.1	0.0	0.0
Silicates	97.5	97.5	97.5	97.5	97.5
FeAsO$_2$*2H$_2$O	0.0	0.0	1.1	1.7	2.2
Fe$_2$O$_3$	0.0	0.0	0.3	0.4	0.6

during pressure oxidation, the gold content in the residue was practically the same as in the ore, i.e. 5.7 g/t.

Figure 4 shows the effect of sulphide breakdown on the recovery of gold in cyanide leaching. In the test series the recovery of gold was 68% without pressure oxidation. After 2 hours of treatment in the autoclave the breakdown of the sulphide/arsenide phase was 93% and the recovery of gold was 90%. The results indicate that almost complete breakdown of sulphides and arsenides is required to achieve an acceptable recovery of gold by cyanide leaching.

The maximum recovery of gold by cyanide leaching with pressure oxidation pretreatment was 92.7%. The corresponding gold recovery from the concentrate was 96.3%. For the concentrate, total gold recovery was only 69% due to losses during flotation. The significant increase in gold recovery achieved with pressure oxidation indicates that a large portion the gold is locked in sulphides or arsenides. The gold not recovered by pressure oxidation/cyanide leaching is enclosed in silicates that are not markedly affected by the autoclave treatment.

Discussion of gold recovery

A major problem in beneficiation of the Osikonmäki ore appears to be the low recovery of gold by flotation. The most likely explanation is that some gold particles are locked in silicate minerals. Only small amount of gold gold is locked in in sulphide and arsenide minerals because the recovery of sulphides and arsenides was over 90% but that of gold 70%. A further indication that gold is locked in silicate grains is that with ultra-fine grinding, gold recovery increases along with the recovery of silicate minerals.

Low recovery of gold in flotation is sometimes due to contamination of free gold particles which makes them non-floatable with conventional flotation reagents such as xanthates. Although there is no clear evidence of such behaviour in the flotation of the Osikonmäki ore, the association of gold with bismuth may well impede the floatability of gold particles. Anyhow, the non-floatable gold causes significant losses in flotation recovery.

The pressure oxidation increased gold recovery in cyanide leaching by 15 - 25%, implying that

gold was liberated from sulphide and arsenide minerals. Only about 7% of the gold was not recovered after pressure oxidation. This outcome challenges the notion that a great deal of the gold not recovered by flotation is locked in silicate grains. A partial explanation lies in the microscope observations of unliberated gold particles containing both silicates and sulphides. Pressure oxidation may therefore have liberated gold from grain boundaries between silicate and sulphide/arsenide minerals.

The conclusion from pressure oxidation data is that less than 10% of the gold is contained within silicate minerals. The increase of 10% to 20% in gold recovery after cyanide leaching with pressure oxidation indicates that this gold fraction held within sulfides and arsenides. The remainder of the gold, of which 70 to 80% is directly amenable to cyanidation, comprises "free" gold, which is predominantly floatable, though a proportion of this is "non-floatable". The flotation results in fact imply that the fraction of non-floatable gold is up to 10 to 20% of the total gold.

Process options

Because gold recovery from the Osikonmäki ore by flotation is low, the method preferred for beneficiation is pressure oxidation/cyanide leaching without concentration. Conventional gravity separation methods can be applied before other processes, provided that there is enough coarse gold. Naturally, processing the ore as a whole in autoclave requires a larger volume than does the treatment of a flotation concentrate. On the other hand, the pulp density can be considerably higher in the treatment of the ore than in the treatment of the concentrate.

In the pressure oxidation treatment of the ore, all the arsenic goes into the waste as ferric arsenate, which may cause environmental problems

when the waste is stockpiled. Generally, ferric arsenate is classified as an acceptable waste (Papassiopi et al. 1987). Neutralisation of the sulphuric acid generated by the pressure oxidation of sulphides consumes large amounts of lime or limestone, resulting in masses of gypsum. The volume of the waste is therefore much larger than that of ore. If flotation were carried out first, most of the arsenic would go into tailings as sulphides or arsenides in an environmentally safe form. Consequently, the amount of harmful waste would be relatively small and easily disposable.

Considering the relatively small size of the Osikonmäki deposit, pressure oxidation of the ore

may not be commercially viable. Besides, more economical and efficient methods are currently available for oxidising of sulphides. The most interesting option, with low capital and operation costs, is bio-oxidation, a process in which decom-position of sulphide minerals is assisted by bacterial action (Lawrence and Marchant 1987). Atmospheric chemical oxidation could also be considered as a potential low-cost process option for refractory gold.

CONCLUSIONS

Beneficiation studies of the Osikonmäki ore were carried out with a composite sample made of three subsamples blasted from a study pit. The recovery of gold from the ore was studied with froth-flotation, cyanide leaching and pressure oxidation. The following conclusions are drawn.

1. In conventional bulk-flotation, gold recovery is only about 70% despite almost complete recovery of the sulphides/arsenides. The arsenic content in the bulk concentrate is high, up to 10 - 25%. Gold in flotation tailings is locked in silicates, as grains containing bismuth, and as other poorly floatable grains.

2. Depending on the grinding fineness, the maximum recovery of gold in cyanide leaching is 75 - 80%. Sodium cyanide consumption is from moderate to high.

3. Pressure oxidation increases gold recovery in cyanide leaching by 10% to 20%, maximum recovery being over 90%. The increase in gold recovery was proportional to the breakdown of sulphides.

4. Future beneficiation research should be focused on development of more effective and selective flotation, improvement of cyanide leaching, and cost-effective oxidation methods for the sulphide/arsenide phase (e.g. bio-oxidation).

ACKNOWLEDGEMENTS

REFERENCES

Berezowsky, R. 1989. Refractory gold: The role of pressure oxidation. In: Bhappu, R.B.& Harden, R.J. (eds.) Gold Forum on technology and Practice - World Gold '89. SME-AIME, 295-304.

Jha, M.C. 1987. Refractoriness of certain gold ores to cyanidation. Probable causes and possible solutions. Mineral Processing and Extractive Metallurgy Review (2) 331-350.

Kontoniemi, O. 1990. Osikonmäen kulta-aiheen tutkimukset Rantasalmella vuosina 1985-1989. M19/3233/-90/1/10. Unpublished report, Geological Survey of Finland. 36 p.

Kontoniemi, O. 1998. An overview of the geology in the Osikonmäki area, Rantasalmi, southeastern Finland: Especially as a promising environment for epigenetic gold mineralization. In: Kontoniemi, O. & Nurmi, P.A. (eds.) Geological setting and characteristics of the tonalite-hosted Paleoproterozoic gold deposit at Osikonmäki, Rantasalmi, southeastern Finland. Geological Survey of Finland, Special Paper 25, 7-18.

Kontoniemi, O., Johanson, B., Kojonen, K. & Pakkanen, L. 1991. Ore mineralogy of the Osikonmäki gold deposit, Rantasalmi, southeastern Finland. In: Autio, Sini (ed.) Geological Survey of Finland, Current Research 1989-1990. Geological Survey of Finland, Special Paper 12, 81-89.

Kontopoulos, A. & Stefanikis, M. 1987. Process options for refractory sulphide gold ores: Technical, environmental and economic aspects. Extraction & Processing Division Congress 90, Anaheim, TMS-AIME, 393-412.

Laukkanen, J. & Leppinen, J. 1994. Application of eMAX image analysis to pressure oxidation of refractory gold ores. Minerals Engineering (7) 239-249.

Lawrence, R.W. & Marchant, P.B. 1987. Biochemical pre-treatment of arsenical gold ore processing. In: Reddy, R., Hendricks, J. & Quenau, P. (eds.) Arsenic Metallurgy - Fundamentals and Applications. TMS-AIME, Warrendale, PA, 201-211.

Nurmi, P.A., Johansson, B. & Kojonen, K. 1992. Kullan esiintyminen eräissä Suomen uusissa kultamalmiaiheissa. Summary: Mineralogical distribution of gold in selected new gold prospects in Finland. Vuoriteollisuus - Bergshanteringen 2 (50), 70-75.

Papassiopi, N., Stefanikis, M. & Kontopoulos, A. 1987. Removal of arsenic from solution by precipitation as ferric arsenates. In: Reddy, R., Hendricks, J. & Quenau, P. (eds.) Arsenic Metallurgy - Fundamentals and Applications,, TMS-AIME, Warrendale, PA, 321-334.

Wahyudi, T. 1993. Mineralogy and characteristics that affect recoveries of gold from the tonalite-hosted Osikonmäki gold deposit, Finland. Unpublished Master of Science thesis. Michigan Technological University, Houghton, U.S.A. 40 p.

A COMPARATIVE STUDY OF CYANIDE AND BROMINE RECOVERY OF GOLD FROM A ROASTED OSIKONMÄKI GOLD ORE, FINLAND

by

T. Wahyudi, T. J. Bornhorst and C. Nesbitt

Wahyudi, T. & Bornhorst, T. J. & Nesbitt, C. 1998. A comparative study of cyanide and bromine recovery of gold from a roasted Osikonmäki gold ore, Finland. *Geological Survey of Finland, Special Paper 25*, 111 - 119. One figure and 5 tables.

Comparative leaching studies were conducted on roasted ore samples of the Osikonmäki deposit in Finland. The complex mineralogy of the material made roasting necessary to reduce the refractory nature of the ore. The ores were dry ground to -200 mesh and roasted for 24 hours at 750°C. Two lixivation strategies were compared: cyanide and bromide leaching. Gold recoveries in excess of 75% were obtained using cyanide and bromine leaching. The cyanidation was conducted in bottle roll experiments in which samples were mixed with 4g/l cyanide solutions for 24 hours. The bromination was conducted using GeoBromTM solutions in an agitated beaker test. In kinetic tests, maximum gold recovery was achieved in only 8 hours as compared to the cyanidation which required nearly 24 hours to complete.

Key words (GeoRef Thesaurus, AGI): gold ores, beneficiation, thermal treatment, leaching, cyanides, bromides, experimental studies, Osikonmäki, Finland

Wahyudi, T. & Bornhorst, T. J., Department of Geological Engineering and Sciences, Michigan Technological University, Houghton, MI 49931 U.S.A. Nesbitt, C., Department of Metallurgical and Materials Engineering, Michigan Technological University, Houghton, MI 49931 U.S.A.

INTRODUCTION

A complete understanding of mineralogy is important for those engaged in gold metallurgy. Efficient beneficiation is achieved only if metallurgical test work is combined with detailed mineralogical information of the ore (Gasparini 1983; Petruk 1989; Henley 1989; Cook 1990).

Gold often occurs in either the native state or in one of a few gold-bearing minerals such as the gold-tellurides. Recovery is usually excellent if gold occurs as large grains or nuggets, and thus, is readily exposed to leaching solution. However, the problems arise when gold is locked in sulfide min-

erals or when the mineralogy is complex. Detailed mineralogical investigation is necessary and serves as the first step in the development of recovery techniques.

Mineralogical studies have been made on the Osikonmäki ores (Kontoniemi et al. 1991; Kontoniemi, this volume; Wahyudi 1993). Gold is sited in silicates and sulfides as well as within fine fractures of gangue minerals. Overall, the gold is microscopic, disseminated, and low grade (3 g/t) but in high grade areas sometimes the grade is up to 27 g/t. The complex mineralogy of the Osikonmäki ores provides a good sample for laboratory leach-ing experiments.

Cyanide has been used for gold extraction for many years. The toxicity and slow kinetic performance of cyanide in recovering gold has led to the search for alternative leachants that are safer and more effective. Of the various leachant studies, bromine is one of the most promising because of its ability in dissolving gold and less environmental restrictions (Sergent et al. 1988; Pesic and Sergent 1991).

This study compares the extraction of sodium cyanide and a liquid bromine carrier from Osikonmäki ores.

METHOD OF STUDY

Olavi Kontoniemi, Geological Survey of Finland, provided a 60 kg bulk sample of mineralized tonalite from the Osikonmäki gold deposit with a grade of over 5 ppm Au. The study employed a polarizing microscope in both transmitted and reflected light for mineralogical study. Detailed mineral identification, including composition, was performed by electron microprobe using an acceleration of 20 kV and a specimen current of 25 nA.

Metallurgical experiments were conducted using both cyanide and bromine leaching. Prior to leachings, the ore was ground to -200 mesh and roasted overnight at 750°C as a pre-treatment to the ores. Cyanidation was carried out using a rolling bottle technique while bromination used the overhead stirring method. Analysis of both pregnant solutions and residues was completed by AAS and fire assay.

GEOLOGY AND MINERALOGY

At Osikonmäki, gold occurs in a 3-km long, E-W trending shear zone in the northern part of a tonalite intrusion (Kontoniemi, this volume). The ore minerals occur as disseminations and consist mainly of pyrrhotite, arsenopyrite, löllingite, and chalcopyrite in a matrix of biotite, quartz, potassium feldspar, sericite, diopside, epidote, and sphene. Lesser minerals are ilmenite, rutile, sphalerite, galena, stannite, tetrahedrite, boulangerite, molybdenite, pyrite, marcasite, and covellite.

Physical encapsulation is the most common microtexture between gold and its hosts. The gold along with hedleyite, native bismuth, and ikunolite is included within arsenopyrite or löllingite. Gold with maldonite, native bismuth, arsenopyrite, chalcopyrite, and pyrrhotite is also encapsulated by quartz and/or altered plagioclase. In addition, the gold is also distributed along the border between grains, either silicates or sulfides, forming fine veinlets as well as a larger rounded grains.

ROASTING OF ORES

Since significant fine gold particles are present in both sulfide and non-sulfide portions, concentration/flotation is basically not practical for Osikonmäki gold ores. Depending on ore mineralogy, two different roasting processes are possible.

In a one-stage process, the ore is only subject to elevated temperature in an oxidizing atmosphere. In two-stage roasting, the ore is first heated in a reducing atmosphere to increase porosity prior to a second oxidizing stage. For this study, one-stage

Geological Survey of Finland, Special Paper 25

A comparative study of cyanide and bromine recovery of gold...

oxidizing roast was used. The thermal effect on roasted ores was determined on concentrates of arsenopyrite, pyrrhotite, and quartz obtained by heavy liquid and magnetic separation. The concentrates were roasted at temperature of 450, 500, 600 and 750 °C with adjusted air-flow rate (4 L/min.) to provide enough oxidation. The thermal effect on roasted ore was determined for mineral phases and microtextures using reflected-light microscopy, x-ray diffraction and scanning electron microscopy-energy dispersive analysis.

Due to its refractory character, quartz seems unaffected by temperature. No phase changes occur within the quartz matrix. However, micro-fractures are developed at high temperature (600 to 750 °C). This feature is rarely present at low temperatures (<600 °C). Microfracture development in silica is essential for liberating gold distributed along the grain boundaries. For gold enclosed within silicates, the particles still remain in the host and are not affected by temperature.

The sulfide minerals respond adequately to the thermal effect with substantial phase and micro-texture changes. At lower temperature (450 °C), both arsenopyrite and pyrrhotite are still stable in their natural forms. No phase changes occur until the temperature is raised to 500 °C when arseno-pyrite particles start decomposing to intermediate pyrrhotite and a small amount of magnetite. However, remnant arsenopyrite is present in the center of grains. The arsenic is assumed to diffuse through the thermally expanded lattice and is later volatilized at the surface. At higher temperature (600 and 750 °C), the intermediate product pyrrhotite is more oxidized to magnetite and subsequently to hematite. The textural changes seem to develop gradually. At 500 °C, more fractures occur on arsenopyrite surfaces and as the temperature increases, the fractures expand to fibrous-like hematite in which porosity and permeability have developed adequately. The high degree of porosity allows lixiviants to reach any locked-gold particles that might be present. At this stage, a specific texture termed "butterfly morphology" by Hagni et al (1992) generally occurs.

Fissures develop normal to the particle surfaces during roasting in excess of 500 °C, especially in pyrrhotite and arsenopyrite. At this point, desulfurization allows the sulfur to migrate to the particle surface. The sulfur then volatilizes leaving various degrees of porosity. As the temperature increases to 600 °C, the intermediate product mag-netite is more completely oxidized to hematite. At this stage a circular rim of hematite forms but its dense texture makes it different from the hematite formed in the central portion of the grains, which is more porous than that of the rim. Marsden and House (1992) suggest that the rim results from too rapid a heating rate. From the gold extraction point of view, the existence of the rim is a disadvantage as it will inhibit solution access to the central porous particles. Similar to roasted arsenopyrite, the butterfly-shaped particles also develop at high temperatures (600 and 750 °C) which consist of porous hematite. Porosity and permeability are fully develop at this stage.

Marsden and House (1992) illustrate the thermal effect on gold during the roasting process. For gold associated with sulfides, gold particles and/or gold in solid solution migrate towards pores or boundaries in the direction of diffusion or sulfur or arsenic. The gold coalesces in the liquid phase. As the sulfur or arsenic volatilize, further coalescence is thought to occur at the mineral surface resulting in bigger gold particle formation. The thermal effect on gold distributed in a fine fracture is supposed to occur in the same way as that of gold within sulfides, i.e., coalesced gold in a liquid phase ends up with bigger gold particles along the fracture. A table summarizing mineralogical changes and microfracture development is presented in Table 1.

T. Wahyudi, T. J. Bornhorst & C. Nesbitt

Table 1. Mineralogical and microfracture changes due to thermal effect for different mineral including phases.

Quartz

Roasting temp.	Microfract. dev.	Effect on gold extr.
Unroasted	-	-
450 °C	-	-
500 °C	L	-
600 °C	M	-
750 °C	A	good

phase is unaffected by temperature
dash: no microfracture development
L: less microfracture development

M: minor microfracture development
A: abundant microfracture development

Arsenopyrite

Roasting temp.	FeAsS	Fe$_{1-x}$S	Fe$_3$O$_4$	Fe$_2$O$_3$	Texture	Effect on gold extraction
Unroasted	A	-	-	-	-	-
450 °C	A	-	-		few fractures	-
500 °C	M	M	M	L	more fract., fibrous-like	-
600 °C	-	-	M	A	rim	bad
					porous butterfly	good
750 °C	-	-	-	A	high porosity	good

Pyrrhotite

Roasting temp.	Fe$_{1-x}$S	Fe$_3$O$_4$	Fe$_2$O$_3$	Texture	Effect on gold extraction
Unroasted	A	-	-	-	-
450 °C	A	-	-	few features	-
500 °C	M	M	L	fibrous-like	-
600 °C	-	-	A	rim	bad
				porous butterfly	good
750 °C	-	-	A	high porosity	good

dash: no phase changes
L: less phase
M: minor phase
A: abundant phase

EXPERIMENTAL PROCEDURES

Since the gold particles are present in both sulfide and non-sulfide portions, ore concentration, such as froth floatation or gravitational, was not attempted prior to leaching experiments. Approximately 60 kg of bulk sample, representing a high grade deposit (> 5 ppm), was received. The ores were crushed to -10 mesh and split into individual 500 g charges for testing. The grinding tests were conducted at dry condition in laboratory rod mills using a 20 minute grind time. A sieve analysis suggests that the 80 wt. % passing size is 85 microns (Table 2). Thus, the ores to be leached were ground to -200 mesh. A flowsheet describing sample preparation is presented in Figure 1.

The high sulfur content and the presence of refractory elements such as Te, Bi, Sb (Bornhorst et. al., this volume) may affect extraction. Therefore, pre-treatment of samples prior to leaching is required. Sulfur can consume O$_2$ or CN$^-$ during cyanidation. Antimony minerals commonly develop coating over gold particle in solution and gold-bearing tellurium dissolves slowly (Gasparini 1983).

Experiments have been conducted to determine roughly the effect of cyanide and bromine on the dissolution of particular minerals. Due to difficulties in concentrating the minerals from the Osikonmäki ores, the experiments used substitute minerals from various places in the USA that might be different in composition. The experimental procedure consists of agitating

Table 2. Screen analysis of Osikonmäki ores.

Screen size (mesh)	(μ)	Weight (g)	Weight (%) Cumulative retained
-48+65	300	4.40	0.88
-65+100	212	13.10	3.50
-100+150	150	61.50	15.80
-150+200	106	31.75	22.15
-200+270	75	9.25	28.00
-270+325	53	4.75	28.95
-325+400	45	5.00	29.95
-400	38	348.50	100.00

Starting weight. 500g
Lost weight: 1.75 g
Grinding time: 20 minutes

Received 60 kg bulk sample

Jaw Crusher

Roll Crusher

10 Mesh Screen —— +10 Mesh

- 10 Mesh

Rod Mill

200 Mesh Screen —— +200 Mesh

Head assay analysis of -200 Mesh ore (100 g)

Leaching samples (cyanide & bromine) (-200 Mesh)
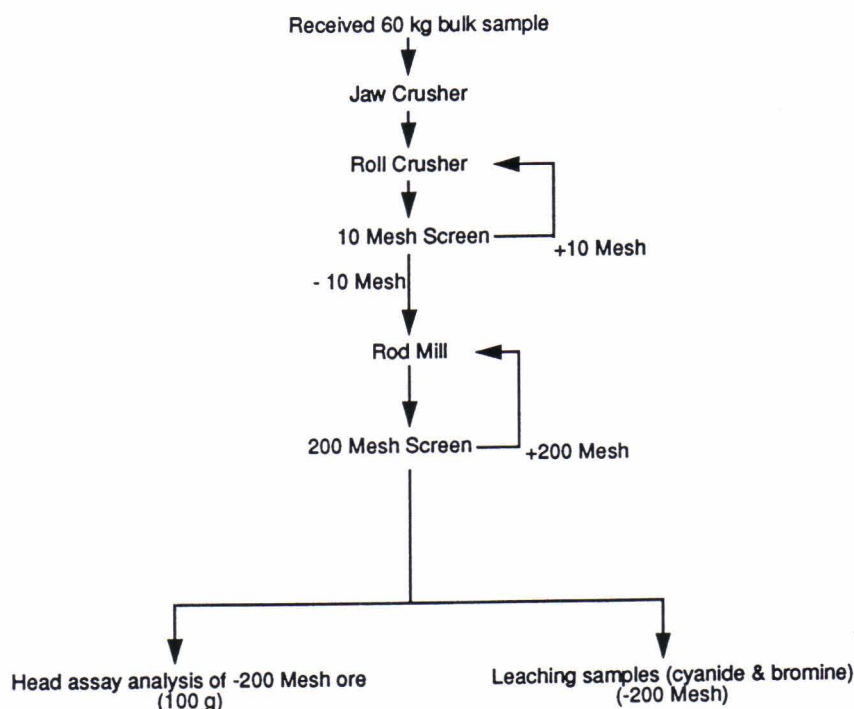
Fig. 1. Flowsheet of sample preparation of Osikonmäki ores.

each of mineral grains (0.25 g) in 20 ml solution of cyanide/bromine. The concentration of both solutions is 4 g/l, the optimum leach solution mixture for the Osikonmäki ores. By weighing residue after 24-hour leaching, the percentage of the solved minerals was calculated. Results of the experiments are presented in Table 3. Of the common sulfides, arsenopyrite, pyrite, chalcopyrite, and sphalerite are relatively inert in both lixiviants. This inert behavior is an advantage, where dealing with coarser gold grains, but a disadvantage with fine gold as Osikonmäki ores due to difficulties in breaking down the host mineral. Galena and pyrrhotite are markedly soluble and may produce oth-

er complexes in ligands that affect adversely the dissolution and precipitation of gold. Tetrahedrite is sufficiently soluble in cyanide and bromine solution and may cause excessive loss of ligands as well as may result in fouling solutions with antimony. Covellite is inert in bromine but soluble in cyanide, enough to cause cyanide loss. Most of the silicates and oxides, represented by quartz, biotite, diopside, and ilmenite, are relatively stable in both lixiviants. The presence of epidote may result in excessive consumption of bromine and sphene may consume a lot of cyanide.

Typically, roasting is carried out between 500 - 750 °C. The thermal tests suggests that the high

Table. 3. Effect of cyanide and bromide solution on the dissolution of particular minerals.

Mineral	% dissolved by	
	cyanide	bromine
Arsenopyrite	0.79	0.65
Pyrite	0.96	1.24
Chalcopyrite	6.95	4.80
Sphalerite	19.50	20.05
Covellite	24.00	9.07
Tetrahedrite	24.95	21.70
Pyrrhotite	44.03	40.46
Galena	68.28	67.55
Quartz	0.08	0.12
Biotite	5.03	3.29
Diopside	9.76	12.12
Epidote	11.60	39.67
Sphene	48.27	28.80
Ilmenite	10.78	3.95

degree of porosity of roasted products from sulfides as well as microfracture expansion of quartz developed adequately at 750 °C. Thus, the ground ores were roasted at a temperature of 750 °C to make them amenable to both cyanide and bromine leach. A. Dadgar of Great Lakes Chemical Co. (personal communication, 1992) suggested that for a well oxidized ore, the concentration of carbon and sulfur should be about 0.1%. The sulfur content of unroasted ore (100 g) was 3.58% which then decreased to 0.037% after overnight roasting at 750 °C. Carbon content is actually not a problem for these ores as the carbon content in both roasted and unroasted ores are less than 0.1%.

The rolling-bottle technique is the method employed for cyanidation to reduce cyanide losses by volatilization (Dadgar, personal communication 1992). Typically, cyanidation tests are performed at high pH (9.50 - 11.00) to prevent excessive loss of cyanide due to hydrolysis. This can be achieved by adding lime to the slurry. However, lime consumption might be high if the calcines contain soluble compounds such as magnesium and iron sulfate which consume lime as well. To overcome this problem, the samples need pre-leaching using hot water (80 °C) prior to the test so that the harmful components are removed from the calcines. Cyanidation experiments discussed in this chapter were performed using both washed and unwashed calcines to evaluate its effect on gold recovery and to calculate how much lime is needed in the tests for both types of calcines.

For cyanidation tests, 50 g of calcines were pulped with water. The pulp density was 20%, a standard condition for optimizing different parameters. The concentration of sodium cyanide within the pulp was 4 g/l and the maximum leach time was limited to 24 hours. To determine the effect of leach time, samples were taken at 2, 4, 6, 8, 12, 18, and 24 hours. The tests were also conducted for concentrations of 3 and 5 g/l sodium cyanide. For comparison, the tests were performed at 30% pulp density with the amount of water constant but the calcines increased to 86 g.

As bromination requires pH/Eh monitoring, which is difficult if using bottle-roll technique, overhead stirring was used to agitate the pulp within a bottom round flask (Dadgar, personal communication, 1992). The flask was placed in a water bath with the water temperature adjusted to (25 °C) but the pH of solution was not adjusted. Actually, it is not easy to compare extraction results from cyanide test using bottle-roll technique and bromine leaching using overhead stirring method. Both are diffusion limited reactions. Moreover, the amount of oxygen in a capped and sealed bottle of cyanidation is limited and after 24 hours of leaching it may limit further leaching of gold. Sergent et. al. (1988) state that there is no appreciable effect on bromine leaching using either bottle-roll or overhead stirring method.

Studies on the effect of pH on gold dissolution rate by Pesic and Sergent (1991) suggest that bromination occurs in three distinct dissolution regions with respect to pH: the region independent of pH (pH = 1-6), the region in which pH increase has a negative effect (pH 6-10), and the region in which there is no gold dissolution (pH>10). The decrease in gold dissolution rate as pH increases is accounted for by the consumption of bromine in reaction with hydroxide ions followed by the rapid redox reaction of the hypobromite. Therefore, a standard condition for pH and Eh in the bromine leach test was 2-4 and 750-900 mV, respectively (Dadgar, personal communication, 1992).

Prewashing with hot water can basically be skipped as the pre-leaching does not affect gold extraction by bromination (Sergent et al. 1988; Dadgar 1989). However, one exploratory test, using washed calcine, has been performed to confirm that washing is not important.

The amount of calcines in the bromine test were similar to that of the cyanide test for both pulp densities. Reagent parameters included Geobrom™ 3400A and sodium bromide. Maximum leach tests as well as kinetic tests similar to that of cyanidation experiments were conducted. No analyses were made on final cyanide or bromine concentrations; therefore, consumption was not determined. Head assay of -200 mesh roasted and unroasted ore samples are 10.64 g/t and 9.64 g/t, respectively.

RESULTS

Cyanidation

Preliminary cyanidation test work on the unconcentrated, roasted-Osikonmäki ores was performed without lime addition to evaluate final pH and how much gold was recovered at that condition. For a 24-hour leaching, the test showed pH value of 10.20, the number of which is still in the range for optimum leaching conditions of gold by cyanide (Dadgar 1989; Marsden and House 1992). The relatively high pH occurs because of high alkalis in the ore. Without lime, gold recovery was 68%. However, all additional experiments were conducted at an adjusted pH (10.50 - 11.00) by adding lime as well as using the washed and unwashed calcines in order to optimize gold extraction.

Results of cyanidation tests are presented in Table 4. After 24 hours, the highest extracted gold was achieved by 4 g/l of cyanide concentration although the amount of recovery is still only 75%. No improvement was observed when increasing cyanide concentration to 5 g/l. The reason is not well understood but it is assumed that high pH also affected dissolution. Tests using unwashed calcines with similar conditions to the previous tests show similar recoveries. The extracted gold ranged from 65 to 75%. The results also confirm that 4 g/l NaCN and pH 10.80 are the optimum condition for this ore and the high pH due to increasing cyanide concentration yields low extraction as seen in tests 3 and 6. Increasing pulp density to 30% solid resulted in higher gold extraction (test 7 and 8), yet lime consumption decreases to 0.98 kg/t for the washed calcines and 1.00 kg/t for the unwashed calcines to keep pH value approximately at 10.80. To establish the optimum leaching time, kinetic tests were performed under conditions similar to test 2. After two hours, the dissolved gold in the leachant was 45% and increased with time. It is presumed that the total dissolution of gold would be higher if the leach time were extended as the extraction versus time curve has not reached a maximum.

Table 4. Results for extraction of gold using cyanide.

Test	Pulp density (%)	pH (g/l)	NaCN (kg/t)	NaCN (kg/t)	Lime (kg/t)	Au ext. (%)	Au in res. (g/t)
1	20	11.00	3.00	11.00	1.63	72.73	2.86
2	20	10.80	4.00	14.52	1.60	75.76	2.55
3	20	11.90	5.00	18.15	1.64	65.76	3.51
4	20	10.50	3.00	10.88	3.30	72.12	2.79
5	20	10.75	4.00	14.55	3.25	75.15	2.48
6	20	10.80	5.00	18.25	3.22	66.67	3.42
7	30	10.80	4.00	15.00	0.98	77.27	2.33
8	30	10.80	4.00	15.00	1.00	76.67	2.40

Bromination

The concentration of Geobrom™ 3400A was kept constant at 3 g/l but that of NaBr varied from 2 to 10 g/l in the first three tests (test 9-11). The results indicate that for these conditions the average gold extraction is similar to that of cyanidation tests. The average final recovery is achieved at 75%. The next tests were performed under condition of 4 to 5 g/l Geobrom™ 3400A (Table 5). Gold recovery was maximized at 4 g/l of Geobrom™ 3400A, however, the tests show that the maximum amount of extracted gold is limited to 81% and gold residues vary from 1.50 to 3.50 g/t. To confirm that of 4 g/l Geobrom™ 3400A is the optimum condition, five confirma-tory tests were performed (test 19-23) as summarized in table 5, but pulp density was increased to 30%. The results show conditions similar to test 15 yields higher final recovery than that of the other tests.

Complete leach tests were conducted to evaluate bromine response to time at 2, 4, 6, 8, 12, 18, and 24 hours using conditions similar to test 15. After 2-hour leaching, the amount of dissolved gold is less than anticipated if compared to 2-hour cyanide leaching, yet the recovery increased rapidly after 4 hours. Since recovered gold seems constant after 8-hours of leaching, a leach time of 8 hours is sufficient instead of 24 hours.

Table 5. Results for extraction of gold using bromine.

Test	Pulp dens. (%)	GB™3400A (g/l)	GB™3400A (kg/t)	NaBr (g/l)	NaBr (kg/t)	Au ext. (%)
9	20	3	10.90	2	7.26	73.94
10	20	3	10.90	4	14.52	74.85
11	20	3	10.90	10	36.29	76.60
12	20	4	14.52	0	0	65.00
13	20	4	14.52	2	7.26	79.39
14	20	4	14.52	4	14.52	79.70
15	20	4	14.52	10	36.29	80.91
16	20	5	18.15	2	7.26	72.48
17	20	5	18.15	4	14.52	78.61
18	20	5	18.15	10	36.29	79.03
19	30	3	10.90	10	36.29	74.24
20	30	4	14.52	10	36.29	83.33
21	30	4	14.52	4	14.52	81.00
22	30	4	14.52	2	7.26	80.95
23	30	5	18.15	10	36.29	79.39

CONCLUSIONS

Generally, ore mineralogy of the Osikonmäki gold deposit is characterized by sulfide and silicate phases with gold as native grains associated more often with silicates than sulfides. Gold is mostly found as inclusions in minerals and along fine fractures. Sometimes, gold is completely encapsulated by more than one mineral which hampers liberation. Most sulfides as well as bismuth-minerals in Osikonmäki ores are harmful to the leaching solution ("preg-robber").

Laboratory experiments using both cyanide and bromine show that 20 to 25 wt. % of contained gold would be lost to the tailings. Low recovery is apparently controlled by unliberated gold within silicate inclusions. Chemical breakdown of silicate needs to be made prior to leaching to over-come this problem and leaching of finer size (-325 to -400 mesh) needs to be conducted to explore leaching characters at this condition. Air pollution by SO_2 and arsenic emissions might be minimized using an autoclave.

Bromine lixiviants could be used for leaching the gold from the Osikonmäki ores. Regardless of low final recoveries, the kinetics of bromination is considerably faster than that of cyanidation. The 8-hours of bromine leaching yields as much gold as that of 48-hour cyanide leaching. However, this study did not address the issue of gold recovery from bromine leach pulp and solution (after solid/liquid separation) using activated carbon, ion exchange resins, and zinc precipitation.

The use of cyanide as a leachant is basically

acceptable for Osikonmäki ores. The gold is physically accessible to the leachant. The principal problem is dissolution rate of gold. The

rate is relatively slow and regardless of feed characteristics, the rate effects final recovery.

REFERENCES

Bornhorst, T.J., Kontoniemi, O., & Nurmi, P., this volume. Geochemistry of gold and associated elements in the Paleoproterozoic Osikonmäki gold deposit, southeastern Finland. In: Kontoniemi, O. & Nurmi, P. A. (eds.) Geological setting and characteristics of the tonalite-hosted Paleoproterozoic gold deposit at Osikonmäki, Rantasalmi, southeastern Finland. Geological Survey of Finland, Special Paper 25. 81-90.

Cook, N.J., 1990. Mineralogical examination of gold samples: Canadian Institute of Mining Bulletin 83, 51-55.

Dadgar, A., 1989. Refractory concentrate gold leaching: Cyanide vs. bromine: Journal of The Minerals, Metals & Materials Society 41(12), 37-44.

Gasparini, C., 1980. The role of the ore microscope and electron microprobe in the mining industry: Canadian Institute of Mining Bulletin 73, 73-85.

Hagni, A.M., Hagni, R.D., & Taylor, P.R., 1992. Process mineralogy of roasted pyrite and arsenopyrite: Journal of The Minerals, Metals & Materials Society, 44(4), 36-38.

Henely, K.J., 1989. A combined mineralogical/metallurgical approach to determining the nature and location of gold ores and mill products: Mineral Engineering 2, 459-470.

Kontoniemi, et. al., 1991. Ore mineralogy of the Osikonmäki gold deposit, Rantasalmi, southeastern Finland: Geological

Survey of Finland, Special Paper 12, 81-89.

Kontoniemi, O., this volume. Geological setting and characteristics of the Paleoproterozoic tonalite-hosted Osikonmäki gold deposit, southeastern Finland. In: Kontoniemi, O. & Nurmi, P. A. (eds.) Geological setting and characteristics of the tonalite-hosted Paleoproterozoic gold deposit at Osikonmäki, Rantasalmi, southeastern Finland. Geological Survey of Finland, Special Paper 25. 39-80.

Mardsen, J., & House, I., 1992. The chemistry of gold extraction: New York: Ellis Harwood. 595p.

Pesic, B., & Sergent, R.H., 1991. A rotating disk study of gold dissolution by bromine: Journal of The Minerals, Metals & Materials Society, 43(12), 35-37.

Petruk, W., 1976. The application of quantitative mineralogical analysis of ores to ore dressing: Canadian Institute of Mining Bulletin 69, 146-153.

Sergent, R.H., et al., 1988. A comparison of bromine and cyanide leaching for a refractory gold concentrate: Symposium on Precious and Rare Metals, Albuquerque, New Mexico, 6-8 April, 1988.

Wahyudi, T., 1993. Mineralogy and characteristics that affect recoveries of gold from the tonalite-hosted Osikonmäki gold deposit, Finland: M.S. Thesis, Michigan Technological University, Houghton, Michigan, U.S.A. 40 p.